Enamines and Enol-ethers: Enabling Dienophiles for Sydnone Cycloadditions

Christopher Paul Lakeland

Supervisor: Prof. J. P. A Harrity

August 2020

Submitted to the University of Sheffield in partial fulfilment of the requirements for the award of Doctor of Philosophy

Department of Chemistry, University of Sheffield, Sheffield, S3 7HF, UK.

E-mail: cplakeland1@sheffield.ac.uk

Contents

Abbreviations

(9-Mes-10-Me-Acr)$^+$ = 9-mesityl-10-methylacridinium

1,2-DBE = 1,2-dibromoethane

BCN = *exo*-((1*R*,8*S*)-bicyclo[6.1.0]non-4-yn-9-yl)methanol

BDE = bond dissociation energy

BET = back electron transfer

BHT = butylated hydroxytoluene

Boc = *tert*-butyloxycarbonyl

BOR = Bestmann-Ohira reagent

bpy = 2,2'-bipyridyl

bpz = 2,2'-bipyrazine

BSTFA = *N*,*O*-bis(trimethylsilyl) trifluoroacetamide

Cbz = benzyloxycarbonyl

CFL = compact fluorescent light-bulb

CSA = camphorsulfonic acid

CuAAC = copper catalysed azide-alkyne cycloaddition

CuSAC = copper catalysed sydnone-alkyne cycloaddition

DABCO = 1,4-diazabicyclo[2.2.2]octane

DBU = 1,8-diazabicyclo[5.4.0]undec-7-ene

DCE = 1,2-dichloroethane

DCM = dichloromethane

DDQ = 2,3-dichloro-5,6-dicyano-1,4-benzoquinone

DFT = density functional theory

DIBAC = dibenzoazacyclooctyne

DIBAL = diisobutylaluminium hydride

DIBO = dibenzocyclooctyne

DIPEA = *N*,*N*-Diisopropylethylamine

DMA = dimethylacetamide

DMAP = 4-(dimethylamino)pyridine

DME = 1,2-dimethoxyethane

DMF = dimethylformamide

DMSO = dimethylsulfoxide

DPE = 1,1-diphenylethylene

EDG = electron donating group

EnT = energy transfer

EPR = electron paramagnetic resonance

E_T = triplet excited state energy

EVI_2 = ethyl viologen diiodide

EWG = electron withdrawing group

Fc = ferrocene

Fc^+ = ferrocinium

FCC = flash column chromatography

GC-MS = gas chromatography-mass spectrometry

HAT = hydrogen atom transfer

HOMO = highest occupied molecular orbital

IAN = isoamylnitrite

IR = infrared

ISC = intersystem crossing

LC-MS = liquid chromatography-mass spectrometry

LED = light emitting diode

LFP = laser flash photolysis

LUMO = lowest unoccupied molecular orbital

MCR = multi component reaction

MLCT = metal to ligand charge transfer

MS = molecular sieves

$MVCl_2$ = methyl viologen dichloride

MW = microwave

NBS = *N*-bromosuccinamide

NCS = *N*-chlorosuccinamide

NMP = 1-methyl-2-pyrrolidinone

NMR = nuclear magnetic resonance

NUV = near ultraviolet

o-DCB = 1,2-dichlorobenzene

P = product

PC = photocatalyst

PMP = para-methoxyphenyl

ppm = parts per million

PPTS = pyridinium *p*-toluenesulfonate

ppy = 2-phenylpyridinato

PSEC = photocatalytic sydnone-enamine cycloaddition

RBF = round bottom flask

RSM = returned starting material

RT = room temperature

SA = sodium ascorbate

SCE = standard calomel electrode

S_EAr = electrophilic aromatic substitution

SEO = single electron oxidation

SER = single electron oxidation

SET = single electron transfer

SM = starting material

SPSAC = strain promoted sydnone-alkyne cycloaddition

SS = solid support

T = temperature

t = time

TBABr = tetra-*n*-butylammonium bromide

TBAF = tetra-*n*-butylammonium fluoride

TBS = *tert*-butyldimethylsilyl

TCO = *trans*-cyclooct-4-en-1-ol

TEMPO = (2,2,6,6-tetramethylpiperidin-1-yl)oxyl

TFA = trifluoroacetic acid

TFAA = trifluoroacetic anhydride

THF = tetrahydrofuran

THFu = tetrahydrofuranyl

THPy = tetrahydropyranyl

TM = transition metal

TMEDA = tetramethylethylenediamine

TMNO = trimethylamine N-oxide

TMS = trimethylsilyl

TMTH = 3,3,6,6-tetramethylthiacycloheptyne

Troc = 2,2,2-trichloroethoxycarbonyl

UV = ultraviolet

VCB = vinylcyclobutane

VLPC = visible light photocatalysis

XPhos = 2-dicyclohexylphosphino-2′,4′,6′-triisopropylbiphenyl

Acknowledgements

To my supervisor, Joe. Without your help and guidance, always unstingingly given, the completion of this work would have been markedly more difficult. Your passion for science and desire to share your knowledge and experience (along with a beer or two…) have been equally valuable in creating fond memories of the last 4 years. I hope you enjoyed our foray into visible light driven chemistry as much as myself, and I look forward to seeing further progress from the Harrity group in the future!

To Dr David Watson, I couldn't have asked for a better supervisor during my stay in Cambridge. Your assistance and constant suggestions have undoubtedly helped to improve my PhD project. Good luck in your future ventures!

To Ben Allen (Benoir), your experience and guidance upon my arrival to the Harrity group were pivotal in creating this body of work. For this, and your enthusiasm for Friday night pub sessions, I am immensely grateful.

To Wheatdogg (Matt Wheatley), our constant association during the completion of this work has been most pleasurable.

To Marie, through the medium of coffee and crisps, you have made the undertaking of this PhD far less stressful! Although I sometimes wish your columns were finished a little faster, there is nobody else I'd rather have by my side. Here's to a thesis powered by bacon frazzles and Jammy Red Roo!

To my family, this thesis is dedicated to you. I am incredibly appreciative of the never-ending support you have provided me throughout my education, without which, I would certainly not be in the position I am today.

To the rest of the harrity group – thank you for all the beer and good times! I wish everyone the best of luck in the completion of their studies.

Finally, a debt of gratitude is owed to all of the academic, administrative and technical staff within the Department of Chemistry for their assistance in both scientific and non-scientific matters.

Abstract

Several new pyrazole syntheses, based on the cycloaddition reactions of sydnones and functionalised alkenes, are reported. The methods take advantage of a cycloaddition-retrocycloaddition-elimination concept to achieve an *in situ* oxidation level adjustment which leads to the selective formation of pyrazole products.

Under thermal promotion, the reactions of sydnones and a range of enol-ethers was found to deliver the corresponding 1,4-disubstituted pyrazoles in good yield and with high levels of regiocontrol. When cyclic enol ethers are employed in these reactions in the absence of any additives, acetal containing pyrazoles are isolated. However, the addition of stoichiometric potassium carbonate leads to the corresponding alcohol containing products. Further investigations found the scope of this process to be limited with respect to both substrates; *N*-arylsydnones bearing different functional groups are reactive but *N*-alkylsydnones and *C*4-substituted sydnones do not form the desired pyrazoles. Additionally, examination of a number of other dipolarophile substrates was met with limited success.

Following these investigations, a visible light promoted photocatalytic cycloaddition procedure was developed. The synergistic combination of organocatalysis and visible light photocatalysis was found to promote a reaction between enamines and *N*-arylsydnones at ambient temperature under irradiation with blue light. This reaction leads to the exclusive formation of 1,4-disubstituted pyrazoles in high yield across a range of structurally varied enamines and *N*-arylsydnones. However, scope investigations uncovered a number of limitations including the non-reactivity of *N*-alkyl and *C*4-substituted sydnones. A series of mechanistic investigations (Stern-Volmer luminescence quenching, radical traps/clocks, cyclic voltammetry and isotopic labelling) indicate that this novel reactivity is driven by a triplet energy transfer from the photocatalyst to the sydnone substrate, leading to an excited state sydnone intermediate which reacts further to form the observed products.

1. Introduction

1.1 Pyrazoles

Pyrazole containing molecules are of paramount importance. This five-membered heterocycle containing two adjacent nitrogen atoms was first synthesised by Knorr in 1883 through the condensation of *N*-arylhydrazines and 1,3-dicarbonyl compounds.[1] Since this report, a large number of bioactive molecules based on the pyrazole core have been discovered including celecoxib[2] and rimonabant[3] (Figure 1.1), while the pyrazole motif is also prevalent in a number of blockbuster agrochemicals.[4,5] Furthermore, pyrazoles have been shown to have wide ranging industrial applications.[6,7]

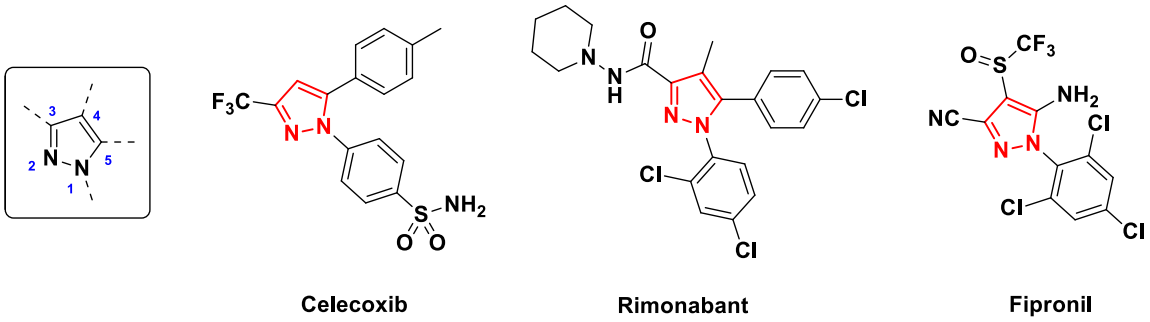

Figure 1.1 – bioactive molecules containing the pyrazole core

Owing to this widespread utility, there has been much interest in the development of novel methodologies for the synthesis of pyrazole derivatives. Generally these approaches can be classified into one of two main categories; 1) condensation reactions between hydrazines and 1,3-biselectrophiles forging two new *C-N* bonds (Figure 1.2, path a) or 2) cycloaddition reactions between various 1,3-dipoles and suitable dipolarophiles leading to the formation of one *C-C* and one *C-N* bond (Figure 1.2, path b). Alternative approaches using multi-component reactions (MCRs) and transition metal catalysis have also been reported but will not be discussed further.[6,8]

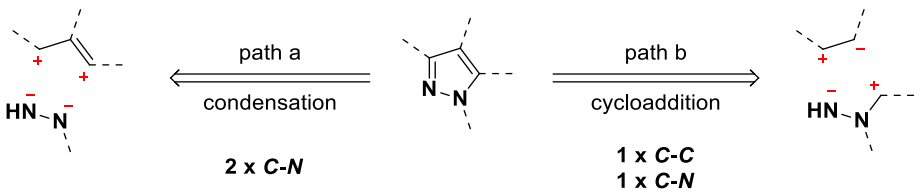

Figure 1.2 – typical approaches towards pyrazole synthesis

1.1.1 Condensation Reactions

Classical methods for the synthesis of pyrazoles have been largely based on the condensation of hydrazine derivatives with 1,3-dicarbonyl compounds such as diketones and α,β-unsaturated ketones/aldehydes (Scheme 1.1). Elguero and co-workers have postulated a mechanism for the condensation of hydrazides with 1,3-diketones whereby addition to both carbonyl groups leads to the formation of diaminal intermediates **1a** and **1b**, which then lose two molecules of water to furnish the pyrazole products.[7] In this proposal, the formation of both *C-N* bonds leading to **1a**/**1b** is considered to be reversible while the subsequent loss of water to form **2a**/**2b** is irreversible. As such, the ratio of product regioisomers is determined by the rates of dehydration of intermediates **1a**/**1b** (Scheme 1.1). These methods generally proceed with high levels of efficiency but provide regioisomeric mixtures of pyrazole products when unsymmetrical electrophiles are employed, because the regioselectivity is controlled by reactivity differences between the two termini of the bis-electrophile. As such, the observed ratios are heavily substituent dependant. A similar mechanism may also be invoked for the reaction of enones, except that in this case the immediate product of the reaction is pyrazoline **3a**/**3b** which must be subsequently oxidised to the corresponding pyrazole.

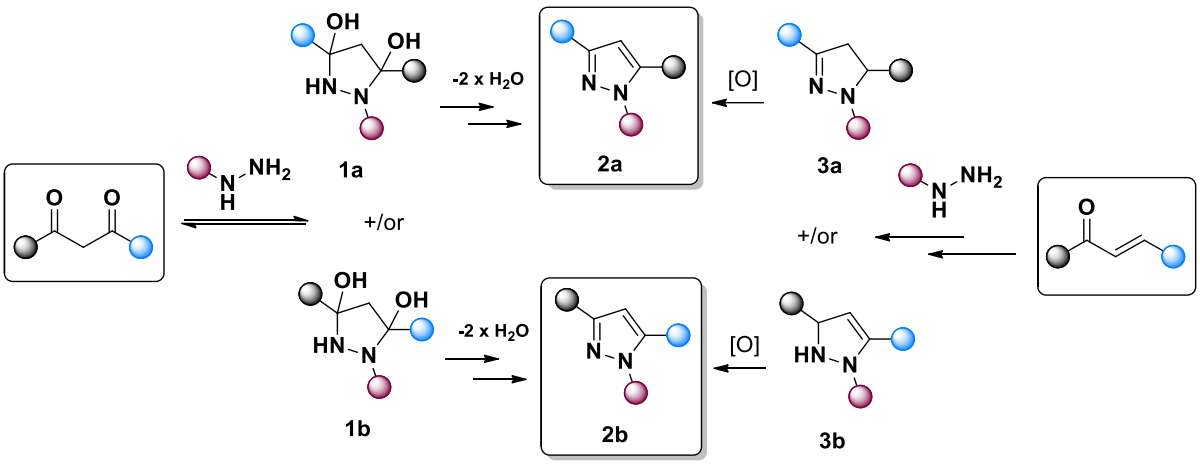

Scheme 1.1 – proposed mechanism for the condensation of hydrazines and 1,3-dicarbonyl compounds or α,β-unsaturated carbonyl compounds

Alternatively, if the α,β-unsaturated carbonyl compound contains a suitable leaving group at the α- or β-position then the pyrazoline intermediate can undergo an *in situ* oxidation level adjustment to deliver the pyrazole directly. Such a strategy was reported Katritzky and co-workers in the reaction of α-benzotriazolyl-α,β-unsaturated ketones and *N*-alkyl/aryl hydrazines (Scheme 1.2).[9] In the case of aryl substituted enones the reaction initially forms the stable pyrazoline intermediates **5** which can undergo conversion to the corresponding pyrazoles using excess base. On the other hand, alkyl substituted enones form the pyrazole products directly.

In addition to its role as a leaving group, the benzotriazole moiety also enhances the regioselectivity of the reaction and, for aryl substituted pyrazolines **5**, allows the introduction of additional functionality due to the acidity of the α-hydrogen atom. Numerous other elegant methods to achieve regiocontrol in condensation reactions have been reported, resulting in a diverse library of pyrazole derivatives becoming accessible using this strategy.

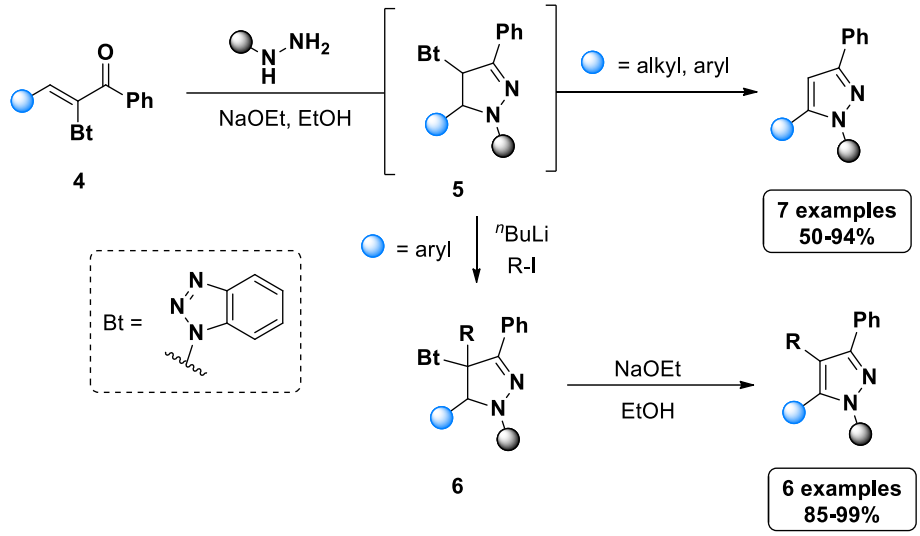

Scheme 1.2 – synthesis of pyrazoles using benzotriazole substituted enones

1.1.2 Cycloaddition Reactions

An alternative approach for pyrazole synthesis centres on the 1,3-dipolar cycloaddition reactions of [*C-N-N*] dipoles such as diazoalkanes, nitrilimines and azomethine imines with suitably substituted alkene or alkyne dipolarophiles (Scheme 1.3). In comparison to the condensation methods described above, dipolar cycloadditions are typically more regioselective as a consequence of the intrinsic polarity across the dipole resulting from the large electronegativity difference between the *C* and *N* atoms.

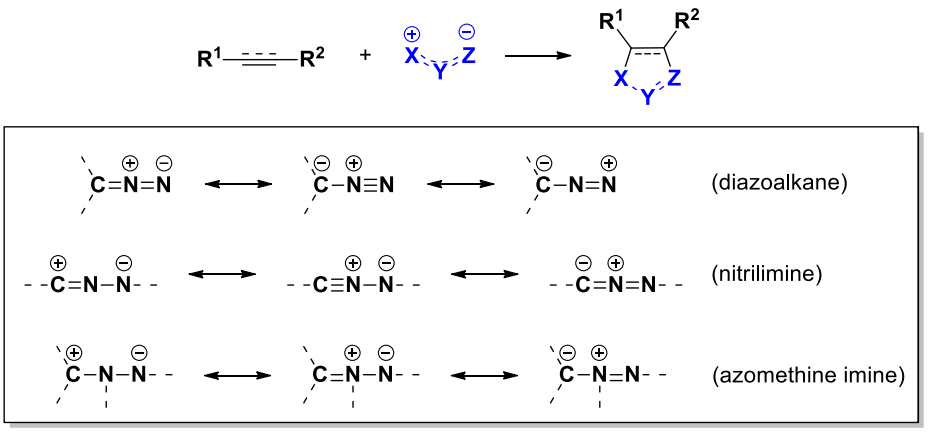

Scheme 1.3 – common dipolar reagents used for pyrazole synthesis

1.1.2.1 Diazoalkanes as 1,3-dipoles

Amongst their many uses in synthetic chemistry, diazoalkanes are especially prominent as substrates for thermally promoted cycloaddition reactions with alkenes and alkynes to form pyrazoles. Due to the high reactivity and toxicity of these intermediates, they are often prepared *in situ* from tosylhydrazone precursors (Scheme 1.4A). Upon exposure to a suitable base, the tosylhydrazone undergoes an elimination event to form the desired diazoalkane which can then react with the dipolarophile partner. For example, Aggarwal showed that aryl substituted diazoalkanes **8** could be trapped with *N*-vinylimidazole (an acetylene equivalent) or a range of propiolates to produce the corresponding pyrazoles in high yields and with excellent regioselectivities.[10]

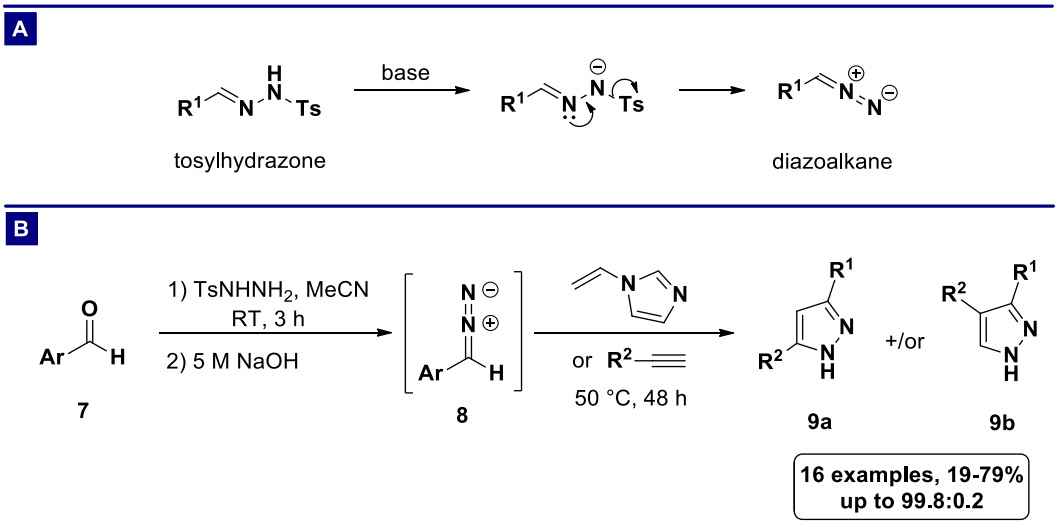

Scheme 1.4 - a) base promoted conversion of tosylhydrazones into diazoalkanes; b) cycloaddition reactions of *in-situ* generated diazoalkanes

A few years later, Muruganantham *et al.* reported the synthesis of a range of phosphonyl pyrazoles (Scheme 1.5).[11] A base-mediated acyl cleavage from the Bestmann-Ohira reagent (BOR)[12,13] **11** generates the reactive diazoalkane **13** which reacts with the nitroolefin partner to afford the desired pyrazoles as a single regioisomer. These reports highlight the excellent levels of regiocontrol that can be attained in these dipolar cycloaddition reactions and again demonstrate the utility of exploiting a leaving group elimination to attain the pyrazole oxidation level.

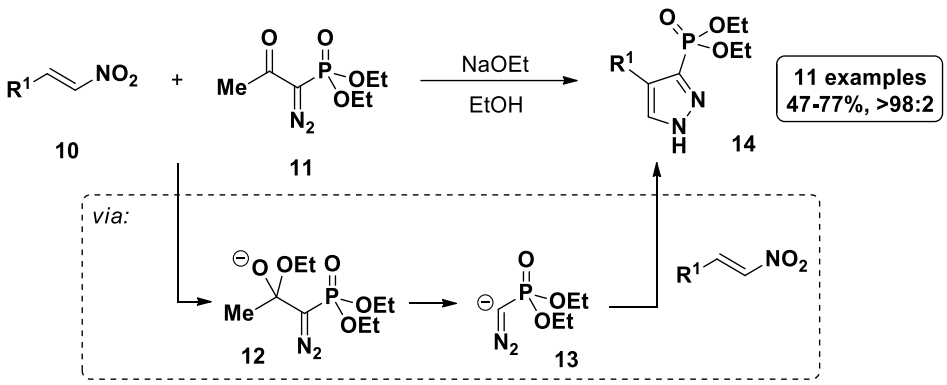

Scheme 1.5 – synthesis of 3-phosphonyl pyrazoles

1.1.2.2 Nitrilimines as 1,3-dipoles

Analogous to diazoalkanes, nitrilimines are usually generated *in situ* by the treatment of hydrazonoyl halides with a base (Scheme 1.6A). The use of this class of dipole for the synthesis of pyrazoles has been known for over 30 years and has subsequently been employed in the regioselective synthesis of several bioactive molecules.[14,15] In contrast to the reactions with diazoalkanes, the cycloaddition reaction between nitrilimines and alkynes often exhibits low levels of regioselectivity and therefore remains relatively unexplored. However, the reaction of nitrilimines with alkenes is highly regioselective and hence more synthetically valuable. In 2001, Donohue reported the reaction between nitrilimines and resin-bound enamines **15**, leading to the formation of pyrazoline intermediates **17**.[16] Subsequent treatment with trifluoroacetic acid (TFA) induces an elimination event that concurrently oxidises the pyrazoline and cleaves the target pyrazole from the solid support (Scheme 1.6B).

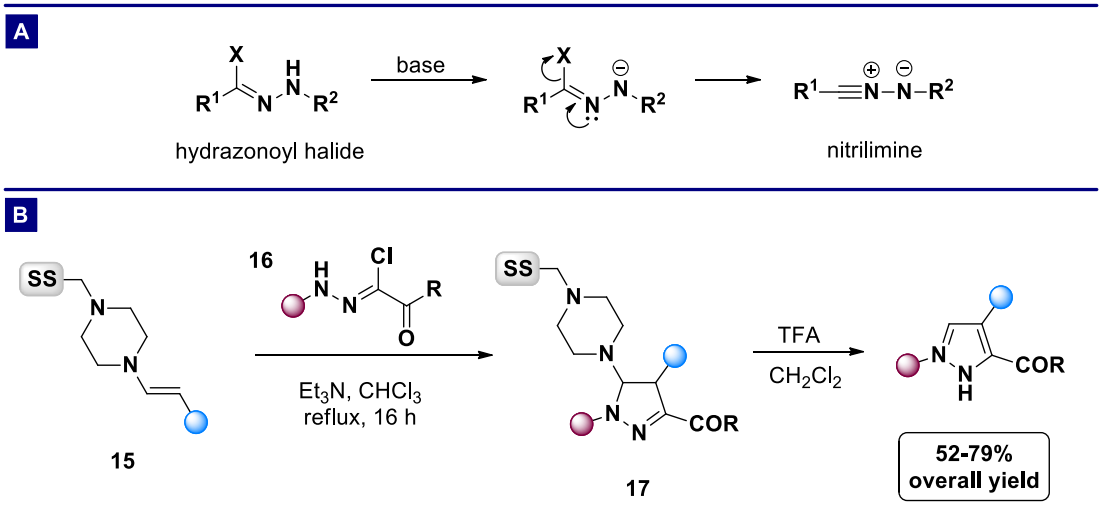

Scheme 1.6 – a) base promoted conversion of hydrazonoyl halides into nitrilimines. b) polymer supported synthesis of pyrazoles from enamines and nitrilimines; SS = solid support

Further reports from Abunada and co-workers showed that nitrilimines generated from hydrazonoyl bromides **18** undergo successful reaction with active methylene compounds **19** and **21** to deliver densely functionalised pyrazoles in moderate to high yields.[17] In the case of pyrazoline cycloadduct **20**, the elimination of a molecule of water forms the pyrazole product, while **22** undergoes a tautomerisation to form the desired product. In combination, these methods demonstrate that incorporating a heteroatom based leaving group into the dipolarophile partner can enhance dipolar cycloaddition reactions by: 1) Polarising the frontier molecular orbitals of the dipolarophile leading to higher levels of regiocontrol. 2) Removing the necessity for further oxidative manipulation of the cycloadducts.

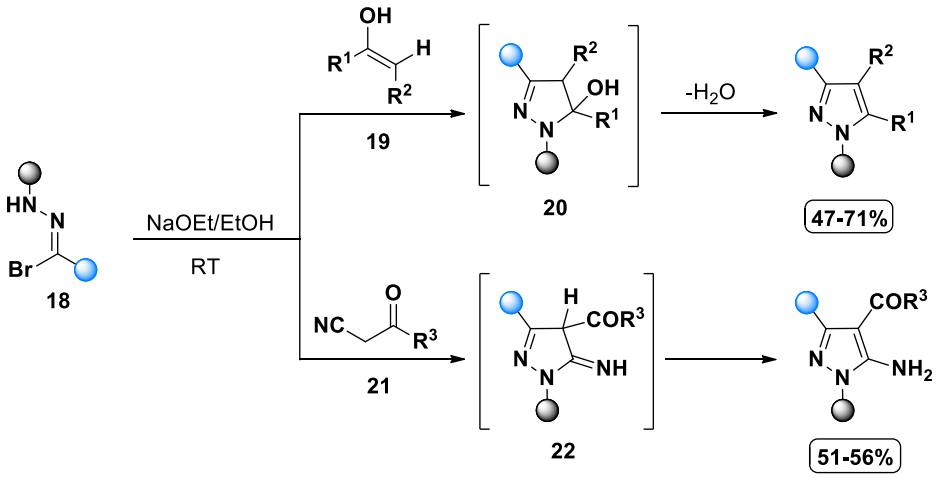

Scheme 1.7 – cycloaddition reactions of nitrilimines with active methylene containing compounds

1.1.2.3 Azomethine imines as 1,3-dipoles

The final class of 1,3-dipoles which may be utilized in the synthesis of pyrazoles are azomethine imines. Reports using this class of dipole are much less prevalent than diazoalkanes/nitrilimines, and mainly involve strongly oxidising conditions to convert pyrazoline intermediates into the desired pyrazoles. For example, Kirar *et al.* showed that cyclic azomethine imines **24** react with acetylene amide **25** to form bicyclic pyrazolidinones **26** in moderate yield.[18] Electron rich pyrazolidinone **26a** could then be subjected to a copper-catalysed oxidative hydrolytic ring-opening to the corresponding pyrazole **27**.

On the other hand, sydnones have been widely used as dipolar reagents for the synthesis of pyrazoles. This class of heterocycles may essentially be regarded as azomethine imine type dipoles linked to a molecule of carbon dioxide; the elimination of which both oxidises the intermediate and drives the reaction forward. This makes sydnones highly versatile precursors to a wide range of pyrazole containing molecules (*vide infra*).

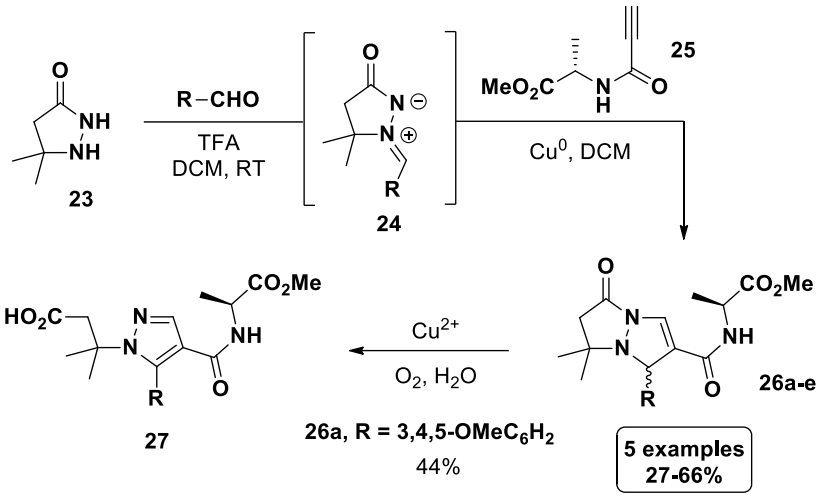

Scheme 1.8 – synthesis of pyrazoles from azomethine imines

1.2 Sydnones

Sydnones were discovered in 1935 by Earl and Mackney who observed that treating *N*-nitrosophenylglycine with acetic anhydride gave rise to a crystalline solid; *N*-phenylsydnone.[19] This was later found to be a general process and the early chemistry of sydnones was subsequently reviewed by Ollis and Stewart.[20,21] Synthetic interest in sydnones has steadily increased over the last century due to the discovery of many bioactive sydnone containing molecules including antibacterials,[22] antimicrobials,[23] and antineoplastics.[24] Additionally, sydnones serve as effective precursors to a range of 5-membered heterocycles including pyrazoles and pyrazolines through their cycloaddition reactions with alkynes and alkenes, respectively.[25]

1.2.1 Structure and Properties

Ever since their discovery, the structure of sydnones has attracted much debate. Initial proposals for the structure of sydnones included the strained bicyclic β-lactam **28**, based on the observations that alkaline hydrolysis of *N*-phenylsydnone produced *N*-nitroso-*N*-phenylglycine in high yield and treatment with aqueous acid gave *N*-phenylhydrazine, formic acid and carbon dioxide (Scheme 1.9A). What is now considered the correct structure was first proposed by Baker, Ollis and Poole in 1949.[26] Experiments by Kenner and Mackay concluded that sydnones are optically inactive,[27] leading Baker and Ollis to propose a five-membered mesoionic structure **29**, in which the positive charge is delocalised over the ring system while the negative charge is localised mainly on the exocyclic oxygen (Scheme 1.9B). This problem has also been approached computationally through a series of molecular orbital calculations.[28] The calculated bond orders corroborate the presence of an enolate type exocyclic oxygen and the calculated net charges also indicate an iminium type *N*3 nitrogen (large positive charge) and enolate like oxygen atom (large negative charge) (Figure 1.3A). However, these

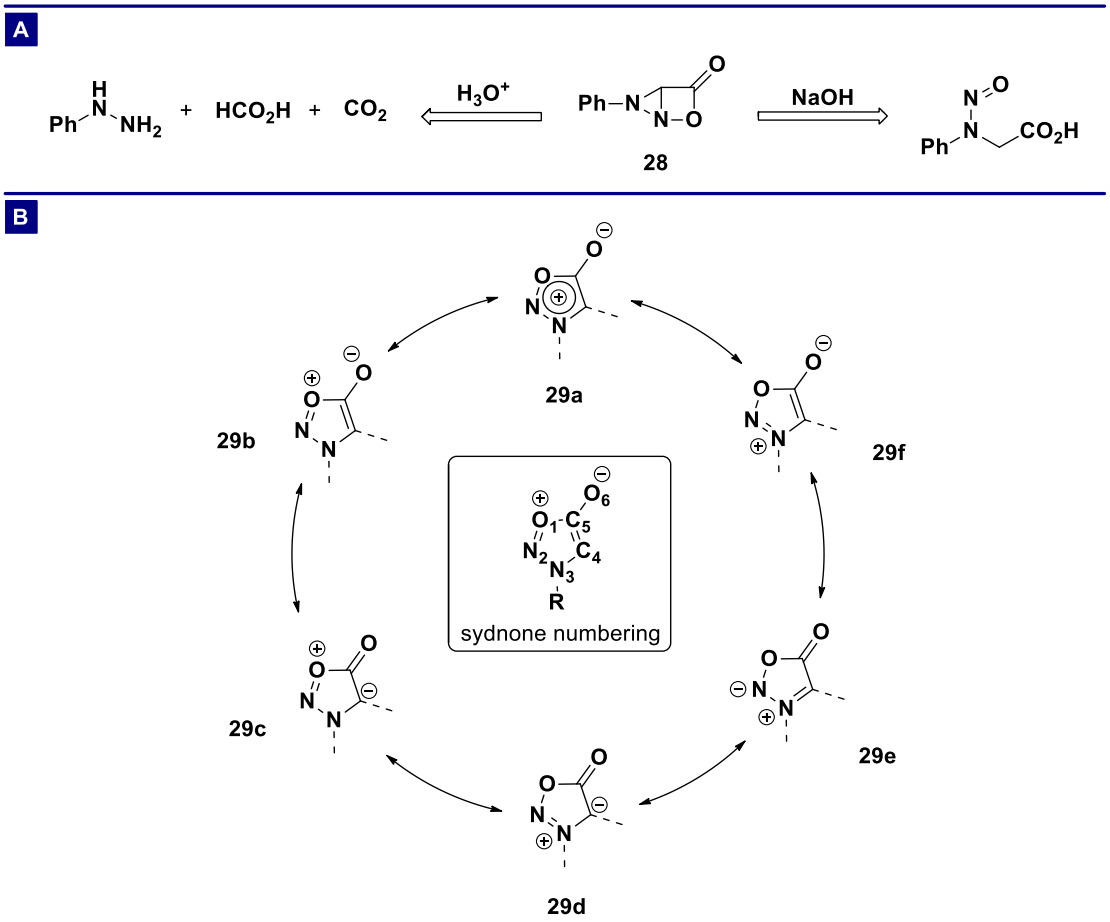

Scheme 1.9 – a) proposed β-lactam structure of sydnones; b) proposed mesoionic structure of sydnones

conclusions are contradicted by the observation that the proton on the sydnone *C*4 carbon is relatively acidic (pKa ~18),[29] indicating the presence of a ketone type carbonyl group. Infra-red spectra of sydnones also show an intense peak in the carbonyl region (~1730 cm^{-1}) further complicating the picture. Gratifyingly, synthetic studies indicate that a combination of the various predicted properties is correct and a general reactivity profile for sydnones is shown in Figure 1.3B.

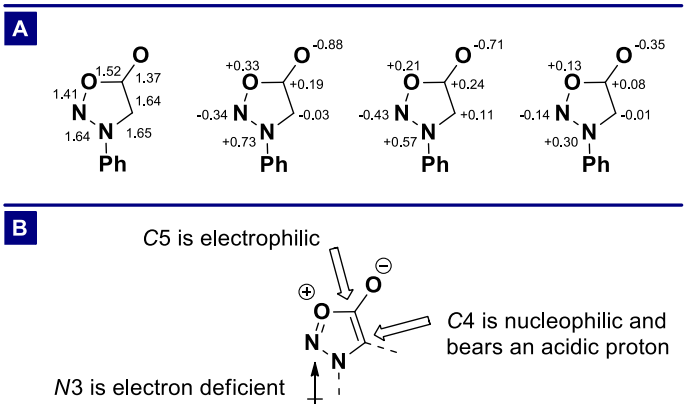

Figure 1.3 – a) calculated bond orders and net charges in *N*-phenylsydnone; b) general reactivity profile of sydnones

1.2.2 Synthesis of Sydnones

Sydnones can be readily synthesised in two steps from the corresponding *N*-substituted amino acids **30** (Scheme 1.10). Treatment with sodium nitrite in a solution of aqueous hydrochloric acid generates nitrosamine intermediate **31** which can then undergo cyclodehydration in the presence of acetic anhydride. The sydnone products are, with the exception of *N*-methylsydnone, crystalline solids that show remarkable stability under ambient conditions (*N*-phenylsydnone is stable at ambient temperature >5 years). More recent modifications of this protocol include using isoamyl nitrite (IAN) to allow the incorporation of acid sensitive functional groups and the employment of trifluoroacetic anhydride (TFAA) due to the increased rate of cyclodehydration. It should be noted that the use of *N*-substituted amino acids is necessary; treatment of the unsubstituted amino acid (R = H) with a nitrosating reagent simply results in the formation of the corresponding diazonium salt. Further refinement of this reaction has been investigated leading to methods which achieve higher levels of purity and avoid handling the highly carcinogenic nitrosamine intermediates through means of a one-pot process.[30–32]

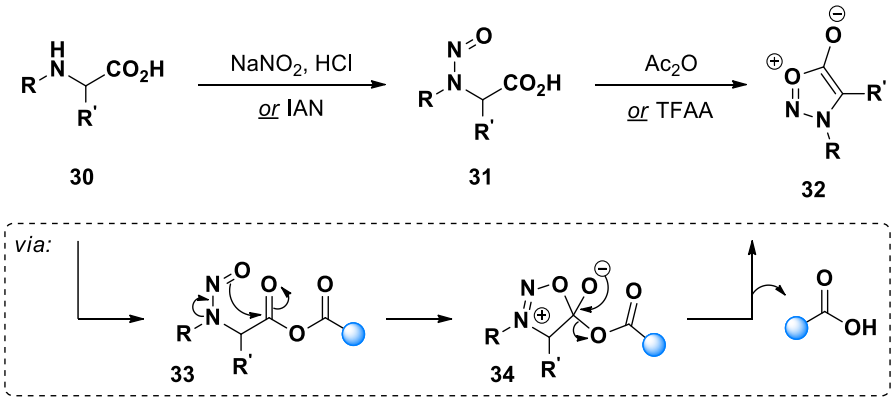

Scheme 1.10 – general procedure for the synthesis of sydnones

1.2.3 *C*4 Functionalisation

The functionalisation of sydnones at the *C*4 position is arguably the most common, and important, means of derivatizing these mesoionic heterocycles. Given both the nucleophilicity of sydnones at the *C*4 carbon and the presence of an acidic proton in the same position, it is unsurprising that a large number of *C*4 functionalisation reactions have been reported.[25] Reported techniques include electrophilic aromatic substitution (S_EAr), lithiation and electrophilic trapping and transition metal catalysed cross-coupling reactions. The combination of these methods allows the introduction of a diverse range of functional groups at the *C*4 position of the sydnone ring.

1.2.3.1 *C*4 Halogenation

The halogenation of sydnones has been known for over 70 years and serves as a linchpin for sydnone functionalisation due to the diverse array of chemistry applicable to the halogenated products. Many reagents have been shown to successfully promote this transformation including bromine, chlorine, *N*-bromosuccinamide (NBS) and *N*-chlorosuccinamide (NCS).[33–36] The reaction exhibits a wide scope with respect to the sydnone *N*-substituent including both alkyl and aryl groups. In the latter example one might imagine a competitive halogenation process between the sydnone and aryl rings, however, systematic studies by Turnbull discovered that only the presence of a 2-amino group was sufficient for achieving selective bromination on the aryl ring.[37] These results indicate a strong deactivating effect on the aryl ring due to the electron withdrawing nature of the sydnone *N*3 atom. In contrast to the effortless bromination/chlorination of sydnones, iodination reactions with iodine proceed in markedly decreased yields. Reports from Dumitraşcu demonstrated how to overcome this challenge using a mixture of iodine monochloride, glacial acetic acid and sodium acetate (Scheme 1.11B).[38,39] This reaction works in high yield for a range of *N*-alkyl/*N*-aryl sydnones and was unaffected by the electronic character of the nitrogen substituent. The fluorination of sydnones via reductive elimination from a Pd-fluoride complex has also been reported,[40] while the dehalogenation of 4-halosydnones can also be achieved using a number of conditions.[41–44]

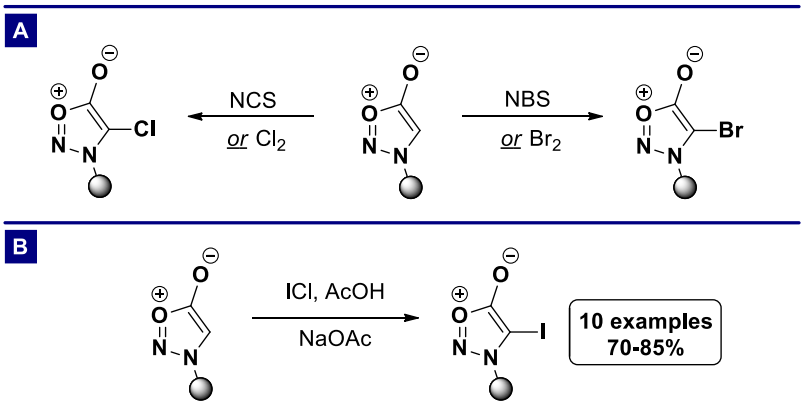

Scheme 1.11 – a) chlorination and bromination of sydnones; b) iodination of sydnones using ICl

1.2.3.2 *C*4 Acylation

The *C*4 acylation of sydnones is another important transformation because of the versatility of the carbonyl group within organic synthesis. Interestingly, the classical Friedel-Crafts conditions for achieving acylation (acid chloride and $AlCl_3$) are inoperative when used on sydnones,[45] presumably due to sequestration of the Lewis acid by the exocyclic oxygen of the sydnone. The first sydnone acylation reaction was reported by Greco who showed that treating *N*-phenylsydnone with *n*-butyllithium (^{n}BuLi) produced lithiated species **36** which could be trapped with carbon dioxide to

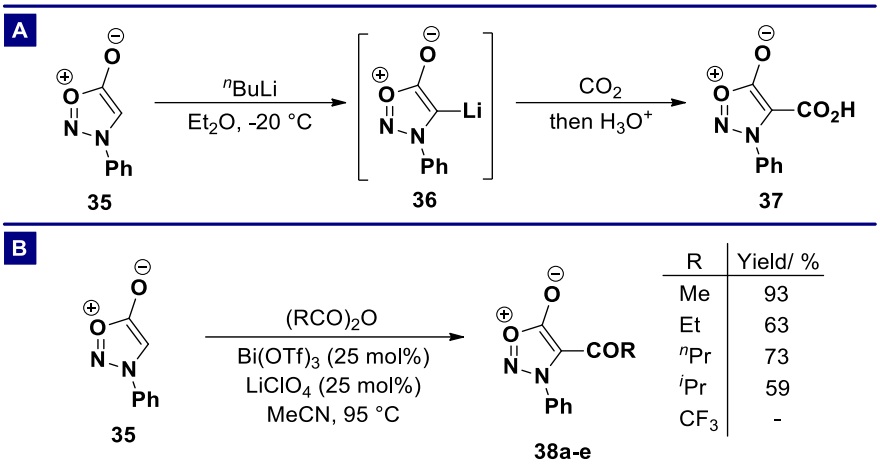

Scheme 1.12 – a) acylation of sydnones with carbon dioxide; b) Lewis acid catalysed acylation of sydnones

produce sydnone **37**.[33] Alternatively, the generation of the *C*4 Grignard reagent from the appropriate 4-bromosydnone has been exploited for the synthesis of 4-acetylsydnones and this metalation/electrophilic trapping strategy has also been expanded to disulphide, phosphinous chloride and silyl chloride electrophiles along with a variety of acyl donors.[25] Furthermore, Turnbull has reported a metal triflate catalysed system for achieving *C*4 acylation;[46–48] the first example of a Lewis acid catalysed sydnone acylation (Scheme 1.12B). Using bismuth triflate (25 mol%) and a lithium perchlorate co-catalyst (25 mol%) in the presence of acetic anhydride gave excellent yields of 4-acetyl-3-phenylsydnone in only 2 hours. Longer reaction times were found to decrease product yield (likely due to increased acid-mediated degradation of the sydnones (*vide supra*)) as did decreasing either the catalyst loadings or temperature. The reaction is also tolerant of different acid anhydride substrates although the reaction fails to provide any product when TFAA is used, possibly due to the inductive effects of the fluorine atoms leading to decreased coordination of the Lewis acid. Myriad other methods have been reported for this transformation thus allowing acylation of the sydnone ring regardless of the *N*3-substituent.[25]

1.2.3.3 *C*4 Functionalisation using Transition Metal Catalysis

Significant advancements in transition metal catalysed cross-coupling and *C-H* activation reactions have been achieved over the last few decades,[49,50] the importance of which has been recognised by the awarding of both the 2005 and 2010 Nobel prize in Chemistry. These processes have provided chemists with an abundance of ways to rapidly functionalise molecules and these techniques have subsequently been applied to sydnones to further increase the functional group diversity available at the *C*4-position. The first example of sydnone cross-coupling came from Kalinin who showed that cuprate **39**, generated by deprotonation of *N*-phenylsydnone with ^{n}BuLi and transmetalation with copper (I) bromide, underwent palladium catalysed cross-coupling with aryl and alkenyl halides to

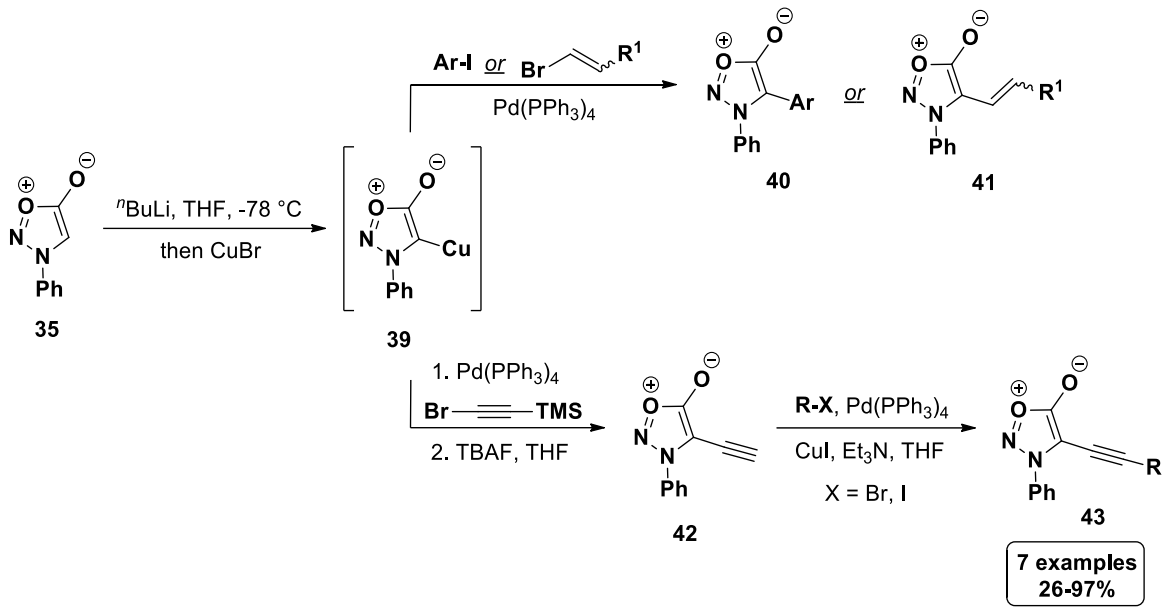

Scheme 1.13 – Pd-catalysed sydnone functionalisation via cuprate **39**

afford sydnones **40** and **41**, respectively (Scheme 1.13).[51] Attempts to directly introduce different ethynyl groups with this methodology failed but this could be circumvented using a Sonogashira coupling of intermediate **42**.[52] A more efficient synthesis of 4-alkynylsydnones came from Turnbull in 2002 who demonstrated that 4-bromosydnones were susceptible to a direct Sonogashira coupling reaction with terminal alkynes,[53] delivering the corresponding 4-alkynylsydnones in high yield. The main advantage of this method is the relative ease of synthesising 4-halosydnones (Section 1.2.3.1). Further coupling reactions of 4-halosydnones include the microwave assisted Suzuki-Miyaura coupling of 4-bromosydnones with aryl boronic acids (Scheme 1.14).[54] This procedure is tolerant of numerous palladium pre-catalysts, solvents and boron activating species including potassium hydrogen fluoride (KHF_2) which, at the time, represented an unprecedented acid-mediated Suzuki-Miyaura cross-coupling. The reaction was found to give high yields of the coupled products independent of the

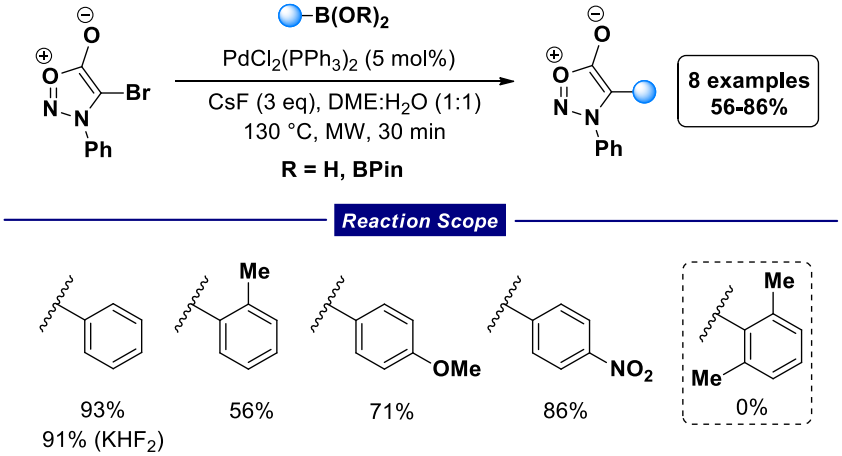

Scheme 1.14 – microwave assisted Suzuki-Miyaura cross-coupling of 4-bromosydnones

electronic nature of the boronic acid, but more sterically hindered boronic acids gave lower yields.

In recent years attention has turned to *C-H* activation methods for achieving *C*4 functionalisation. By comparison to traditional cross-coupling techniques which require two activated substrates, *C-H* activation reactions make use of one,[55] or two,[56] unactivated substrates and are therefore less time consuming due to a decreased requirement for precursor synthesis. In 2009, Moran disclosed that *N*-arylsydnones **44** can undergo a direct reaction with iodobenzenes at 120 °C under air to produce diarylsydnones **45** in high yield.[57] Optimisation studies found the high temperature was essential for an efficient reaction with *N*-arylsydnones while a decreased temperature of 80 °C also allowed *N*-alkylsydnones to participate in the reaction, albeit with lower yields. A further report from Moran's group extended this catalyst system to include alkenyl halide electrophiles,[58] thus rendering this system highly useful for sydnone *C*4-functionalisation.

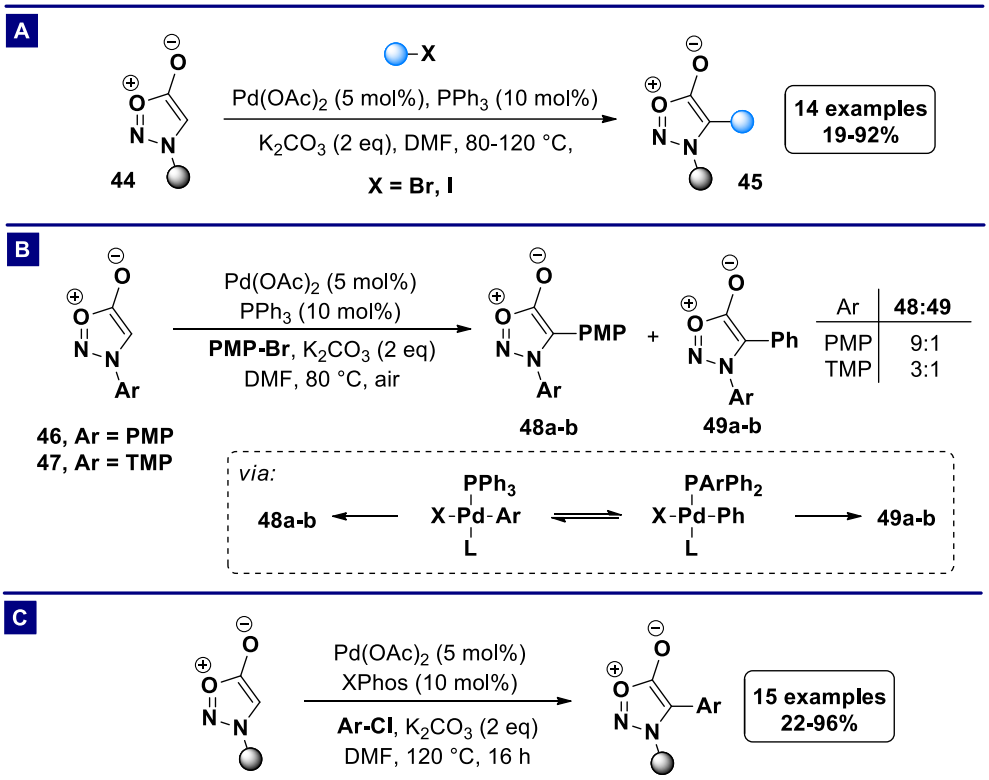

Scheme 1.15 – a) direct *C-H* arylation of sydnones; b) by-product formation under *C-H* arylation conditions using PPh_3 as a ligand; c) improved *C-H* arylation conditions using XPhos as a ligand; PMP = 4-methoxyphenyl; TMP = 3,4,5-trimethoxyphenyl

Later investigation in the Harrity group revealed a side reaction under Moran's conditions when electron rich sydnone substrates were employed (Scheme 1.15B).[59] Alongside the desired products **48a** and **48b**, small amounts of the 4-phenyl substituted sydnones **49a** and **49b** were also isolated. The authors hypothesised that the by-products arise due to an exchange process between the palladium centre and the triphenylphosphine ligand, which becomes kinetically competitive due to a slow

transmetalation step. The use of the Buchwald biaryl phosphine ligand XPhos (10 mol%) in place of PPh_3 eliminated this unproductive side reaction and also allowed aryl chlorides to be used as substrates.[60] Exploration of the reaction scope found the reaction to be unaffected by the electronic nature of the sydnone, but electron rich aryl chlorides were significantly less active than electronically poor/neutral counterparts (Scheme 1.15C).

1.2.2 Sydnone Cycloaddition Reactions

1.2.2.1 Cycloaddition Reactions with Alkynes

Arguably the most important synthetic application of sydnones is their 1,3-dipolar cycloaddition reaction with alkynes. This reaction leads to the formation of pyrazoles **52** by an initial cycloaddition to form bridged intermediate **51**, followed by a retrocycloaddition with the extrusion of carbon dioxide (Scheme 1.16).

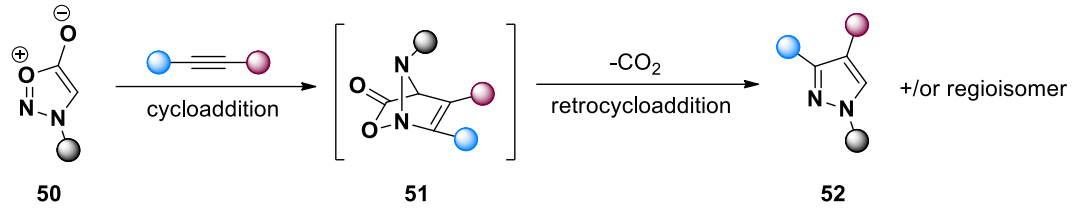

Scheme 1.16 – general mechanism of sydnone-alkyne cycloaddition reactions

This mode of reactivity was discovered by Huisgen in 1962 with the reaction between sydnones and alkynes bearing hydrocarbon, ketone, ester, alcohol and acetal groups at high temperature.[61] Many other examples employing both symmetrical and unsymmetrical dipolarophiles have since been reported, leading to a diverse range of functional groups and pyrazole substitution patterns becoming accessible using this chemistry.[62–69] Often, the observed regioselectivity is hard to predict and appears to arise from a combination of steric and electronic factors.[70] Another common feature of these reactions is the requirement for high temperatures (>140 °C) and long reaction times (>16 h).

On the other hand, systems which can reliably control the regioselectivity of organic reactions are highly sought after. Moreover, those which proceed under mild conditions offer further advantages with respect to functional group tolerance. Following on from the widespread success of the copper catalysed azide-alkyne cycloaddition (CuAAC),[71–73] Taran reported the regioselective copper catalysed sydnone-alkyne cycloaddition (CuSAC) reaction (Scheme 1.17A).[74] The combination of catalytic quantities of copper (II) sulphate (20 mol%) and ligand **L1** efficiently promoted the reaction of *N*-arylsydnones and terminal alkynes to form 1,4-disubstituted pyrazoles exclusively. The postulated mechanism involves the formation of a Cu-acetylide species which coordinates to the *N*2 atom of the sydnone ring. This coordinating interaction then controls the geometry of the dipolarophile during the

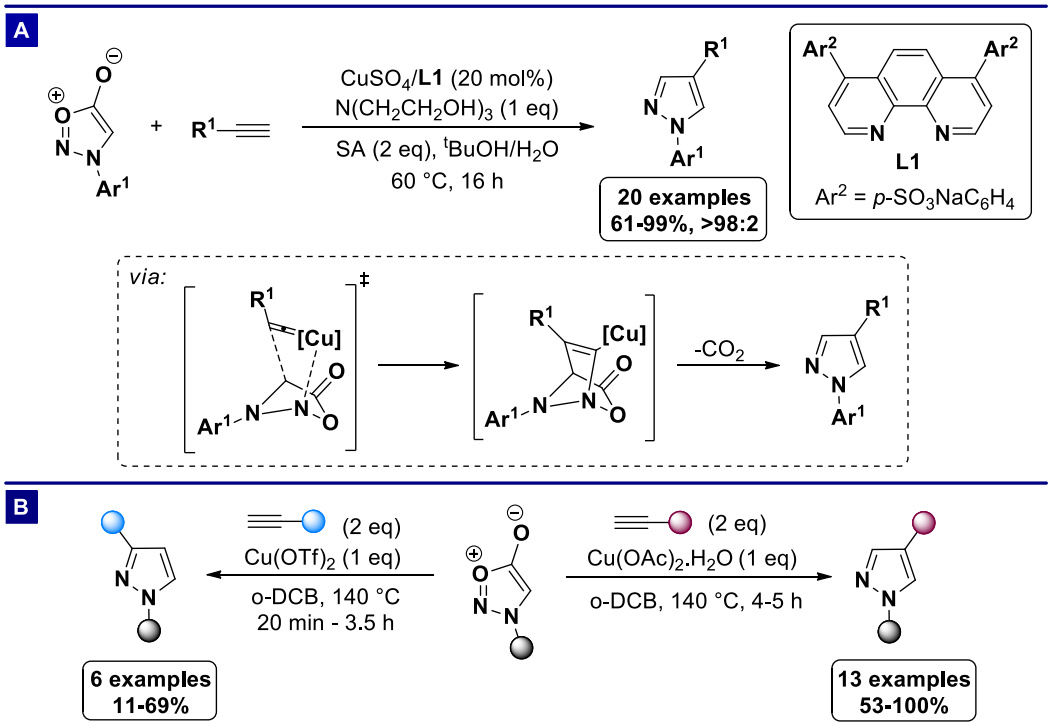

Scheme 1.17 – a) Cu-catalysed sydnone-alkyne cycloaddition (CuSAC); b) regiodivergent Cu-promoted sydnone-alkyne cycloadditions; SA = sodium ascorbate; *o*-DCB = 1,2-dichlorobenzene

cycloaddition reaction, leading to the observed selectivity. The promoting effect of copper salts on sydnone cycloadditions has also been reported by the Harrity group (Scheme 1.17B).[75,76] These studies demonstrated that the addition of $Cu(OAc)_2$ (1 eq) gave the 1,4-regioisomer selectively, while the addition of $Cu(OTf)_2$ (1 eq) gave the 1,3-regioisomer. Density functional theory (DFT) calculations propose that the observed regioselectivity switch is the result of a change in mechanism; $Cu(OAc)_2$ produces the Cu-acetylide (c.f. $CuSO_4$) while $Cu(OTf)_2$ coordinates to the exocyclic oxygen of the sydnone ring, lowering the energy of the transition state to form the 1,3-disubstituted pyrazole. Other regioselective sydnone-alkyne cycloadditions include a substrate controlled reaction between 4-pyridylsydnones **53** and alkynyltrifluoroborate salts **54** (Scheme 1.18).[77] Exposure of trifluoroborate **54** to a fluorophilic Lewis acid generates the corresponding difluoroborane *in-situ* which then forms a Lewis acid-base complex with the nitrogen donor in the pyridine substituent. The formation of this interaction templates the cycloaddition process, enhancing both the regioselectivity and rate of reaction. As a consequence, this reaction proceeds under remarkably mild conditions compared to other sydnone-alkyne cycloaddition reactions (140 °C -> 25 °C).

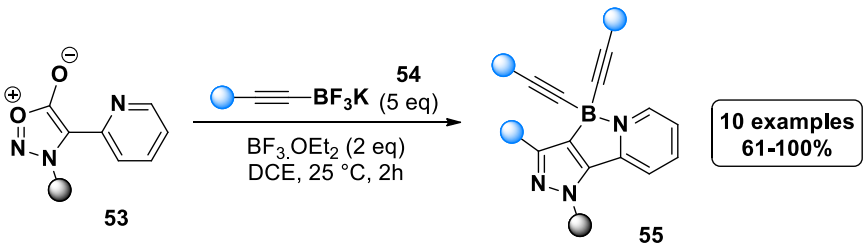

Scheme 1.18 – Lewis acid-base promoted sydnone cycloaddition reaction

Much of the recent literature has focused on the application of sydnones in bioorthogonal cycloadditions, driven by the discovery that *N*-phenylsydnone reacts rapidly with *exo*-((1*R*,8*S*)-bicyclo[6.1.0]non-4-yn-9-yl)methanol (BCN) under ambient conditions (Scheme 1.19A).[78] A more rigorous evaluation of the substituent effects on the rate of these reactions was then performed by Taran's group.[79] Among the more interesting results, the presence of a halogen atom on the sydnone *C*4-position was found to dramatically increase the rate of the reaction. Specifically, iodine provided a 5-fold rate enhancement while a chlorine substituent increased the rate by over 15 times. Later work found an even larger effect in the presence of fluorine,[40] while a computational investigation of the reaction using the "distortion/interaction" model was performed to try and understand the origin of this phenomenon.[80] Furthermore, computational analysis of different dipolarophile partners in bioorthogonal cycloadditions using *N*-phenylsydnone led to the discovery of dibenzoazacyclooctyne (DIBAC) as a more efficient coupling partner (Scheme 1.19B).[81] The culmination of these reports begins to address the problems associated with the harsh conditions of sydnone cycloadditions, although further work is required to expand the scope of these processes.

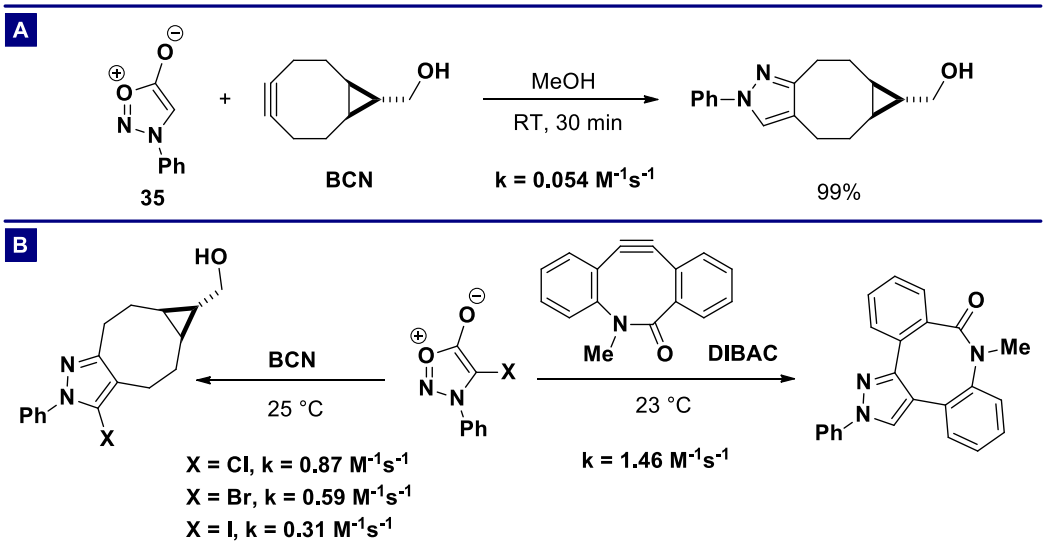

Scheme 1.19 – a) discovery of strain promoted sydnone-alkyne cycloadditions (SPSAC); b) investigation of 4-halosydnones and alternative dipolarophiles in the SPSAC reaction; RT = room temperature

1.2.2.2 Cycloaddition Reactions with Alkenes

The first sydnone-alkene cycloadditions were reported around the same time as the sydnone-alkyne equivalent.[82] In spite of this, far fewer examples of this class of cycloaddition can be found in the literature. The reaction is again thought to proceed via a cycloaddition-retrocycloaddition mechanism however, due to the oxidation level difference in the dipolarophile, the product of this process is no longer a pyrazole (Scheme 1.20). Instead, 1,3-dipolar intermediate **58** is formed and the unpredictable fate of this species is likely responsible for the relatively limited number of sydnone-alkene cycloadditions. As reported by Huisgen, **58** can undergo a simple proton shift to form the corresponding pyrazolines **59**.[82] Alternatively, a second 1,3-dipolar cycloaddition gives rise to bridged heterocycles of type **60**,[83] while an oxidation event can also lead to pyrazole products **61**.[84] Indeed, the propensity of these dipoles to undergo further cycloaddition reactions has been exploited within polymer synthesis.[85,86]

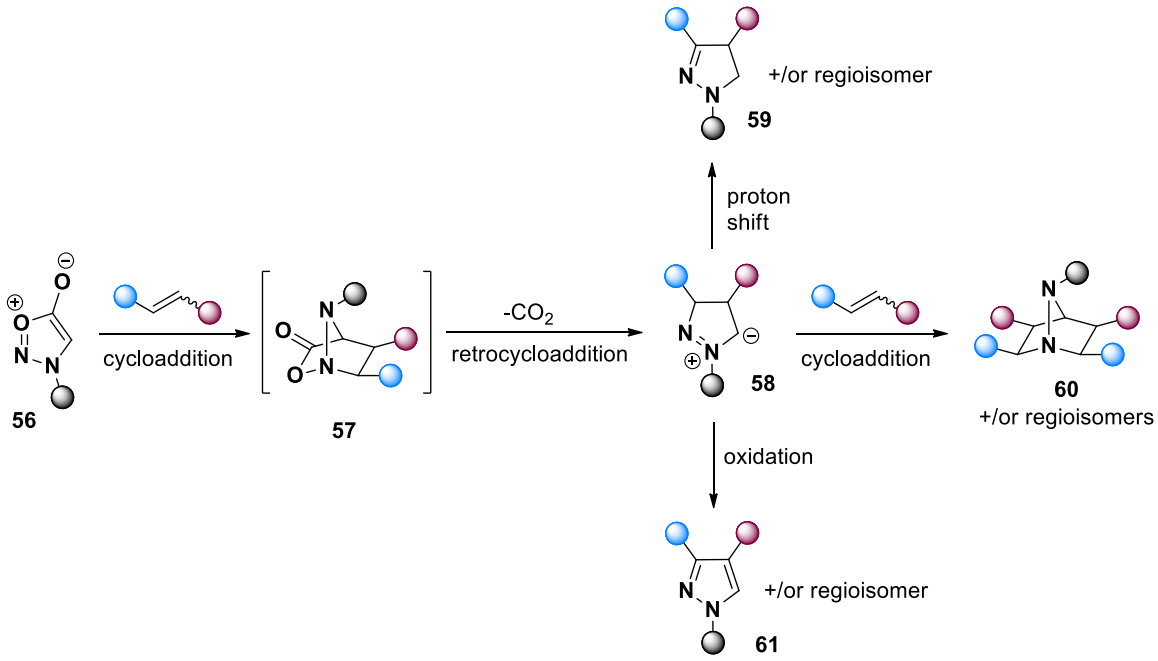

Scheme 1.20 – general sydnone-alkene cycloaddition

In addition to these general processes, substrate specific rearrangements can lead to even further possibilities. For example, Sasaki has described the reaction of *N*-phenylsydnone with 7-azanorbornene **62** in refluxing toluene to produce polycyclic adducts **63a** and **63b**.[87] The reaction begins with the usual cycloaddition-retrocycloaddition to form dipole **64**. However, instead of undergoing one of the aforementioned transformations, the dipolar intermediate eliminates a molecule of *N*-phenylpyrazole to form isoindole **65** which participates in a [4+2] cycloaddition with the azanorbornene **62** to produce **63a** and **63b**.

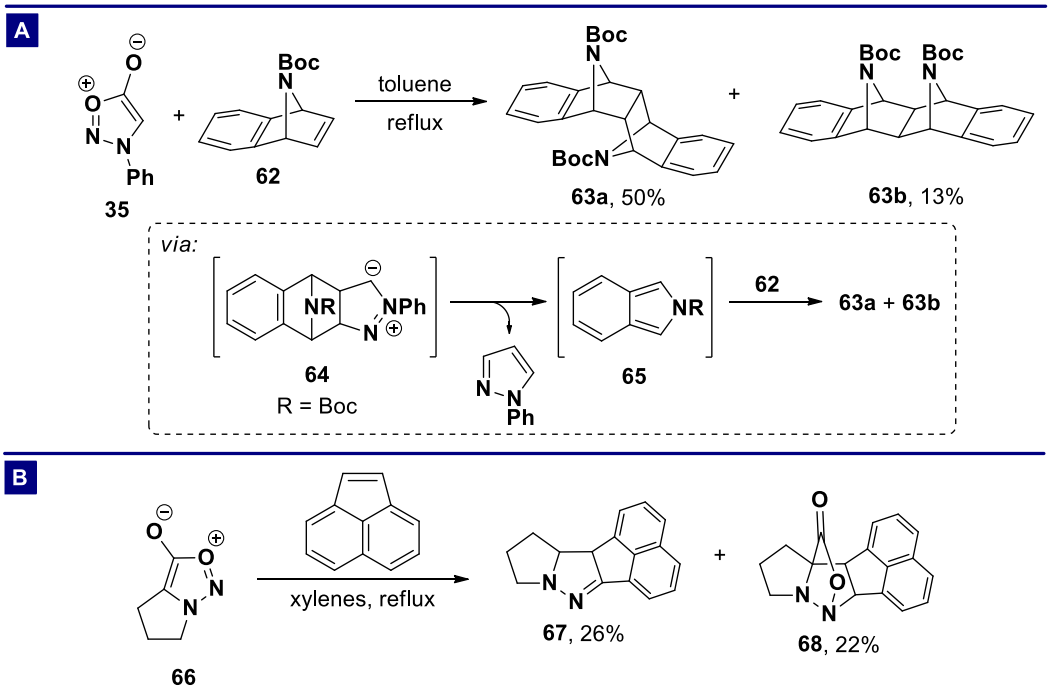

Scheme 1.21 – a) formation of polycycles from sydnone-alkene cycloaddition; b) unexpected formation of CO_2 containing adduct **68**

Another surprising result can be found in the reaction of proline derived sydnone **66** with acenaphthylene (Scheme 1.21B).[88] Along with the expected product **67**, adduct **68** was also formed in 22% yield. In this instance, extrusion of carbon dioxide (usually a barrierless process) has failed to proceed to completion. Finally, during Huisgen's preliminary investigations into sydnone-alkene cycloadditions a surprising elimination reaction was observed.[82] The reaction of *N*-phenylsydnone with α-methylstyrene was found to produce 1,3-diphenylpyrazole through the elimination of methane, possibly proceeding via pyrazoline **69**. The potential application of this unexpected hydrocarbon elimination was then examined further by Larsen using bicyclic sydnone **70**.[89] The reaction of a number of α,β-unsaturated ketones proceeded in high yield and, while the alkyl substituted examples gave mixtures of elimination products, aryl substituted enones produced only products arising from the elimination of hydrogen. Overall, the above examples serve to highlight the somewhat unpredictable nature of sydnone-alkene cycloadditions.

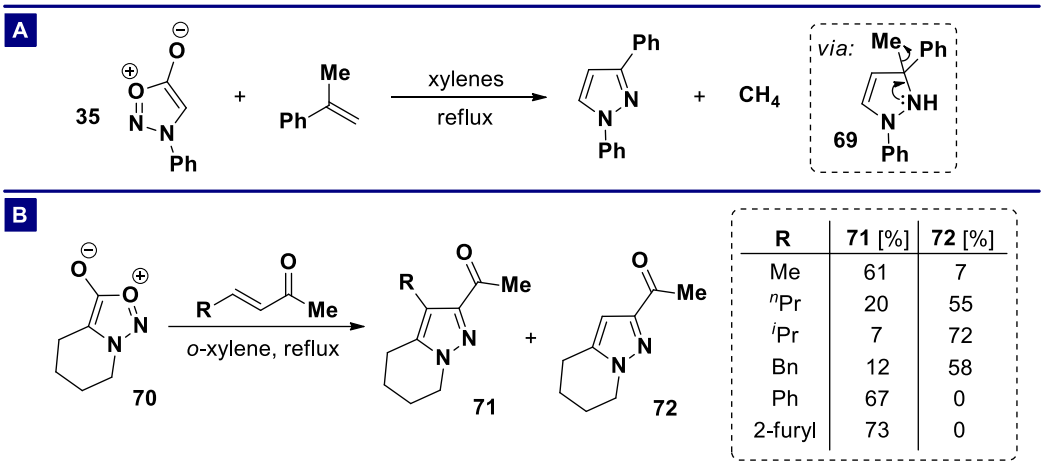

Scheme 1.22 – a) methane elimination observed by Huisgen; b) hydrocarbon eliminations in the cycloaddition reactions of enones with sydnones

1.3 Conclusions

Since their discovery, a large amount of research into the chemistry of sydnones has uncovered a number of interesting and unique chemical and physical properties. The development of a variety of methods to functionalise sydnones at the *C*4-position have allowed the creation of a vast array of sydnone containing compounds with relative ease. Furthermore, the cycloaddition reactions of sydnones and alkynes is well studied and, when combined with the methods to achieve *C*4-functionalisation, allows for the rapid construction of diverse pyrazole libraries. However, in spite of this progress, the vast majority of sydnone cycloaddition reactions require high temperatures to proceed efficiently and afford regioisomeric mixtures of pyrazole products. Therefore, further research focusing on enhancing both the reactivity and regioselectivity of sydnone cycloaddition reactions remains highly desirable.

2 Thermal Cycloaddition Reactions

2.1 Aims

As described, the platform of sydnone-alkyne cycloadditions offers access to a highly diverse set of pyrazole containing molecules. However, with the exception of copper-promoted systems and directed cycloadditions, these reactions often give rise to inseparable mixtures of pyrazole regioisomers. Those reactions that are highly selective often rely on steric interactions to achieve such an outcome, limiting the application of less hindered functional groups. Literature precedence from other classes of dipolar cycloaddition indicates that alkenes substituted with a heteroatom can act as efficient alkyne equivalents (Scheme 2.1A).

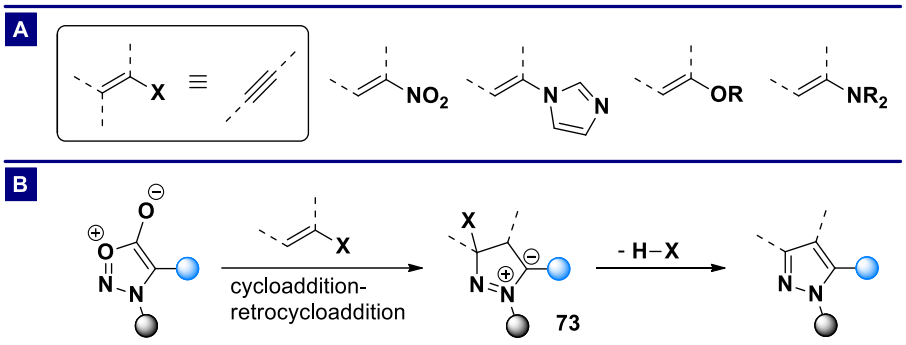

Scheme 2.1 – a) assortment of "alkyne equivalent" alkenes; b) leaving group elimination as a means of controlling the fate of 1,3-dipolar intermediate **73**

Moreover, the electronically polarising nature of these substituents confers a degree of asymmetry to the π/π* orbitals, often leading to predictable and high levels of regiocontrol. Additionally, this may result in increased overlap between the frontier molecular orbitals involved in the cycloaddition and lead to reduced activation barriers. In the context of sydnone cycloadditions, these leaving groups may also allow the fate of the dipolar intermediate to be controlled because an intramolecular elimination event should outcompete further cycloaddition reactions, hopefully resulting in exclusive formation of the corresponding pyrazoles (Scheme 2.1B). Indeed, this strategy has been investigated by Gribble in the cycloaddition of münchnones (another class of mesoionic heterocycles) and nitroalkenes.[90] Due to the structural diversity associated with compounds that fit the above description, a number of scaffolds may become accessible using this reaction manifold (Scheme 2.2).

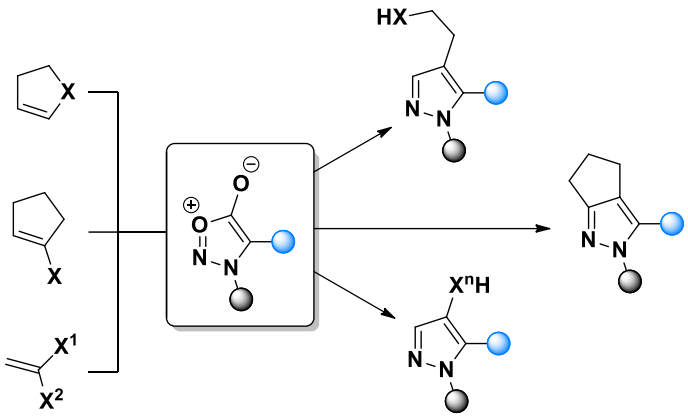

Scheme 2.2 – potential scaffolds accessible using sydnone-alkene cycloadditions

Thus, the aims at the outset of the project were:

1) To investigate the scope (both in terms of structure and substitution) of alkene type dipolarophiles in sydnone cycloadditions reactions.

2) Examine the possibility of using this chemistry to overcome the issues associated with regiocontrol in sydnone cycloaddition reactions.

3) Determine whether the inherent polarisation of the dipolarophile offers any advantage in terms of reaction rate.

2.2 Cyclic Enamide Dipolarophiles I

To begin investigating the above hypotheses we first required reasonable quantities of starting materials. *N*-Phenylsydnone was selected as the dipolar substrate for these investigations due to its availability in multi-gram quantities and remarkable stability under ambient conditions. Thus, according to the procedure of Turnbull, treatment of *N*-phenylglycine with IAN in 1,2-dimethoxyethane (DME) afforded nitrosamine **75**.[91] Due to its highly carcinogenic nature, handling of this intermediate was kept to a minimum and therefore the solvent was removed under vacuum and the crude oil dissolved directly in dichloromethane (DCM) under a nitrogen (N_2) atmosphere and treated with TFAA. A standard aqueous work-up (dilution with sat. $NaHCO_3$ solution and extraction with DCM) followed by recrystallisation from hot ethanol (EtOH) then afforded *N*-phenylsydnone (**35**) as a tan solid in 72% yield.

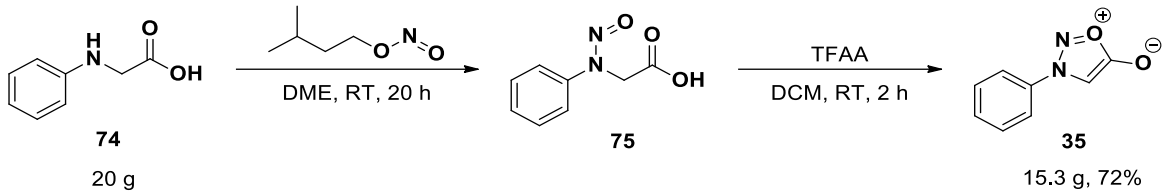

74
20 g

75

35
15.3 g, 72%

Scheme 2.3 – synthesis of *N*-phenylsydnone from *N*-phenylglycine; DME = 1,2-dimethoxyethane; RT = room temperature

In order to rapidly investigate the key cycloaddition reaction, we then selected commercially available enamide **76** (n = 1) as the starting dipolarophile. A test reaction in 1,2-dichlorobenzene (*o*-DCB) at 150 °C overnight showed the formation of 1,4-disubstituted pyrazole **78a** which could be isolated in 6% yield following column chromatography. Generally, the regiochemical assignment of the disubstituted pyrazoles formed during sydnone cycloadditions can be made purely on the basis of ^{1}H NMR spectroscopy because of the drastically different signals produced by the pyrazole ring protons in each case. Firstly, the *H*4 and *H*5 protons in 1,3-disubstituted pyrazoles appear as a pair of doublets (with a coupling constant in the order of 1.5-3.0 Hz) at 6.5-7.0 ppm and 7.5-8.0 ppm, respectively. Contrastingly, the *H*3 and *H*5 protons in 1,4-disubstituted pyrazoles appear as singlets, with both signals in the region of 7.5-8.0 ppm. In the case of **78a**, analysis of the ^{1}H NMR spectrum shows two singlets at 7.55 ppm and 7.74 ppm, consistent with the 1,4-regioisomer. Despite the low conversion and yield, this experiment provided two key results: 1) Sydnones successfully react with enamides to form pyrazoles. 2) Pyrazole **78a** was formed as a single regioisomer (the other regioisomer was not detectable by ^{1}H NMR spectroscopy of the crude material), indicating the potential of these reactions to achieve high levels of regiocontrol. Despite this initial success, our attempts to optimise the reaction by altering variables such as the solvent, temperature, time, concentration and enamide ring size failed to afford synthetically useful yields of the corresponding pyrazoles (Table 2.1).

Table 2.1 – optimisation of the reaction between *N*-phenylsydnone and enamides **76**/**77**[a]

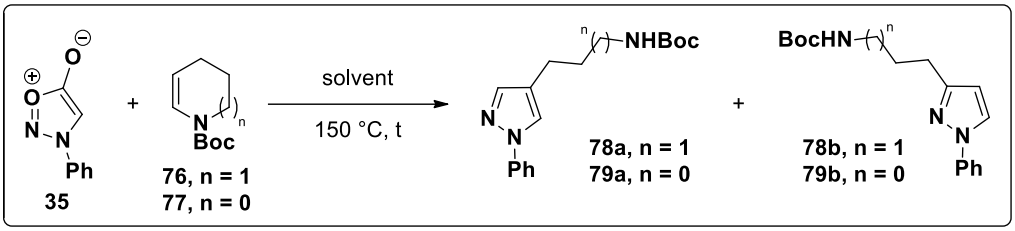

Entry	S	Solvent	Concentration [M]	t [h]	P	Yield [%][b]	a:b[c]
1	**76**	*o*-DCB	0.5	24	**78**	6	>98:2
2	**76**	xylenes	0.5	24	**78**	8	>98:2
3	**76**	toluene	0.5	24	**78**	8	>98:2
4	**76**	*o*-DCB	0.5	48	**78**	7	>98:2
5	**76**	*o*-DCB	1.0	24	**78**	5	>98:2
6	**77**	*o*-DCB	0.5	24	**79**	5	>98:2

[a] Reaction conditions: *N*-phenylsydnone (0.5 mmol), enamide (1.0 mmol), solvent (0.5-1.0 mL) at 150 °C for the specified time; [b] yield of isolated compound; [c] ratio determined by ^{1}H NMR analysis; *o*-DCB = 1,2-dichlorobenzene; S = substrate; P = product

We suspected that the lack of improvement in product yield could be a consequence of thermal deprotection of the Boc-group, which could limit the product yield in at least two ways. Firstly, deprotection of the starting material would provide enamine **80** which could tautomerise to imine **81** and undergo side reactions, reducing the quantity of substrate available for the desired cycloaddition (Scheme 2.4A). Alternatively, deprotection of the initial cycloadduct **78a** would produce the free amine **82** which might prove difficult to isolate by silica column chromatography due to its high polarity. An LC-MS analysis of the crude reaction mixture identified amine **82**, confirming the viability of Boc-deprotection under the reaction conditions. Regardless of the explanation for the low product yields under these conditions, this observation indicated the requirement for a more thermally stable *N*-protecting group; benzyloxycarbonyl (Cbz) for example.

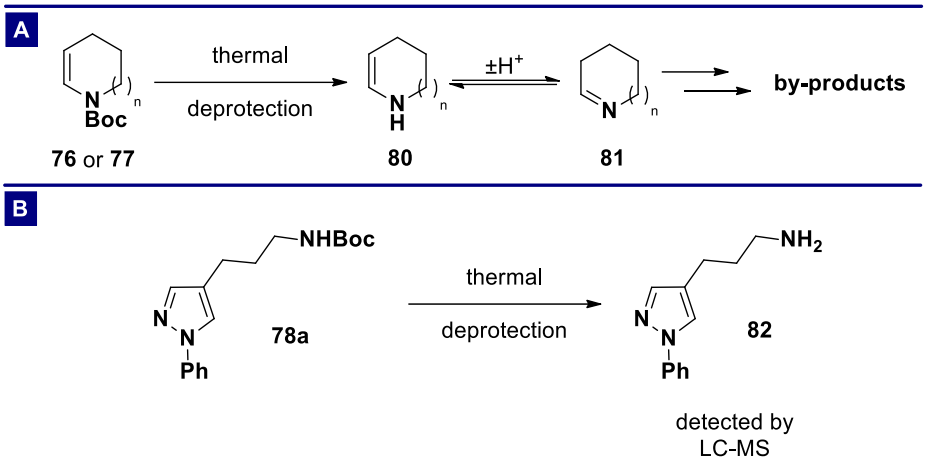

Scheme 2.4 – a) thermal deprotection of Boc protected enamide substrates; b) thermal deprotection of Boc protected pyrazoles

Although the Cbz protected enamide **84** is commercially available, it is rather expensive (>£130 per gram at the time) and as such a 3 step synthesis starting from δ-valerolactam was employed.[92] Initial protection of the amide nitrogen with benzyl chloroformate (Cbz-Cl) following deprotonation with ^{n}BuLi gave imide **83** which was used in crude form in the next steps. Selective reduction of the endocyclic carbonyl group with sodium borohydride ($NaBH_4$) and subsequent dehydration using sulphuric acid (H_2SO_4) produced enamide **84** in 41% yield over the 3 steps.

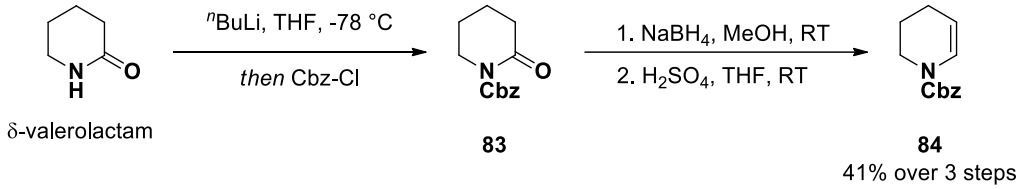

Scheme 2.5 – synthesis of Cbz protected enamide **84**

The use of Cbz protected enamide **84** in sydnone cycloaddition reactions was then investigated (Table 2.2). However, these attempts were unsuccessful and failed to afford any of the desired product despite prolonged heating at high temperature (180 °C for 48 h). The reduced reactivity of **84** relative to **76** is not easily understood due to the similarity of the two protecting groups, but the low reactivity of these enamide substrates in general, compared to alkynes, is also interesting. Previous work on sydnone-alkyne cycloadditions has suggested that sydnone cycloadditions may operate under inverse electron demand, due to the increased rate of reaction when using electron deficient *N*-arylsydnones in comparison to those with neutral or electron rich groups.[70] Therefore, the presence of a carbamate protecting group may prevent efficient donation of the nitrogen lone pair into the alkene, leading to a decreased HOMO energy and less-efficient orbital overlap. However, this is contradicted by the observation that sydnones react efficiently with both propiolate and acetylene dicarboxylate

Table 2.2 – attempted optimisation of the reaction between *N*-phenylsydnone and enamide **84**[a]

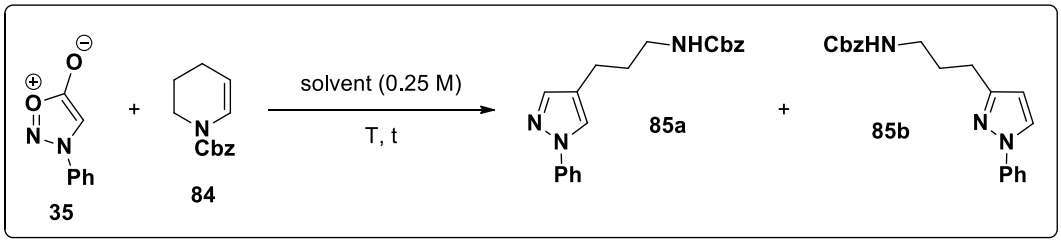

Entry	Solvent	eq. 84	T [°C]	t [h]	Yield [%][b]
1	*o*-DCB	2	150	24	0
2	*o*-DCB	2	150	48	0
3	xylenes	2	150	24	0
4	*o*-DCB	5	150	24	0
5	*o*-DCB	2	180	24	0

[a] Reaction conditions: *N*-phenylsydnone (0.5 mmol), **84** (1.0-2.5 mmol), solvent (2.0 mL) at the specified temperature and time; [b] yield of isolated compound; *o*-DCB = 1,2-dichlorobenzene

dipolarophiles.[25] Thus, it is possible that the enamide dipolarophiles are neither electron rich nor electron poor enough to efficiently react with sydnones. Further investigation of this hypothesis would be possible using an enamine bearing an electron donating (or less withdrawing) *N*-substituent (Figure 2.1). Given the limited number of reported methods to synthesise compounds of this type, we decided to pursue other avenues of investigation.

Figure 2.1 – possible enamine dipolarophiles

2.3 Cyclic Enol Ether Dipolarophiles I

Following the limited success employing cyclic enamides in sydnone cycloaddition reactions, attempts were made to incorporate 3,4-dihydro-2*H*-pyran (**86**) in a reaction with *N*-phenylsydnone. It was envisaged that the lack of a heteroatom protecting group should simplify the analysis because deprotection steps are no longer possible. Initial attempts to promote the reaction at 150 °C were found to be unproductive, with the sydnone substrate returned intact. However, increasing the temperature to 180 °C resulted in conversion of the sydnone, evidenced by the formation of a diagnostic pyrazole proton at δ7.74 ppm in the ^{1}H NMR spectrum. More interestingly, analysis of the crude ^{1}H NMR spectrum also identified another signal at δ4.58 ppm which integrated 1:1 relative to the pyrazole proton. Following column chromatography this reaction was found to produce

Table 2.3 - optimisation of the reaction between *N*-phenylsydnone and enol ether **86**[a]

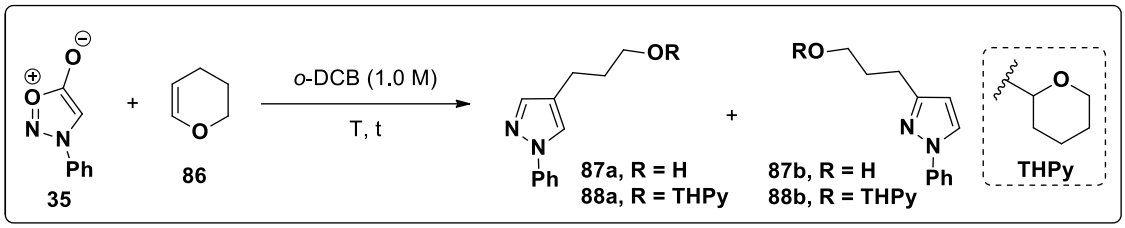

Entry	T [°C]	t [h]	P	Yield [%][b]	a:b[c]
1	150	24	-	0	-
2	150	48	-	0	-
3	180	24	**88**	26	>98:2
4	180	48	**88**	39	>98:2
5	200	24	**88**	20	>98:2

[a] Reaction conditions: *N*-phenylsydnone (0.5 mmol), **86** (2.0 mmol) in *o*-DCB (0.5 mL) at specified time and temperature; [b] yield of isolated compound; [c] ratio determined by ^{1}H NMR analysis; *o*-DCB = 1,2-dichlorobenzene; THPy = tetrahydropyranyl

tetrahydropyranyl (THPy) ether containing pyrazole **88** rather than the desired alcohol containing pyrazole **87**, the formation of which appears to be the result of **87** reacting with another equivalent of **86**. Once again, the regiochemical assignment is made on the basis of two singlet peaks at 7.56 ppm and 7.74 ppm, consistent with a 1,4-disubstituted pyrazole isomer. Attempts to increase the yield by lengthening the reaction and increasing the temperature ultimately resulted in a modest 39% yield of **88a**, but as a single regioisomer (Table 2.3).

In order to examine the electronic effect of the sydnone *N*-substituent a small number of *N*-arylsydnones were then employed in a cycloaddition reaction with **86** (Table 2.4). The desired THPy ether containing pyrazole products were obtained in 24-48% yield, with the reaction proving more efficient for electron withdrawing/neutral aryl substituents than the one electron rich group tested. Furthermore, the reaction was found to be highly selective in all cases, with only the 1,4-regioisomer isolated.

Table 2.4 – scope of the 1,4-regioselective cycloaddition between *N*-arylsydnones and **86**[a]

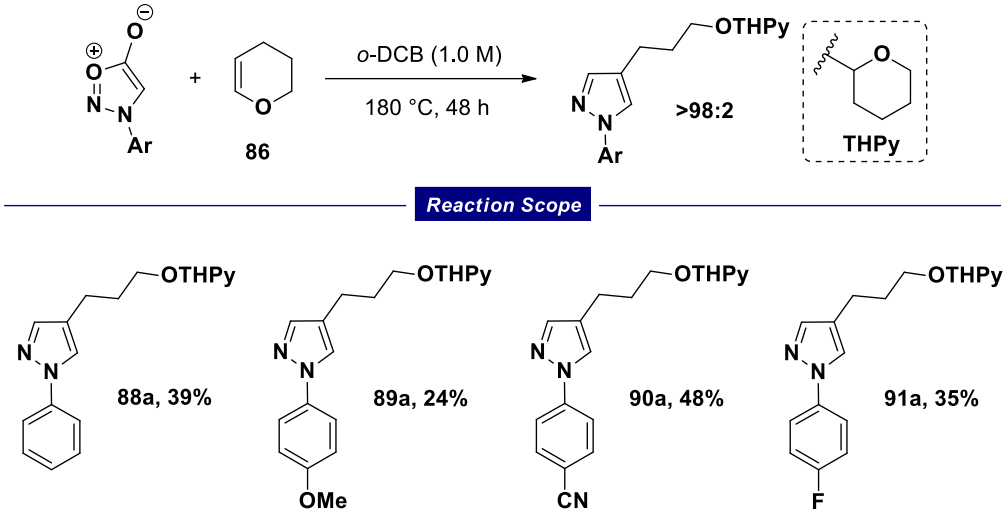

[a] Reaction conditions: *N*-arylsydnone (0.5 mmol), **86** (2.0 mmol), *o*-DCB (0.5 mL), 180 °C, 48 h; *o*-DCB = 1,2-dichlorobenzene; THPy = tetrahydropyranyl

With enol ethers established as more reactive substrates under these conditions than the cyclic enamides, we next turned our investigations to probing the effect of changing ring size (Table 2.5). In stark contrast to **86**, 2,3-dihydrofuran **92** reacted smoothly with *N*-phenylsydnone at 150 °C (c.f. 180 °C for **86**), leading to 100% conversion and a 54% yield of **94a**. Pleasingly, this reaction was found to furnish the analogous tetrahydrofuranyl (THFu) ethers as the major product, although careful examination of the crude ^{1}H NMR spectrum showed the free alcohol containing product **93a** as a minor component. A decreased temperature of 100 °C was also found to promote this reaction, leading to 40% conversion of the starting material and a mixture of products (Table 2.5, entry 2). Increasing the temperature beyond 150 °C provided no further benefit but decreasing the concentration of the reaction mixture gave a much cleaner crude ^{1}H NMR spectrum and a combined product yield of 98% following column chromatography (Table 2.5, entry 5).

Table 2.5 – optimisation of the reaction between *N*-phenylsydnone and enol ether **92**.[a]

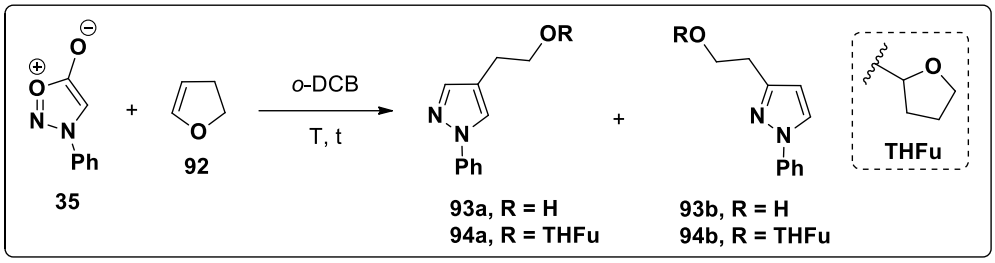

Entry	eq 92	Concentration [M]	T [°C]	t [h]	Yield 94 [%][b]	a:b[c]
1	4	1.0	150	24	54	>98:2
2	4	1.0	100	24	8[d]	>98:2
3	4	1.0	180	24	59	>98:2
4	6	1.0	150	24	47	>98:2
5	4	0.25	150	24	65[e]	>98:2
6	4	0.25	150	48	67[f]	>98:2
7[g]	4	0.25	150	1	50	>98:2
8[g]	4	0.25	150	2	55	>98:2
9[g]	4	0.25	180	2	64	>98:2

[a] Reaction conditions: *N*-phenylsydnone (0.5 mmol), **92** (n mmol), *o*-DCB (0.5-2.0 mL) at specified temperature and time; [b] yield of isolated compound. [c] ratio determined by ^{1}H NMR analysis; [d] 34% of **93a** isolated; [e] 33% of **93a** isolated; [f] 30% of **93a** isolated; [g] reaction performed using microwave irradiation; *o*-DCB = 1,2-dichlorobenzene; THFu = tetrahydrofuranyl

Interestingly, neither increasing the length of the reaction (compare entries 5 and 6) or the equivalents of 2,3-dihydrofuran (compare entries 1 and 4) resulted in further conversion to **94**. Assuming **94** arises from the reaction of **93** and 2,3-dihydrofuran, there may be a few possible explanations for this observation. Either the reaction has reached a thermal equilibrium after 24 hours and therefore the product distribution will be unaffected by further heating, or the concentration of enol ether **92** has decreased sufficiently after 24 hours that further reaction to the THF ether product is slow/no longer possible. It should be noted that the boiling point of 2,3-dihydrofuran is ~55 °C and significant vapour pressure would be expected under the reaction conditions. In line with this expectation, a large amount of liquid was observed to condense inside the reaction vessel when running these reactions (albeit far below the solvent boiling point), indicating that the concentration of **92** in solution should be lower than expected. Given that a subsequent control experiment heating an isolated sample of **93a** in *o*-DCB in the presence of **92** verified the formation of acetal products from the free alcohol under these conditions (Scheme 2.6A), it is probable that the lack of increased conversion to **94** is the result of one of the above explanations.

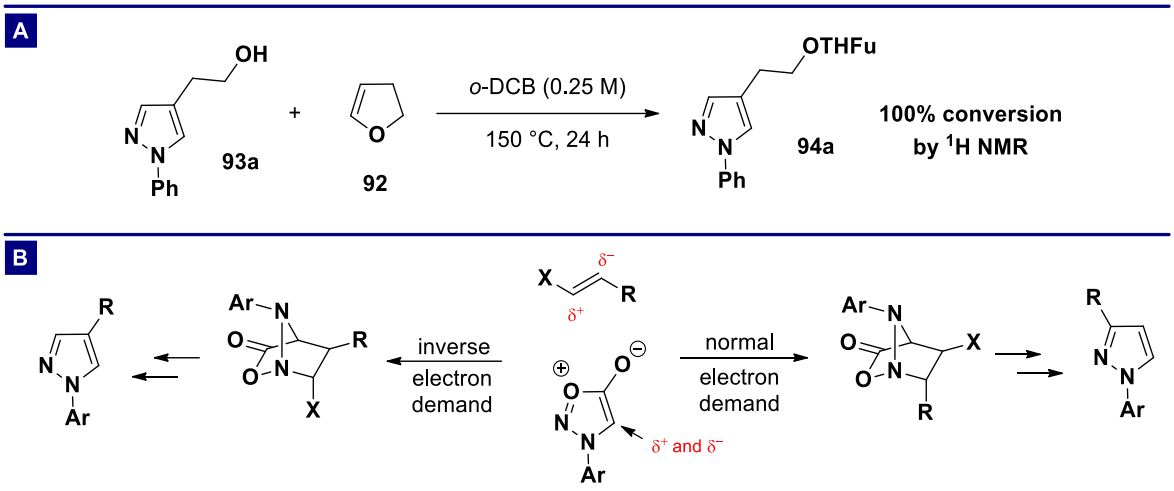

Scheme 2.6 – a) conversion of alcohol containing pyrazoles into the corresponding acetals; Reaction conditions: **93a** (0.25 mmol), **92** (1.0 mmol), *o*-DCB (1.0 mL), 150 °C, 24h; b) mechanistic pathways for normal and inverse electron demand cycloadditions between sydnones and alkenes; *o*-DCB = 1,2-dichlorobenzene; THFu = tetrahydrofuranyl

Due to the prolonged reaction times, the feasibility of using microwave irradiation to drive the reaction between **92** and *N*-phenylsydnone was also investigated (Table 2.5). A temperature of 150 °C and reaction length of 2 hours was found to be insufficient for complete conversion of the starting material, while increasing the temperature to 180 °C gave complete conversion and a 64% yield of **94a**; comparable to the optimised conditions under conventional heating.

The observed regioselectivity and apparently high levels of regiocontrol observed in the sydnone-alkene cycloadditions investigated so far is interesting. In particular, the high levels of selectivity are in stark contrast to many sydnone cycloaddition reactions.[25,93] Early work by Huisgen and Gotthardt found that the rate of sydnone-alkyne cycloadditions is only slightly decreased by increasing solvent polarity, indicating that sydnone cycloadditions likely proceed via a concerted mechanism.[94] Moreover, the reaction of 4-methyl-3-phenylsydnone with different acetylene derivatives showed that the rate of reaction increased dramatically when electron deficient acetylenes were used, pointing to a normal electron demand (i.e. the reaction is controlled by the sydnone HOMO and dipolarophile LUMO). On the other hand, calculations by Houk and Varnek propose that sydnones possess a low energy LUMO and thus their cycloadditions reactions should operate under inverse electron demand.[95,96] This is consistent with the observation of a positive Hammett value (p ~ +0.8) in the reaction of a series of 4-arylsydnones, indicating an increase in reaction rate for electron deficient sydnones. Curiously, molecular orbital calculations on sydnones have indicated that a larger coefficient of both the HOMO and LUMO orbitals is found on the *C*4 atom than on the *N*2 atom.[97] Therefore, any observed selectivity would be derived from the dipolarophile only. In the case of these sydnone-alkene cycloadditions using enamides/enol ethers, the predicted selectivity for a normal

electron demand cycloaddition gives rise to the opposite regioisomer to that observed (Scheme 2.6B). Conversely, the predicted selectivity for an inverse electron demand cycloaddition would result in the same regioisomer to that which is isolated in the reactions investigated so far. Ultimately, it would appear that sydnone cycloadditions can operate via either the sydnone HOMO or LUMO orbitals, and the contributions of each in a given reaction depend on both the sydnone substitution pattern and the electronic characteristics of the dipolarophile. In the reaction of *N*-arylsydnones and enamides/enol ethers, the observed selectivity is best explained by an inverse electron demand cycloaddition reaction, but further experimental work would be required to verify this.

The scope of this 1,4-regioselective cycloaddition process was then examined using a number of different sydnone substrates (Table 2.6). Sydnones containing strongly electron withdrawing *N*-substituents produced good yields of the 1,4-disubstituted pyrazoles (**97a**-**99a**), as did sydnones containing F, Cl, or Br substituents (**100a**-**102a**). Sydnones with strongly electron donating *N*-substituents required higher concentrations to react efficiently, but nevertheless gave good yields of the corresponding pyrazoles **95a** and **96a**. Unfortunately, the reaction was not compatible with *N*-alkyl sydnones: those with methyl (**103**), isopropyl (**104**) and benzyl (**105**) substituents were unreactive while a carboxymethyl substituted sydnone (**106**) decomposed under the reaction conditions. The origin of this reactivity difference is not entirely clear, but could be due decreased transition state stabilisation in the absence of an adjacent π-system. Additionally, the reaction of 4-substituted sydnones bearing either acyl or aryl groups all failed to produce any detectable quantities of pyrazole products. In this instance the lack of reactivity is probably caused by detrimental steric interactions between the enol ether and the *C*4-substituent. Both of these observations are consistent with the reduced reactivity of *N*-alkyl and *C*4-susbtituted sydnones when reacting with alkynes.

Table 2.6 – scope of the 1,4-regioselective cycloaddition between *N*-arylsydnones and **92**[a]

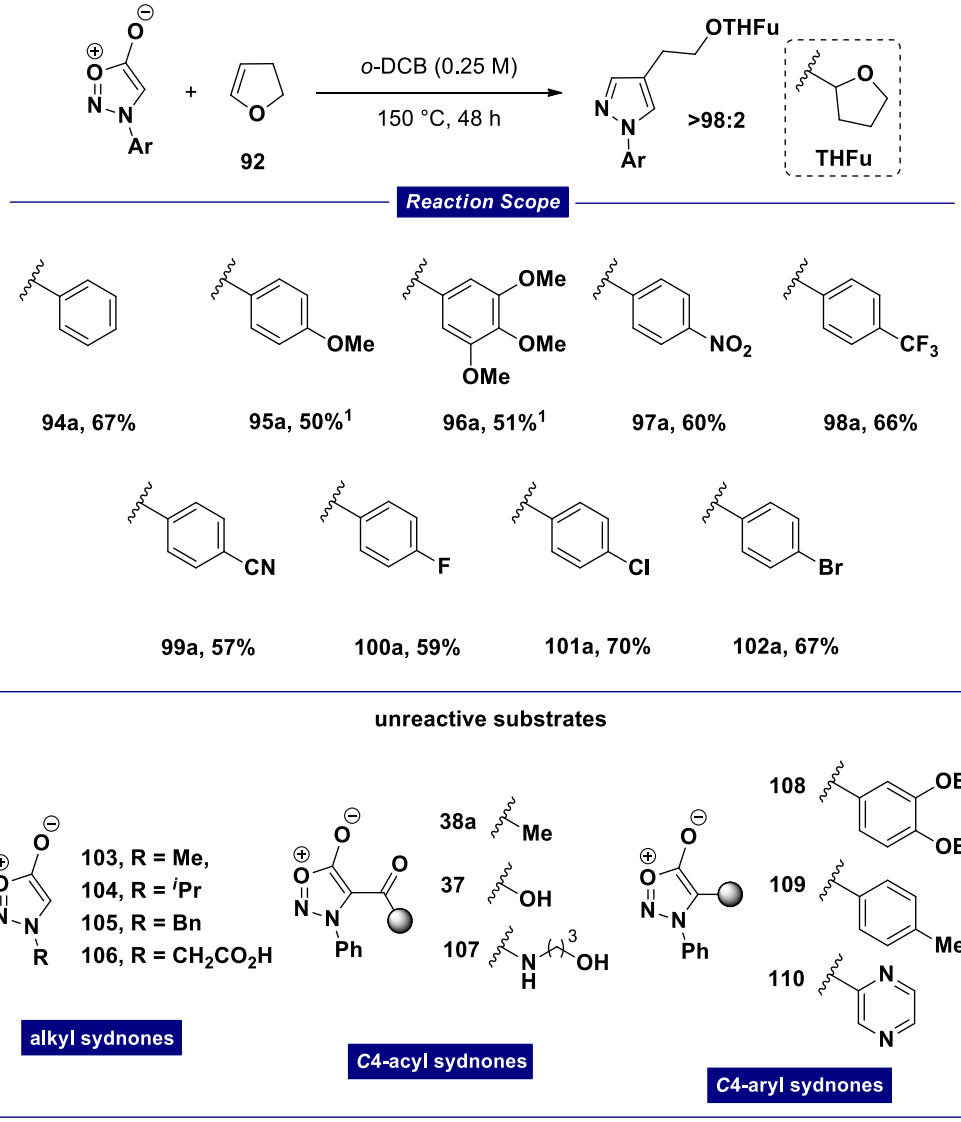

[a] Reaction conditions: *N*-arylsydnone (0.5 mmol), **92** (2.0 mmol), *o*-DCB (2.0 mL), 150 °C, 48 h; [1] reaction performed at 1.0 M; *o*-DCB = 1,2-dichlorobenzene; THFu = tetrahydrofuranyl

The apparent reactivity difference between **86** and **92** is surprising, given their structural similarity, and we hypothesised that it might arise from an electronic difference between the *C-C* double bond in each of the substrates. To investigate this, ^{13}C NMR spectra of both **86** and **92** were recorded; if one double bond is significantly more electron rich or poor than the other, then the alkene signals would be shifted either up or down field in the spectrum, respectively. In the event, as can be seen in Figure 2.2, the spectra of both substrates are very similar, indicating no major electronic difference between the two double bonds.

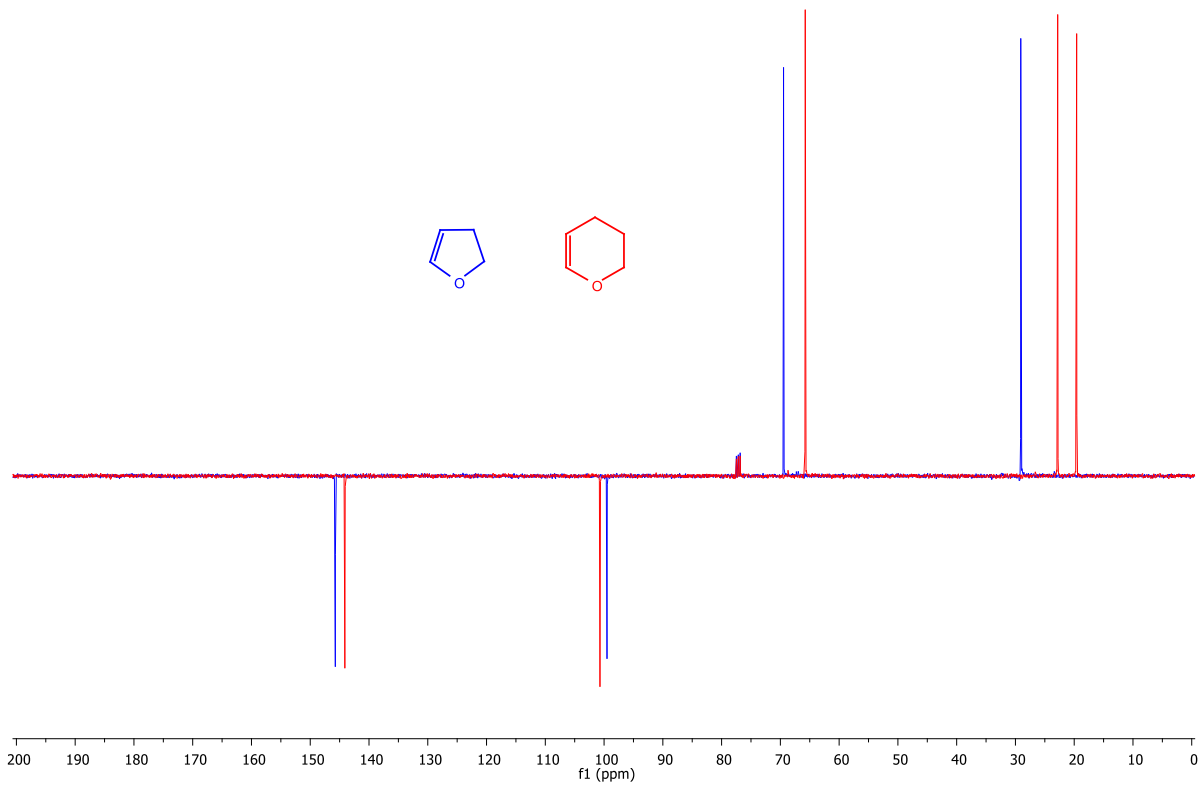

Figure 2.2 – ^{13}C NMR spectra of enol ethers **86** (red) and **92** (blue)

Next, the role of ring strain in the reaction was investigated. Given that five-membered ring systems contain a moderate degree of ring strain (~ 6 kCal.Mol^{-1} for cyclopentane),[98] while six-membered ring systems are relatively strain free, it is possible to imagine that the release of ring strain in the elimination step might help to drive the reaction of **92** towards the pyrazole product. An initial competition reaction between **86** and **92** was performed to gauge their relative reactivity, with the two alcohol products being obtained in a 94:6 ratio (Scheme 2.7A, path a). An unfortunate limitation of this experiment is the need to hydrolyse the mixture of THFu/THPy ethers obtained after the first step as one must assume that all intermediates are hydrolysed to an equal extent. Nevertheless, this experiment provides further evidence of a significant reactivity difference between **86** and **92**. A cycloaddition reaction between *N*-phenylsydnone and ethyl vinyl ether **111a** (essentially **92** but without the ring strain) was then performed under the optimised conditions and, to our surprise, this reaction delivered *N*-phenylpyrazole (**112**) in an outstanding 94% yield (Scheme 2.7A, path b). Moreover, a competition reaction between **92** and **111a** afforded the corresponding products in fairly similar yields. In combination, these experiments suggest that ring strain is not an important factor in the cycloaddition reaction between sydnones and enol ethers. Finally, a series of experiments were conducted to investigate the effect of vinyl ethers with varying steric bulk (Scheme 2.7C). In comparison to ethyl vinyl ether (1^0 substituted), cyclohexyl vinyl ether **111b** (2^0 substitution) and

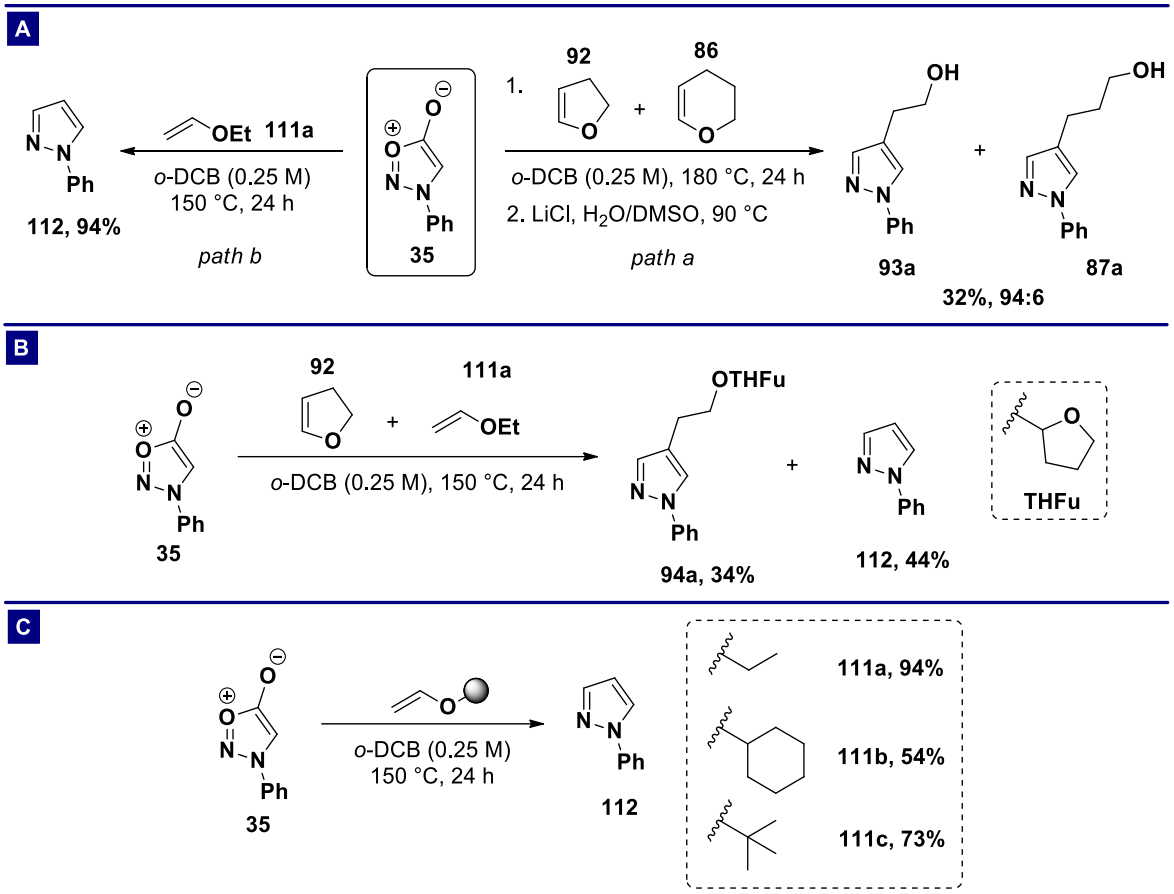

Scheme 2.7 – a) competition reaction between enol ethers **86** and **92** (path a) and cycloaddition reaction between *N*-phenylsydnone and ethyl vinyl ether (path b); b) competition reaction between **92** and ethyl vinyl ether; c) reaction of *N*-phenylsydnone with sterically variable vinyl ethers; *o*-DCB = 1,2-dichlorobenzene; DMSO = dimethylsulfoxide; THFu = tetrahydrofuranyl

tert-butyl vinyl ether **111c** (3^0 substitution) both produced *N*-phenylpyrazole in diminished yields. However, the origin of this reduction in yield is currently unclear because in both cases the reaction reached 100% conversion and the crude ^{1}H NMR spectra showed no other phenyl containing species. Overall, it is possible that the steric hindrance in this position can have an impact on the efficiency of sydnone-enol ether cycloaddition reactions.

2.4 Acyclic Dipolarophiles

The discovery that acyclic enol ethers are also reactive in sydnone-alkene cycloadditions prompted use to carry out a more thorough examination of the scope of this class of dipolarophile. First, the reaction of commercially available enol ether **113** with a number of sydnones was evaluated. *N*-Phenylsydnone and *N*-(4-nitrophenyl)sydnone reacted within 24 hours to afford high yields of 4-methyl substituted pyrazoles **114a** and **115a**, respectively. As noted previously, the reaction with *N*-(4-methoxyphenyl)sydnone was much slower, requiring 2 days to reach a high level of conversion (**116a**). Enol

Table 2.7 – scope of the 1,4-regioselective cycloaddition between *N*-arylsydnones and **113**[a]

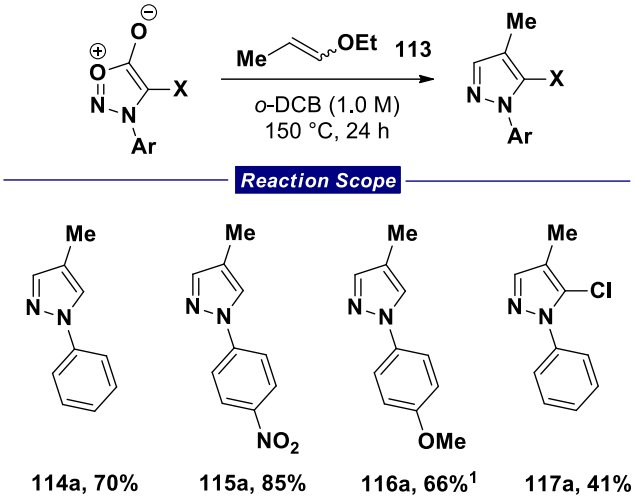

[a] Reaction conditions: *N*-arylsydnone (0.5 mmol), **113** (2.0 mmol), *o*-DCB (2.0 mL), 150 °C, 24 h. [1] 48 h; *o*-DCB = 1,2-dichlorobenzene

ether **113** then proved to be a particularly reactive substrate, achieving a successful reaction with 4-chloro-3-phenylsydnone to give **117a** in moderate yield.

Although the ability to selectively introduce a methyl group into the pyrazole scaffold is useful, an expansion to further functional groups was required. As such, a number of other substrates were synthesised to further this investigation. The Wittig olefination of either benzaldehyde or *p*-anisaldehyde (chosen as a particularly electron rich example) gave the corresponding methyl enol ethers **118** and **119** in high yield as a mixture of geometrical isomers (Scheme 2.8A).[99] Alkyl substituted

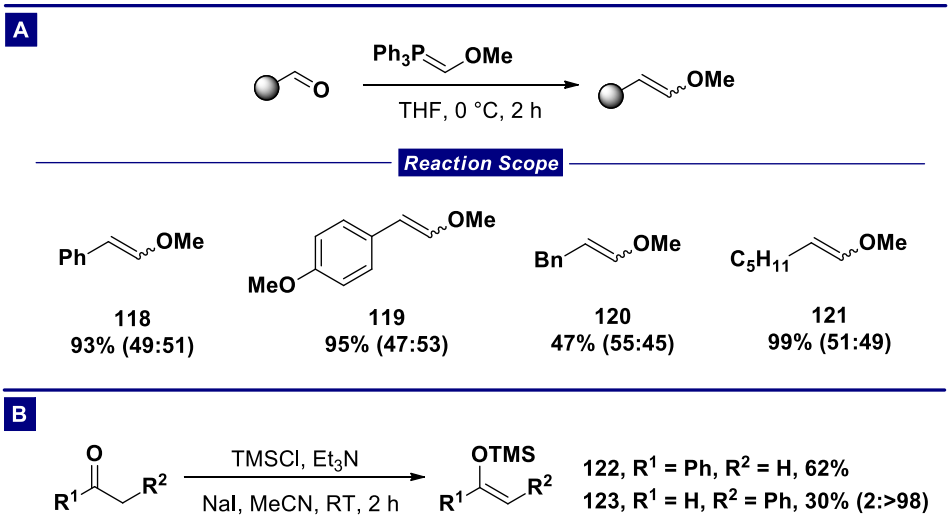

Scheme 2.8 – a) synthesis of enol ethers via the Wittig olefination of various aldehydes; b) synthesis of silyl enol ethers from carbonyl compounds. Values in parentheses indicate *E*:*Z* ratios of the isolated compounds as determined by ^{1}H NMR analysis; THF = tetrahydrofuran

enol ethers could also be synthesised by the reaction of phenylacetaldehyde (for **120**) or hexanal (for **121**) under the same conditions. Additionally, silyl enol ethers **122** and **123** could be isolated by trapping the enolates of acetophenone or phenylacetaldehyde with chlorotrimethylsilane.[100] Curiously, the silyl enol ether derived from phenylacetaldehyde (**123**) was isolated exclusively as the *Z*-isomer.

The scope of the cycloaddition reactions of these substrates was then investigated and, unfortunately, a lack of reactivity was observed in many cases including aryl substituted enol ethers **118**/**119** and silyl enol ethers **122**/**123**. However, alkyl substituted enol ethers **120** and **121** did participate in a cycloaddition reaction to give the 1,4-disubstituted pyrazoles **131** and **132** in moderate yield. As a final attempt to extend this reaction to more interesting and highly substituted products, silyl ketene acetal **124** was reacted with *N*-phenylsydnone (Table 2.8, entries 9 and 10). Despite heating up to 180 °C this reaction gave no trace of the desired product, instead returning the unreacted sydnone. Overall these results indicate that this approach may serve as a useful method for the synthesis of alkyl substituted pyrazoles in a regiocontrolled manner. Interestingly, the reaction remains highly regioselective in the presence of a sydnone *C*4-substituent, thus indicating that the observed selectivity may arise from an electronic preference. It remains unclear whether aryl substituted enol ethers are unreactive due to steric or electronic factors.

Although these results showed promise, a number of deficiencies remained. For example, the reaction is limited (with the exception of 1 example) to the synthesis of disubstituted pyrazole scaffolds and the enol ether substrates are prone to decomposition under a number of conditions. A brief investigation of other leaving groups was therefore performed to ascertain whether any reactivity enhancement could be achieved by the manipulation of this substituent. Maintaining a focus on oxygen substituted dipolarophiles, a reaction with vinyl acetate (**125**) demonstrated the enhanced reactivity of these dipolarophiles; even with an electron withdrawing group on oxygen this reaction affords *N*-phenylpyrazole in 75% yield (Table 2.8, entry 11). However, the use of a more strongly electron withdrawing tosyl group prevented the reaction of vinyl tosylate **126**.

Table 2.8 – cycloaddition reactions of *N*-phenylsydnone and enol ethers[a]

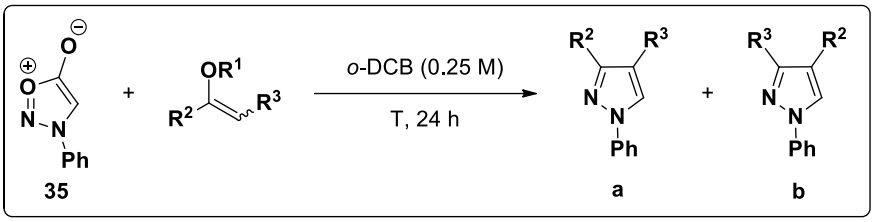

Entry	Substrate[b]	R^1	R^2	R^3	T [°C]	Product	Yield [%][c]	a:b[d]
1	**122**	TMS	Ph	H	150	**127**	0	-
2	**122**	TMS	Ph	H	180	**127**	0	-
3	**123 (2:>98)**	TMS	H	Ph	150	**128**	0	-
4	**118 (49:51)**	Me	H	Ph	150	**129**	0	-
5	**118 (49:51)**	Me	H	Ph	180	**129**	0	-
6	**119 (47:53)**	Me	H	PMP	150	**130**	0	-
7	**120 (55:45)**	Me	H	Bn	150	**131**	41	>98:2
8	**121 (51:49)**	Me	H	C_5H_{11}	150	**132**	30	>98:2
9	**124 (85:15)**	TMS	OMe	^{n}Bu	150	**133**	0	-
10	**124 (85:15)**	TMS	OMe	^{n}Bu	180	**133**	0	-
11	**125**	Ac	H	H	150	**112**	75	-
12	**126**	Ts	H	H	150	**112**	0	-

[a] Reaction conditions: *N*-phenylsydnone (0.5 mmol), dipolarophile (2.0 mmol), *o*-DCB (2.0 mL) at specified temperature for 24 h; [b] values in parentheses indicate the *E*:*Z* ratio of the substrate; [c] yield of isolated compound; [d] ratio determined by ^{1}H NMR analysis; *o*-DCB = 1,2-dichlorobenzene.

Finally, 2,3-dihydroisoxazole **134**, available in 3 steps from benzaldehyde, was investigated in the hope of introducing a useful amino functional group.[101] Despite numerous attempts, and despite the structural similarity between **134** and 2,3-dihydrofuran **92**, this substrate failed to participate in sydnone cycloaddition reactions. Moving away from oxygen based leaving groups, vinyl halides **136-*E*** and **136-*Z*** were synthesised from 1-octyne (Scheme 2.9B).[102,103] Although the double bond geometry should have no impact on the final product structure in these reactions, we were intrigued as to whether or not this structural feature would have any effect on reactivity. Unfortunately, neither the *E* or *Z* isomer reacted under any of the conditions investigated.

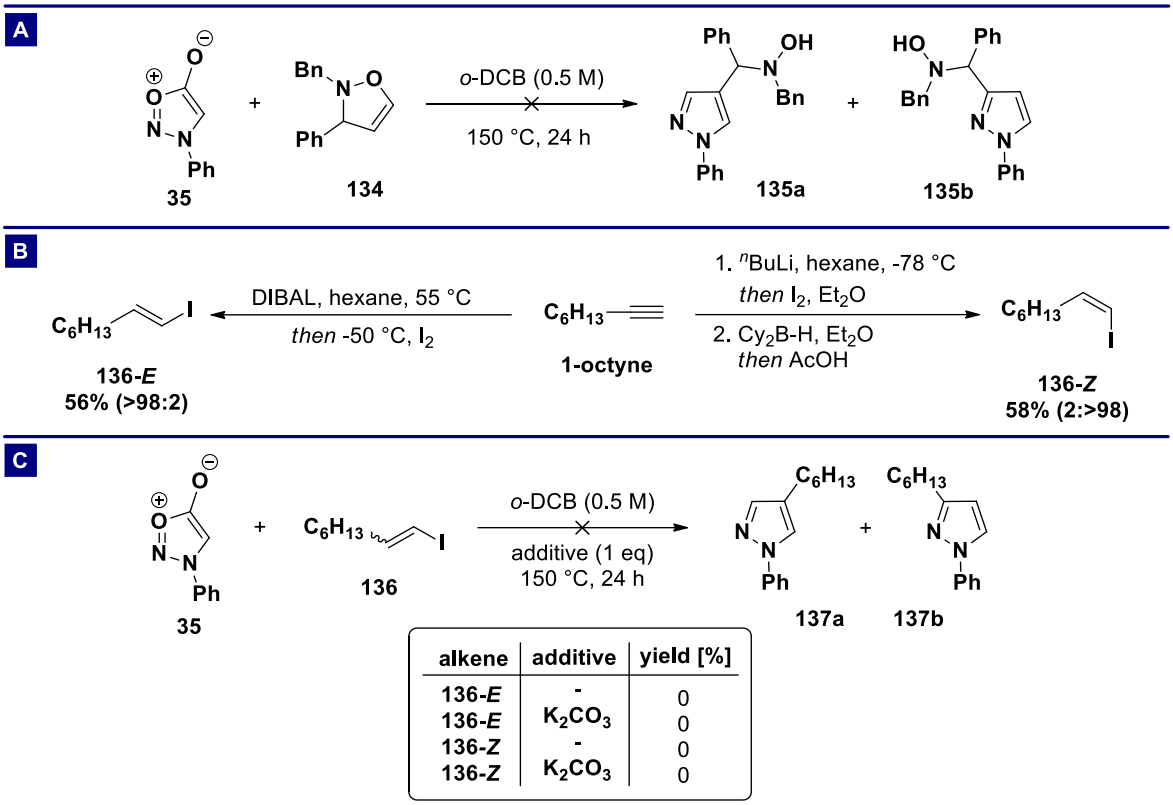

alkene	additive	yield [%]
136-*E*	-	0
136-*E*	K_2CO_3	0
136-*Z*	-	0
136-*Z*	K_2CO_3	0

Scheme 2.9 – a) attempted reaction between *N*-phenylsydnone and dihydroisoxazole **134**; b) synthesis of *E*- and *Z*-alkenyl iodides from 1-octyne. Values in parentheses indicate *E*:*Z* ratios of isolated compounds; c) attempted cycloaddition reactions of *N*-phenylsydnone and alkenyl iodides

The enhanced reactivity of electron rich enol ethers also prompted us to test the reaction of various enamines. Moreover, given the highly regioselective nature of these reactions, we were interested in the possibility of tuning the enamine structure as a means of achieving regiodivergence (Scheme 2.10).

The reaction of *n*-butyl substituted enamine **138** was first performed to gauge the reactivity of these substrates. Surprisingly, under our optimal conditions, the amide **139** was isolated in quantitative yield. The formation of this by-product is unusual and appears to arise from a hydrolysis of the enamine starting material followed by nucleophilic ring opening of *N*-phenylsydnone with the resulting piperidine. Attempts to reduce this non-productive pathway by employing more strictly anhydrous conditions were unsuccessful and further examination of a number of enamine substrates found this to be a general process under the current conditions. Therefore, investigation of a possible

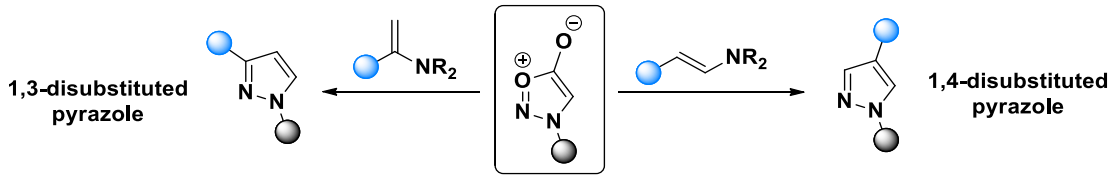

Scheme 2.10 – using enamines for a regiodivergent pyrazole synthesis

regiodivergent synthesis was performed using 2-methoxypropene **143**, leading to 1,3-disubstituted pyrazole **114b** in 54% yield. This is the opposite regioisomer to that obtained in the reaction of **113** with *N*-phenylsydnone (Table 2.7) and this result provides further indication that the regioselectivity in these reactions is governed primarily by electronic factors. A couple of other details from this reaction are worth mentioning: only a small amount of conversion is observed at 150 °C (unlike enol ether **113**) and even at 180 °C, the reaction remains incomplete after 24 h (~70% conversion). Both of these details highlight the significantly detrimental impact steric interactions have on this class of cycloaddition reaction.

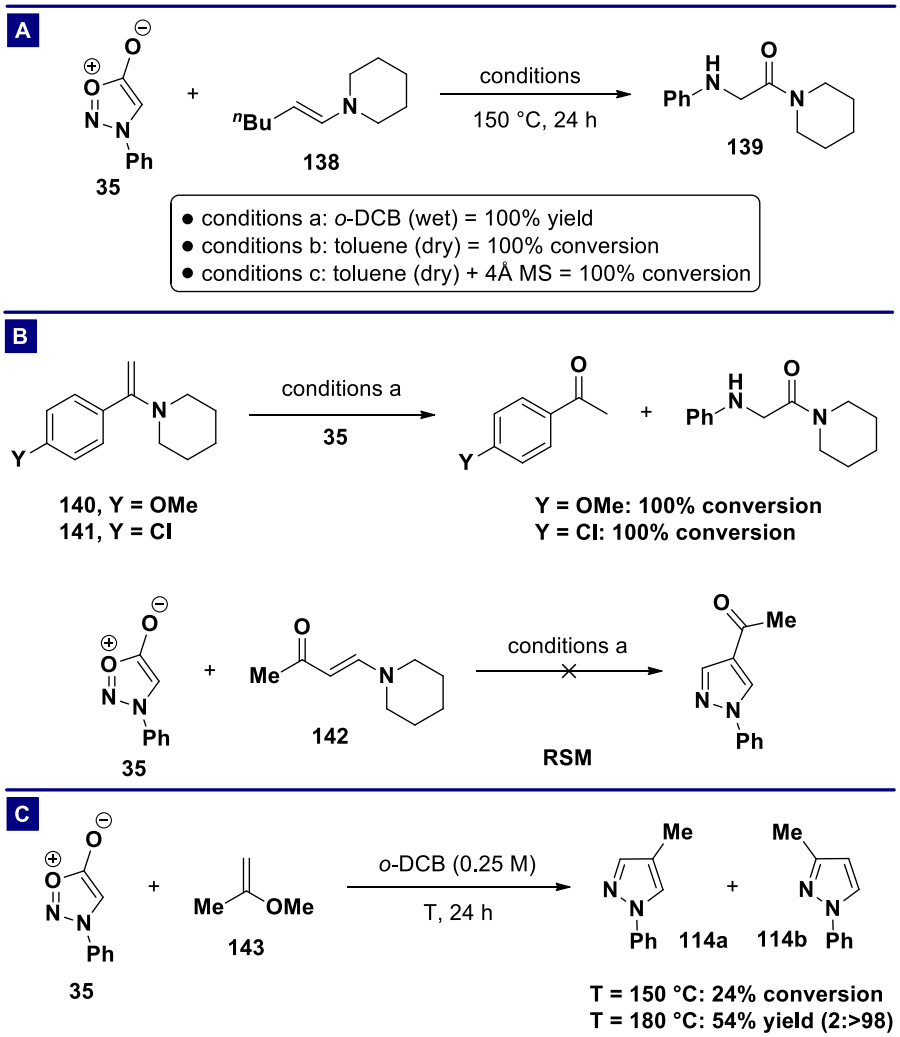

Scheme 2.11 – a) attempted cycloaddition reaction of *N*-phenylsydnone and enamine **138**; b) cycloaddition reactions of *N*-phenylsydnone and various enamines; c) 1,3-regioselective cycloaddition reaction between *N*-phenylsydnone and **143**; *o*-DCB = 1,2-dichlorobenzene; MS = molecular sieves

2.5 Cyclic Enamide Dipolarophiles II

The investigation of sydnone-enol ether cycloadditions uncovered an intriguing relationship between dipolarophile ring size and reactivity. Although our initial attempts to use 6-membered cyclic enamides failed, we postulated that this reactivity enhancement might assist our efforts. To aid with this investigation, a 3 step synthesis of Cbz protected 2,3-dihydropyrrole **146** was devised.[104] An initial Cbz protection of 4,4-diethoxybutan-1-amine **144** under biphasic conditions proceeded quantitatively, but subsequent hydrolysis of the acetal moiety using pyridinium *p*-toluenesulfonate (PPTS) and dehydration in anhydrous toluene proceeded in poor yield and gave a mixture of compounds. Nevertheless, this synthesis provided sufficient quantities of **146** for cycloaddition studies.

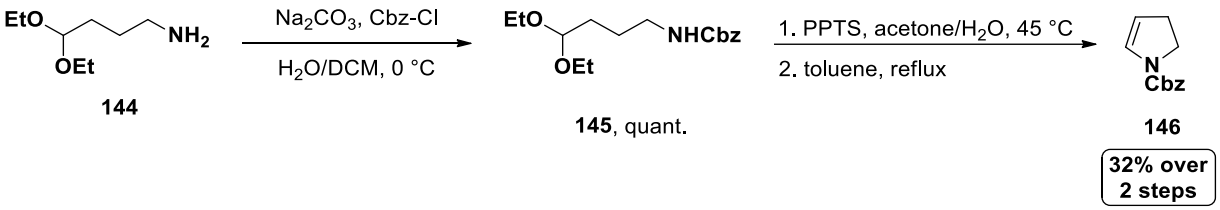

Scheme 2.12 – synthesis of Cbz protected enamide **146**

A test reaction using 2 eq. of **146** in *o*-DCB at 150 °C demonstrated that this reactivity trend also extends to enamides (Table 2.9, entry 1). Indeed, 100% conversion (c.f. 0% conversion for **84**) of the sydnone was observed alongside formation of a 1,4-disubstituted pyrazole product, as evidenced by the appearance of two singlets at δ7.56 ppm and δ7.75 ppm in the crude ^{1}H NMR spectrum. However, following purification by column chromatography the desired product was obtained in low yield. Furthermore, the ^{1}H NMR spectrum of the isolated compound did not fit the structure of **147a**; there were too many aromatic protons. An LC-MS analysis revealed that this observation was the result of several products co-eluting from the column during purification. In addition to the mass peak of the desired product *m*/*z* 322.2 $(M+H)^+$, a peak at *m*/*z* 412.2 $(M+H)^+$ is also observed, consistent with the benzylated structure **148a**. The exact mechanism by which this product is formed is unclear, but the obvious benzyl donor molecule is enamide starting material **146**. In accordance with this, a small quantity of amide **149** was isolated alongside the pyrazole products. It is possible that debenzylation/oxidation of enamide **146** leads to the formation of pyrrole which can then cause ring opening of *N*-phenylsydnone to produce **149** (c.f. scheme 2.11A). Additionally, this helps to explain the low isolated yields in spite of the high conversion of sydnone starting material. We next undertook a small survey of conditions to try and minimise the amount of benzylation, hoping that a concomitant increase in sydnone stability might also be observed. Decreasing the equivalents of enamide **146** reduced the conversion of sydnone but all of the identified by-products were still visible on ^{1}H NMR and LC-MS analyses. Heating the reaction to 180 °C and varying the substrate stoichiometries provided

Table 2.9 – optimisation of the reaction between *N*-phenylsydnone and enamide **146**[a]

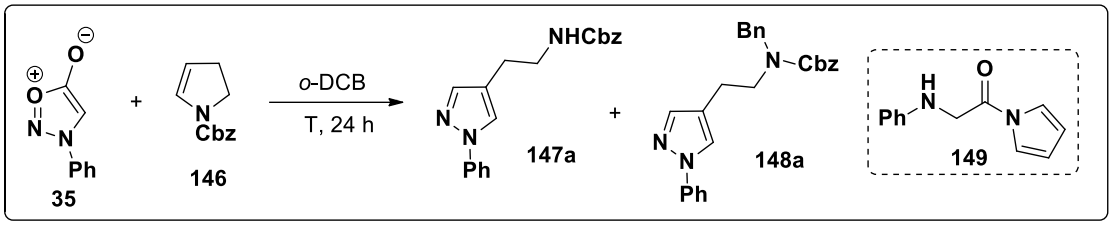

Entry	eq 146	Concentration [M]	T [°C]	Conversion [%][b]	Yield [%][c]
1	4	0.25	150	100	20
2	4	0.13	150	100	24
3	2	0.25	150	65	19
4[d]	4	0.25	150	100	<5
5	4	0.25	180	100	18
6	2	0.25	180	100	10
7	4	0.13	180	100	15
8[e]	4	0.13	150	100	<5

[a] Reaction conditions: *N*-phenylsydnone (0.13 mmol), **146** (0.25-0.50 mmol), *o*-DCB (0.5-1.0 mL) at specified temperature for 24 h; [b] conversion estimated by the ^{1}H NMR ratio of **147a** to *N*-phenylsydnone; [c] yield of isolated mixture of **147a** + **148a**; [d] K_2CO_3 (2 eq) added; [e] DABCO (2 eq) added; *o*-DCB = 1,2-dichlorobenzene

almost identical results. On the basis that enamide decomposition is an acid catalysed process, we examined the effect of adding different bases to the reaction. The addition of potassium carbonate (K_2CO_3) provided no noticeable change to the outcome of the reaction, while the organic base 1,4-diazabicyclo[2.2.2]octane (DABCO) prevented the formation of amide **149** but also reduced the amount of pyrazole product even at 100% conversion. Although these reactions reinforce the idea that ring size affects reactivity in sydnone-alkene cycloadditions, the use of enamines poses a number of challenges which are yet to be overcome.

2.6 Cyclic Enol Ether Dipolarophiles II

The ability to predictably switch the selectivity of a reaction by the addition or removal of a single reagent is highly desirable in synthetic chemistry as a means of accessing more diverse chemical space from common starting materials. Often this means searching for conditions which achieve a switch in either regio- or stereoselectivity, but other options are also possible. Protecting groups are highly useful in organic synthesis for allowing control over a chemical reaction, but their removal must occur under orthogonal conditions to other protecting groups within the molecule. Therefore, being able to control the fate of a functional group in a given reaction is highly important.

In the case of cyclic enol ethers **86** and **92**, the reaction with *N*-arylsydnones was found to produce either the THPy or THFu ethers, respectively. In the event that the free alcohol containing product is desired, an additional deprotection step would be required leading to decreased yields and increased time consumption. The formation of THFu/THPy ethers is usually an acid catalysed process whereby protonation of **86** forms the oxocarbenium intermediate **150** which can undergo attack by an alcohol nucleophile to form the desired product **152** (Scheme 2.13).

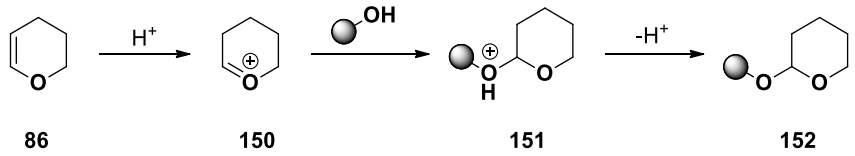

Scheme 2.13 – mechanism of formation of THP ethers

Based on this mechanism, we hypothesised that adding a base to our otherwise optimal conditions might lower the pH of the reaction medium sufficiently as to prevent the formation of the acetal products. An initial test reaction between *N*-phenylsydnone and **92** in the presence of 1 equivalent of K_2CO_3 validated this hypothesis (Table 2.10, entry 1). Analysis of the crude ^{1}H NMR spectrum showed no evidence of the acetal product at 100% conversion and, following column chromatography, alcohol **93a** was isolated in 56% yield as a single regioisomer. However, further experimentation found this result hard to replicate despite numerous attempts, with varying quantities of the acetal product observed each time. Coincidentally, this turned out to be the result of different amounts of pre-stirring between *N*-phenylsydnone and K_2CO_3 before the addition of **92** and eventually a 1 hour pre-stir was employed as the optimal method for preventing acetal formation. A screen of other bases including 1,4-diazabicyclo[2.2.2]octane (DABCO), 1,8-diazabicyclo[5.4.0]undec-7-ene (DBU) and 4-(dimethylamino)pyridine (DMAP) produced mixed results; many gave lower conversions or didn't completely prevent acetal formation, while DBU produced a complex mixture from which only small quantities of **93a** could be isolated. The observation of numerous high molecular weight by-products via LC-MS (possibly from further reactions of the dipolar intermediate) then prompted us to try running the reaction at lower concentrations, resulting in a final 70% yield of **93a** (Table 2.10, entry 10).

Table 2.10 – optimisation of the base-buffered cycloaddition reaction between *N*-phenylsydnone and **92**[a]

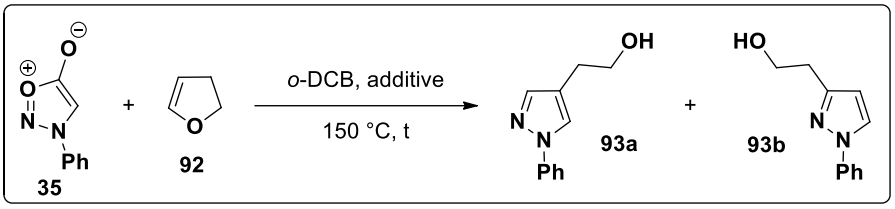

Entry	Additive (eq)	Concentration [M]	t [h]	Yield [%][b]	a:b[c]
1	K_2CO_3 (1.0)	1.0	24	56	>98:2
2	K_2CO_3 (0.5)	1.0	24	66	>98:2
3	K_2CO_3 (0.1)	1.0	24	50	>98:2
4	K_2CO_3 (2.0)	1.0	24	41	>98:2
5	DABCO (1.0)	1.0	24	64	>98:2
6	DBU (1.0)	1.0	24	17	>98:2
7	DMAP (1.0)	1.0	24	45	>98:2
8	K_2CO_3 (1.0)	0.25	24	52	>98:2
9	K_2CO_3 (2.0)	0.25	24	40	>98:2
10	K_2CO_3 (2.0)	0.17	48	70	>98:2
11	K_2CO_3 (2.0)	0.13	72	65	>98:2
12	DABCO (2.0)	0.17	72	18	>98:2

[a] Reaction conditions: *N*-phenylsydnone (0.5 mmol), **92** (2.0 mmol), additive (0.05-1.0 mmol), *o*-DCB (0.5-3.0 mL) at 150 °C for the specified time; [b] yield of isolated compound; [c] ratio determined by ^{1}H NMR analysis; *o*-DCB = 1,2-dichlorobenzene.

Other *N*-arylsydnones were then surveyed under these conditions and although no obvious electronic trends were apparent, several alcohol containing pyrazoles could be synthesised in good yield and with good regioselectivity (Table 2.11).

Table 2.11 – scope of the 1,4-regioselective base-buffered cycloaddition between *N*-arylsydnones and **92**[a]

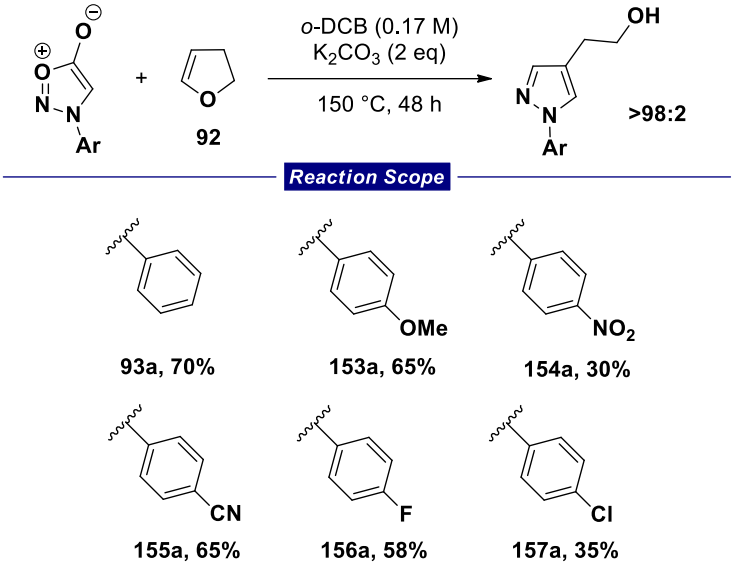

[a] Reaction conditions: *N*-arylsydnone (0.5 mmol), **92** (2.0 mmol), K_2CO_3 (1.0 mmol), *o*-DCB (3.0 mL), 150 °C, 48 h; *o*-DCB = 1,2-dichlorobenzene

In order to compare and contrast this method with sydnone-alkyne cycloadditions we performed a reaction between *N*-phenylsydnone and 3-butyn-1-ol **158** (Scheme 2.14A). Interestingly this reaction proceeds at a similar rate to the reaction with **92** (incomplete conversions were observed after 24 hours) and crucially, leads to **93a**/**93b** in 65% yield and a ratio of 17:83. The key conclusions derived from this experiment are: 1) The reaction between *N*-arylsydnones and enol ethers offers complementary regioselectivity to sydnone-alkyne cycloadditions. 2) The reaction between *N*-arylsydnones and enol ethers offers higher levels of regiocontrol than sydnone-alkyne cycloadditions. These key details highlight the utility of enol ethers in expanding the scope of sydnone cycloaddition reactions. Although earlier experiments had confirmed the conversion of **93a** to **94a** (Scheme 2.6), one might argue that the observed results upon adding K_2CO_3 to the cycloaddition reaction conditions are the consequence of a change in mechanism rather than simply preventing the reaction of **92** and **93a**. This may be refuted by the observation that heating **93a** in the presence of **92** and K_2CO_3 simply returns the starting material intact, with 0% conversion to the acetal (Scheme 2.14B). Once again, a pre-stirring period with **93a** and K_2CO_3 was found to be essential for consistent results. Finally, a competition reaction between 5-membered enol ether **92** and 6-membered **86** was performed under the newly optimised conditions (Scheme 2.14C). Earlier competition experiments had required a secondary hydrolysis step (Scheme 2.7A), thus to draw any conclusion from this experiment we had to assume that the observed product ratio was unaffected by this step. Under the base buffered conditions, the reactivity of **92** and **86** could be directly compared and it was found that the corresponding products were formed in a 63% yield and 94:6 ratio. The observed ratio is identical to

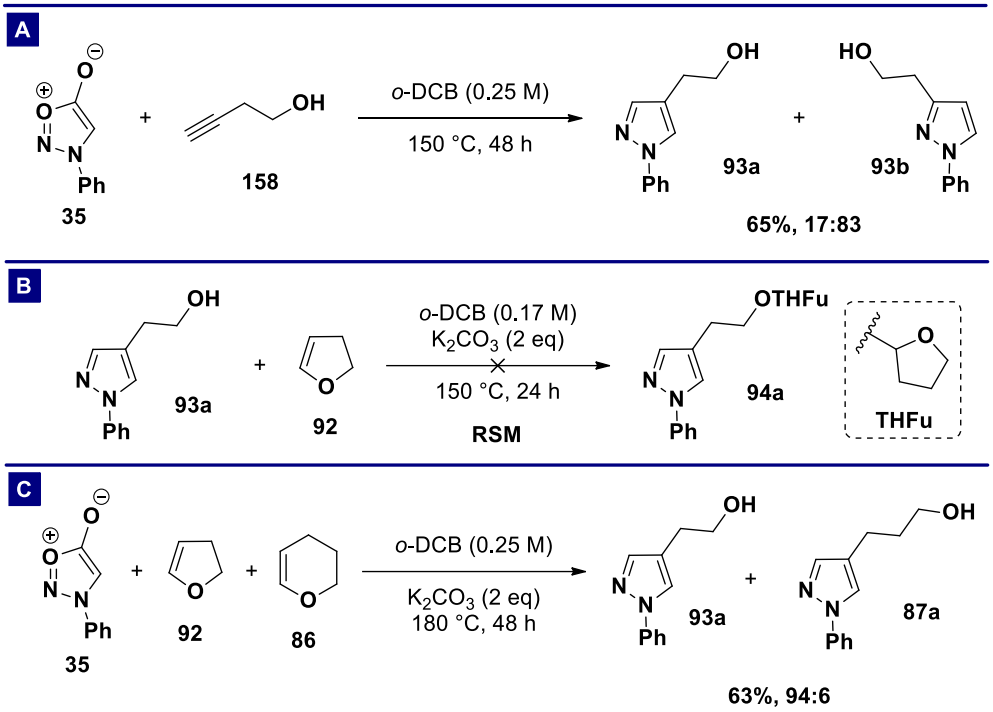

Scheme 2.14 – a) reaction of *N*-phenylsydnone with alkyne **158**; b) failed reaction of alcohol **93a** with enol ether **92** in the presence of K_2CO_3; c) competition reaction between **92** and **86** under base-buffered conditions; *o*-DCB = 1,2-dichlorobenzene; THFu = tetrahydrofuranyl; RSM = return of starting material

that found in the earlier experiment, validating our assumption and further confirming the enhanced reactivity of **92** relative to **86**.

2.7 Substituted Cyclic Enol Ether Dipolarophiles

Our initial experiments used only the unsubstituted 2,3-dihydrofuran **92** and 3,4-dihydro-2*H*-pyran **86** as substrates in sydnone cycloaddition reactions. Primarily, this was a consequence of the formation of THFu/THPy ethers which, upon the use of substituted dihydrofuran substrates, would lead to diastereoisomeric mixtures of acetal protected products and potential purification problems (Scheme 2.15A). However, the discovery that adding K_2CO_3 to the reaction medium prevents this additional step opened up the possibility of using more highly substituted enol ether substrates. Previous literature precedence indicated that 4-substituted-2,3-dihydrofurans **159** are accessible using a transition metal catalysed cycloisomerisation of the corresponding homopropargyl alcohols **160** (Scheme 2.15B). Given the contrasting regioselectivity of sydnone-alkyne and sydnone-enol ether cycloadditions, we envisioned that this cycloisomerisation might also function as a regioselectivity switch within these reactions (Scheme 2.15C).

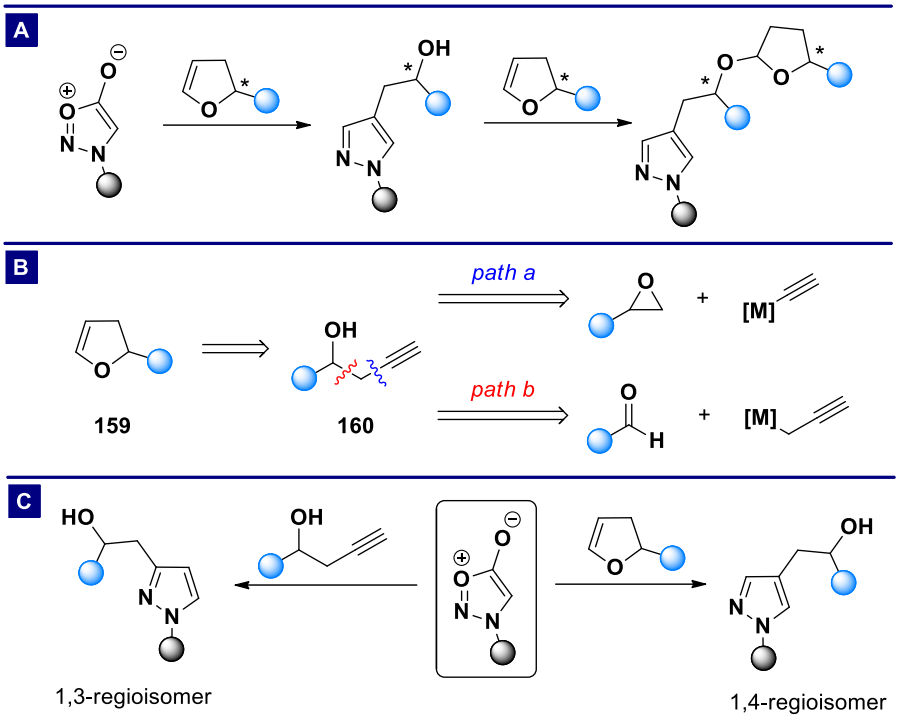

Scheme 2.15 – a) reaction of sydnones and substituted dihydrofurans to form diastereoisomeric mixtures; b) retrosynthetic analysis of homopropargylic alcohols; c) regiodivergent cycloadditions using a cycloisomerisation switch

A simple retrosynthetic analysis identified two potential routes by which these compounds might be synthesised; the addition of alkynyl nucleophiles to epoxides (Scheme 2.15B, path a) or the addition of propargylic nucleophiles to aldehydes (Scheme 2.15C, path b). In the case of the former, achieving high levels of regiocontrol is potentially problematic, especially for aryl substituted epoxides.

Therefore we began by exploring the reaction between benzaldehyde (**161**) and propargyl Grignard (derived from propargyl bromide) in THF, however, none of the desired product (**163**) was observed and benzaldehyde was returned intact (Table 2.12). Furthermore, large quantities of magnesium turnings remained visible at the base of the reaction flask (in spite of a 1:1 stoichiometry of propargyl bromide:Mg), indicating a lack of Grignard formation. To try and achieve a more effective activation of the magnesium, a flame dried round bottomed flask (RBF) containing Mg turnings under argon was stirred for 3 hours prior to the addition of THF, two crystals of iodine (I_2) and propargyl bromide and the mixture was then heated to 50 °C for 2 hours. A series of colour changes (red → orange → yellow) were observed over the course of this reaction but analysis of the crude ^{1}H NMR again showed no formation of the desired product and formation of a complex mixture of products. It is therefore possible that the observed colour changes were simply the result of iodine consumption, with no subsequent formation of the propargyl Grignard. Indeed, the difficulty of forming propargylic Grignard reagents is documented in the chemical literature, with their formation often requiring the use of sub-

stoichiometric quantities of highly toxic mercury (II) salts. Additionally, the basic nature of these reagents can result in the formation of alkynyl Grignard reagents **165**, leading to isomeric mixtures of products. In order to avoid these problems it was decided to investigate the reaction of the corresponding propargyl zinc reagent. An initial reaction employing activated zinc (activated according to the procedure of Baran)[105] in place of the magnesium turnings, and this showed complete consumption of benzaldehyde and the formation of homopropargylic alcohol **163** alongside minor quantities of allenic alcohol **164**, which could be isolated in a combined 97% yield after purification (Table 2.12, entry 4). This reaction was found to work with almost equal efficiency using non-activated zinc powder, giving a 91% combined product yield with the same ratio of regioisomers (entry 5). Unfortunately, these mixtures proved difficult to separate chromatographically and so we sought more selective conditions. Interestingly, higher levels of selectivity could be achieved by performing the reaction in a mixture of THF and saturated ammonium chloride (NH_4Cl) solution (1:1, v/v).[106] While this reaction proceeds with lower levels of conversion, almost complete selectivity for the homopropargylic alcohol **163** (**163**:**164** = 96:4 in the crude product) was observed and **163** could be isolated as a single compound following column chromatography. A number of different homopropargylic alcohols were then synthesised following this procedure (Table 2.13).

Table 2.12 – optimisation of the synthesis of homopropargylic alcohol **163**

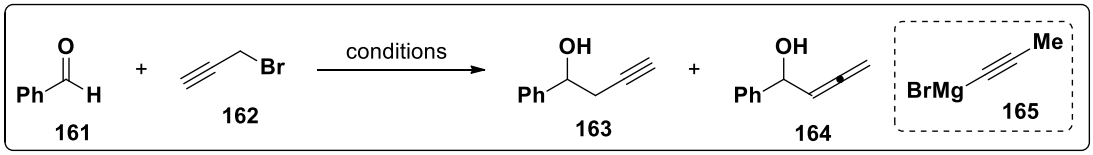

Entry	Conditions	Yield [%][a]	163:164[b]
1[c]	Mg turnings, THF, reflux → 0 °C	0	-
2[d]	Mg turnings, THF, 50 °C → 0 °C	0	-
3[e]	Mg turnings, THF, 50 °C → 0 °C	0	-
4[f]	Zn powder, THF, RT	97	88:12
5[g]	Zn powder, THF, RT	91	88:12
6[h]	Zn powder, THF/NH_4Cl, 0°C → RT	59	>98:2

[a] yield of the isolated compound; [b] ratio determined by ^{1}H NMR analysis; [c] **162** (2 eq), Mg (2 eq), I_2 (cat.), reflux then **161** (1 eq), 0 °C; [d] **162** (2 eq), Mg (2 eq), I_2 (cat.), 50 °C then **161** (1 eq), 0 °C; [e] Mg (2 eq), RT, 3 h then **162** (2 eq), I_2 (cat.), 50 °C then **161** (1 eq), RT; [f] activated Zn (2 eq), LiCl (2 eq), TMSCl (5 mol%), 1,2-DBE (5 mol%), THF, RT then **161** (1 eq), **162** (1 eq); [g] Zn (2 eq), 1,2-DBE (2 eq), **162** (2 eq), THF, RT then **161** (1 eq); [h] activated Zn (2 eq), **162** (2 eq), THF/NH_4Cl (1:1, 0.5 M), 0 °C then **161** (1 eq), RT. 1,2-DBE = 1,2-dibromoethane

Table 2.13 – synthesis of homopropargylic alcohols[a]

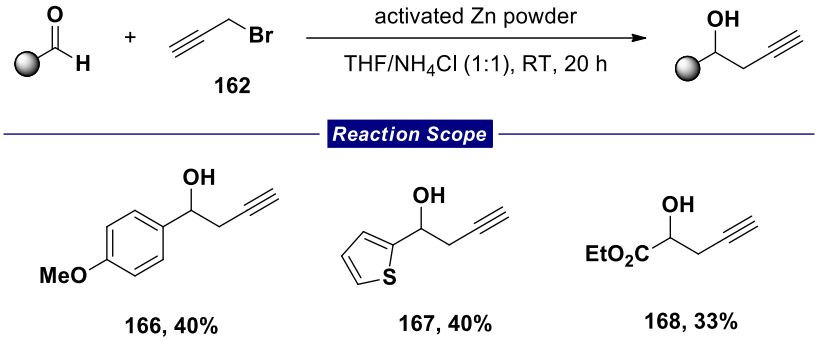

[a] Reaction conditions: aldehyde (9.8 mmol), **162** (20 mmol), activated Zn (20 mmol), THF/NH_4Cl (1:1, 20 mL). THF = tetrahydrofuran

With sufficient quantities of **163** in hand, we then examined the cycloisomerisation step under conditions reported by McDonald.[107] The reaction of **163** with sub-stoichiometric quantities of $Mo(CO)_6$ and trimethylamine *N*-oxide (TMNO) in a mixture of triethylamine (Et_3N) and diethyl ether (Et_2O) at 20 °C proceeded in low conversion even after 2 days (table 2.14, entry 1).

Table 2.14 – optimisation of the cycloisomerisation of **163**[a]

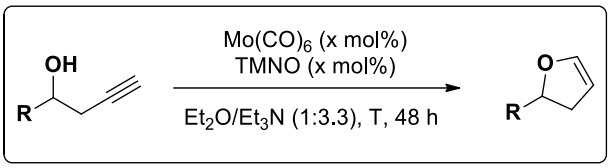

Entry	SM	R	x	Concentration [mM]	T [°C]	P	Conversion [%][b]
1	**163**	Ph	50	23	20	**169**	23
2	**163**	Ph	50	46	20	**169**	51
3	**163**	Ph	50	46	30	**169**	73
4	**163**	Ph	50	46	40	**169**	35
5	**163**	Ph	50	46	50	**169**	75 (70)
6	**163**	Ph	100	46	20	**169**	24
7	**163**	Ph	50	93	20	**169**	45
8	**163**	Ph	50	190	20	**169**	35
9[c,d]	**166**	PMP	50	46	50	**170**	100 (82)
10[c,d]	**167**	2-thiophenyl	50	46	50	**171**	100 (90)
11[c,d]	**168**	CO_2Et	50	46	50	**172**	100 (52)

[a] Reaction conditions: homopropargyl alcohol (0.34 mmol), $Mo(CO)_6$ (0.17-0.34 mmol), TMNO (0.17-0.34 mmol), Et_2O/Et_3N (1:3.3, 1.8-15 mL), at specified temperature for 48 h; [b] conversion estimated by ^1H NMR ratio of SM and P. Values in parentheses are yields of isolated compound; [c] homopropargyl alcohol (2.3 mmol); [d] 60 h; SM = starting material; P = product; TMNO = trimethylamine *N*-oxide

A two-fold increase in concentration provided a marked increase in conversion, but higher concentrations were less effective (compare entries 1, 2, 7 and 8). Increasing the temperature also resulted in higher levels of conversion up to 75% at 50 °C, allowing 2,3-dihydrofuran **169** to be isolated in 70% yield. These optimised conditions were then used in the synthesis of a number of other 2,3-dihydrofurans (**170**-**172**) (Table 2.14, entries 9-11).

Although successful, the linear nature of this protocol results in a diminished quantity of material throughput. Thus, a more rapid synthesis of aryl-substituted 2,3-dihydrofurans could be achieved using a Pd-catalysed Heck reaction under conditions reported by Lory.[108,109] The initial migratory insertion and β-hydride elimination is thought to produce isomeric 2,5-dihydrofuran **173** which then undergoes sequential hydropalladation and β-hydride elimination to afford the desired product. Consequently, aryl substituted dihydrofurans with phenyl (**169**), *para*-methyl (**174**), fluoro (**175**) and nitro (**176**) groups could be synthesised in 58%, 42%, 50% and 56% yield respectively, in only one step from commercially available 2,3-dihydrofuran.

Table 2.15 – Pd-catalysed synthesis of 4-aryl-2,3-dihydrofurans[a]

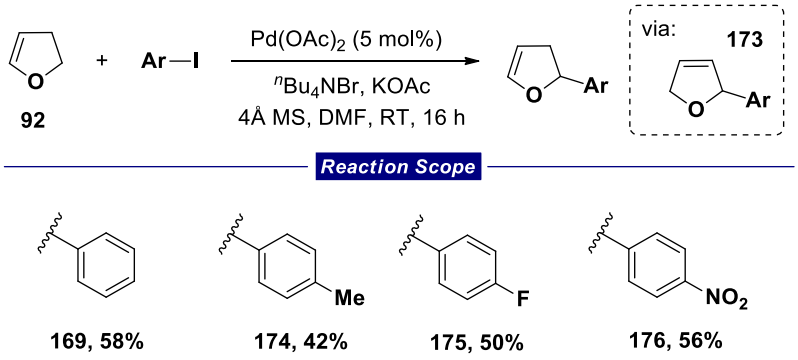

[a] Reaction conditions: aryl iodide (1 eq), **92** (10 eq), $^{n}Bu_4NBr$ (2.5 eq), KOAc (2.5 eq), $Pd(OAc)_2$ (5 mol%), 4Å MS, DMF, RT, 20 h; DMF = dimethylformamide; MS = molecular sieves

With a library of 4-substituted-2,3-dihydrofurans available we were then able to examine their sydnone cycloaddition reactions. A reaction between *N*-phenylsydnone and **169** in the presence of 1 equivalent of K_2CO_3 at 150 °C for 24 hours produced 1,4-disubstituted pyrazole **177a** in 37% yield (Table 2.16, entry 1). Increased reaction times had no positive impact on the reaction but a temperature of 180 °C gave a higher yield of 48%.

Table 2.16 – optimisation of the reaction between *N*-phenylsydnone and **169**[a]

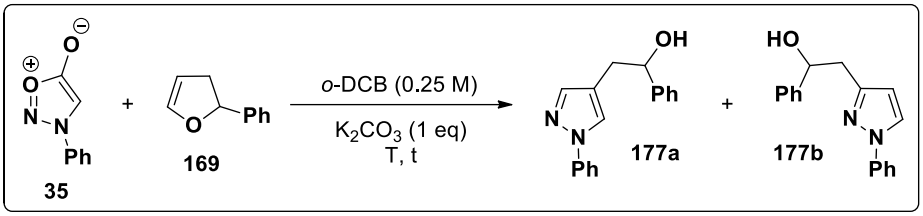

Entry	T [°C]	t [h]	Yield [%][b]	a:b[c]
1	150	24	37	>98:2
2	150	48	35	>98:2
3	180	24	48	>98:2
4	180	48	40	>98:2

[a] Reaction conditions: *N*-phenylsydnone (0.34 mmol), **169** (0.68 mmol), K_2CO_3 (0.34 mmol) *o*-DCB (1.3 mL) at the specified temperature and time; [b] yield of isolated compound; [c] ratio determined by ^{1}H NMR analysis. *o*-DCB = 1,2-dichlorobenzene

The application of these conditions to other dihydrofuran substrates gave a range of alcohol containing pyrazoles bearing both electron rich and electron deficient aryl groups (**178a**, **181a**, **182a**), a heteroaryl substituent (**179a**) and a synthetically useful ester moiety (**180a**). As would be expected, the electronic and steric profile of these substituents had little impact on their reactivity. Unfortunately, the pyrazole containing a *para*-nitrophenyl substituent could not be purified despite several attempts. The investigation of homopropargylic alcohols in sydnone cycloadditions then verified the possibility of using the cycloisomerisation as a regioselectivity switch. For instance, the phenyl substituted alkyne **163** reacted with *N*-phenylsydnone to afford 1,3-disubstituted pyrazole **177b** in 42% yield as a single regioisomer. Further reactions with *para*-methoxyphenyl (**178b**), 2-thiophenyl (**179b**) and ester (**180b**) substituted alkynes all produced the corresponding 1,3-disubstituted pyrazoles exclusively, albeit in low yield (Table 2.17).

Table 2.17 – regioselective synthesis of alcohol containing pyrazole derivatives[a,b]

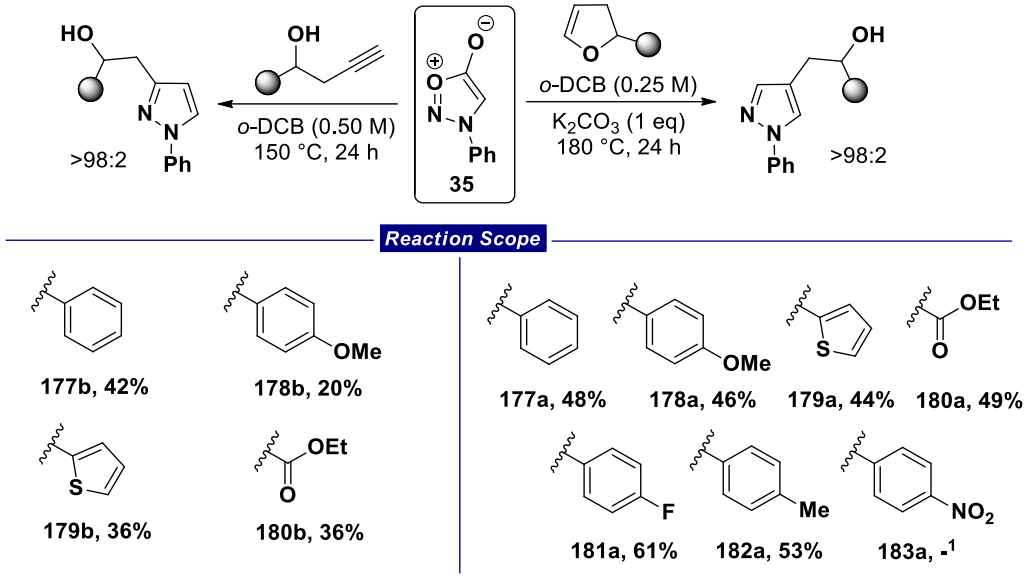

[a] Reaction conditions: *N*-phenylsydnone (0.31 mmol), dihydrofuran (0.62 mmol), K_2CO_3 (0.31 mmol), *o*-DCB (1.2 mL), 180 °C, 24 h; [b] Reaction conditions: *N*-phenylsydnone (0.31 mmol), homopropargyl alcohol (0.93 mmol), *o*-DCB (0.62 mL), 150 °C, 24 h; [1] unable to purify product; *o*-DCB = 1,2-dichlorobenzene

2.8 Conclusions

The cycloaddition of sydnones and enol ethers has been successfully demonstrated as a means of achieving high levels of regiocontrol in sydnone cycloaddition reactions. A range of both cyclic and acyclic enol ethers react with sydnones to afford 1,4-disubstituted pyrazoles exclusively in good yields. In the case of cyclic enol ethers, acetal containing pyrazoles are isolated in the absence of any additives, while the addition of a stoichiometric quantity of K_2CO_3 leads to the isolation of the corresponding alcohols. However, the scope of these reactions remains somewhat limited; only *N*-arylsydnones react successfully whereas *N*-alkylsydnones and *C*4-substituted sydnones (with a single exception) fail to provide any trace of product under the investigated conditions. Additionally, enol ethers are currently the only viable dipolarophiles in this reaction; a range of other dipolarophiles including enamines, enamide and alkenyl halides were shown to be unreactive. Given the high temperatures, long reaction times and limited substrate scope, it seems likely that the solution to these limitations lies in the use of alternative forms of promotion (vide infra).

3 Visible Light Photocatalysis

3.1 Introduction

Catalysis plays a pivotal role within organic synthesis. Indeed, the development of both metal-based and purely organic catalyst structures has allowed both the enhancement of known processes and the discovery of novel transformations. Among all of the reported catalytic manifolds, visible light photocatalysis (VLPC) has been shown to play a unique role in uncovering novel complexity building transformations.[110–112] Traditionally, the role of synthetic photochemistry has remained limited due to a number of complications, both chemical and practical. Many organic molecules exhibit only weak interactions with light and therefore ultraviolet (UV) irradiation is required to achieve their excitation, however, the use of such high energy photons can often result in undesirable photodecomposition processes, especially in highly functionalised molecules. Furthermore, the setups required to generate UV radiation can be expensive and hazardous to use and the combination of these issues has meant that many photochemical transformations are limited in overall scope and applicability. More recently, a number of approaches have been taken to combat these deficiencies. Specifically, the incorporation of flow-chemistry techniques has allowed circumvention of some of the practical issues,[113,114] while the discovery of photocatalysts capable of absorbing visible light has greatly expanded the scope of synthetic photochemistry.

Although the application of this strategy to organic synthesis has been known for a number of decades, the true potential of this approach has been realised only recently by the synthetic community (Figure 3.1). This resurgence followed independent reports from the laboratories of MacMillan,[115] Yoon,[116] and Stephenson,[117] and has resulted in photocatalysis becoming a key area of research interest in organic chemistry.

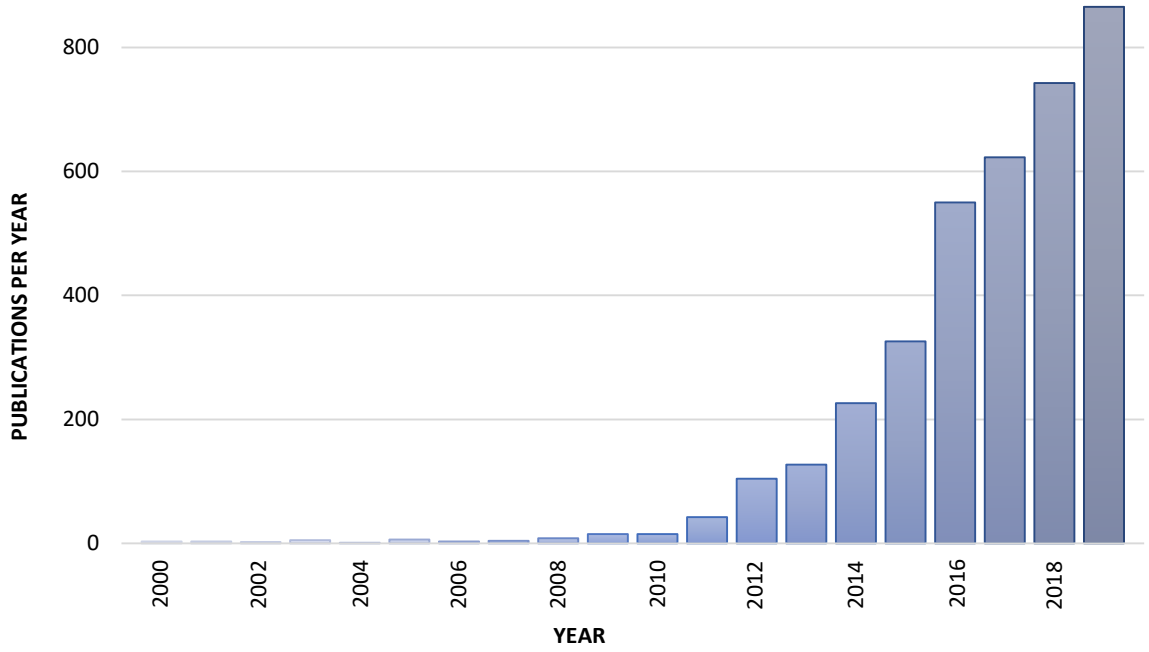

Figure 3.1 – Number of publications per year since 2000 for the keyword search "photoredox catalysis" on SciFinder®. Search conducted: 06/03/2020

3.2 Mechanisms of Photocatalysis

At its core, VLPC involves the conversion of light energy into synthetically useful chemical energy (via energy transfer) or chemical potential (via electron or atom transfer) by means of a light absorbing photocatalyst. Absorption of a photon by the photocatalyst generates an excited state photocatalyst which can interact with organic molecules in a number of ways (vide infra), each of which leads to uniquely reactive intermediates (Scheme 3.1). Essentially, the photocatalyst acts as a conduit through which visible light can be used to excite a wide variety of organic molecules. The operative mechanism within a specific transformation is primarily determined by the structure of the chosen catalyst and understanding the potential mechanisms for each is crucial for designing new photocatalytic reactions.

3.2.1 Photoinduced Electron Transfer

The primary factor responsible for the renewed interest in photocatalytic transformations is the ability of excited state photocatalysts to participate in single electron transfer (SET) events. Using transition-metal photocatalysts as an exemplar, excitation with visible light promotes a metal to ligand charge transfer (MLCT) creating an electron hole pair (a similar charge separation is responsible for the reactivity of organic photocatalysts but the orbitals involved are reliant upon the individual catalyst structure). This charge transfer increases the positive charge on the metal centre and negative charge on the ligand, thus conferring the remarkable property that the excited photocatalyst is

simultaneously more oxidising *and* more reducing than in the ground state. Therefore, quenching of this excited state can occur via the transfer of an electron to an acceptor molecule (oxidative quenching) or from a donor molecule (reductive quenching). The terms oxidative and reductive refer to the change in oxidation state of the photocatalyst as a result of the quenching step. In the case of an oxidative quenching cycle (Scheme 3.1, path a), the resulting PC^{+} is then an even more powerful oxidising agent, capable of removing an electron from another organic molecule. Conversely, a reductive quenching (Scheme 3.1, path b) generates the powerfully reducing PC^{-} which can donate an electron to an organic molecule. Overall, the catalyst harnesses visible light to act as a "shuttle" of electrons from a donor to an acceptor.

3.2.2 Photoinduced Energy Transfer

The second commonly reported quenching mechanism involves a triplet energy transfer (EnT), commonly termed "photosensitisation", from the excited state photocatalyst to an organic molecule.[118] Following excitation to the singlet excited state the photocatalyst undergoes intersystem crossing (ISC) to a long lived triplet excited state which can then participate in an energy transfer event to create an excited state substrate and reform the ground state photocatalyst (Scheme 3.1, path c). The most commonly invoked mechanism for this process is a Dexter energy transfer which can be conceptualised as a bilateral electron exchange between the molecules. The resulting diradical species can then undergo different synthetically useful bond forming reactions.

3.2.3 Photoinduced Atom Transfer

The final common quenching mechanism involves direct hydrogen atom transfer (HAT) from the substrate to the excited state photocatalyst, rather than sequential electron transfer and bond cleavage processes (Scheme 3.1, path d).[119] Many examples of this type have been reported and are particularly common for aromatic ketone and polyoxometalate photocatalysts. This mechanistic distinction is important primarily because the feasibility of HAT is dictated by the bond dissociation energy (BDE) rather than the substrate and catalyst reduction potentials (as is the case for electron transfer). The combination of these distinct modes of substrate activation has culminated in a plethora of bond forming processes mediated by visible light photocatalysis.

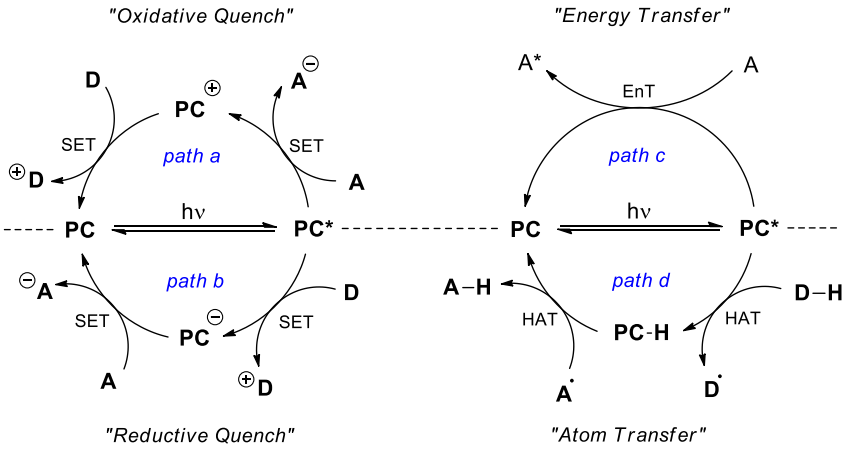

Scheme 3.1 – possible mechanistic outcomes in visible light photocatalysis; PC = photocatalyst; A = acceptor; D = donor; SET = single electron transfer; EnT = energy transfer; HAT = hydrogen atom transfer

3.3 Using Visible Light photocatalysis for Constructing Cyclic Molecules

Given the prevalence of carbo- and heterocyclic motifs within natural products and compounds exhibiting useful bioactive properties, it is unsurprising that many reports utilising VLPC have focused on their construction. For the purposes of the following section there will be a focus on reactions which proceed by cycloaddition/annulation processes, while those utilising cyclisations will not be discussed.[120–122]

3.3.1 Synthesis of 3-Membered Rings

The synthesis of 3-membered cyclic motifs is highly desirable due to the defined and rigid conformations of such molecules, in combination with their use as substrates in the assembly of larger cyclic systems. Although examples of 3-membered ring synthesis using VLPC are more limited than larger ring systems, several interesting examples are reported in the literature. For example, work in the laboratory of Yoon highlighted the synthesis of aziridines from alkenes and azidoformate **184** (Scheme 3.2A).[123] Previous attempts to promote this same transformation by other methods including direct UV photolysis resulted in the formation of mixtures of products arising from aziridination and *C-H* activation processes. Based on the assumption that these arose from the non-selective formation of both singlet and triplet nitrene intermediates, Yoon proposed that excitation of iridium complex **185** followed by energy transfer to **184** would lead to selective generation of the triplet nitrene, thereby providing a platform to control product formation. Indeed, irradiating a mixture of azidoformate **184** and various di-, tri- and tetra-substituted alkenes with blue light in the presence of iridium complex **185** delivered the corresponding aziridines in high yields and with excellent selectivity. The reaction is chemoselective for electron rich alkene substrates as shown in the formation of **188**, while the reaction of electron rich enol ether substrates such as benzofuran afforded

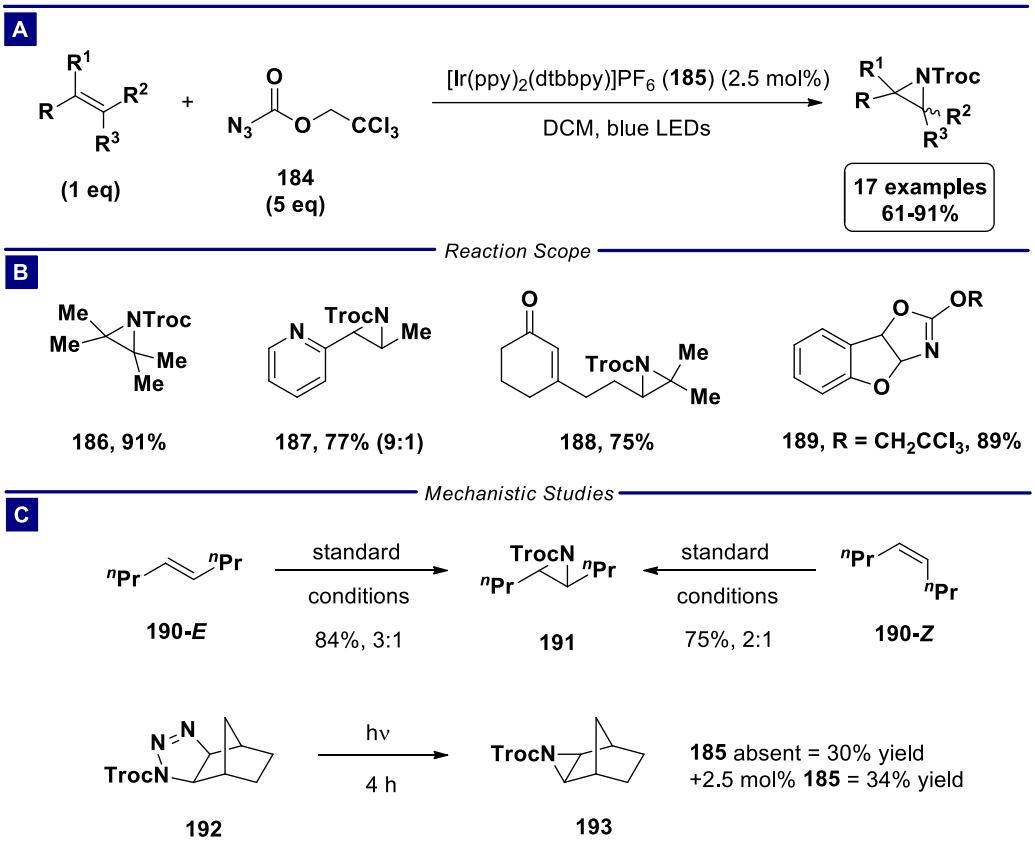

Scheme 3.2 – a) photocatalytic aziridination of alkenes using Ir-catalyst **185**; b) partial reaction scope. Values in parentheses indicate the diasteroisomeric ratio; c) mechanistic studies of photocatalytic aziridination; Troc = 2,2,2-trichloroethoxycarbonyl

the isomeric oxazoline product **189**. Mechanistic investigations support the reaction proceeding via a stepwise diradical mechanism rather than azide-alkene cycloaddition followed by rearrangement due the stereoconvergent nature of the reaction and the lack of rate enhancement on the photodecomposition of **192** in the presence of photocatalyst (Scheme 3.2C).

VLPC may also be used in the synthesis of cyclopropanes, as demonstrated by Ferreira with the photooxidising Cr(III) catalyst **196** (Scheme 3.3) and others.[124] In comparison to oxidative transformations using Ru(II) and Ir(III) complexes, oxidative transformations using first row transition metal (TM) complexes are more rare. However, in addition to the obvious advantages of first row TMs in terms of cost/availability, the photoexcited states of first row TM complexes also offer interesting and unique properties.[125,126] Thus Ferreira demonstrated that photocatalyst **196** could promote the cyclopropanation of a large number of electron rich styrenes under mild conditions. In this instance, the authors propose a mechanism whereby the styrene substrate undergoes single electron oxidation (SEO) to form radical cation **197** followed by addition of the diazo compound to form the first *C-C* bond (Scheme 3.3A). Loss of nitrogen from **198** leads to the "long-bonded" radical cation **199** which

undergoes single electron reduction (SER) to form the final product. An important consequence of these mechanistic details is found in the observed chemoselectivity (Scheme 3.3B).

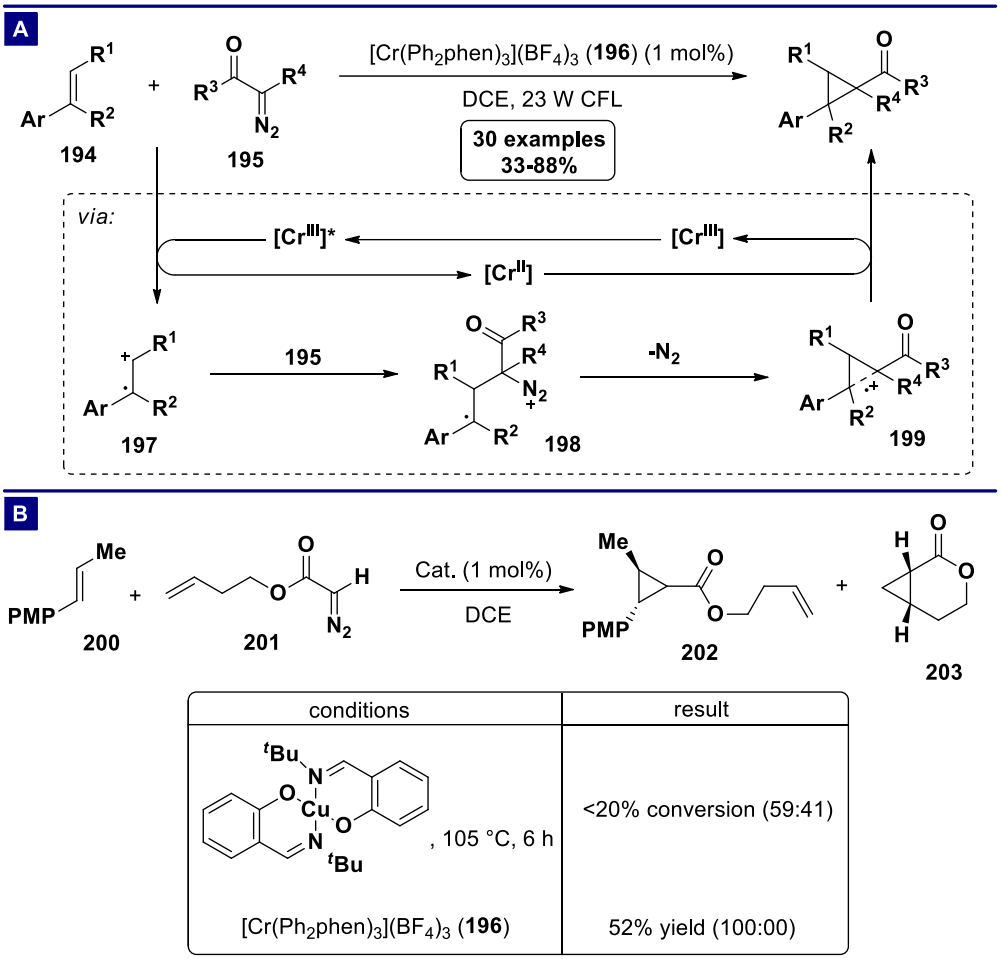

Scheme 3.3 – a) chromium photocatalysed cyclopropanation of radical cations; b) demonstration of the chemoselectivity in the chromium photocatalysed cyclopropanation. Values in parentheses indicate the ratio **202**:**203**; CFL = compact fluorescent light bulb; PMP = 4-methoxyphenyl

The reaction of *trans*-anethole (**200**) with diazo ester **201** using Cu-catalysed cyclopropanation delivers an isomeric mixture of products **202** and **203** with low conversion. On the other hand, Cr-catalyst **196** provides a moderate yield of the intermolecular cyclopropanation product **202** exclusively, due to the necessity for SEO of the alkene to initiate the reaction.

3.3.2 Synthesis of 4-Membered Rings

Arguably the principal application of traditional photochemistry has focused on the promotion of [2+2] cycloaddition reactions of unsaturated hydrocarbons. Analogously, the majority of VLPC cycloaddition reactions focus on the [2+2] cycloaddition of a wealth of different substrates. Interest in this area was sparked by reports from Yoon describing the intramolecular radical anion cycloaddition reactions of aryl substituted enones (Scheme 3.4A).[116] Key observations from the optimisation studies include the

necessity for both *N*,*N*-diisopropylethylamine (DIPEA) and lithium tetrafluoroborate ($LiBF_4$) (changing either ion inhibits conversion) in order for the reaction to proceed. The dependency on DIPEA is thought to arise from a reductive quench of $[Ru(bpy)_3]^{2+}$ to the highly reducing $[Ru(bpy)_3]^{+}$ species ($E_{1/2}$ = -1.33 V vs. SCE), while the lithium cation is proposed to act as a Lewis acid and the tetrafluoroborate anion aids with catalyst solubility. On this basis the authors proposed a mechanism initiated by SER of lithium coordinated enone **205** using $[Ru(bpy)_3]^{+}$ to generate radical anion **206** which then cyclises onto the second α,β-unsaturated system. A secondary bond forming cyclisation creates the 4,5-bicyclic intermediate **208** which undergoes SEO as part of a chain propagation step to form the product.[127] Investigations of the scope showed tolerance of a variety of aryl substituents along with Michael acceptors including enones, enoates and enamides and importantly, the products were obtained with uniformly high diastereoselectivity. However, the reaction fails to proceed in the absence of at least one aryl enone moiety, presumably because reduction of the substrate is endergonic in this case. Later reports from the same group overcame this limitation by employing a cleavable redox auxiliary to allow the synthesis of diester and diamide products.[128,129]

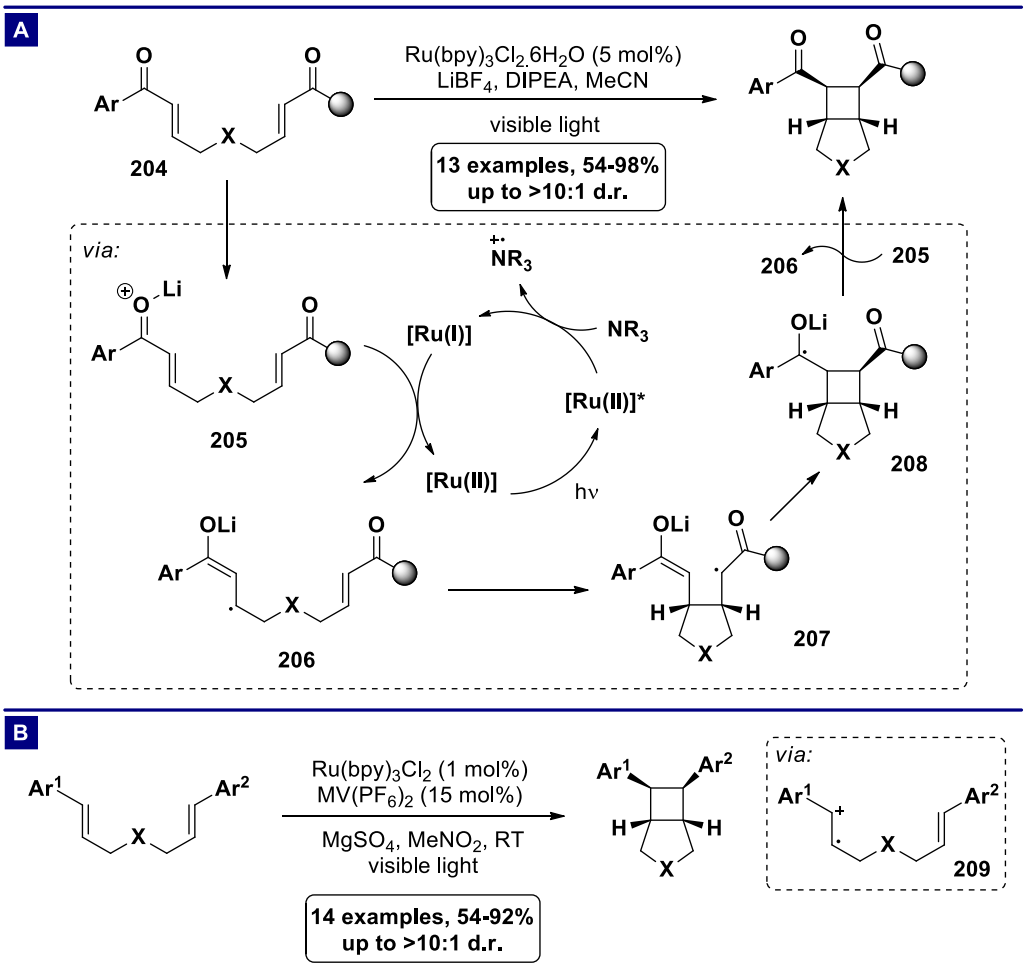

Scheme 3.4 – a) radical anion [2+2] cycloaddition of aryl enones and α,β-unsaturated carbonyl compounds; b) radical cation cycloaddition of electron rich styrenes; $MV(PF_6)_2$ = methyl viologen dihexafluorophosphate

Despite this, an obvious limitation to this methodology lies in the fact that the substrate must possess a suitable reduction potential in order for the reaction to proceed. However, by exploiting the capability of $[Ru(bpy)_3]^{2+}$ to undergo SEO, Yoon's lab were also able to incorporate a range of electron rich alkenes (Scheme 3.4B).[130] The methyl viologen additive is proposed to oxidise the excited state photocatalyst, generating the highly oxidising $[Ru(bpy)_3]^{3+}$ species (+1.29 V vs. SCE) which subsequently oxidises the styrene substrate to radical cation **209**. A series of cyclisation steps and SER then generates the product, analogously to the radical anion cycloadditions. Limitations were also uncovered when surveying the scope because in this instance an electron rich styrene is required for the reaction to be successful. This is best demonstrated by the fact that *ortho*- and *para*-methoxy substituted styrenes are reactive, but the *meta*-substituted analog is not. Indeed, although the author's ingenuity allowed a broad scope of substrates to participate in these processes, these examples do highlight the predominant problem within photoredox catalysis; the scope of reactions is limited by the redox properties of the chosen substrates which must participate in SET events. A series of other publications dealing with intermolecular variants of this reaction have also been made using transition metal,[131,132] heterogeneous,[133] and organic photoredox catalysts.[134]

More recent advances in VLPC [2+2] cycloadditions have focused on the ability of numerous photocatalysts to promote the triplet sensitisation of various alkenes. Inspired by Kutal's work on the valence photoisomerisation of a substituted norbornadiene,[135] Yoon's group reported the intramolecular [2+2] cycloaddition of various styrenes proceeding via an energy transfer mechanism.[136] Importantly, the scope of this reaction was found to be independent of the electronic nature of the styrene substituent, leading to a range of bicyclic products in high yield and with good diastereoselectivity (Scheme 3.5A). A particularly impressive demonstration of the mild nature of this protocol is the synthesis of **211** from an alkenyl iodide substrate. Moreover, the utility of this method was demonstrated in the synthesis of (±)-cannabiocicyclolic acid (**214**) and a subsequent report extended the method to include 1,3-dienes as the acceptor alkene.[137] In addition to expanding the scope of photocatalytic cycloadditions, energy transfer manifolds are also useful for attaining new selectivity. For example, the intramolecular [2+2] cycloaddition of styrenes and enones provides the "straight" addition products in all radical-ion cycloadditions. Conversely, a report from Kwon showed that a [2+2] cycloaddition of substrates **215** under energy transfer conditions produced bridged adducts **216** selectively.[138] Computational calculations into the origins of this selectivity suggest it arises as a result of the varying stability of 1,4-diradicals **217a-d**, formed following the first *C-C* bond formation (Scheme 3.5B). The more stable diradical **217a** then participates in a combination event to form the bridged products selectively. In addition to these methodologies, a number of systems using iridium,[139–141] ruthenium,[142] and flavin derived photocatalysts have also been described.[143,144]

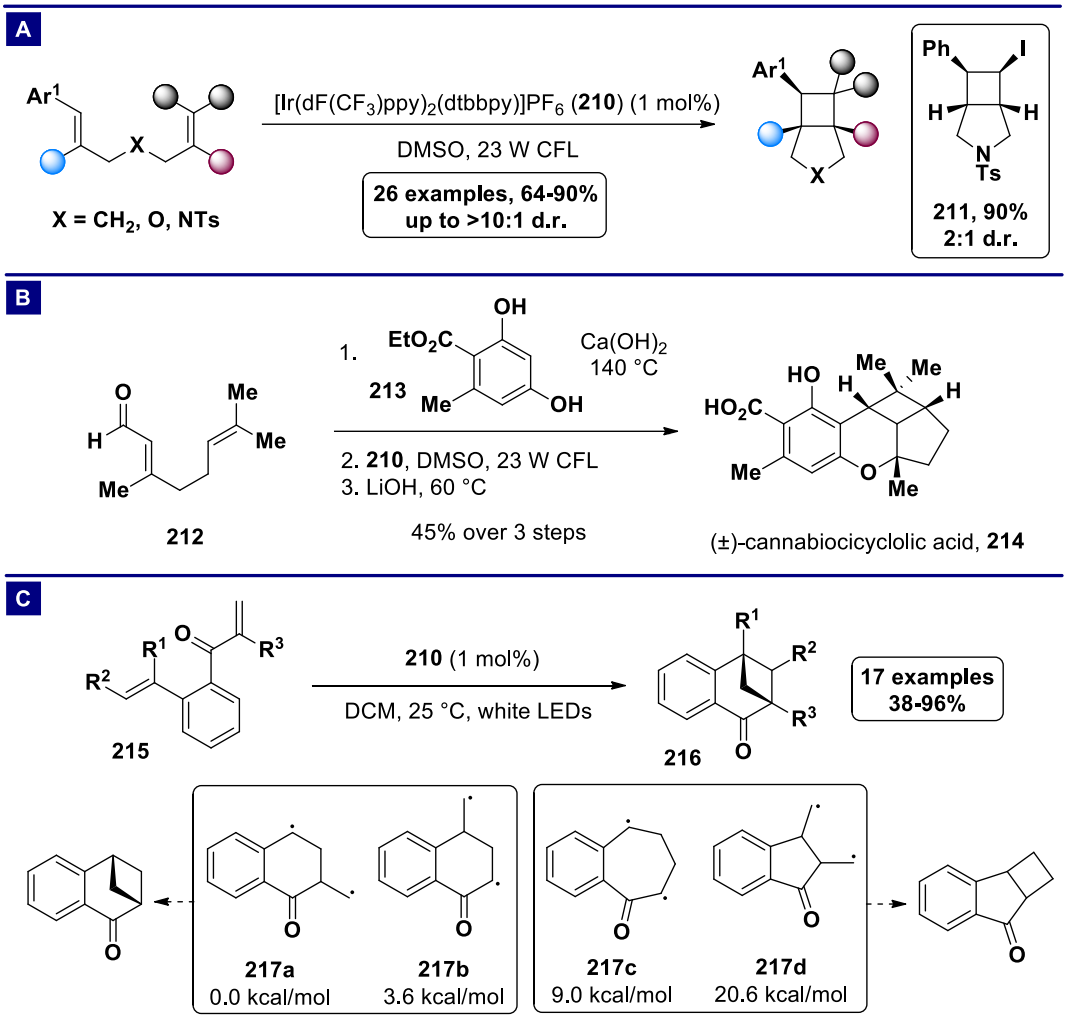

Scheme 3.5 – intramolecular [2+2] cycloaddition of styrenes by an energy transfer mechanism; b) synthesis of (±)-cannabiocicyclolic acid using Ir-catalysed triplet sensitisation; c) synthesis of bridged carbocycles using a [2+2] cycloaddition; CFL = compact fluorescent light bulb

Perhaps the most notable extension of this concept has been the development of enantioselective photocatalytic cycloaddition reactions. One such example involves the reaction of 2-hydroxychalcones **218** with dienes **219** under a dual catalytic system (Scheme 3.6).[145] Central to the design of this system is the principal that coordination of a Lewis acid to the substrate can result in a decrease of the substrate's triplet energy level. In their unbound state, 2-hydroxychalcones **218** possess a triplet energy level which is too high (54 kcal/mol) to participate in productive energy transfer with $[Ru(bpy)_3]^{2+}$ (46 kcal/mol). However, coordination of the scandium Lewis acid to both the phenolic and carbonyl oxygen atoms leads to a >20 kcal/mol reduction in the triplet energy, verified both experimentally and computationally, leading to the Sc-bound complex **220** readily participating in an energy transfer with photoexcited $[Ru(bpy)_3]^{2+}$. By exploiting this interaction, a potential non-selective background reaction is circumvented and therefore the vinylcyclobutane (VCB) products are obtained in high yield and with excellent enantioselectivity. This principle has since been disclosed in a number

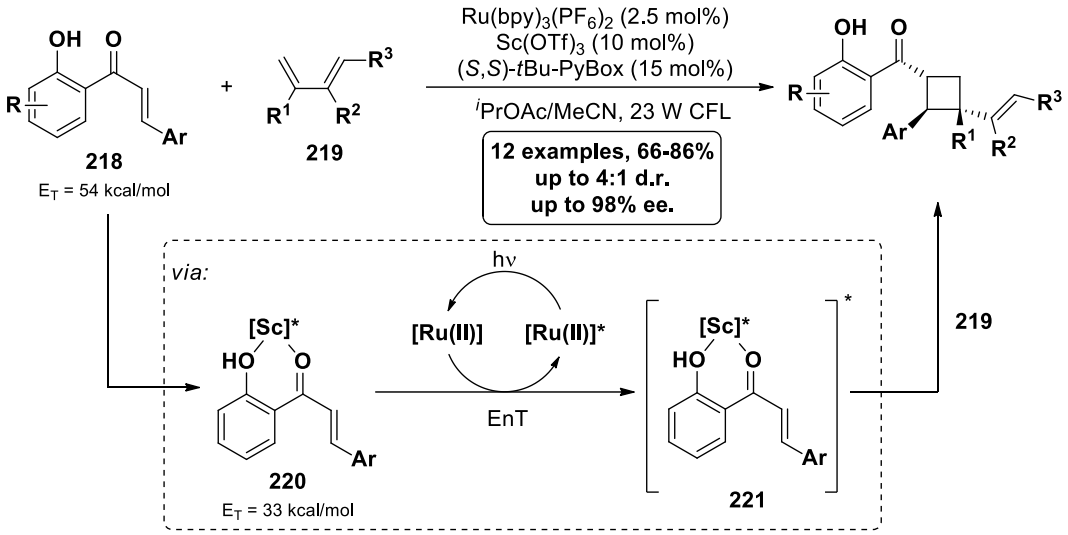

Scheme 3.6 – enantioselective [2+2] cycloaddition of 2-hydroxychalcones by Lewis acid catalysed triplet sensitisation; CFL = compact fluorescent light bulb; EnT = energy transfer

of other reports using Lewis acids and hydrogen bonding catalysts,[146–148] while many direct photochemical cycloadditions exploiting intermolecular interactions are also known.[149,150,159–161,151–158]

3.3.3 Synthesis of 5-Membered Rings

Another thriving area of research in photocatalysis involves the synthesis of 5-membered ring systems. The synthesis of carbocyclic motifs has largely focused on the [3+2] radical ion cycloadditions of α-cyclopropylketones which, analogously to the previously described [2+2] cycloadditions, are initiated by SET from the photocatalyst to a Lewis acid bound ketone (Scheme 3.7).[162] This intermediate then undergoes rapid ring opening to form distal radical **222** which is followed by 5-exo-trig cyclisation onto the alkene, secondary ring closure and SEO to afford the observed products. In this way, aryl cyclopropyl ketones could be coupled with various α,β-unsaturated carbonyls, alkenes and alkynes in good yield and diastereoselectivity. Asymmetric versions have since been reported and the principal of cyclopropyl ring opening has also been used in a number of other settings,[163–170] rendering this a useful method of synthesising cyclopentane containing compounds.

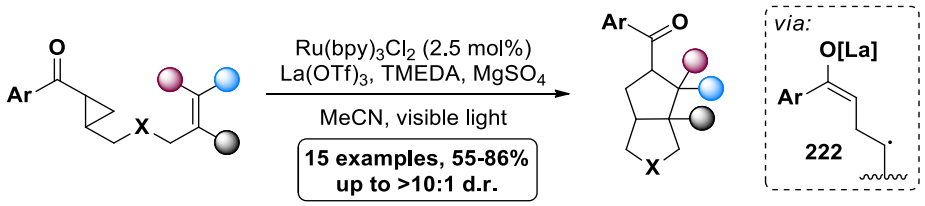

Scheme 3.7 – [3+2] radical anion cycloadditions of aryl cyclopropyl ketones

5-Membered heteroaromatic compounds are also accessible using photocatalysis, as demonstrated by Xiao in the synthesis of polysubstituted pyrroles from 2*H*-azirines (Scheme 3.8A).[171] Earlier reports

from Mattay had shown that 2*H*-azirines **223** were susceptible to SEO by the highly oxidising Fukuzumi catalyst, followed by a ring opening event.[172] By intercepting this intermediate with a range of electron deficient alkynes including propiolates and acetylenedicarboxylates, the desired pyrroles could be accessed in good yield. Furthermore, this strategy can also be used for the synthesis of oxazole containing compounds if the alkyne substrate is replaced by an aldehyde.[173] Expanding the repertoire of heterocycles accessible using VLPC, the same group described the synthesis of highly functionalised imidazoles from β-keto-*N*-arylamines and tosylmethylisocyanides (Scheme 3.8B).[174] This reaction exploits the propensity of amines to undergo SEO followed by the overall loss of a hydrogen atom to form imines **230** which can then react with isocyanides in a formal [3+2] cycloaddition. The mild nature of this oxidation step eliminates the necessity for handling potentially sensitive imine intermediates and allows the synthesis of *N*-aryl acyl substituted imidazoles in good yield. The combination of a photoinduced oxidation and annulation has also been used for the synthesis of pyrazole derivatives from hydrazines and 1,3-bis-electrophiles (Scheme 3.8C).[175] Although the condensation of hydrazines and 1,3-bis-electrophiles is widely reported, it often requires high temperature and/or hazardous oxidising agents. Comparatively, the addition of $Ru(bpy)_3Cl_2$ (2 mol%) and irradiation with visible light under air promoted the annulation of *N*-alkylhydrazines and electrophiles including malonitriles, malonates and enones in high yield under mild conditions. Although the role of the photocatalyst in this system is simply for the oxidation of the hydrazine substrates to the corresponding diimides **232**, it highlights how photocatalytic promotion of a reaction may allow it to proceed under unusually mild conditions.

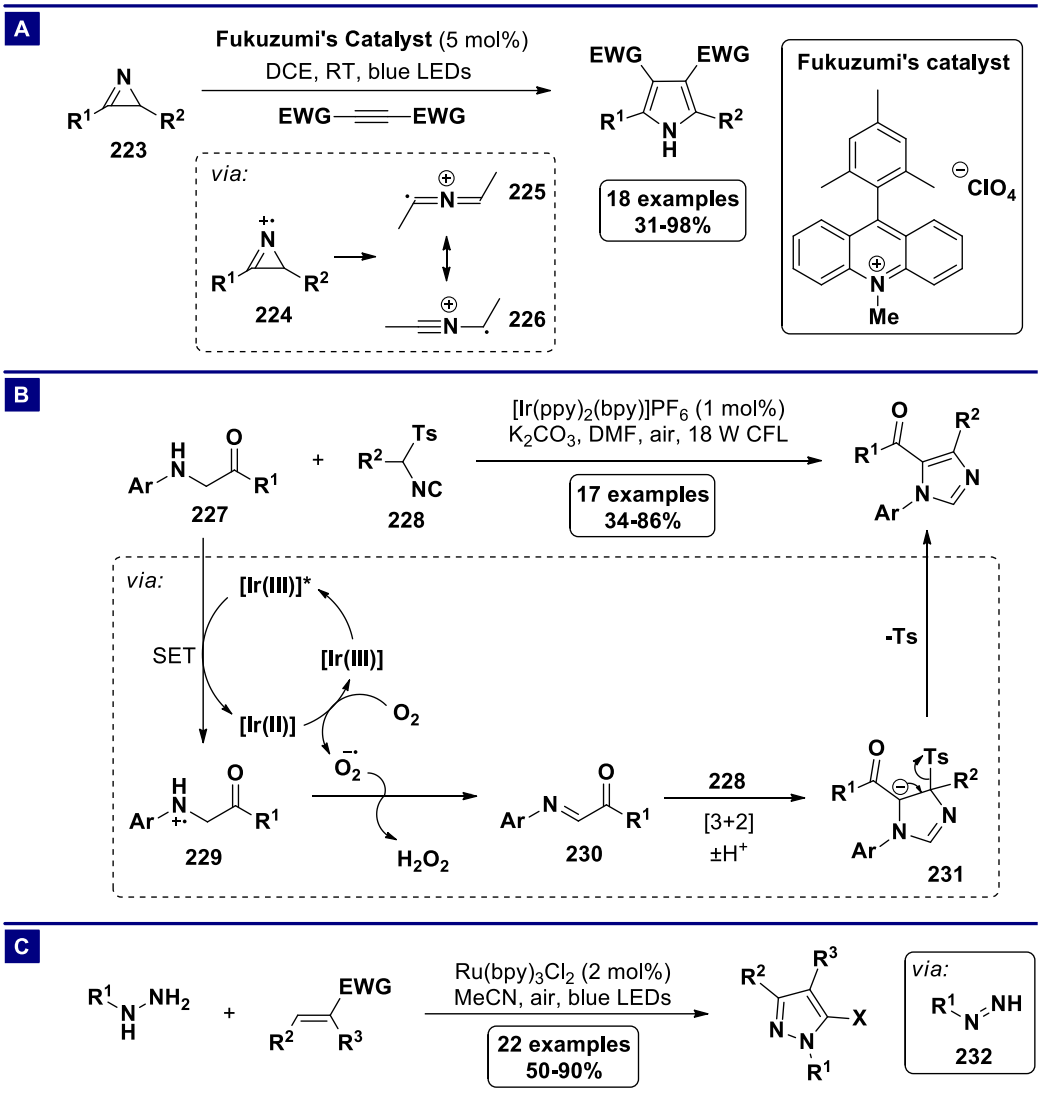

Scheme 3.8 – a) photocatalytic synthesis of polysubstituted pyrroles; b) photocatalytic annulation of *N*-arylamines and tosylmethylisocyanides; c) photocatalytic synthesis of pyrazoles; EWG = electron withdrawing group; CFL = compact fluorescent light bulb; SET = single electron transfer; LED = light emitting diode

In a similar manner, many photocatalytic systems have been developed as a means of accessing traditional dipolar reagents under mild conditions. The first such examples came almost simultaneously from Xiao[176] and Rueping[177] who disclosed the generation of azomethine ylides from tetrahydroisoquinolines and their subsequent [3+2] cycloaddition with different dipolarophiles (Scheme 3.9). The reaction begins with SEO of the amine by the excited state photocatalyst to produce radical cation **234** and Ru(I) species **235**, which reduces a molecule of oxygen to superoxide to return to the ground state. Hydrogen atom transfer and deprotonation of **234** by superoxide then creates the key azomethine ylide **236** which reacts with the dipolarophile to form the azacyclic products. Using this approach Rueping was a able to synthesise a range of polycyclic pyrrolidine derivatives, while a subsequent oxidation step in Xiao's procedure provided pyrrolo[2,1-a]isoquinolines in high yield. The

success of this methodology and the presence of the resulting product motifs in a vast array of alkaloid natural products resulted in a number of further reports utilising this approach.[178–181]

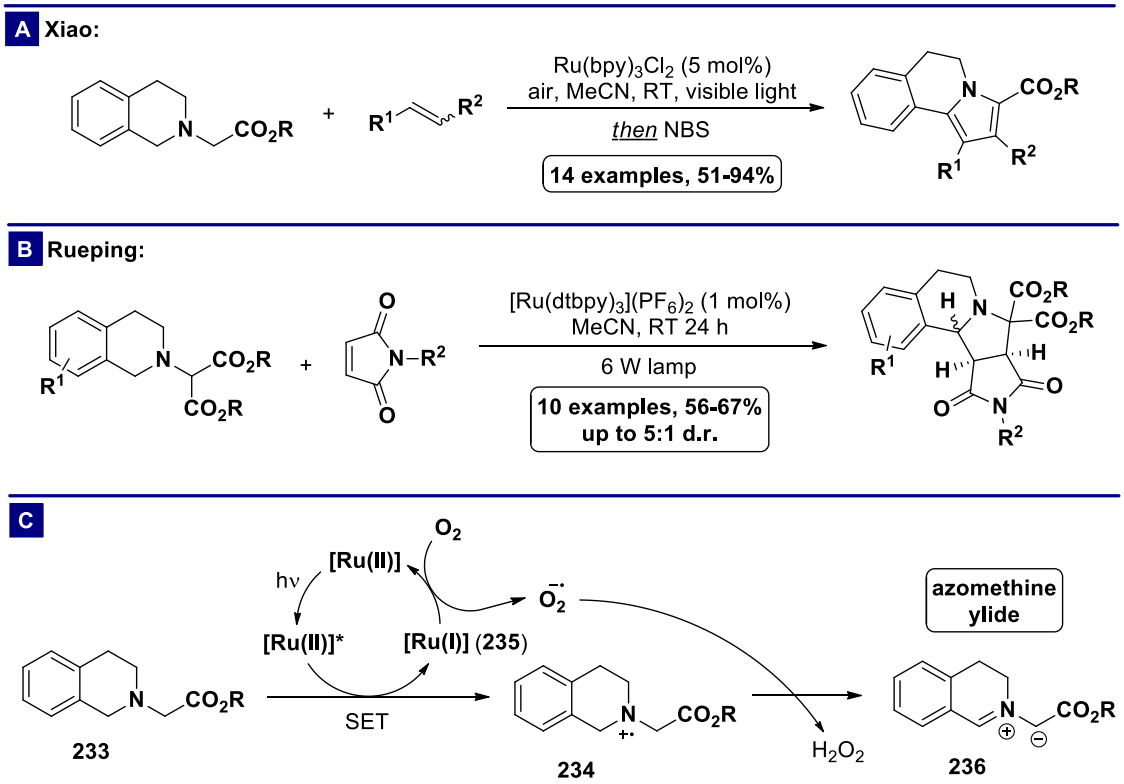

Scheme 3.9 – a) photocatalytic synthesis of pyrrolo[2,1-a]isoquinolines; b) photocatalytic [3+2] cycloaddition of azomethine ylides and maleimide derivatives; c) photocatalytic formation of azomethine ylides from tetrahydroisoquinolines; SET = single electron transfer

Nitrone cycloadditions are also known under VLPC conditions and utilise the same principles.[182,183] For example, *N*-arylhydroxylamines **237** derived from glyoxylic esters undergo oxidation and deprotonation to afford nitrones **239** which react in a [3+2] cycloaddition with alkenes **238** to form isoxazolidines (Scheme 3.10A). The scope is broad and the reaction was found to be tolerant of various ester substituents, a number of electronically varied *para*-substituted *N*-aryl groups and dipolarophiles including maleimides, styrenes and enol ethers. Alternatively, nitrones can be accessed from oxaziridines by means of a ring opening oxidation using Fukuzumi's catalyst (Scheme 3.10B).[184] Using Stern-Volmer luminescence quenching the authors were able to verify the presence of an interaction between the excited state photocatalyst and the oxaziridine substrate, reportedly leading to nitrone **242**. The subsequent addition of electronically activated alkynes and the ensuing [3+2] cycloaddition led to the production of a range of 4-isoxazoline products in variable yield.

The final class of dipolar reagent generated under VLPC conditions are nitrile oxides (Scheme 3.10C).[185] The authors reasoned that oxidative decarboxylation of imines **243** should generate nitrile oxide intermediates which could be intercepted by a range of Michael's acceptors. Indeed, Stern-Volmer

analysis shows oxone as the photoexcited state quenching species and the subsequent Ru(III) complex ($E_{1/2}$ = +1.29 V vs. SCE) is sufficiently oxidising to perform SEO of the carboxylate **244** ($E_{1/2}$ = +1.31 V vs.

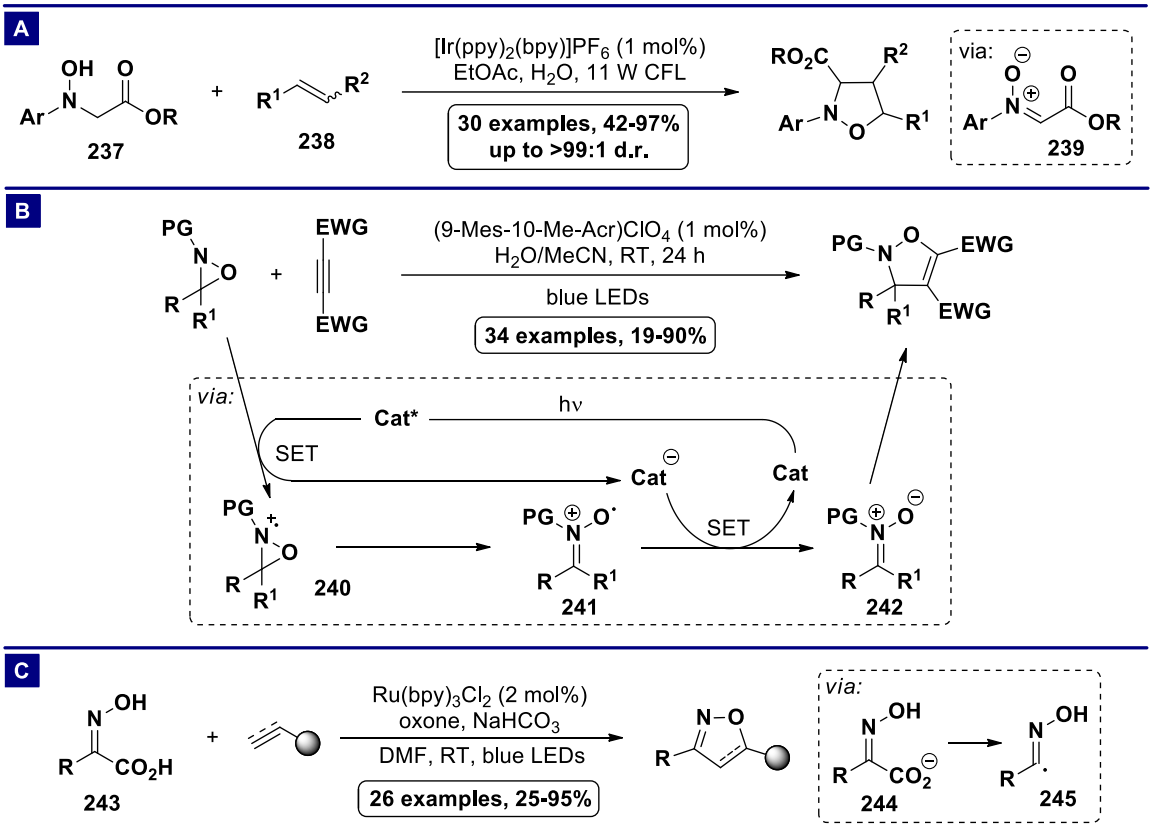

Scheme 3.10 – a) photocatalytic synthesis of nitrones from *N*-arylhydroxylamines; b) photocatalytic synthesis of nitrones from oxaziridines; c) photocatalytic synthesis and reactions of nitrile oxides; CFL = compact fluorescent light bulb; PG = protecting group; EWG = electron withdrawing group; SET = single electron transfer; LED = light emitting diode

SCE), leading to C-centred radical **245**. A second SEO event then generates the critical nitrile oxide dipole which reacts in a [3+2] cycloaddition. The substrate scope of this procedure was found to be very broad, incorporating both *N*-alkyl and *N*-aryl nitrile oxides in a reaction with alkenes bearing aldehyde, ketone, nitrile, sulfone and aryl/alkyl substituents. Moreover, alkynes are also suitable reaction partners for the synthesis of isoxazole heterocycles.

3.3.4 Synthesis of 6-Membered Rings

The synthesis of 6-membered rings using the Diels-Alder reaction is one of the most important bond forming reactions in organic chemistry and, due to this prominence, the factors governing the kinetics and regio- and stereoselectivity within the Diels-Alder reactions are well understood. Importantly, understanding the frontier molecular orbitals involved in the Diels-Alder reaction has led to the knowledge that reactions between electron rich dienes and electron poor dienophiles are facile compared to the reaction of two electron rich substrates, due to unfavourable orbital overlap in the

latter case. In this context, SEO of electron rich alkenes to create a radical cation intermediate can assist the Diels-Alder reaction of two electron rich substrates by: 1) increasing the overlap of the orbitals involved in the reaction, thus enhancing the rate; 2) switching the inherent polarisation of the two carbon synthon, leading to the opposite regioselectivity to that expected under thermal conditions.[186] Photocatalytic conditions that achieved the generation of a radical cation mediated Diels-Alder reaction were first reported Yoon and involved the reaction of electron rich alkene derivatives with an assortment of dienes (Scheme 3.11A).[187] Examination of the scope found the reaction to be compatible with electron rich styrenes, enamines and enol ethers as the dienophile, while substitution at various points around the diene is also tolerated. Advantageous to the photon promoted nature of this reaction, no dimerisation of the styrene substrate is observed which contrasts with electrochemical promotion of this reaction. Furthermore, due to the aforementioned features, this methodology could be employed in the synthesis of heitziamide A. A number of other groups have also reported on the [4+2] cycloaddition including Ferreira who used a photooxidising Cr(III) catalyst (Scheme 3.11B).[188–193] This study demonstrated that $[Cr(Ph_2phen)_3(BF_4)_3]$ **196** could catalyse a [4+2] radical cation Diels-Alder reaction with similar efficiency (in terms of yield and regio-/stereoselectivity) to the Ru-catalysed method developed by Yoon. However, an interesting dependence on oxygen was also observed under these conditions: although all steps of the proposed catalytic cycle are thermodynamically feasible in the absence of O_2, no reaction is observed under anaerobic conditions.

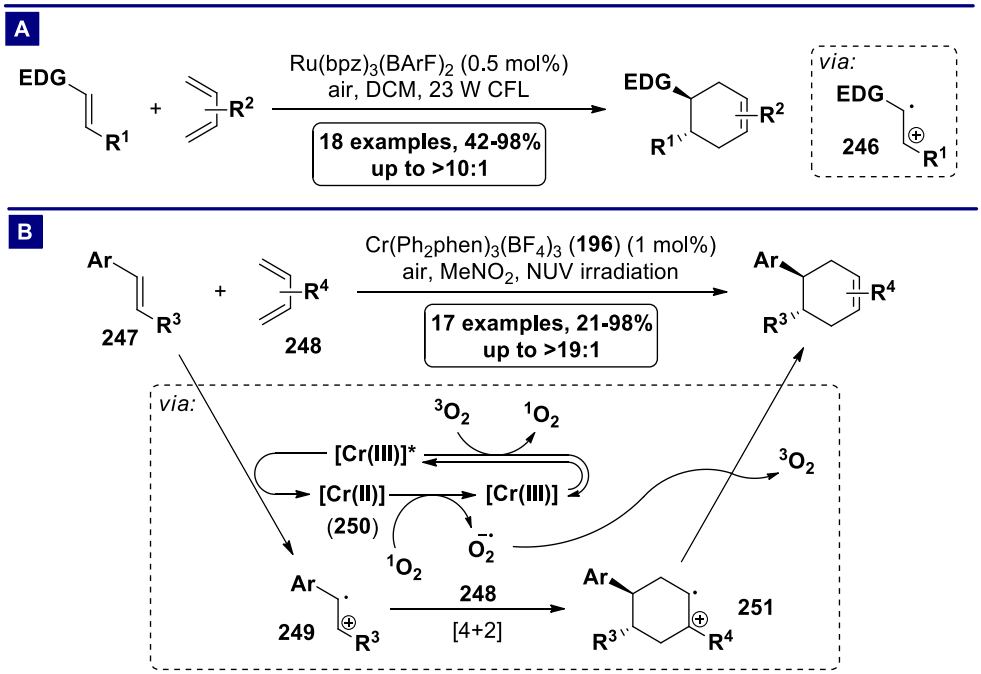

Scheme 3.11 – a) radical cation Diels-Alder reaction of electron rich styrenes; b) Cr-catalysed radical cation Diels-Alder reaction; EDG = electron donating group; CFL = compact fluorescent light bulb; NUV = near ultraviolet

Further mechanistic investigations by the same authors and others propose a dual role for oxygen in this system.[194,195] Firstly, triplet oxygen present in the reaction mixture can lead to a quenching of the excited state photocatalyst with concomitant generation of singlet oxygen. Secondly, the singlet oxygen generated *in situ* acts as an electron shuttle between Cr(II) species **250** and the cycloadduct **251.** It should be noted that singlet oxygen is required for the oxidation of Cr(II) species **250** ($E_{1/2}$ = -0.27 V vs. SCE) because triplet oxygen is not sufficiently oxidising ($E_{1/2}$ = -1.01 V vs. SCE). Therefore, although the first step initially seems unproductive it is vital for the success of this reaction. The enhanced utility of employing Cr-photocatalysts in this reaction has been further demonstrated by an extension to electron deficient styrene substrates (something which is usually precluded by unfavourable electron transfer) via an EnT mechanism.[196,197] Furthermore, photocatalytic cycloadditions reporting the synthesis of various tetrahydroquinoline[198,199] and chromane[200] derivatives have also been made.

4 Light Driven Reactions of Sydnones

4.1 Photochemical Reactions of Sydnones

4.1.1 Traditional Photochemistry

In addition to the well described thermal cycloaddition chemistry of sydnones, photochemical reactions, promoted by UV light, are also known. Indeed, the first report describing the interaction of sydnones with UV light was made over 50 years ago when Krauch disclosed the photochemical rearrangement of *N*-phenylsydnone into 3-phenyl-1,3,4-oxadiazol-2(3*H*)-one **252** (Scheme 4.1A).[201] Although the mechanistic pathway from the sydnone to **252** is not obvious, the observation that the reaction evolved CO_2 upon exposure to UV light caused the authors to propose nitrilimine **253** as an intermediate. The potential existence of a nitrilimine intermediate was corroborated by George's reports on the photochemical cycloaddition of 3,4-diphenylsydnone with diethylacetylene dicarboxylate (Scheme 4.1B).[202] Unlike the thermal cycloaddition process which affords pyrazole **255a**, the photochemical reaction was found to produce isomeric pyrazole **255b** and in order to explain this observation, the authors suggested that the reaction initially proceeds to nitrilimine **256** followed by a [3+2] cycloaddition with the alkyne dipolarophile. Further evidence for nitrilimines was found from the photolysis of 3,4-diphenylsydnone in benzene in the absence of other reactants, which created a mixture of products derived from nitrilimine **256**.[203] Initially, **256** undergoes photochemical dimerisation to dihydrotetrazine **257** which can undergo electrocyclic ring opening to common intermediate **258**. From this point, a series of HAT events, presumably from the solvent, leads to the reduced species **259**. Alternatively, ring closure and elimination of phenylnitrene creates 2,4,5-triphenyl-1,2,3-triazole **261**. On the other hand, amide adduct **263** is probably formed by the reaction of nitrilimine **256** with aniline to give hydrazone **262** which is hydrolysed on work up.

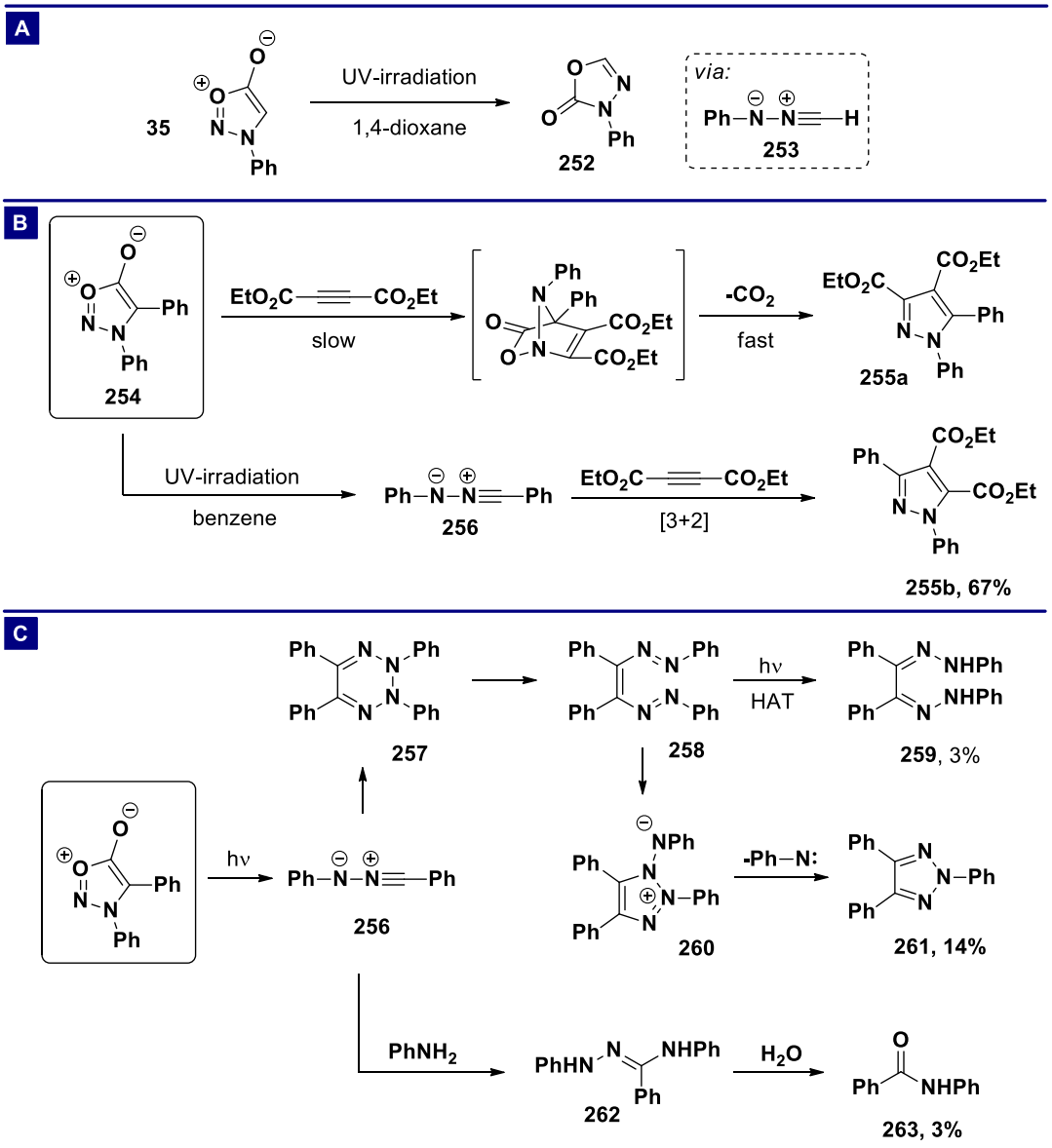

Scheme 4.1 – a) photochemical rearrangement of *N*-phenylsydnone; b) photochemical reaction of *N*-phenylsydnone and diethylacetylene dicarboxylate; c) photolysis of *N*-phenylsydnone; UV = ultraviolet; HAT = hydrogen atom transfer

More convincing evidence was obtained by the reaction of 3,4-diphenylsydnone with various additives.[204] The addition of methanol and trimethylborate produces hydrazonate **264** in 64% yield, evidenced by ^{1}H NMR spectroscopy and through observation of the phenylhydrazine and methyl benzoate hydrolysis products. Additionally, acetic acid reacts with **256** to form hydrazonic anhydride **265** which undergoes an intramolecular acyl group transfer to form the hydrazide product **266** in quantitative yield. Definitive evidence for the existence of nitrilimine intermediates was later obtained using laser flash photolysis (LFP).[205] This investigation observed an absorbance increase around 380 nm following the laser pulse, analogous to that observed in the photolysis of diphenyltetrazole and consistent with the formation of *C*,*N*-diphenyl nitrilimine **256**. However, the authors did not propose

a mechanism for this transformation. Further attempts to characterise the intermediates involved in this process have also been made with varying degrees of success. Analysis of the photolysis of different sydnone substrates using electron paramagnetic resonance (EPR) spectroscopy indicated the involvement of radical intermediates, although no mechanistic interpretations were put forward to explain these observations.[206,207] Alternatively, a combined experimental and computational study by Wentrup observed the formation of a lactone intermediate in the matrix photolysis of *N*-phenylsydnone.[208] During the course of the photolysis there is an accumulation of an intermediate which absorbs at 1881 cm^{-1} in the infrared (IR) spectrum, possibly due to bicyclic lactone **28**. In light of these studies, the commonly accepted mechanism for photochemical sydnone cycloadditions is shown in Scheme 4.2C. The reaction begins with excitation of the sydnone precursor **267** with UV light which then undergoes a formal electrocyclisation to lactone **268**. This is followed by the loss of carbon dioxide to give diazirine **269** which rearranges to the reactive nitrilimine **270**, followed by a [3+2] cycloaddition to form the observed products. More comprehensive investigations into the scope of this process have been made over many years and in all cases, the observed regiochemical outcome is consistent with the formation of a nitrilimine intermediate.[209–216]

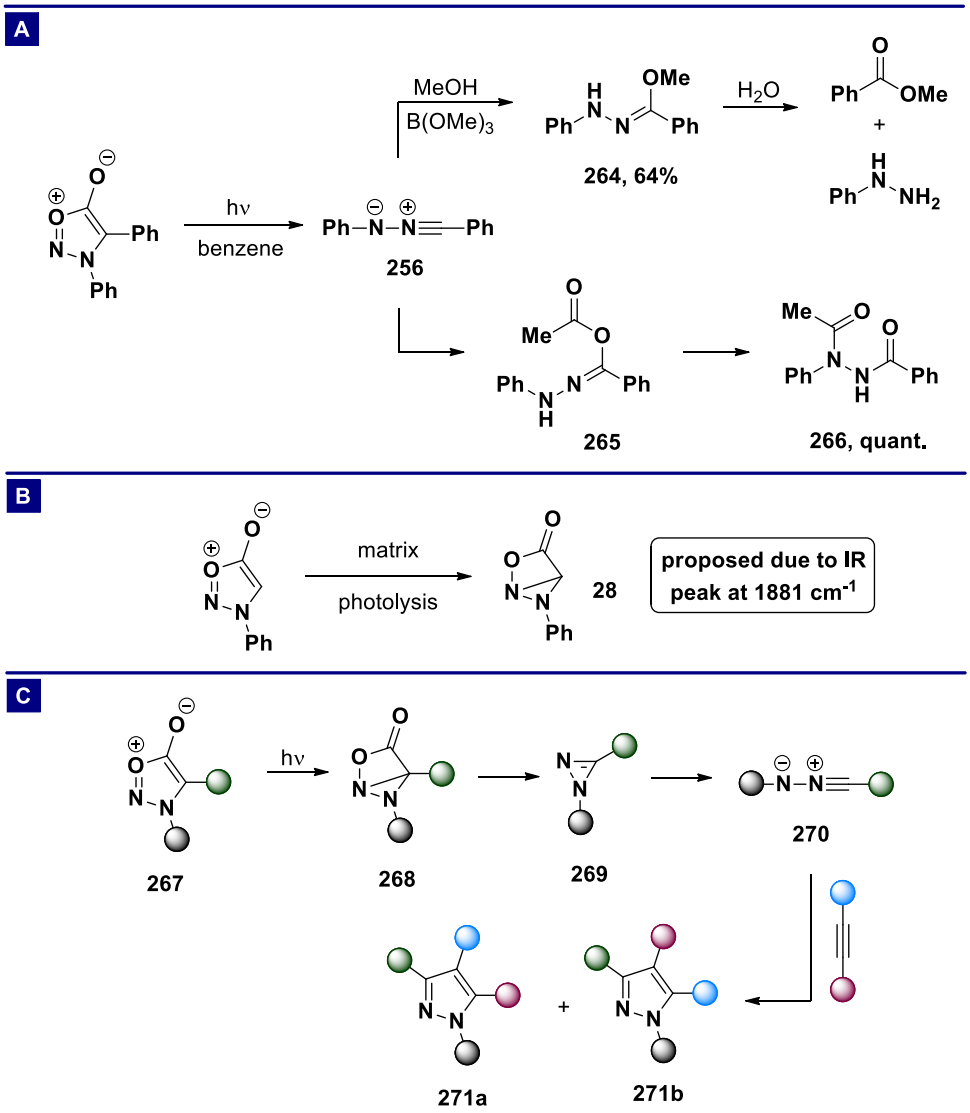

Scheme 4.2 – a) photochemical reaction of *N*-phenylsydnone and various additives; b) proposed bicyclic lactone intermediate in sydnone photolysis; c) accepted mechanism for photochemical sydnone cycloadditions; IR = infrared

4.1.2 Bioorthogonal Reactions

More recent advancements in the photochemistry of sydnones have focused on the development of photoclick reactions with a particular emphasis on their application to bioorthogonal chemistry. In comparison to other click reactions, light driven photoclick reactions offer a higher degree of spatial and temporal control rendering their development highly desirable for use in fields such as optochemical biology.[217] In the context of sydnones, Yu has shown that a variety of 3,4-diarylsydnones can undergo UV-promoted cycloaddition reaction with alkenes to produce pyrazoline products (Scheme 4.3A).[218] This reaction works with a number of electron deficient (**272**-**273**) and neutral (**274**-**275**) alkenes, giving the product in high yield but with varying degrees of regio- and stereocontrol. More importantly, the pyrazoline products formed in a reaction with *trans*-cyclooct-4-en-1-ol **274**

(TCO) were found to exhibit large degrees of fluorescence turn on (from 120 fold to 320 fold) along with a large Stokes shift (>150 nm). By varying the sydnone *N*- and *C*-substituents the authors discovered that the key to the obtaining favourable photophysical properties in the pyrazoline products was the use of sydnones bearing electron rich *N*-aryl groups and electron deficient *C*-aryl groups. Furthermore, the advantageous properties of the products were subsequently employed in cellular imaging by the same group.[219] Another study found that the same strategy could also be applied to the reaction of strained alkynes such as BCN, dibenzocyclooctyne (DIBO) and 3,3,6,6-tetramethylthiacycloheptyne (TMTH) for the synthesis of pyrazoles (Scheme 4.3B).[220] In this instance the reaction does not cause a fluorescence "turn on" but the highly reactive nature of the alkynes means the reactions are complete in significantly shorter times (<2 minutes). Therefore, the authors were able to use this approach to perform a bioorthogonal conjugation reaction.

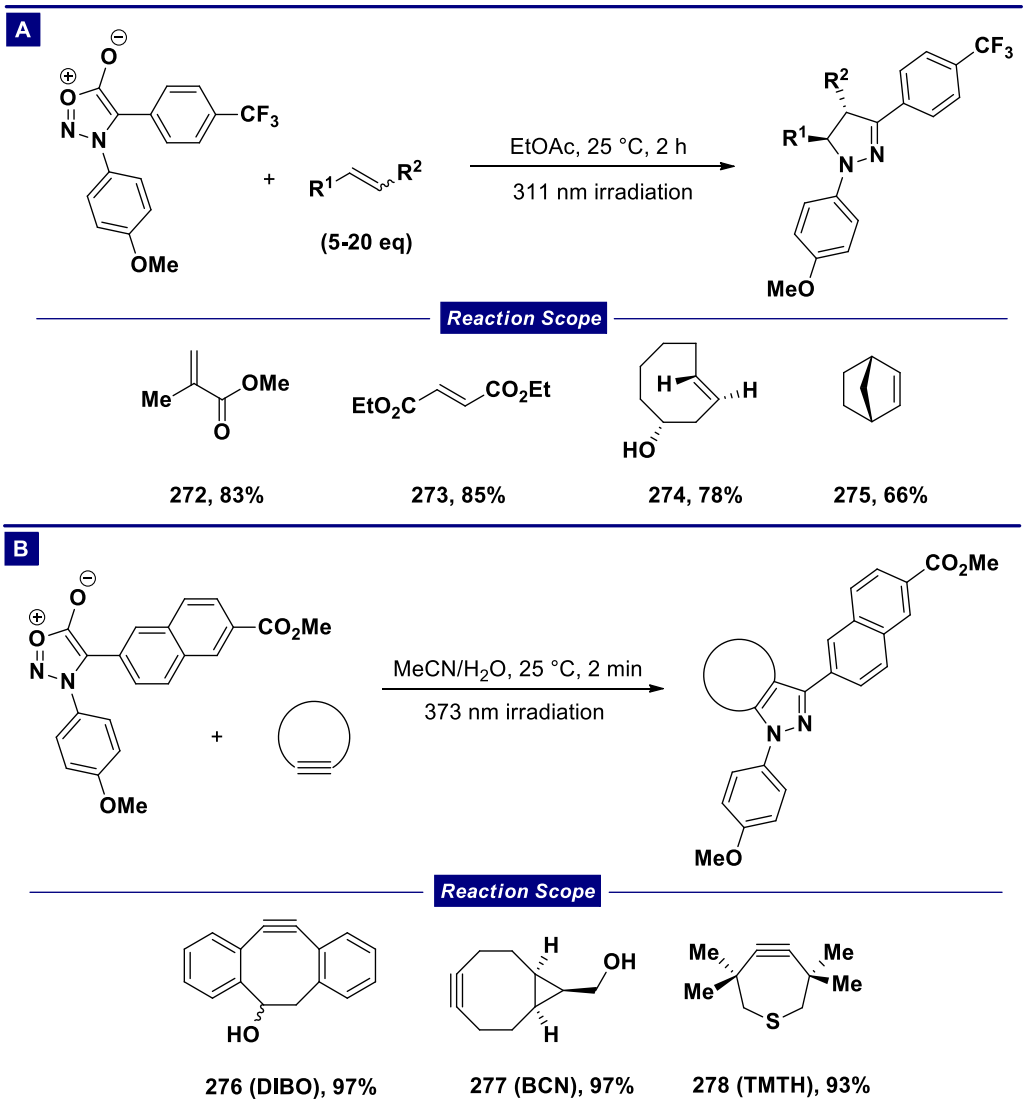

Scheme 4.3 – a) photoclick reaction of diarylsydnones and alkenes; b) photoclick reaction of diarylsydnones and strained alkynes

4.1.3 Conclusions

Sydnones are known to undergo UV promoted cycloaddition reactions with various alkenes and alkynes to form pyrazolines and pyrazoles, respectively. From a synthetic perspective, the potential of these reactions lies in the formation of alternative product regioisomers to those observed under thermal conditions, due to a photochemically induced sydnone-nitrilimine rearrangement. In spite of this, sydnone photochemistry has remained primarily limited to intramolecular reactions, while the recently reported photoclick reactions are performed on small scales (<30 mg) with a large excess (>5 eq) of dipolarophile. Thus, the development of a more general light induced sydnone cycloaddition protocol remains desirable.

4.2 Photocatalytic Sydnone Cycloadditions

4.2.1 Aims

At this juncture, our investigation into the cycloaddition reactions between sydnones and alkene dipolarophiles had encountered numerous problems. These reactions required high temperatures (>140 °C) and long reactions times (>24 h) to proceed efficiently and exhibited a fairly narrow substrate scope with respect to both reaction partners. As described above, sydnones participate in UV light promoted cycloadditions with numerous dipolarophiles and although these reactions proceed at ambient temperature, the development of a general visible light promoted sydnone cycloaddition protocol remained elusive and desirable. Given the Harrity group's longstanding interest in sydnone chemistry, and the ascendance of VLPC as a means of promoting transformations under benign conditions, we were intrigued to investigate the possibility of developing a photocatalytic sydnone cycloaddition reaction. In particular, we were interested in the radical cation [4+2] cycloaddition developed by several groups (vide supra) as a means of achieving this goal, based on the idea that sydnones can be considered as a 4-atom *N*-*O*-*C*-*C* synthon (Scheme 4.4).[187,188,192,196,221] An additional consideration in the case of sydnones is that following the cycloaddition-retrocycloaddition cascade a potentially promiscuous dipolar intermediate would be formed. Thus, we proposed that the fate of this dipole might be controlled by employing enamines as the dienophile in this process due to their ability to undergo SEO,[222] and the ability of the amine moiety to function as a leaving group following the cycloaddition step. Combining these considerations led to the mechanistic proposal shown in scheme 4.4B. Excitation of the photocatalyst with visible light creates the excited state catalyst **282** which performs SEO of the enamine **281** to create radical cation **283**. A [4+2] cycloaddition between **283** and the sydnone substrate **280** forms cycloadduct **284** which eliminates CO_2 to form dipolar intermediate **285**. Finally, SER and elimination of the amine would form the desired pyrazole products.

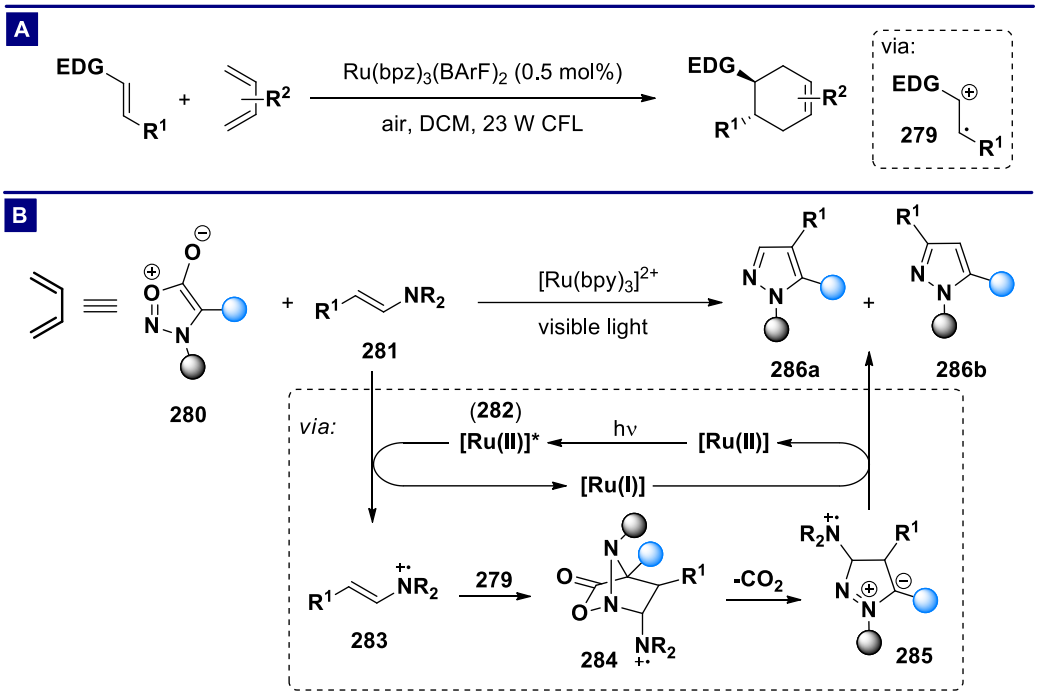

Scheme 4.4 – a) photoredox catalysed radical cation Diels-Alder reaction; b) proposed photocatalytic sydnone cycloaddition reaction; CFL = compact fluorescent light bulb

Therefore, the aims at the outset of this investigation were:

1) To investigate the possibility of using visible light photocatalysis to overcome the high temperatures (>140 °C) required for thermally promoted sydnone cycloadditions.

2) To examine whether the photocatalytic activation of sydnone-alkene cycloaddition reactions offers any additional advantages in terms of substrate scope.

4.2.2 Optimisation of the PSEC Reaction

To begin our examination of a potential photocatalytic sydnone-enamine cycloaddition (PSEC) reaction we explored the reaction of *N*-phenylsydnone (chosen once again due to its favourable physical and chemical properties) and enamine **138**, available from the condensation of hexanal and piperidine (Table 4.1). To our delight, irradiating a mixture of *N*-phenylsydnone (1 eq), **138** (3 eq) and $Ru(bpy)_3(PF_6)_2$ (5 mol%) in MeCN with blue light for 24 hours provided the corresponding 1,4-disubstituted pyrazole **287a** in 33% yield as a single regioisomer. However, analysis of the crude ^1H NMR spectrum showed complete conversion of the sydnone starting material, in spite of the fairly low yield. This observation led us to investigate the use of oxidising additives, based on the assumption that reductive decomposition of the sydnone may be caused by the highly reducing Ru(I) species (E_{ox} = -1.33 V vs. SCE) formed following SEO of the enamine. The addition of a stoichiometric quantity of methyl viologen dichloride ($MVCl_2$) was found to provide a small increase in yield alongside a

significant reduction in conversion of the sydnone (43% yield at ~50% conversion). It should be noted at this point that the exact role of this additive is still not fully understood, but some possibilities are discussed below (section 4.2.4.6). Nevertheless, these experiments provided a significant conclusion: catalytic quantities of the photosensitiser $[Ru(bpy)_3]^{2+}$ are capable of promoting an ***ambient temperature*** cycloaddition reaction between sydnones and enamines using ***visible light***.

Our efforts then turned to the optimisation of this catalyst system (Table 4.1). A screen of catalysts found the reaction to be unproductive using other ruthenium based photocatalysts and Fukuzumi's catalyst (entries 3, 4 and 6), while an Ir photosensitiser was able to promote the reaction with comparable efficiency (entry 5). It is not clear why using $Ru(bpy)_3Cl_2.6H_2O$ as a catalyst failed to provide any conversion to the products given the light absorbing species is the same as when using $Ru(bpy)_3(PF_6)_2$, but counter ion effects have been observed in other catalyst systems.[223] At this point we decided to perform further optimisation using $Ru(bpy)_3(PF_6)_2$ due to its decreased cost and increased availability relative to $[Ir(dF(CF_3)ppy)_2(dtbbpy)]PF_6$. A screen of solvents showed consistently high conversion and yield in polar aprotic solvents (entries 7-10), while chlorinated solvents also provided moderate conversion (entries 14 and 15). Conversely, the use of ethereal (entries 11-13) and hydrocarbon solvents (entries 16 and 17) provided low yields. Empirical observations would suggest that the observed reactivity differences may result from physical, rather than chemical, phenomena due an increased amount of solid precipitate in reactions which provided poor conversions (particularly Et_2O, $PhCF_3$ and $PhCH_3$). In this case, a reduction in catalyst solubility would result in diminished yields by lowering catalyst concentration and increasing light scattering (due to the turbid reaction mixture), reducing the effectiveness of the excitation step.

Table 4.1 – preliminary optimisation of the PSEC reaction[a]

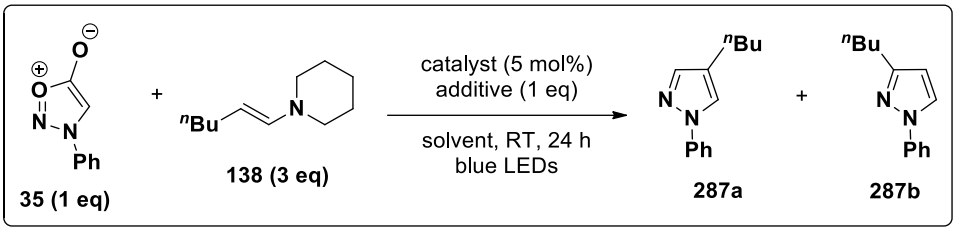

Entry	Catalyst	Additive	Solvent	Yield [%][b]	a:b[c]
1	$Ru(bpy)_3(PF_6)_2$	-	MeCN	33	>98:2
2	$Ru(bpy)_3(PF_6)_2$	$MVCl_2$	MeCN	43	>98:2
3	$Ru(bpy)_3Cl_2.6H_2O$	$MVCl_2$	MeCN	0	-
4	$Ru(bpz)_3(PF_6)_2$	$MVCl_2$	MeCN	0	-
5	$[Ir(dF(CF_3)ppy)_2(dtbbpy)]PF_6$	$MVCl_2$	MeCN	43	>98:2
6	$(9\text{-Mes-10-Me-Acr})ClO_4$	$MVCl_2$	MeCN	0	-
7	$Ru(bpy)_3(PF_6)_2$	$MVCl_2$	DMF	78	>98:2
8	$Ru(bpy)_3(PF_6)_2$	$MVCl_2$	DMA	66	>98:2
9	$Ru(bpy)_3(PF_6)_2$	$MVCl_2$	NMP	82	>98:2
10	$Ru(bpy)_3(PF_6)_2$	$MVCl_2$	DMSO	60	>98:2
11	$Ru(bpy)_3(PF_6)_2$	$MVCl_2$	1,4-dioxane	14	>98:2
12	$Ru(bpy)_3(PF_6)_2$	$MVCl_2$	THF	10	>98:2
13	$Ru(bpy)_3(PF_6)_2$	$MVCl_2$	Et_2O	0	-
14	$Ru(bpy)_3(PF_6)_2$	$MVCl_2$	DCM	35	>98:2
15	$Ru(bpy)_3(PF_6)_2$	$MVCl_2$	DCE	55	>98:2
16	$Ru(bpy)_3(PF_6)_2$	$MVCl_2$	$PhCF_3$	0	-
17	$Ru(bpy)_3(PF_6)_2$	$MVCl_2$	$PhCH_3$	0	-
18	-	$MVCl_2$	NMP	0	-
19	$Ru(bpy)_3(PF_6)_2$	-	NMP	52	>98:2
20[d]	$Ru(bpy)_3(PF_6)_2$	$MVCl_2$	NMP	0	-

[a] Reaction conditions: *N*-phenylsydnone (0.1 mmol), **138** (0.3 mmol), catalyst (5 µmol), additive (0.1 mmol) in solvent (1.0 mL, 0.1 M), 24 h at room temperature under blue LED irradiation; [b] yield determined by ^{1}H NMR spectroscopy using 1,3,5-trimethoxybenzene as an internal standard; [c] ratio determined by ^{1}H NMR analysis; [d] reaction performed in the dark; $MVCl_2$ = methyl viologen dichloride

Further optimisation of the reaction was then performed using as the $Ru(bpy)_3(PF_6)_2$ catalyst and NMP as the solvent (Table 4.2). Varying the substrate stoichiometry (entries 1-3) showed the importance of using an excess of enamine relative to sydnone, although the exact ratio is less important. Changing the enamine structure (entry 4 and 5) provided lower yields, as did either decreasing (entry 6) or increasing (entry 7) the quantity of additive. Investigation of other additives (entries 8-11) found

viologen additives to perform much better than quinone based alternatives and the reaction was also found to provide good conversion with lower catalyst loadings (entries 12-15). Eventually, we chose ethyl viologen diiodide (EVI_2) as the additive due to its comparable performance to $MVCl_2$ (73% vs. 82%) at a significantly reduced cost (EVI_2 = £3.86 g^{-1}, $MVCl_2$ = £48 g^{-1}).

Table 4.2 – further optimisation of the PSEC reaction[a]

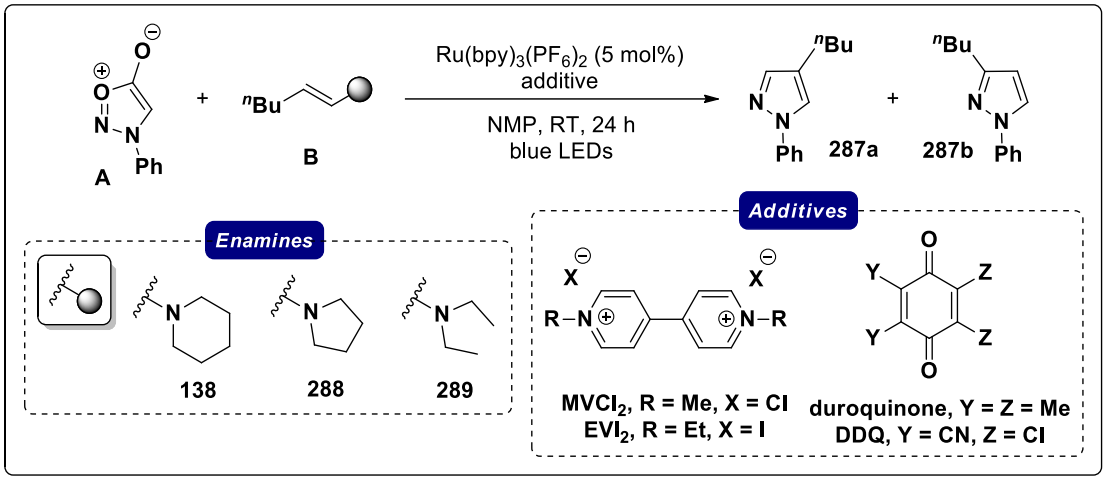

Entry	Enamine	A:B	Additive (eq)	Yield [%][b]	287a:287b[c]
1	**138**	3:1	$MVCl_2$ (1)	43	>98:2
2	**138**	1:2	$MVCl_2$ (1)	75	>98:2
3	**138**	1:4	$MVCl_2$ (1)	72	>98:2
4	**288**	1:3	$MVCl_2$ (1)	36	>98:2
5	**289**	1:3	$MVCl_2$ (1)	61	>98:2
6	**138**	1:3	$MVCl_2$ (0.5)	69	>98:2
7	**138**	1:3	$MVCl_2$ (2)	62	>98:2
8	**138**	1:3	-	52	>98:2
9	**138**	1:3	EVI_2 (1)	73	>98:2
10	**138**	1:3	DDQ (1)	13	>98:2
11	**138**	1:3	Duroquinone (1)	41	>98:2
12[d]	**138**	1:3	EVI_2(1)	47	>98:2
13[e]	**138**	1:3	EVI_2 (1)	67	>98:2
14[f]	**138**	1:3	EVI_2 (1)	59	>98:2
15[g]	**138**	1:3	EVI_2 (1)	60	>98:2

[a] Reaction conditions: *N*-phenylsydnone (0.1 mmol), enamine (0.3 mmol), $Ru(bpy)_3(PF_6)_2$ (5 µmol), additive (0.05-0.2 mmol) in NMP (1.0 mL, 0.1 M), 24 h at room temperature under blue LED irradiation; [b] yield determined by ^1H NMR spectroscopy using 1,3,5-trimethoxybenzene as an internal standard; [c] ratio determined by ^1H NMR analysis; [d] $Ru(bpy)_3(PF_6)_2$ (4 µmol); [e] $Ru(bpy)_3(PF_6)_2$ (3 µmol); [f] $Ru(bpy)_3(PF_6)_2$ (2 µmol); [g] $Ru(bpy)_3(PF_6)_2$ (1 µmol); $MVCl_2$ = methyl viologen dichloride; EVI_2 = ethyl viologen diiodide; DDQ = 2,3-dichloro-5,6-dicyano-1,4-benzoquinone

With an optimised set of conditions developed on NMR scale, we began to increase the scale of the reaction to produce isolable quantities of the pyrazole product (Table 4.3). An increase to 0.5 mmol of sydnone substrate resulted in a significantly decreased yield of 22% after 24 hours alongside a 58% recovery of the unreacted sydnone. Indeed, achieving consistent results when scaling photocatalytic processes is notoriously difficult due to decreased transmission of the incident light through larger volumes of solvent. In the case of the PSEC reaction, it is possible that the decreased conversion at 0.5 mmol stems from this phenomenon: although the reactants are orange, the solution rapidly turns black when everything is mixed together. Increasing the length of reaction to 48 hours provided an increased yield of 50% but longer reaction times gave no further benefit. In addition to the observed rate decrease, the isolated yields of **287a** were diminished by the formation of α,β-unsaturated aldehyde **290** which proved difficult to separate chromatographically. Based on the assumption that **290** arises from the aldol dimerisation of the enamine substrate, we attempted several alterations to the protocol to try and favour the cycloaddition process. Firstly, running the reaction with a large excess of sydnone relative to enamine provided comparative results, while subsequent experiments adding the enamine in either 2 (entry 5) or 3 (entry 6) portions failed to increase the yield of **287a**. Finally, a reaction using a large excess of enamine to compensate for the consumption of **138** by the

Table 4.3 – optimisation of the PSEC reaction at 0.5 mmol scale

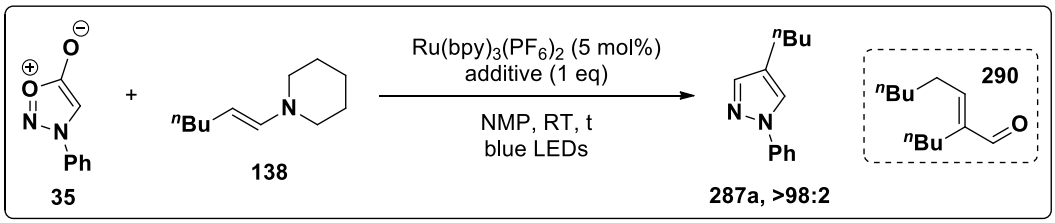

Entry	35:138	Additive	t [h]	Yield [%][b]
1	1:3	EVI_2	24	22
2	1:3	EVI_2	48	50
3	1:3	EVI_2	72	50
4	5:1	-	48	43
5[c]	1:3	EVI_2	48	40
6[d]	1:3	EVI_2	48	36
7	1:3	$MVCl_2$	48	39
8	1:6	EVI_2	48	49[e]

[a] Reaction conditions: *N*-phenylsydnone (0.5 - 2.5 mmol), enamine (0.5 - 3.0 mmol), $Ru(bpy)_3(PF_6)_2$ (25 µmol), additive (0.5 mmol) in NMP (5.0 mL, 0.1 M), for the specified time at room temperature under blue LED irradiation; [b] yield of isolated compound; [c] **138** added in 2 portions; [d] **138** added in 3 portions; [e] **290** isolated in 16% yield; EVI_2 = ethyl viologen diiodide; $MVCl_2$ = methyl viologen dichloride

unproductive pathway provided no benefit to the cycloaddition reaction and the aldehyde **290** was isolated in 16% yield (entry 8).

Different purification methods were also assessed in an attempt to improve the isolated yields (Scheme 4.5). However, stirring the crude product from the cycloaddition reaction with excess piperidine (5 eq) before removal of the solvent under vacuum and filtration through basic aluminium oxide (pH 9-10) proved unsuccessful in removing **290**. Moreover, washing the crude product with a saturated solution of sodium bisulfite ($NaHSO_3$) also failed to remove **290** and although the addition of sodium borohydride ($NaBH_4$) significantly simplified the chromatographic separation, low yields of the desired pyrazole were still obtained.

The lack of success in removing **290** the led to further attempts to reduce the formation of this by-product. It is possible to imagine that the formation of **290** from the enamine substrate might operate under acid catalysed conditions via the corresponding iminium ion species. However, attempts to buffer the reaction mixture through the addition of a stoichiometric quantity of K_2CO_3 proved deleterious to the reaction (possibly as a result of increased turbidity) (Scheme 4.6A, path a). On the other hand, we hypothesised that the formation of **290** might be inhibited using an organocatalytic protocol to reduce the enamine concentration. Gratifyingly, we were able to react *N*-phenylsydnone with hexanal directly in the presence of sub-stoichiometric quantities of piperidine (40 mol%) to provide **287a** in 62% yield (Scheme 4.6A, path b). A decrease in organocatalyst loading to 20 mol% provided an even higher yield of 86% but a further decrease was less effective.

The unique reactivity offered by the development of this dual-catalytic system is highlighted in Scheme 4.6B. The thermally promoted reaction between *N*-phenylsydnone and 1-hexyne requires high

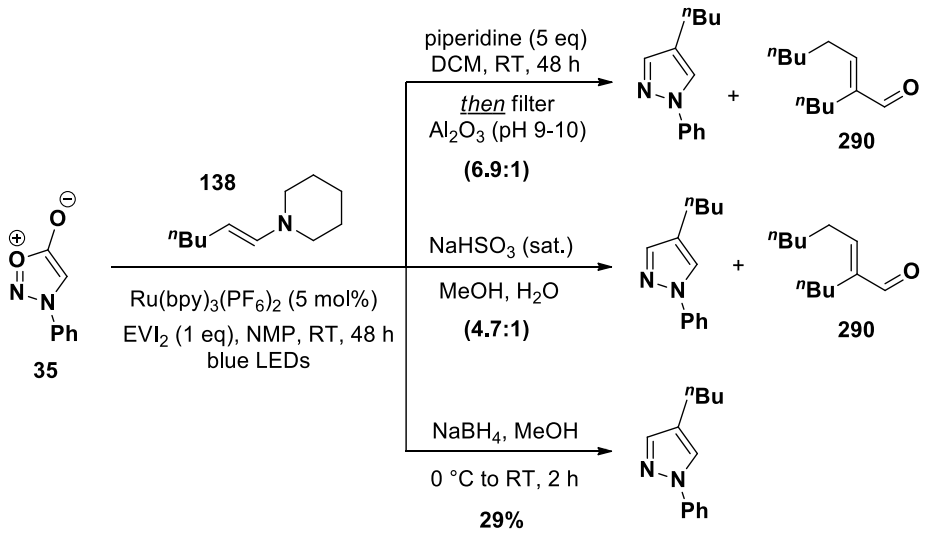

Scheme 4.5 – purification methods attempted for the removal of aldol condensation product **290;** EVI_2 = ethyl viologen diiodide; RT = room temperature

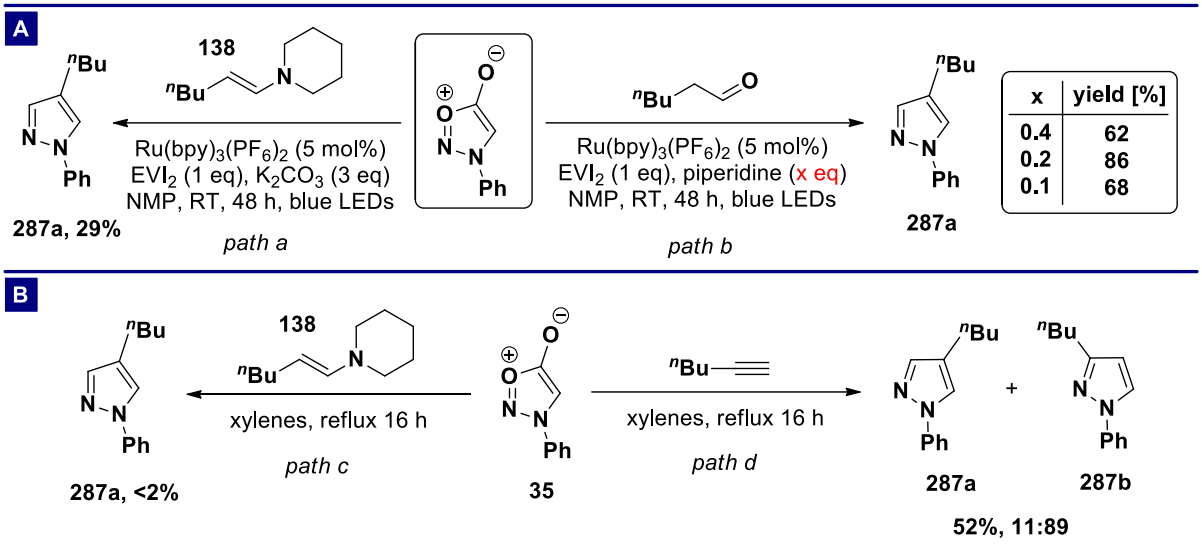

Scheme 4.6 – a) attempted base buffering and organocatalytic PSEC reactions; b) comparison of the PSEC reaction to other sydnone cycloaddition methods; EVI_2 = ethyl viologen diiodide

temperatures and long reaction times to form a regioisomeric mixture of pyrazole products in moderate yield. Additionally, the use of enamines as substrates under thermal conditions fails to achieve conversion to the desired pyrazoles, even after heating over extended periods. Thus, the synergistic combination of VLPC and organocatalysis facilitates a sydnone-enamine cycloaddition reaction under remarkably mild conditions with complementary regioselectivity and higher levels of regiocontrol compared to sydnone-alkyne cycloadditions.

4.2.3 Scope of the PSEC Reaction

Having established successful conditions for an organocatalytic PSEC reaction, we next turned our attention to assessing the reaction scope (Table 4.4). Electronically neutral and electron rich *N*-arylsydnones reacted smoothly to afford pyrazoles **291a**/**292a** in high yield and with complete regioselectivity. Furthermore, sydnones bearing electron withdrawing *N*-aryl groups such as nitrile (**293a**) and halides (**294a**-**296a**) are tolerated, opening up the possibility for further functionalisation. In addition to butyl and isopropyl moieties, other alkyl groups including methyl (**115a**), cyclohexyl (**298a**-**300a**) and benzyl (**131a**) could all be installed into the pyrazole products in high yield. The use of phenylacetaldehyde as a substrate allowed access to 1,4-diphenylpyrazole (**302a**) in moderate yield. Protected amines (**306a**) and alcohols (**303a**) are also applicable and carbonyl derivatives including ester (**304a**) and amide (**305a**) had no adverse impact on the reaction. Throughout the course of this investigation, dimethylamine (Me_2NH) was discovered as a more general organocatalyst for this procedure, offering the advantage of improved yields and atom economy. Limitations in the current methodology were also uncovered; although *meta*-substituted *N*-arylsydnones were found to react smoothly (**301a**), *ortho*-substituted analogues do not participate in the reaction (e.g. **307**).

Table 4.4 – scope of the PSEC reaction[a]

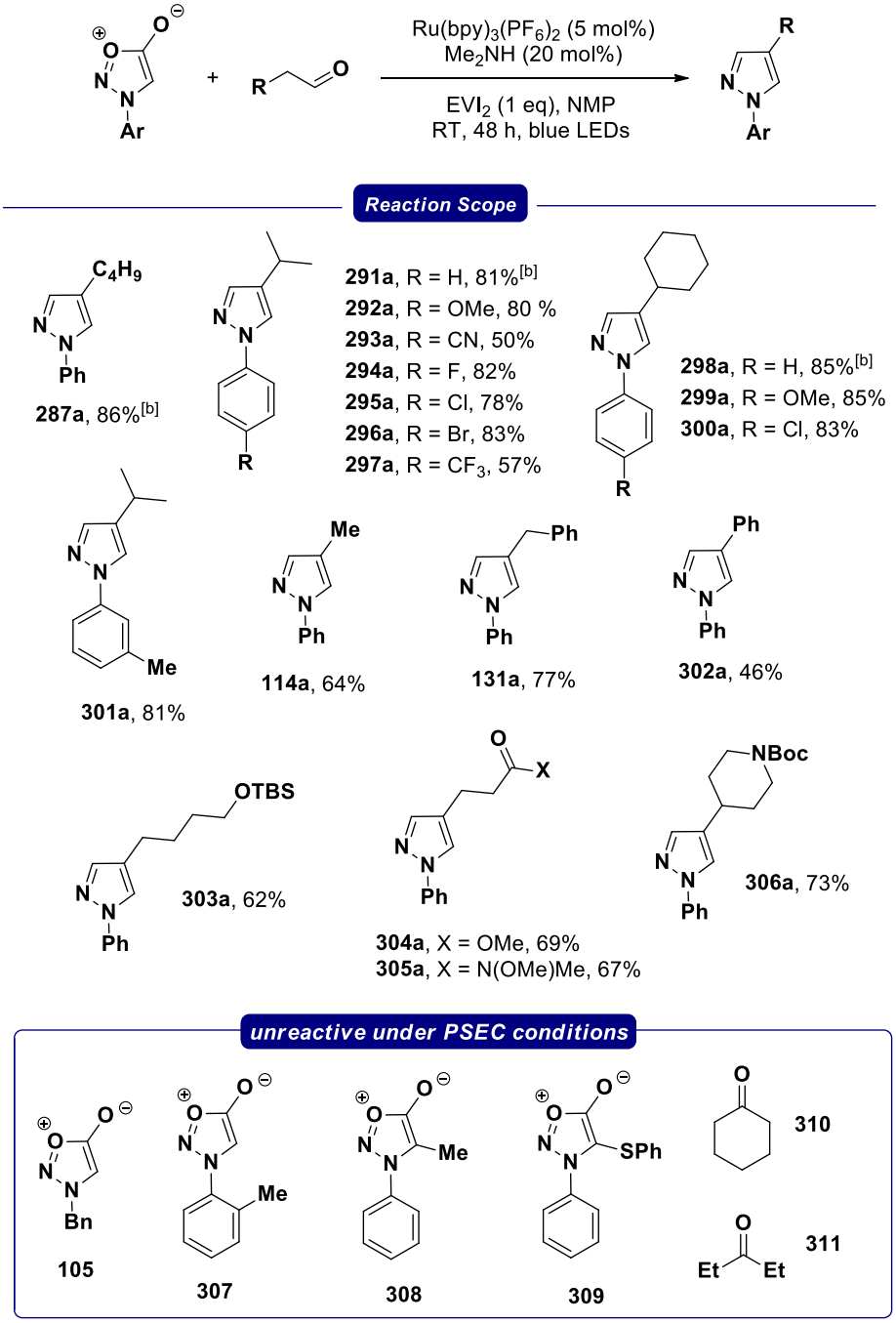

[a] Reaction conditions: sydnone (0.5 mmol), aldehyde (1.5 mmol), Me_2NH (0.1 mmol, 20 mol%), $Ru(bpy)_3(PF_6)_2$ (25 µmol, 5 mol%), EVI_2 (0.5 mmol), NMP (5 mL, 0.1 M), 48 h at room temperature under blue LED irradiation. [b] piperidine (0.1 mmol); EVI_2 = ethyl viologen diiodide

Moreover, *N*-alkylsydnones (**105**) and *C*4-substituted *N*-arylsydnones (**308**/**309**) were found to be inert under PSEC reaction conditions. Several ketone substrates (**310**/**311**) were also surveyed in an attempt to increase the number of substituents on the pyrazole products, but no reactivity was observed. In an effort to expand the scope of the reaction we then targeted the synthesis of several sydnone substrates which might be amenable to an intramolecular PSEC reaction (Scheme 4.7).

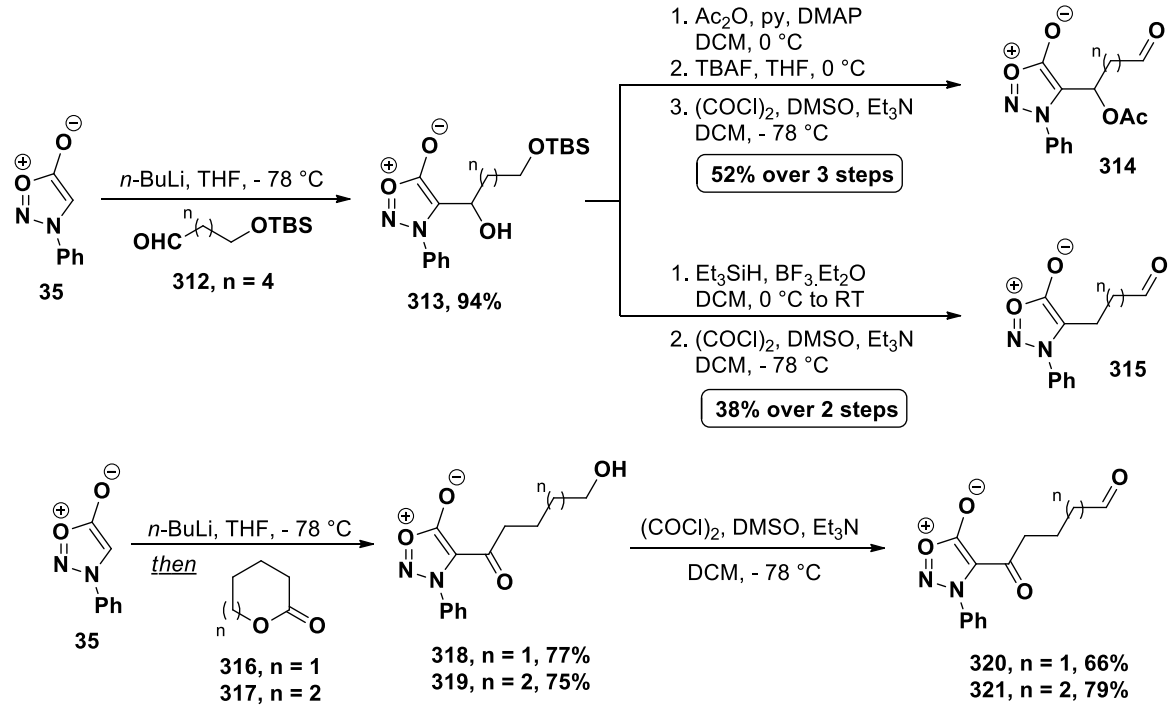

Scheme 4.7 – synthesis of aldehyde tethered sydnones

Initially, deprotonation of *N*-phenylsydnone with *n*-BuLi followed by the addition of aldehyde **312** gave the alcohol containing sydnone **313**. Acetyl protection of the free hydroxyl group followed by removal of the TBS protecting group with *tetra*-*n*-butylammonium fluoride (TBAF) and subsequent Swern-oxidation then provided aldehyde **314** in 52% yield over the 3 steps. Alternatively, cationic reduction of **313** using triethylsilane (Et_3SiH) and boron trifluoride ($BF_3.Et_2O$) achieved simultaneous reduction and removal of the TBS group in moderate yield and a subsequent Swern-oxidation then delivered the aldehyde containing cycloaddition precursor **315** in 38% yield over the two steps. Finally, the reaction of *N*-phenylsydnone with either δ-valerolactone (**316**) or ε-caprolactone (**317**) gave the keto-alcohols **318** and **319** which could be oxidised to the corresponding aldehydes **320** and **321**, respectively. An analysis of the PSEC reactions of these compounds began with keto-aldehyde **320**, but no conversion to the pyrazole product was detected (Table 4.5). Interestingly, keto-aldehyde **321** bearing a longer carbon linker was found to participate in the cycloaddition reaction, but poor yields were observed (entry 2). Conversely, methylene (**315**) and methine (**314**) substituted substrates provided much higher yields of the bicyclic pyrazoles **324** and **325** under PSEC conditions (entries 3 and 6). The cause of this reactivity difference is not immediately apparent, but these results successfully demonstrate an expansion of the current methodology to *C*4-substituted sydnones and also highlight an influence on reactivity caused by the hybridisation state of the carbon atom adjacent to the sydnone ring.

Table 4.5 – scope of the intramolecular PSEC reaction[a]

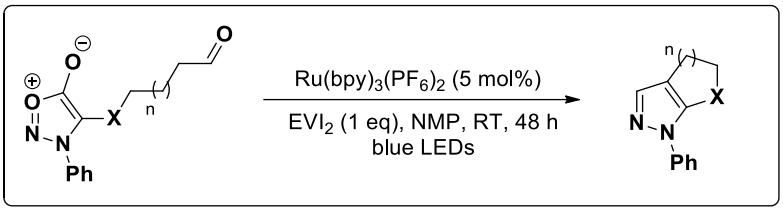

Entry	Substrate	X	n	Concentration [mM]	Product	Yield [%][b]
1	**320**	C=O	1	100	**322**	0
2	**321**	C=O	2	100	**323**	12
3	**315**	CH_2	2	100	**324**	78
4	**314**	CHOAc	2	100	**325**	32
5	**314**	CHOAc	2	50	**325**	34
6	**314**	CHOAc	2	25	**325**	52

[a] Reaction conditions: sydnone (0.13 - 0.50 mmol), Me_2NH (0.03 - 0.1 mmol, 20 mol%), $Ru(bpy)_3(PF_6)_2$ (25 µmol, 5 mol%), EVI_2 (0.5 mmol), NMP (5 mL, 0.025 - 0.1 M), 48 h at room temperature under blue LED irradiation; [b] yield of isolated compound; EVI_2 = ethyl viologen diiodide

4.2.4 Mechanism of the PSEC Reaction

4.2.4.1 Radical Trap and Clock Experiments

Upon the completion of our investigation into the scope of the PSEC reaction, we began to consider how we might interrogate the mechanism of this novel process. Our initial mechanistic proposal for the reaction (Scheme 4.4) hinged upon the formation of aminium radical **283**, thus assessing the importance of this potential intermediate seemed a logical point to begin. Conventionally, radical intermediates are detected by the addition of "trapping" agents which are able to form adducts preferentially with the highly reactive radical intermediates. The mechanism by which these additives inhibit the reaction is structure specific, and several examples are shown in scheme 4.8A. In the case of the PSEC reaction, the addition of super stoichiometric quantities (3 eq) of either (2,2,6,6-tetramethylpiperidin-1-yl)oxyl (TEMPO) or 1,1-diphenylethylene (DPE) was found to have negligible impact on the outcome of the reaction (Scheme 4.8B). These results would suggest that the formation of radical species under PSEC conditions is unlikely, but without knowledge of the rate constants for the reaction between **283** and *N*-phenylsydnone and between **283** and TEMPO/DPE, this cannot be definitively concluded.

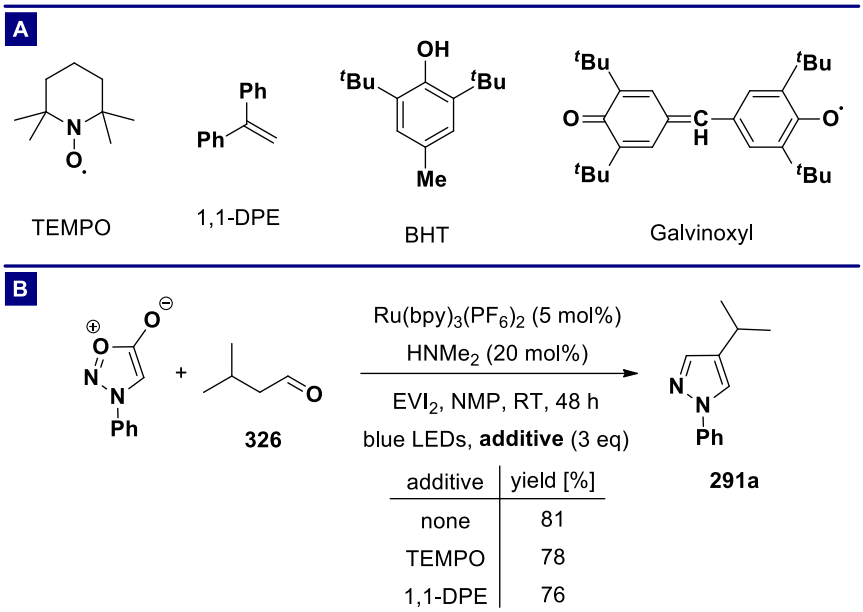

additive	yield [%]
none	81
TEMPO	78
1,1-DPE	76

Scheme 4.8 – a) conventional "radical trapping" agents; b) PSEC reaction with **326** in the presence of different additives; TEMPO = (2,2,6,6-tetramethylpiperidin-1-yl)oxyl; 1,1-DPE = 1,1-diphenylethylene; BHT = butylated hydroxytoluene; EVI_2 = ethyl viologen diiodide; RT = room temperature

Further examination of possible radical intermediates was then conducted using "radical clock" experiments (Scheme 4.9A). This technique makes use of substrates which will, should a radical be formed in a specific position, undergo a known rearrangement process which can be detected through a structural analysis of the isolated products. Moreover, the term "radical clock" is applied because the application of several rearrangement processes with variable rate constants provides one with a rough estimate for the rate of the reaction under study. As such, the tethered alkene containing aldehyde **327** was subjected to our optimised conditions. In the event, no trace of aldehyde **329**, derived from 5-exo-trig cyclisation and subsequent hydrolysis of the proposed aminium radical intermediate, was detected by either GC-MS or ^{1}H NMR spectroscopy and the corresponding 1,4-disubstituted pyrazole **328a** was isolated in 78% yield. Additionally, cyclopropyl substituted aldehyde **330** also produced the cyclopropyl pyrazole **331a** in 55% yield with no trace of any rearranged compounds. These observations can be explained either by a lack of radical formation under PSEC conditions, or by a rapid reaction between *N*-phenylsydnone and the aminium radical intermediates outcompeting the rearrangement processes. Given the rapid rate of the rearrangement processes (2.3×10^5 s^{-1})[224] and (1.2×10^8 s^{-1})[225] and the long reaction times required for the PSEC reaction, the former explanation seems more likely. It should be noted that Chi has previously reported a lack of rearrangement in homoenolate derived radicals, where the presence of radical intermediates has been confirmed using EPR spectroscopy (Scheme 4.9B).[226] The authors rationalised this observation on the basis that the homoenolate derived radical **336** is significantly localised on the carbonyl carbon atom, with little resonance to the β-radical isomer.

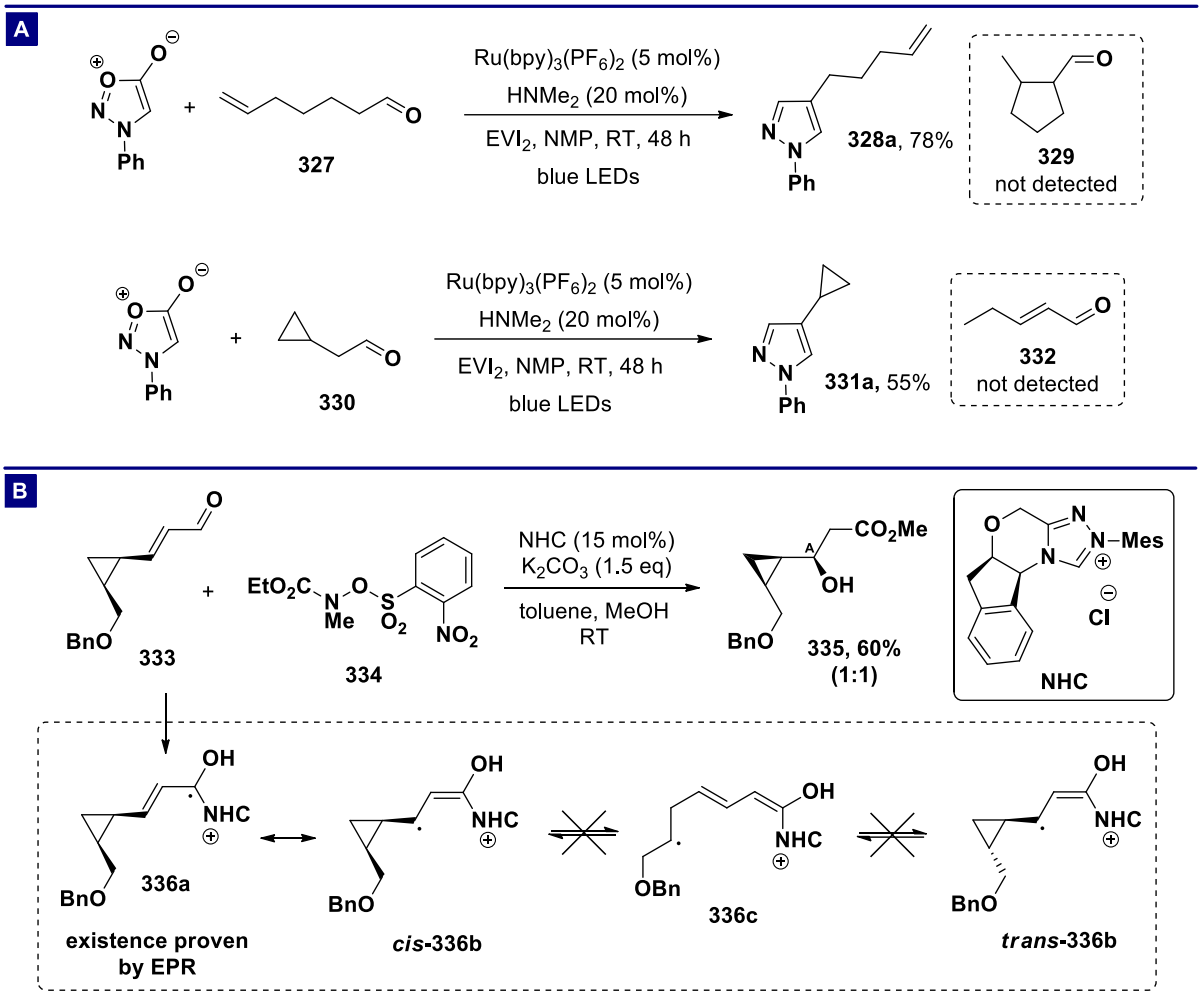

Scheme 4.9 – a) radical clock experiments under PSEC conditions; b) oxidation of homoenolate derived radicals reported by Chi. Values in parentheses indicate the diastereoisomeric ratio; EVI_2 = ethyl viologen diiodide

Therefore, it is possible that the lack of rearrangement observed during our experiments is the result of the aminium radical being localised largely on the nitrogen atom. At this stage, we concluded that while aminium radical formation under PSEC conditions cannot be completely ruled out, the formation of this species seems highly unlikely.

4.2.4.2 Stern-Volmer Luminescence Quenching

The apparent lack of radical formation under our optimum conditions led us to design further experiments with which to probe the PSEC reaction. Control experiments (Table 4.1, entries 18 and 20) and an on/off experiment (Appendix 1) had both demonstrated the light promoted nature of the reaction, thus we set out to ascertain which species was responsible for the catalyst quenching step using fluorescence quenching techniques. In the absence of other molecules, a photoexcited species may return to the ground state through *intramolecular* radiative (e.g. fluorescence, phosphorescence) or non-radiative pathways. The ratio of these processes is defined by the quantum yield (ϕ) and measuring the amount of radiative decay in the absence of additional species creates a baseline

emission intensity (I_0). The addition of other chemical species may accelerate the decay of the photoexcited state by introducing additional non-radiative *intermolecular* transfer processes (e.g. energy or electron transfer), lowering the quantum yield and resulting in a decreased emission intensity (I). Thus, by analysing the relationship between emission intensity (I) and the concentration of the additional chemical species, it is possible to determine whether there is any interaction with the photoexcited state (Stern-Volmer analysis).

By applying this technique to the PSEC reaction, we were able to demonstrate the presence of an interaction between the excited state photocatalyst and enamine **I** (K_{SV} = 9.08 x 10^1 M^{-1}), consistent with the chemical literature (Figure 4.1). Conversely, the corresponding aldehyde **II** exhibited no interaction with $[Ru(bpy)_3]^{2+}$, thus the observed reactivity does not arise from this species. Surprisingly, *N*-phenylsydnone **III** also produced a prominent quenching of the photocatalyst (K_{SV} = 2.01 x 10^2 M^{-1}) while *N*-benzylsydnone **IV** (unreactive under PSEC conditions) gave, by comparison, negligible quenching (Figure 4.1).

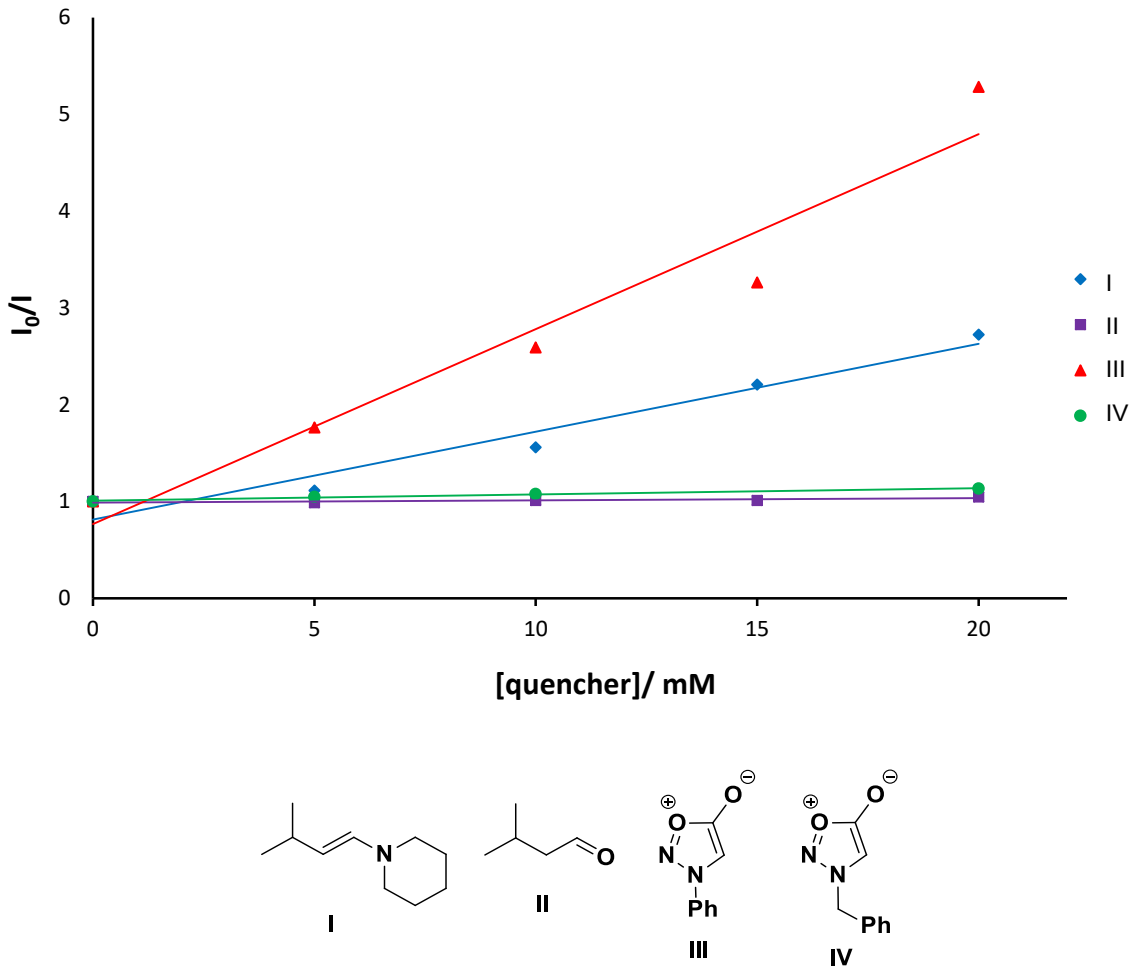

Figure 4.1 – Luminescence quenching studies

The lack of quenching in the case of *N*-benzylsydnone suggests an apparent relationship between catalyst quenching by the sydnone substrate and reactivity under PSEC conditions, therefore, further quenching experiments were conducted to elucidate the importance of this step (Figure 4.2). In contrast to *N*-benzylsydnone, 4-methylsydnone **V** (also unreactive under PSEC conditions) produced a strong fluorescence quenching effect (K_{SV} = 1.48 x 10^2 M^{-1}), similar to *N*-phenylsydnone. Analogously, the tethered aldehyde containing sydnone **VI** (reactive under PSEC conditions) exhibited a catalyst quenching interaction (K_{SV} = 7.29 x 10^1 M^{-1}) but the ortho-substituted sydnone **VII** (unreactive under PSEC conditions) showed much weaker quenching of the photocatalyst (K_{SV} = 1.83 x 10^1 M^{-1}). Indeed, the quenching interaction of **VII** is an order of magnitude less efficient than catalyst quenching by *N*-phenylsydnone. It is possible that this observation is caused by the *o*-methyl substituent causing the sydnone/phenyl rings to sit in a twisted conformation; the sydnone proton in **VII** appears at δ6.48 ppm in the ^{1}H NMR spectrum while the sydnone proton in *N*-phenylsydnone appears at δ6.75 ppm. This observation suggests that the sydnone ring in **VII** is more electron rich, perhaps as a result of decreased conjugation between the two rings.

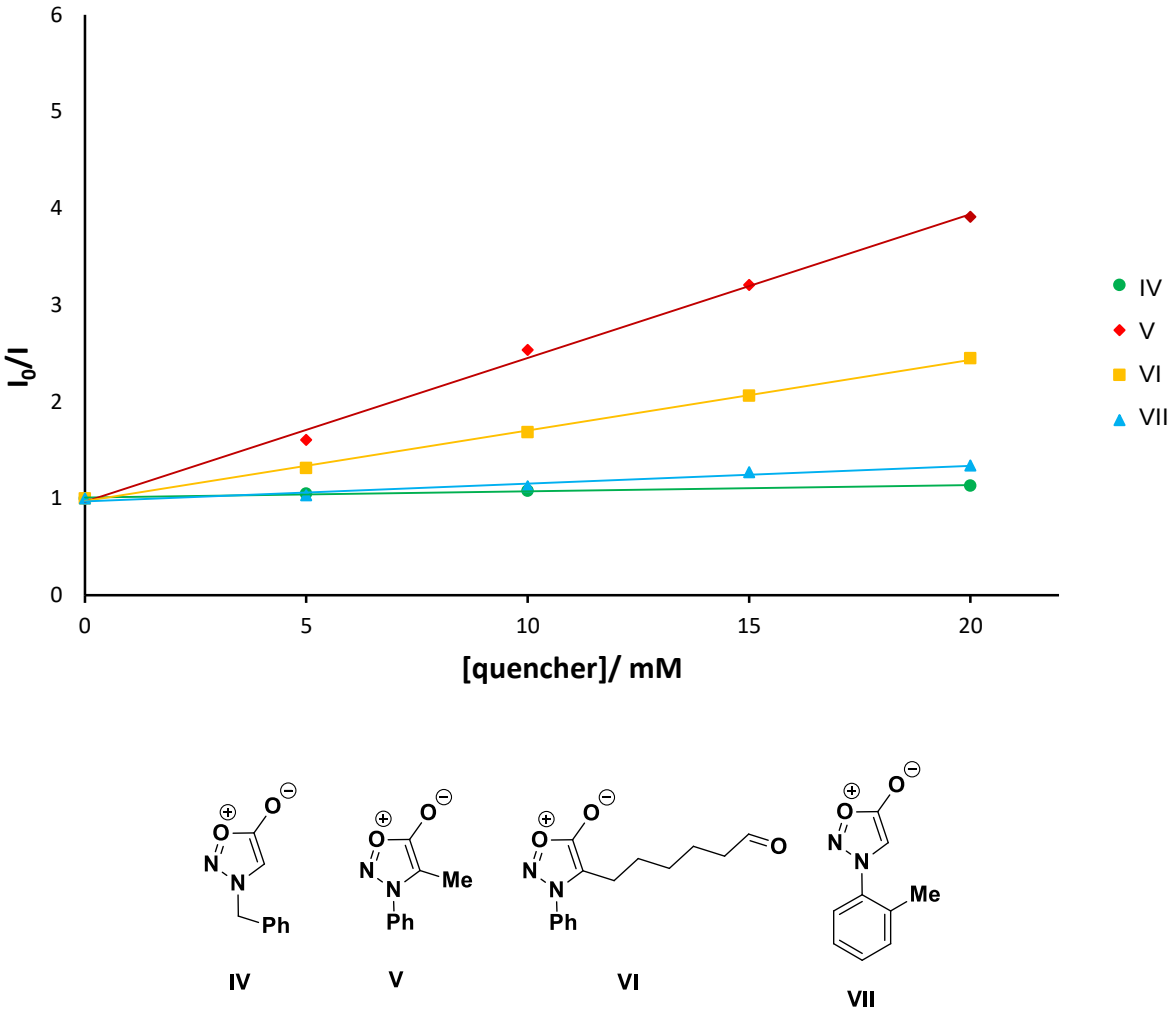

Figure 4.2 – further luminescence quenching studies

This decreased extent of conjugation may then alter the molecular orbitals of **VII** in such a way as to reduce its reactivity under PSEC conditions. Nevertheless, the combination of these results highlights a complex relationship between quenching and reactivity. It can be concluded that the presence of a quenching interaction between the sydnone substrate and excited photocatalyst is necessary for a successful reaction under PSEC conditions, but it is not indicative of success. It seems likely therefore that the observed reactivity is reliant upon this interaction but other steric and electronic factors govern the overall fate of the reaction.

4.2.4.3 Reaction with non-quenching Dipolarophiles

At this stage, the mechanistic details of the PSEC reaction were still unclear. While the radical trap/clock experiments evidence against the formation of radical cation intermediates, the observation that both enamine and sydnone substrates are active quenchers of the photocatalyst meant that elucidation of the key interaction(s) was still required. Theoretically, the observed reactivity under PSEC conditions could arise from a reaction between two excited state substrate molecules, an excited state sydnone and ground state enamine, or an excited state enamine and ground state sydnone (Figure 4.3).

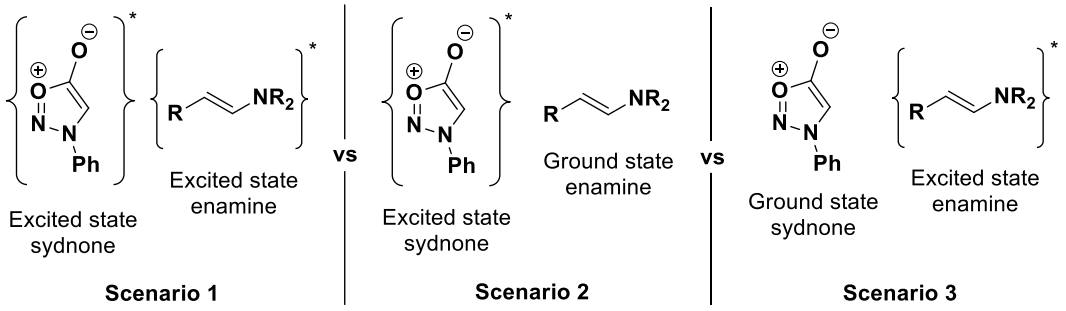

Figure 4.3 – possible mechanistic scenarios under PSEC conditions

While the final possibility can be excluded on the basis that *N*-alkylsydnones are unreactive under PSEC conditions, either of the other mechanisms could be responsible for the observed reactivity. In an attempt to address this mechanistic dichotomy and better understand the role of sydnone based luminescence quenching, we performed photocatalytic cycloaddition reactions with other dipolarophiles; specifically, those which are unable to quench the excited state photocatalyst (Scheme 4.10). If any reaction were to occur under these conditions then it would be reasonable to assume that catalyst quenching by the enamine is irrelevant to the observed outcome of the PSEC reaction. Initially, a reaction between *N*-phenylsydnone and 1-hexyne (1-hexyne possesses no oxidation or reduction peaks within the window of acetonitrile) was performed, however no trace of the corresponding pyrazole was detected. Alternatively, 2,3-dihydrofuran could be employed as the

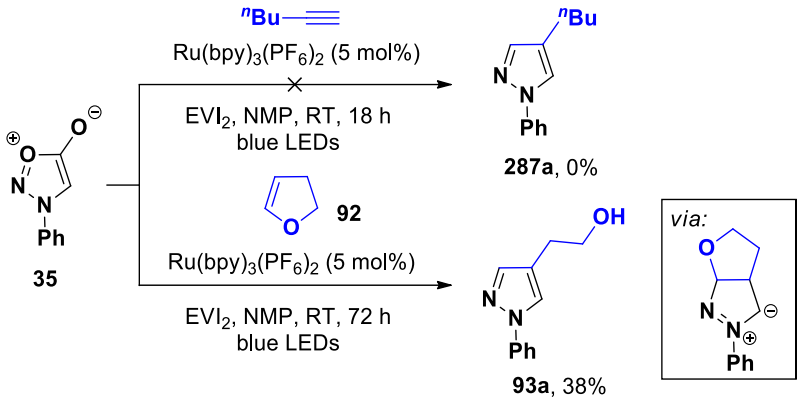

Scheme 4.10 – photocatalytic reactions of non-catalyst quenching dipolarophile; EVI_2 = ethyl viologen diiodide

dienophile partner to afford **93a** in 38% yield as a single regioisomer. Given that the oxidation potential of 2,3-dihydrofuran (E_{ox} ~ +1.5 V vs. SCE) is inaccessible by any of the Ru-species formed under the reaction conditions (the reduction potential of $[Ru(bpy)_3]^{3+}$ is +1.29 V vs. SCE), and the lack of quenching observed in a Stern-Volmer analysis of 2,3-dihydrofuran (Appendix 2), this result clearly demonstrates that photocatalytic activation of the sydnone substrate alone is sufficient for a successful cycloaddition reaction (Scenario 2, figure 4.3). Taken in combination with the relative substrate concentrations (under the optimised conditions, there will be an excess of sydnone relative to *in situ* generated enamine until high reaction conversions) and the superior rate of quenching for *N*-phenylsydnone relative to enamine **I** (Figure 4.1), these results indicate that the sydnone substrate is likely the major photocatalyst quenching species under PSEC conditions. Furthermore, this observation offers an explanation for the improved yield under organocatalytic conditions; if photoredox meditated oxidation of the enamine is responsible for formation of the aldol dimerisation product, then decreased enamine concentration under the organocatalytic conditions would reduce the frequency of this quenching step and ultimately minimise the formation of this by-product.

4.2.4.4 Cyclic Voltammetry

Having established the sydnone as the major quenching species under PSEC conditions, we next set out to establish the nature of this quenching interaction. As described above, the excited state of $[Ru(bpy)_3]^{2+}$ may participate in either electron or energy transfer events with a variety of organic molecules. Thus, using cyclic voltammetry we aimed to establish the feasibility of an electron transfer events between the photocatalyst and sydnone substrate (Figure 4.4). To this end, cyclic voltammetry conducted on *N*-phenylsydnone (2.5 mM) in degassed, anhydrous MeCN containing *n*-Bu_4NPF_6 (0.1 M) as the electrolyte discovered both an irreversible oxidation peak ($E_{p/2}$ = +1.48 V vs. Fc/Fc^+) and an irreversible reduction peak ($E_{p/2}$ = -1.87 V vs. Fc/Fc^+) within the solvent window. Comparison of the

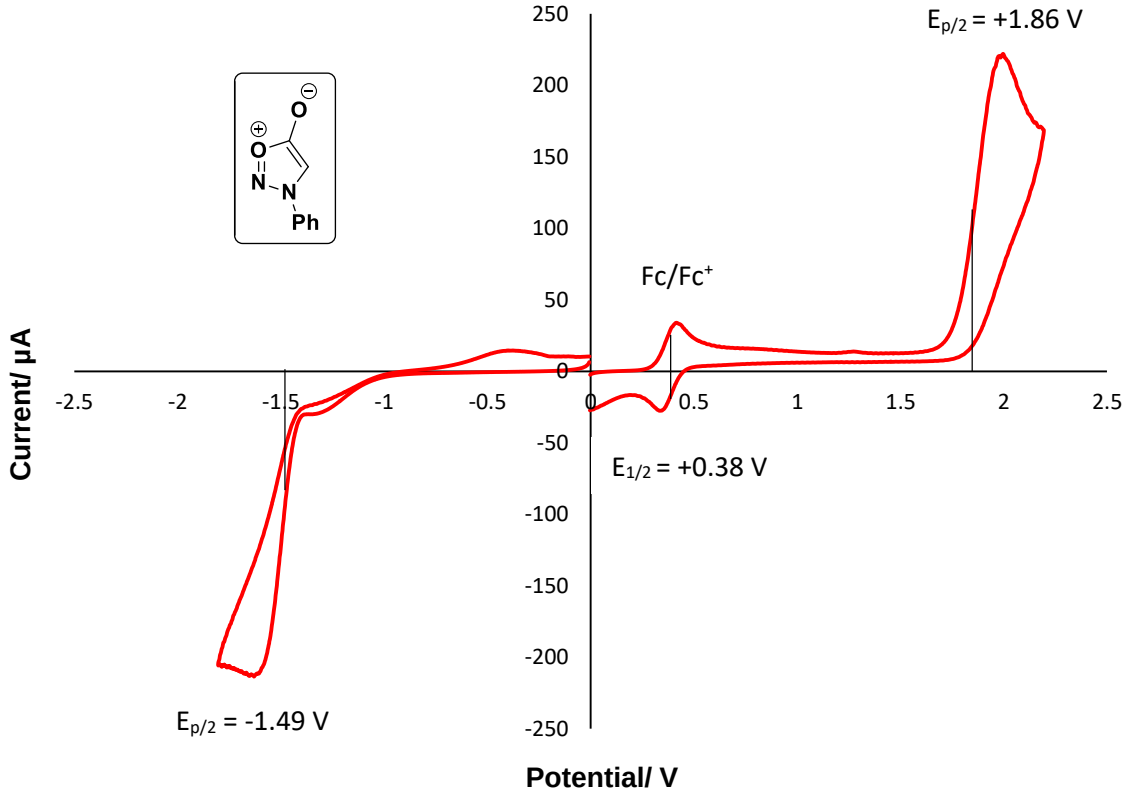

Figure 4.4 – CV spectrum of *N*-phenylsydnone

oxidation potential of *N*-phenylsydnone with the excited state reduction potential of $Ru(bpy)_3(PF_6)_2$ (E_{red} = +0.37 V vs. Fc/Fc$^+$) indicates that a reductive quench of the photocatalyst would be significantly endergonic. Analogously, the reduction potential of *N*-phenylsydnone is more negative than the oxidation potential of the excited state photocatalyst (E_{ox} = -1.21 V vs. Fc/Fc$^+$), rendering an oxidative quench of the photocatalyst endergonic. Overall, these results exclude the possibility of an electron transfer mechanism and indicate the likelihood of a photosensitisation mechanism under PSEC conditions.

4.2.4.5 Fate of the Excited State Sydnone

The discovery that the PSEC reaction is promoted by an energy transfer event between the photocatalyst and sydnone substrate raises a number of additional questions. Firstly, energy transfer to the sydnone could, theoretically, lead to the formation of either the singlet or triplet excited state. Secondly, the previous reports focusing on sydnone photolysis have demonstrated the formation of nitrilimine intermediates which then participate in the subsequent cycloaddition reaction. In the case of the PSEC reaction, it is possible to imagine that the observed products might be derived from a direct, regioselective cycloaddition between the excited state sydnone and the enamine substrate. Alternatively, the formation of an excited state sydnone species could be followed by a

decarboxylative rearrangement to form a nitrilimine which can then participate in a [3+2] cycloaddition with the enamine. It should be noted that the observed regioselectivity under PSEC conditions matches that which would be expected on the basis of previously described nitrilimine-enamine cycloadditions.[16]

We decided to begin by assessing the feasibility of forming a singlet excited sydnone species under the reaction conditions by performing a lambda tail (λ_{tail}) analysis; because the absorption peaks on a UV-vis spectrum represent the excitation of a molecule from the ground state to a variety of energy levels, it is possible to estimate the singlet excited state energy of a given compound from the tail of the longest wavelength absorption peak on its UV-vis spectrum.[227] Performing this analysis with *N*-phenylsydnone produced a λ_{tail} value of 363 nm which, using the equation for the energy of a photon,

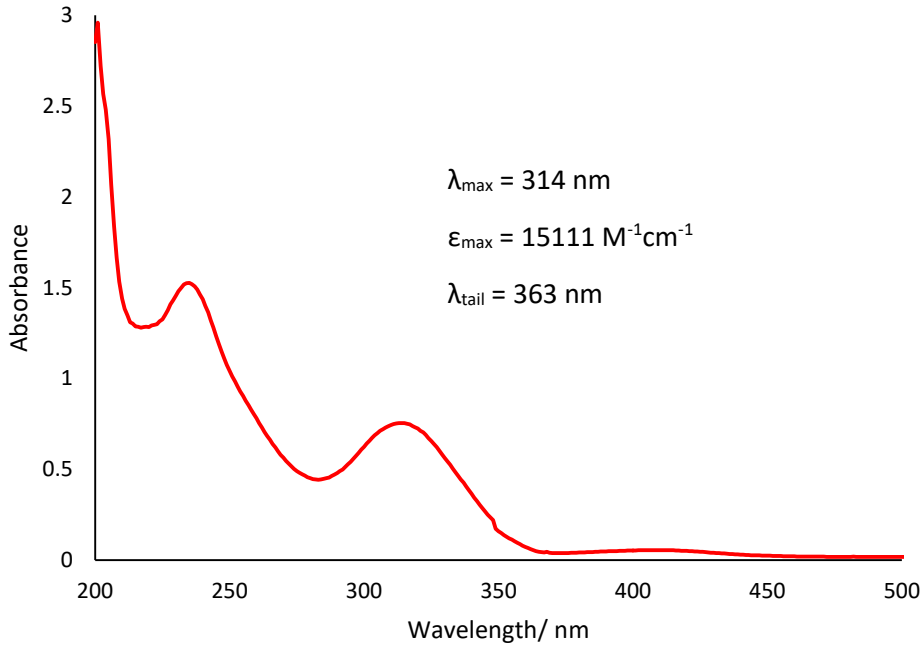

$$E_{00}(X^*/X) \sim hc \,/\, \lambda_{tail} \quad \text{(Equation 1)}$$

Where:

$E_{00}(X^*/X)$ = the estimated energy of the singlet excited state (eV)

h = Planck's constant (4.135667696 x 10^{-15} eV.s)

c = speed of light (299762458 m.s^{-1})

λ_{tail} = wavelength at the tail of the absorption peak (nm)

$$N - \text{phenylsydnone singlet energy} = \frac{(4.135667696\ x10^{-15}).(299792458)}{363\ x10^{-9}} = 3.42\ eV$$

Figure 4.5 – UV-vis spectrum and estimation of the singlet energy of *N*-phenylsydnone

equates to a singlet excited state energy of 3.42 eV or 78.9 kcal/mol (Figure 4.5).

Comparison of this estimated singlet energy with the reported triplet energy of $[Ru(bpy)_3]^{2+}$ (E_T = 2.12 eV or 48.9 kcal/mol)[228] excludes the possibility of singlet excited state formation. Interestingly, the estimated singlet excited state energy of *N*-phenylsydnone is very similar to that observed previously for 3,4-diphenylsydnone (Figure 4.6).[208,229] Moreover, the triplet excited state of 3,4-diphenylsydnone has also been calculated at 48.1 kcal/mol, sufficiently low for productive energy transfer with $[Ru(bpy)_3]^{2+}$. Based on the observation that crystal structures of 3,4-diarylsydnones show the two aryl rings twisted relative to each other,[218] and the comparatively similar singlet energies of 3,4-diphenylsydnone and *N*-phenylsydnone, it is not impossible to imagine that the triplet energies of these two compounds are also similar. Therefore, our current proposal is that $[Ru(bpy)_3]^{2+}$ promotes excitation of the sydnone substrate to its triplet excited state. This would also explain the lack of reactivity in *N*-alkylsydnones, whose calculated triplet energies (E_T = 56.0 kcal/mol for *N*-methylsydnone) are inaccessible by the photocatalyst.

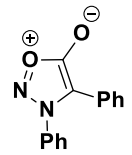

E_S = 79.0 kcal/mol
E_T = 48.1 kcal/mol

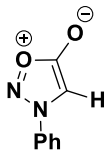

E_S = 79.0 kcal/mol
E_T = **?**

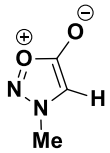

E_S = 99.0 kcal/mol
E_T = 56 kcal/mol

Figure 4.6 – excited state energies of various sydnones; E_S = singlet excited state energy; E_T = triplet excited state energy

We next focused on determining the subsequent fate of the photoexcited sydnone species. According to the two possible mechanisms outlined previously, the hydrogen atom located on the *C*4-position of the sydnone ring could end up on either the *C*3 or *C*5 position of the pyrazole, depending on whether the photoexcited species undergoes a direct cycloaddition or decarboxylative rearrangement, respectively (Scheme 4.11A). To probe this, 4-deuterosydnone ***D*-35** was synthesised from *N*-phenylsydnone by deprotonation with ^{n}BuLi and subsequent trapping with deuterium oxide (D_2O). A PSEC reaction of ***D*-35** under the optimised conditions then proceeded uneventfully to form 3-deuteropyrazole ***D*-291a** as a single regioisomer in 87% yield, the assignment of which is based on a combination of ^{1}H and ^{13}C NMR spectroscopy (Appendix 3 and 4). Indeed, from the ^{1}H NMR spectrum it can be seen that the ratio of pyrazole protons in the product (1:0.16) reflect the extent of deuteration in the sydnone substrate. It can be concluded from this that only one of the postulated mechanisms is active under PSEC conditions because a mixture of competing mechanisms would perturb the ratio in favour of the minor integral. Furthermore, previous characterisation of *N*-phenylpyrazole indicates that the *C*3-carbon atom and the *C*5-carbon atom appear at δ141.1 ppm and

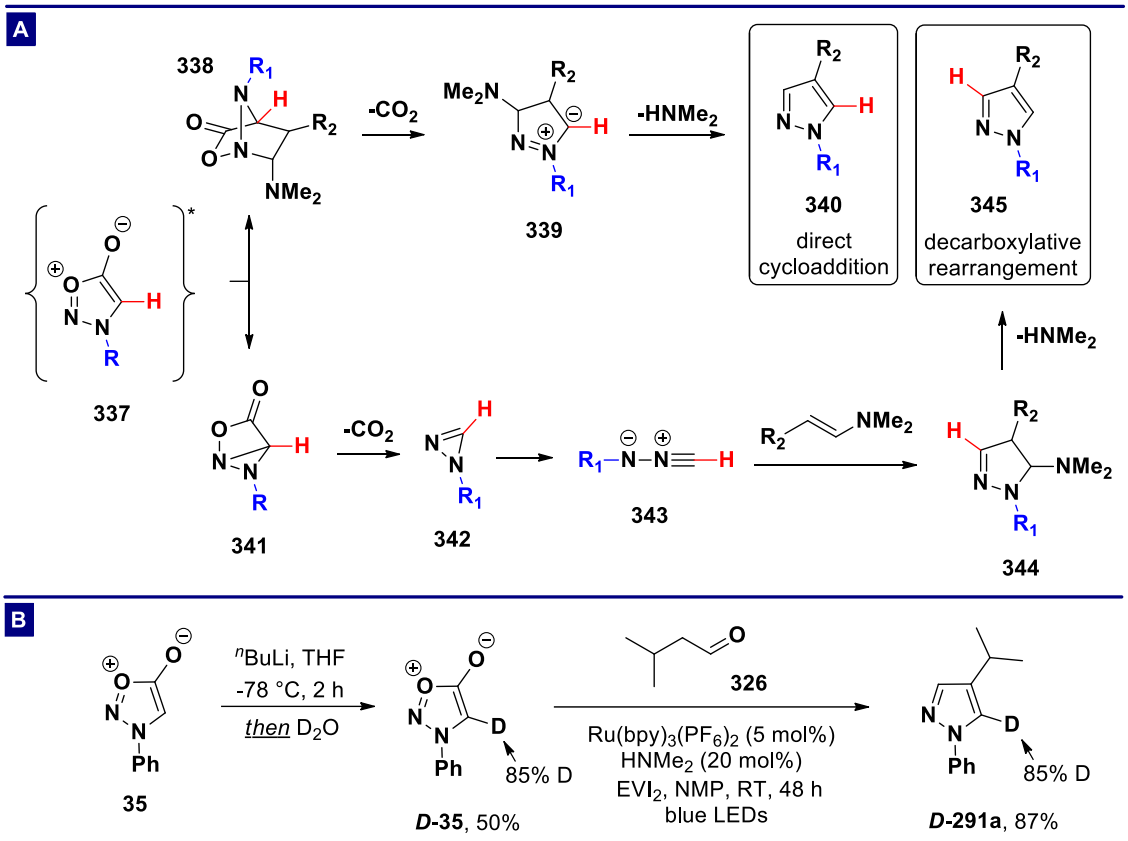

Scheme 4.11 – a) potential mechanistic routes from the excited sydnone species to the observed product; b) PSEC reaction of a deuterated sydnone substrate; EVI_2 = ethyl viologen diiodide

δ126.8 ppm in ^{13}C NMR spectrum, respectively.[230,231] In isopropylpyrazole **291a** the *C*3-carbon would then appear to be the signal at δ139.6 ppm, while the *C*5-carbon appears at δ123.4 ppm. Comparison of the ^{13}C NMR spectra of **291a** and deuterated analog ***D*-291a** reveals a significant reduction in the intensity of the signal at 123.4 ppm (Appendix 4). Moreover, a triplet signal (J = 28.5 Hz) can be seen under the base of the signal at 123.4 ppm, caused by coupling between the carbon and deuterium atoms in ***D*-291a**. This observation indicates that the deuterium atom in ***D*-291a** is attached to the *C*5-carbon atom and results in the conclusion that product formation under PSEC conditions occurs as a result of direct cycloaddition, rather than proceeding via a decarboxylative rearrangement.

4.2.4.6 Proposed Mechanism of the PSEC Reaction

At this point we concluded our investigation into the mechanism of the PSEC reaction. However, before proposing a mechanism, it is worth highlighting the key conclusions drawn from the above investigations:

1) The formation of radical species under PSEC conditions is highly unlikely.

2) The sydnone substrate is the main photocatalyst quenching species under organocatalytic conditions.

3) Electron transfer is significantly endergonic, implicating the existence of an energy transfer mechanism which likely leads to the formation of a triplet excited sydnone.

4) No nitrilimine intermediate is formed en route to the pyrazole product.

The combination of these results allows one to propose the apparently simple mechanism depicted in Scheme 4.12. Excitation of the photocatalyst with visible light creates an excited state species (E_T = 48.9 kcal/mol)[228] which can participate in energy transfer with the sydnone substrate **346** (E_T ~ 48.1 kcal/mol)[208] to create excited state intermediate **347**. This intermediate can then react with the enamine to form **349** following the loss of carbon dioxide. Finally, elimination of the amine moiety from **349** forms the pyrazole product **350** and regenerates the amine organocatalyst.

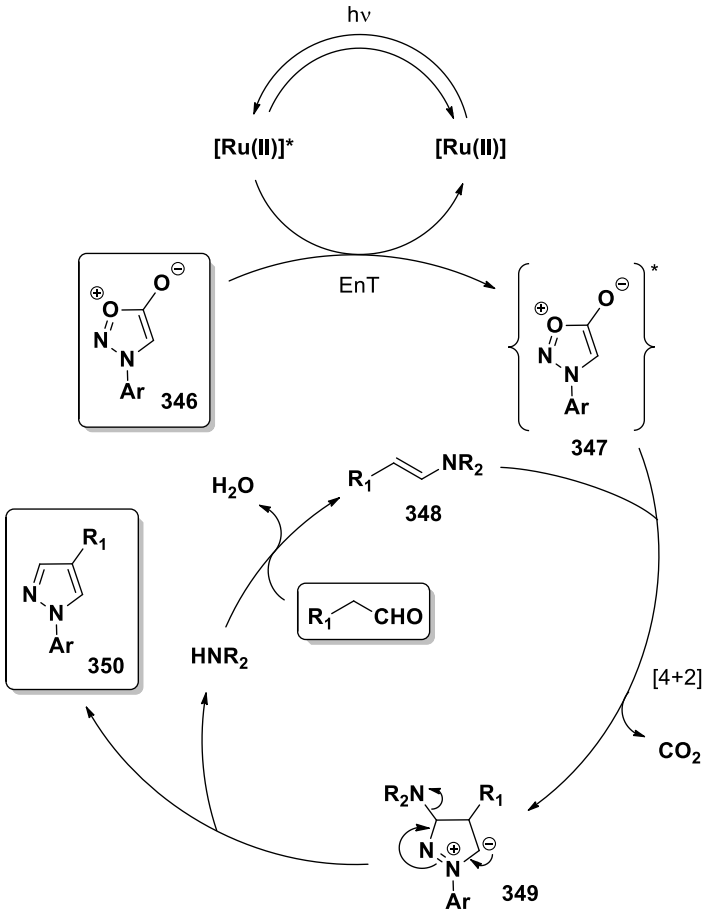

Scheme 4.12 – Initially proposed mechanism of the PSEC reaction

However, a number of questions remain unanswered: what is the role of the viologen additive and what intermediates are involved in the formation of **349** from **347**?

Let us first begin by addressing the role of the viologen additive within the PSEC reaction. Early experiments prove that the presence of viologen *is not* necessary for the observed reactivity. Instead, and despite the known quenching of $[Ru(bpy)_3]^{2+}$ by viologens, the viologen appears to have a positive

effect on the reaction by inhibiting non-productive pathways. Furthermore, the viologen seems likely to interact with the enamine substrate (or intermediates derived therefrom) since its effect is less pronounced under organocatalytic conditions, when the concentration of enamine is lower (Scheme 4.13A). If single electron oxidation of the enamine substrate is responsible for the formation of α,β-unsaturated aldehyde **290** (an interaction between the excited photocatalyst and enamine is observed by Stern-Volmer analysis), then the stoichiometric quantity of amine generated by this process could be responsible for the observed sydnone decomposition (c.f. Scheme 2.11). Therefore, inhibiting the oxidation of the enamine, or its subsequent conversion into aldehyde **290**, would decrease the rate of sydnone decomposition and favour the formation of the desired product. Interestingly, previous reports on both aminium radical,[232] and photoredox catalysed radical cation cycloadditions demonstrate a significant rate retardation in the presence of amine additives.[187] This observation is proposed to arise as a result of back electron transfer (BET) between the radical cation intermediate and the amine additive, regenerating the ground state substrate. Based on this, it is possible to imagine a scenario whereby SEO of the enamine **351** (Scheme 4.13, path b) competes with the formation of excited state sydnone (Scheme 4.13, path a) under PSEC conditions, leading to the formation of radical cation **352**. The viologen additive (**MV^{2+}**, E_{red} = -0.40 V vs. SCE)[110] then participates in a SET event with the reduced photocatalyst (E_{ox} = -1.33 V vs. SCE)[110] to regenerate the ground state catalyst and form **$MV^{\cdot+}$**. The oxidation potential of this species (E_{ox} = +0.40 V vs. SCE) would then allow rapid electron transfer with radical cation **352** (E_{red} = +0.32 V vs. SCE),[233] re-forming the ground state additive and enamine substrate **351**. It should be noted that switching the order in which the enamine and viologen interact with the catalyst would also be thermodynamically feasible. Either way, this scenario would help to explain the apparent dependence on enamine concentration, since higher enamine concentrations would result in a more competitive catalyst quenching step and increased generation of radical cation **352**.

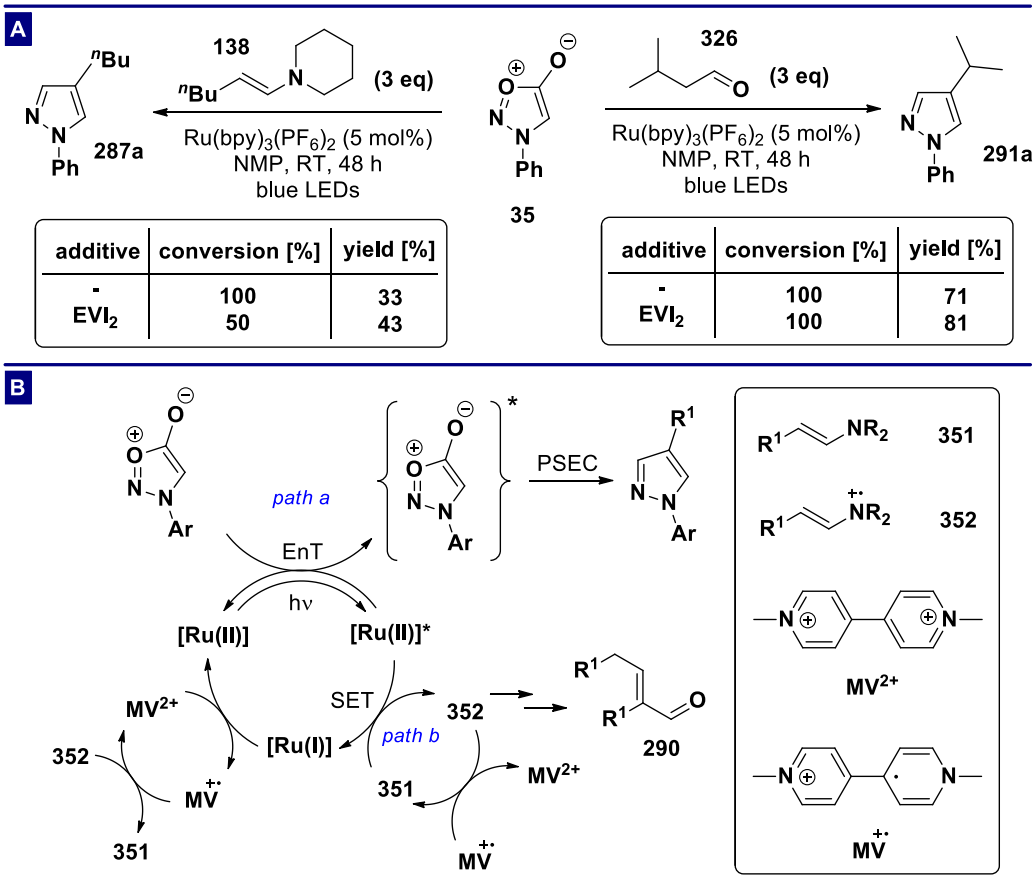

Scheme 4.13 – a) effect of adding viologen additives to the PSEC and organocatalytic PSEC reactions; b) potential mechanistic rationale for the positive effect of adding viologen additives to the PSEC reaction; EVI_2 = ethyl viologen diiodide

With a potential role for the viologen additive proposed, let us now discuss the route from **347** to **349**. The photolysis of sydnones is proposed to proceed through a formal electrocyclisation and loss of CO_2 to form diazirine **354** which can then ring open to nitrilimine **355**. However, isotopic labelling of the PSEC reaction suggests that nitrilimine **355** is not an intermediate under these conditions. Therefore, the pertinent question relates to diazirine **354**; does the loss of CO_2 occur before or after the cycloaddition step? To begin addressing this problem several of control experiments were conducted (Scheme 4.14A). Irradiating a mixture of *N*-phenylsydnone and $Ru(bpy)_3(PF_6)_2$ in either the presence or absence of viologen was found to result in complete consumption of the sydnone starting material. This is further evidence that the viologen additive does not interact with the sydnone under PSEC conditions and suggests that the sydnone does indeed undergo some rearrangement prior to cycloaddition. However, no direct evidence was obtained for the existence of diazirine **354**. Interestingly, shortly after we disclosed our own results, Taran and Glorius described an alternative photocatalytic reaction of sydnones with carboxylic acids (Scheme 4.14B).[234] In this reaction, sydnones with a *C*4-substituent were found to deliver isomeric products compared to *C*4-unsubstituted sydnones, and the authors proposed diazirine **358** as a critical intermediate for explaining this

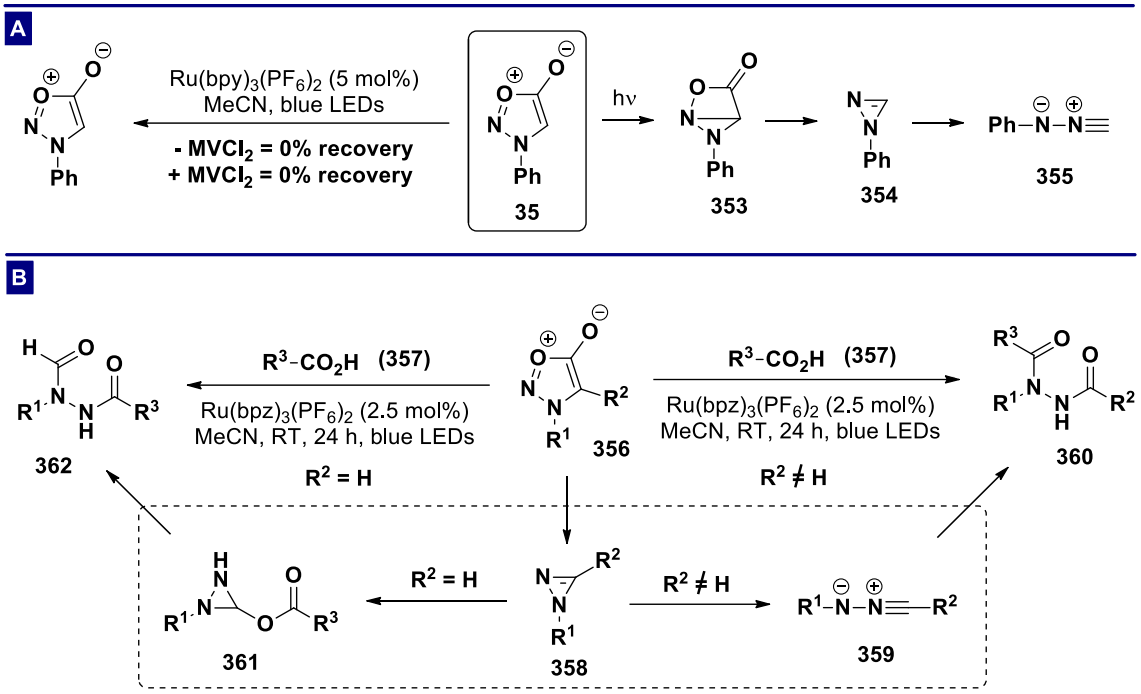

Scheme 4.14 – a) mechanism of sydnone photolysis and effect of viologen additives on sydnone decomposition; b) photocatalytic synthesis of diacylhydrazides from sydnones

regiodivergence. In the case of unsubstituted sydnones, ring opening to the nitrilimine **359** is unfavourable and so the carboxylic acid reacts directly with diazirine **358** to form the observed products following a subsequent rearrangement. Conversely, diazirine intermediates derived from *C*4-substituted sydnones are able to undergo ring opening to the corresponding nitrilimine **359**, which then reacts to form the isomeric product.

Inspired by this report, 3,4-diarylsydnone **363** was investigated in a cycloaddition reaction with both phenylacetylene and isovaleraldehyde (Scheme 4.15). In both cases the observed products correspond to the formation of a nitrilimine intermediate prior to the cycloaddition step and, in spite of the low yields, this result clearly demonstrates the similarity between the photocatalytic mechanism and photolysis mechanism, implicating diazirine **354** as a viable intermediate.

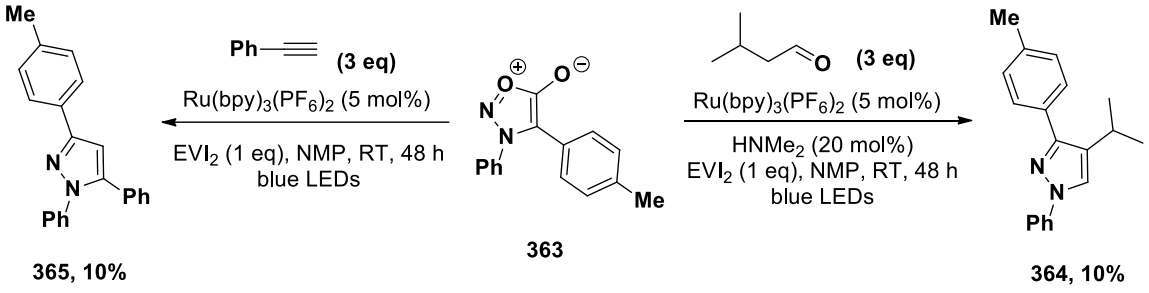

Scheme 4.15 – photocatalytic cycloaddition reactions of 4-arylsydnones

In light of these results, it is possible to propose a unified mechanism that includes a diazirine as a common intermediate and this is described in Scheme 4.16. Excitation of the photocatalyst with visible light and subsequent EnT leads to the key excited state intermediate **367**. From this point, either intermediate **371** (R = H) or nitrilimine **373** (R = Ar) are formed, presumably via diazirine **369**. Elimination of the amine from **371** then leads to the pyrazole products **372** while [3+2] cycloaddition of **373** with enamine **351** leads to pyrazoles **374**. Under the same conditions, SEO of enamine **351** by the photocatalyst creates radical cation **352** which can then react further to aldehyde **290** or participate in SET with the reduced viologen species **MV**$^{\cdot+}$ to reform **351**.

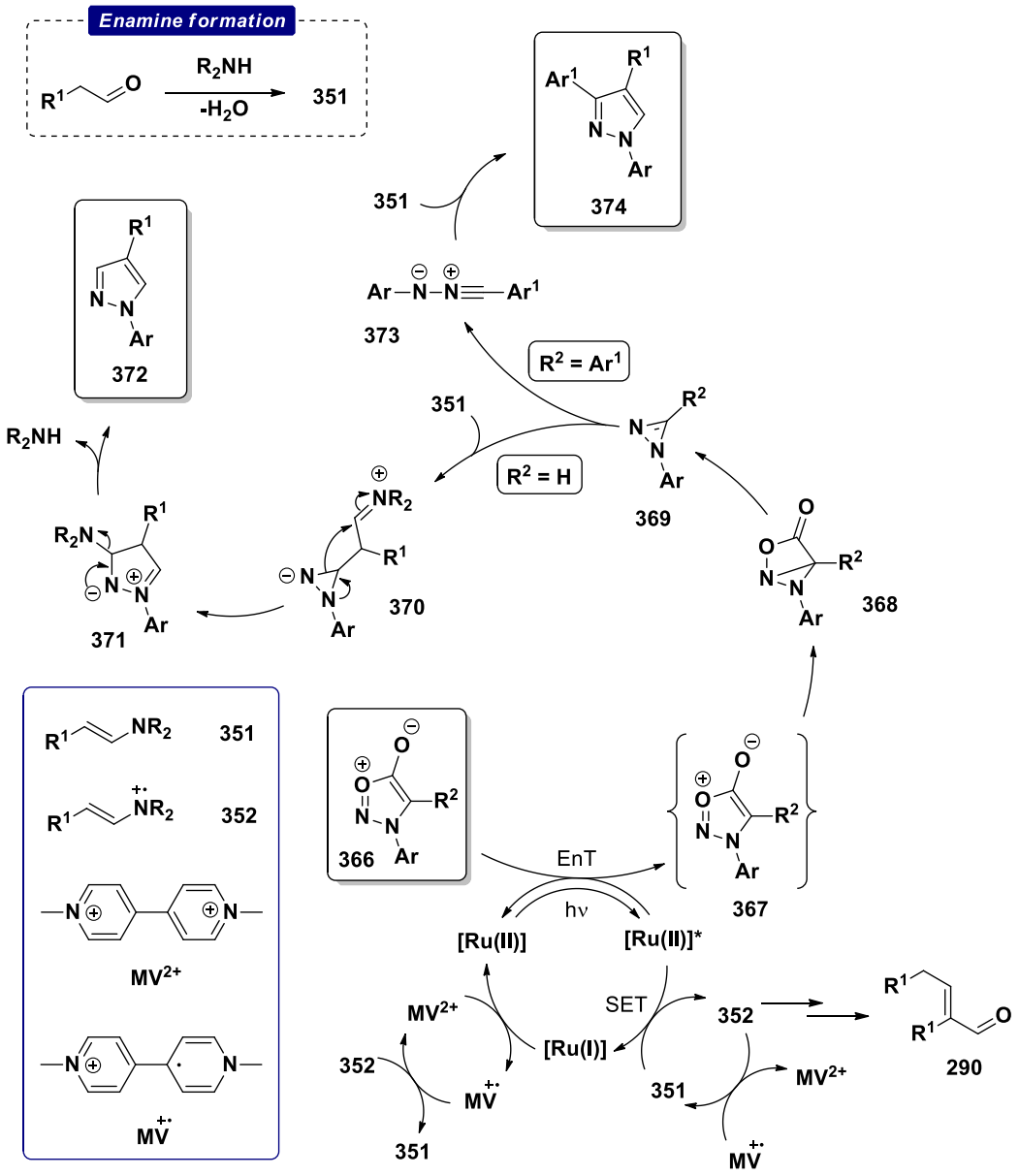

Scheme 4.16 – possible active mechanisms under PSEC conditions; SET = single electron transfer; EnT = energy transfer

4.3 Conclusions

The use of catalytic quantities of a photocatalyst ($Ru(bpy)_3(PF_6)_2$) and organocatalyst (piperidine or $HNMe_2$) has been successfully demonstrated as a means of achieving a sydnone-enamine cycloaddition reaction under irradiation with visible light at ambient temperature. The reaction shows good functional group tolerance in achieving the synthesis of a range of 1,4-disubstituted pyrazole scaffolds in high yield and with excellent regioselectivity. Currently, the scope is limited to sydnone bearing *N*-aryl substituents in both inter- and intramolecular cycloaddition reactions, while *N*-alkylsydnones are not amenable to this process. Mechanistic investigations indicate that this unique reactivity arises from the formation of an excited state sydnone species, formed by an energy transfer event with the photocatalyst, which can then undergo subsequent rearrangement and reaction with the enamine substrate.

4.4 Future Outlook

In general, the platform of sydnone cycloadditions serves as a versatile method for the synthesis of pyrazole containing molecules. The amalgamation of the reported methodologies allows access to a range of pyrazoles containing various substitution patterns, while exploiting a number of catalytic systems and directing interactions has also been demonstrated as a means of achieving high levels of selectivity. Arguably the principal challenge remaining with this class of reaction is the high temperature required to achieve a successful outcome. In this context, the visible light promoted cycloaddition reaction described above offers an opportunity to significantly enhance the synthetic utility of sydnone cycloaddition reactions. Furthermore, the mechanistic insights gathered during the course of this study may be invaluable to achieving this goal.

In particular, the identification of a triplet energy transfer mechanism as the driving force in the PSEC reaction indicates that an expansion of the reaction scope to include *N*-alkylsydnones should be possible by employing a photocatalyst with a sufficiently high triplet energy. Examples of viable catalysts for this purpose include benzophenone (E_T = 69.2 kcal/mol),[134] Michler's ketone (E_T = 62.3 kcal/mol)[134] and $[Ir(dF(CF3)ppy)_2(dtbbpy)]PF_6$ (ET = 61.8 kcal/mol),[234] although this may require the use of a shorter wavelength irradiation source (Scheme 4.17A). Alternatively, it has been demonstrated that Lewis acids are able to interact with the exocyclic oxygen atom of the sydnone ring and similar interactions have been shown to significantly lower the triplet excited state energy of organic molecules.[75,145] Therefore, a screen of Lewis acids may also be a viable method by which to expand the scope of the reaction towards *N*-alkylsydnones (such a screen could be easily performed using fluorescence quenching techniques to reduce time consumption). Further expansion of the scope to include *C*4-substituted sydnone substrates is more challenging. Fluorescence quenching

analysis shows that in the case of *C*4-substituted sydnones, triplet excitation alone is insufficient to achieve a successful reaction under PSEC conditions. Based on the proposed mechanism (Scheme 4.16), this may be a consequence of either poor electrophilicity of the diazirine or poor nucleophilicity of the enamine. In any case, it has been shown that combining photocatalysis with traditional thermal promotion is a viable method by which to "push" particularly difficult reactions under photocatalytic conditions. This strategy may be applicable towards the PSEC reaction with *C*4-substituted sydnones, but requires a more complicated experimental setup. Additionally, it may be possible to increase the scope to include *C*4-substituted sydnones by using a different dipolarophile. This work has demonstrated a successful reaction under photocatalytic conditions when using enamines, enol ethers and alkynes as the dipolarophile partner, indicating that an expansion to other substrates is certainly possible. Furthermore (as highlighted by the reaction *C*4-arylsydnones), an investigation of alternative dipolarophiles may lead to the discovery of new selectivity under photocatalytic conditions.

Indeed, the discoveries presented herein offer a number of exciting possibilities for the future of sydnone cycloaddition reactions.

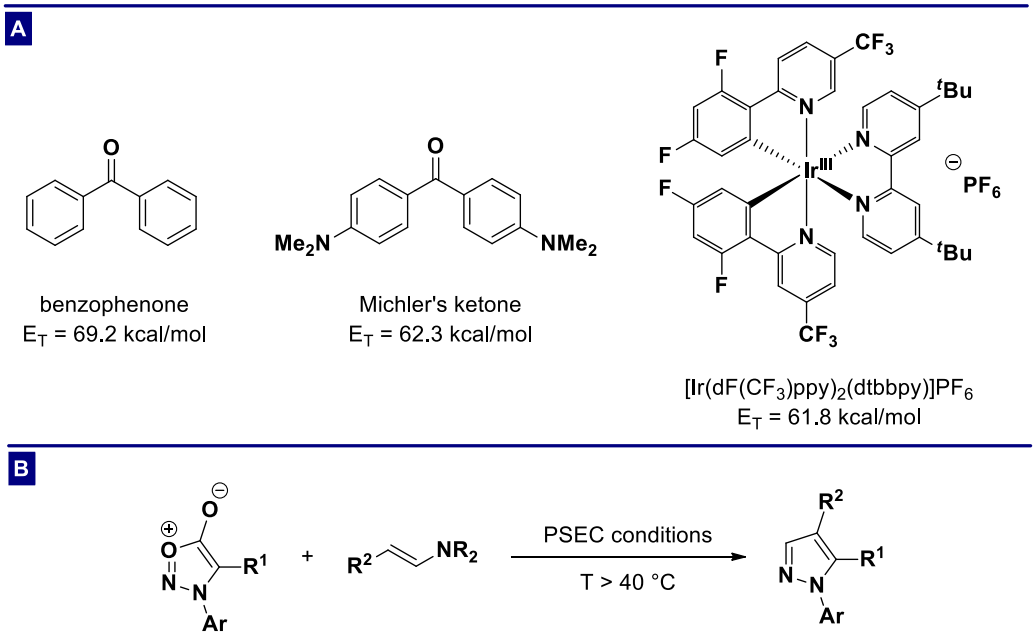

Scheme 4.17 – a) assorted photocatalyst which might be employed under PSEC conditions; b) proposed reaction of *C*4-substituted sydnones using photocatalysis in combination with thermal promotion

5 Experimental

5.1 General Considerations

All chemical transformations requiring an inert atmosphere and vacuum distillations were performed using standard Schlenk-techniques with a 4-port dual manifold (nitrogen/vacuum). Visible light irradiation was achieved using a kessil A160WE tuna blue aquarium LED set to maximum intensity blue emission. Flash chromatography was performed on silica gel (BDH Silica Gel 60 43-60) or Florisil. Thin layer chromatography (TLC) were performed on aluminium backed plates pre-coated with silica (0.2, Merck DC-alufolien Kieselgel 60 F_{254}), which were developed using standard visualizing agents: Ultraviolet light or potassium permanganate. ^{1}H NMR spectra were recorded at 298 K on a Brucker AVIII HD 400 (400 MHz), Brucker AVI 400 (400 MHz), or DPX-400 (400 MHz) supported by an Aspect 3000 data system. Chemical shifts (δ_H) are reported in parts per million (ppm) from tetramethylsilane ($\delta_{H)}$ 0.00 ppm) with the residual protic solvent resonance as the internal reference; $CDCl_3$ (δ_H 7.26 ppm), DMSO (δ_H 2.50 ppm). Data are reported as follows: chemical shift, multiplicity (s = singlet, d = doublet, t = triplet, q = quartet, m = multiplet, br = broad), coupling constant (Hz), integration, assignments. ^{13}C NMR spectra were recorded at 298 K on a Brucker AVIII HD 400 (100 MHz) using the CPD or DEPTQ pulse sequences with broadband proton decoupling using the deuterated solvent as the lock and the residual solvent as the internal reference. Chemical shifts (δ_C) are reported in ppm from tetramethylsilane (δ_C 0.00 ppm) with the solvent as the internal reference; $CDCl_3$ (δ_C 77.16 ppm), DMSO (δ_C 39.52 ppm). Infra-red spectra were recorded on a Perkin-Elmer Paragon 100 FT-IR spectrometer, ν_{max} in cm^{-1}. Samples were recorded as thin films using sodium chloride plates, as a dichloromethane solution or as solids using a solid probe. High-resolution mass spectra (HRMS), recorded for accurate mass analysis, were performed on electrospray mode (TOF ES^+).

Chemicals

All solvents (deuterated, non-deuterated and anhydrous) and chemicals purchased from commercial suppliers were used as supplied or purified according to the procedures described by Perrin and Armarego.[1] Aldehydes were distilled prior to use or prepared as described. All other compounds were synthesised following literature procedures or were prepared as described.

5.2 General Procedures

General Procedure 1 (GP1)

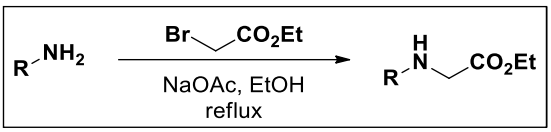

To a suspension of amine (1 eq) and NaOAc (2 eq) in EtOH (0.50 M) under N_2 was added ethyl bromoacetate (1 eq) and the mixture heated to reflux for 4 hours. The reaction mixture was then filtered and the filtrate concentrated under vacuum. DCM (2mL per mmol) was added to the filtrate and the resulting suspension was then filtered and the filtrate concentrated under vacuum. The crude products could be recrystallised from hot EtOH or used without further purification.

General Procedure 2 (GP2)

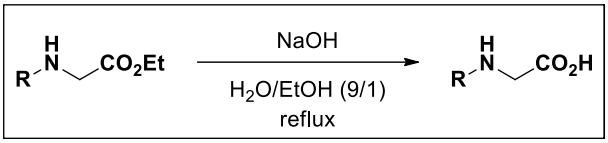

To a solution of ester (1.0 eq) in H_2O/EtOH (0.3 M) was added NaOH (1.5 eq) and the solution heated to reflux for 1.5 hours. The mixture was then cooled to 0 °C and acidified to pH 4 with conc. HCl, causing precipitation of the product which was isolated and dried under vacuum. The products could be further purified by recrystallisation from hot EtOH.

General Procedure 3 (GP3)

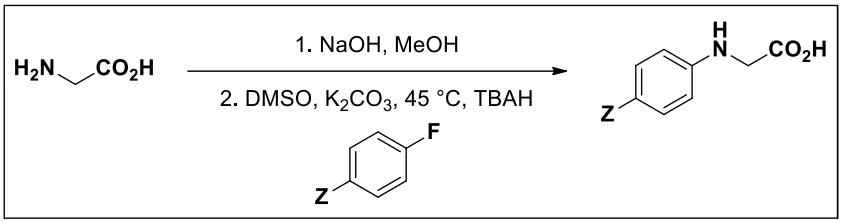

Glycine (1.1 eq) and NaOH (1.1 eq) were suspended in MeOH (2.0 M) and the mixture stirred until homogenous. The volatiles were then removed under vacuum and the resulting solid was dissolved in DMSO (1.0 M). K_2CO_3 (1.2 eq), tetra-*n*-butylammonium hydroxide (1.0 M in MeOH, 6 mol%) and 4-substituted fluorobenzene (1.0 eq) were then added and the mixture was heated to 50 °C for 72 hours. The reaction mixture was poured onto ice and slowly acidified to pH 4 with conc. HCl, causing precipitation of the product which was collected and dried under vacuum. The products could be further purified by recrystallisation from hot EtOH.

General Procedure 4 (GP4)

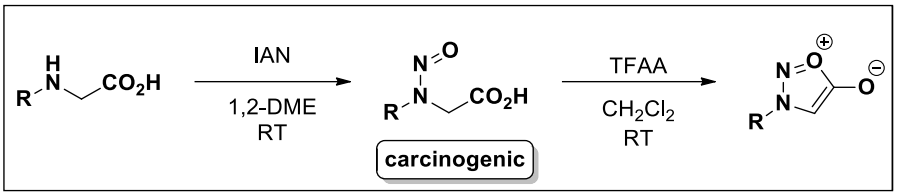

To a round-bottomed flask containing amino acid (1.0 eq) and 1,2-DME (0.25 M) was added IAN (1.1 eq) and the solution stirred at room temperature overnight. The volatiles were then removed under vacuum, petroleum ether/EtOAc (15/1) was added, and the resulting solid was collected and dried under vacuum (**CAUTION:** Highly carcinogenic nitrosamine). The crude material was then suspended in DCM (0.25 M) under N_2 and cooled to 0 °C before the dropwise addition of TFAA (1.5 eq). The reaction mixture was then stirred at room temperature for 90 minutes, after which time the reaction was quenched with sat. $NaHCO_3$ (2mL per mmol) and extracted with DCM (3 x 2mL per mmol). The combined organic layers were then dried over anhydrous $MgSO_4$, filtered and concentrated under vacuum to yield the target sydnones. The products could be further purified by recrystallisation from hot EtOH.

General Procedure 5 (GP5)

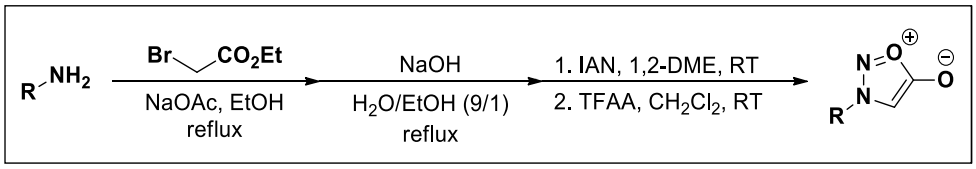

To a suspension of amine (1.0 eq) and NaOAc (2.0 eq) in EtOH (0.50 M) under N_2 was added ethyl bromoacetate (1.0 eq) and the mixture heated at reflux for 4 hours. The reaction mixture was filtered and the filtrate concentrated under vacuum. The crude product was then dissolved in H_2O/EtOH (0.30 M) (9/1) and solid NaOH (1.5 eq) was added and the solution heated at reflux for 1.5 hours. The mixture was then cooled to 0 °C and acidified to pH 4 with conc. HCl, causing precipitation of the product which was isolated and dried under vacuum. The crude product was then dissolved in 1,2-DME (0.25 M) and IAN (1.1 eq) was added and the solution was stirred at room temperature overnight. The volatiles were then removed under vacuum, petroleum ether/EtOAc (15/1) was added and the resulting liquid was decanted and the solid dried under vacuum (**CAUTION:** Highly carcinogenic nitrosamine). The crude solid was then suspended in DCM (0.25 M) under N_2 and cooled to 0 °C before the dropwise addition of TFAA (1.5 eq). The reaction mixture was then stirred at room temperature for 90 minutes, after which time the reaction was quenched with sat. $NaHCO_3$ (2mL per mmol) and extracted with DCM (3 x 2mL per mmol). The combined organic layers were then dried over anhydrous

$MgSO_4$, filtered and concentrated under vacuum to yield the target sydnones. The products could be further purified by recrystallisation from hot EtOH.

General Procedure 6 (GP6)

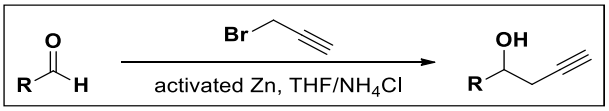

To a solution of aldehyde (1.0 eq), propargyl bromide (2.0 eq) in a mixture of THF (1.0 mL per mmol) and sat. NH_4Cl (1.0 mL per mmol) under argon at 0 °C was added activated Zn (2.0 eq) and the resulting suspension was stirred at room temperature overnight. The product was then extracted with Et_2O (3 x 2 mL per mmol) and the combined organic layers were dried over anhydrous $MgSO_4$, filtered and concentrated under vacuum. Purification by FCC afforded the corresponding homopropargyl alcohols.

Zinc activation: To an RBF containing Zn dust was added 1.0 M HCl (4 mL per g) and the resulting suspension sonicated for 60 seconds. The liquid was then decanted and the process repeated with H_2O, *i*-PrOH, MeOH, and Et_2O and the remaining solid was then dried under vacuum and stored under argon prior to use.

General Procedure 7 (GP7)

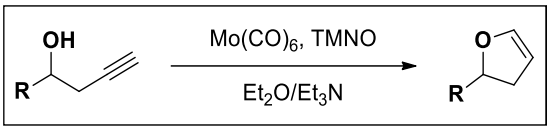

To a solution of $Mo(CO)_6$ (0.50 eq) and TMNO (0.50 eq) in Et_2O (5 mL per mmol) was added Et_3N (16.5 mL per mmol) and the resulting solution heated at 20 °C for 1 hour. The corresponding homopropargyl alcohol (1.0 eq) was then added dropwise and the reaction mixture heated at 50 °C for 60 h. After cooling to room temperature the volatiles were removed under vacuum and the crude residue purified by FCC to afford the title 2,3-dihydrofurans.

General Procedure 8 (GP8)

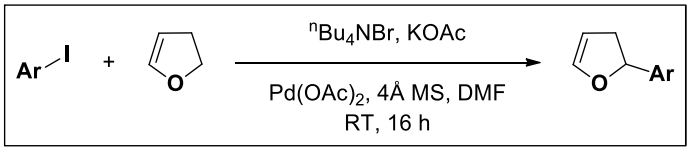

To a stirring suspension of KOAc (2.5 eq), TBABr (2.5 eq), $Pd(OAc)_2$ (5 mol%) and 4Å MS in degassed DMF (0.05 M) was added aryl iodide (1.0 eq) and 2,3-dihydrofuran (10 eq) and the mixture stirred at room temperature for 16 hours. The reaction was then filtered through celite and the filtrate washed

with brine. The organic phase was then dried over anhydrous $MgSO_4$, filtered and concentrated under vacuum. Purification by FCC afforded the target 2,3-dihydrofurans.

General Procedure 9 (GP9)

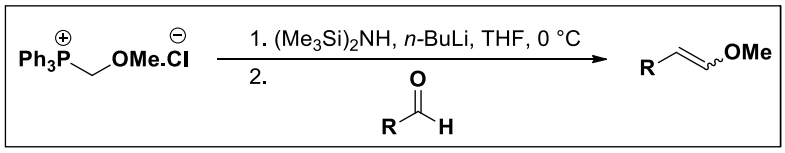

To a solution of hexamethyldisilazane (1.3 eq) in THF (0.33 M) under N_2 at 0°C was added *n*-BuLi (2.5 M in hexanes, 1.3 eq) and the resulting solution stirred at 0 °C for 45 minutes. (Methoxymethyl)triphenylphosphonium chloride (1.3 eq) was added in a single portion as a solid and the resulting solution stirred for 45 minutes at 0 °C before the dropwise addition of aldehyde (1.0 eq) in THF (0.25 M). The reaction was then stirred at 0 °C for 2 hours before dilution with pentane (30 mL per mmol) and filtration through silica. Removal of the volatiles under vacuum afforded the target enol ethers as a mixture of geometrical isomers.

General Procedure 10 (GP10)

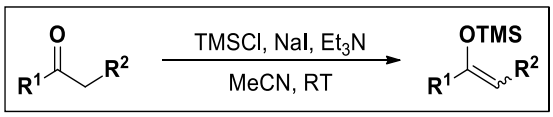

To the appropriate carbonyl compound dissolved in MeCN (0.20 M) under N_2 was added TMSCl (2.0 eq) and Et_3N (1.5 eq). A solution of NaI (1.5 eq) in acetonitrile (1.25 M) was then added dropwise and the resulting mixture stirred at room temperature for 2 hours. The reaction mixture was then concentrated under vacuum and the residual oil purified by FCC to afford the target silyl enol ethers.

General Procedure 11 (GP11)

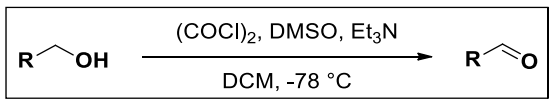

To a solution of $(COCl)_2$ (1.1 eq) in DCM (0.66 M) under N_2 at -78 °C was added DMSO (2.2 eq) dropwise and the resulting mixture stirred at -78 °C for 30 minutes. A solution of the corresponding alcohol (1.0 eq) in DCM (1.5 M) was then added dropwise and the resulting solution stirred at -78 °C for 30 minutes before the addition of Et_3N (5.0 eq). The reaction was then warmed to room temperature for 2 hours before dilution with sat. $NaHCO_3$ (2 mL per mmol) and extraction with DCM (4 x 2 mL per mmol). The combined organic layers were then washed with brine (2 mL per mmol), dried over anhydrous $MgSO_4$, filtered and concentrated under vacuum. Purification by FCC afforded the target aldehydes.

General Procedure 12 (GP12)

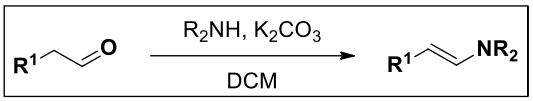

To a suspension of aldehyde (1.0 eq) and K_2CO_3 (2.0 eq) in DCM (1 mL per mmol) under N_2 was added amine (2.2 eq) slowly and the resulting mixture stirred at room temperature overnight. The suspension was then filtered and the filtrate concentrated under vacuum to afford the target enamines.

General Procedure 13 (GP13)

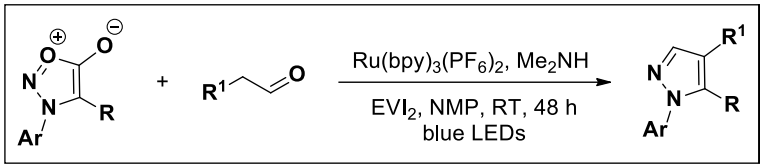

A flame-dried screw cap vial was charged with sydnone (1.0 eq), $Ru(bpy)_3(PF_6)_2$ (5 mol%) and EVI_2 (1.0 eq) under N_2. Anhydrous, degassed NMP (10 mL per mmol) was then added via syringe followed by aldehyde (3.0 eq) and Me_2NH (2.0 M in THF, 0.20 eq). The vial was then subjected to three vacuum/nitrogen cycles, sealed and irradiated at room temperature using a kessil A160WE tuna blue aquarium light for 48 hours. The reaction was then diluted with H_2O (50 mL per mmol) and extracted with Et_2O or EtOAc (4 x 50 mL per mmol). The combined organic layers were then washed with brine (50 mL per mmol), dried over anhydrous $MgSO_4$, filtered and concentrated under vacuum. Purification by FCC then afforded the target pyrazoles.

General Procedure 14 (GP14)

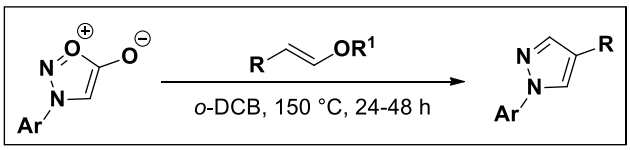

To a sealed tube charged with sydnone (1.0 eq) in *o*-DCB (1.0 M) was added enol ether (4.0 eq) and the resulting mixture heated at 150 °C for 24-48 hours. After cooling to room temperature the mixture was passed through a silica plug (eluting with 40-60 petroleum ether (100 mL per mmol) and then 10% MeOH/DCM (100 mL per mmol)). Purification by FCC then afforded the target pyrazoles.

General Procedure 15 (GP15)

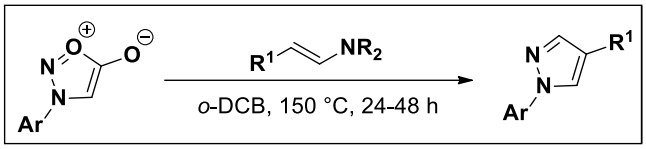

To a sealed tube charged with sydnone (1.0 eq) in *o*-DCB (1.0 M) was added enamine (2.0 eq) and the resulting mixture heated at 150 °C for 24 hours. After cooling to room temperature the mixture was passed through a silica plug (eluting with 40-60 petroleum ether (100 mL per mmol) and then 10% MeOH/DCM (100 mL per mmol)). Purification by FCC then afforded the target pyrazoles.

General Procedure 16 (GP16)

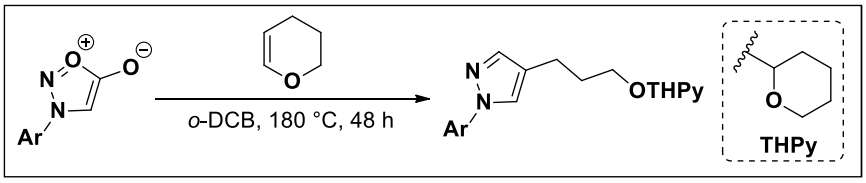

To a sealed tube charged with sydnone (1.0 eq) in *o*-DCB (1.0 M) was added 3,4-dihydro-2*H*-pyran (4.0 eq) and the mixture heated to 180 °C for 48 hours. After cooling to room temperature the mixture was passed through a silica plug (eluting with 40-60 petroleum ether (100 mL per mmol) and then 10% MeOH/DCM (100 mL per mmol)). Purification by FCC then afforded the target pyrazoles.

General Procedure 17 (GP17)

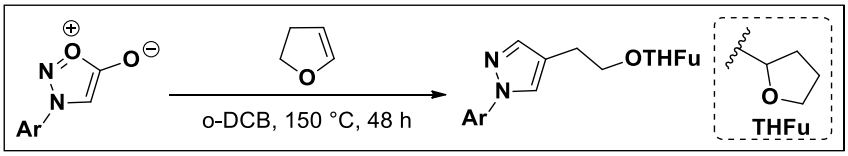

To a sealed tube charged with sydnone (1.0 eq) in *o*-DCB (0.25 M) and 2,3-dihydrofuran (4.0 eq) and the mixture heated to 150 °C for 48 hours. After cooling to room temperature the mixture was passed through a silica plug (eluting with 40-60 petroleum ether (100 mL per mmol) and then 10% MeOH/DCM (100 mL per mmol)). Purification by FCC then afforded the target pyrazoles.

General Procedure 18 (GP18)

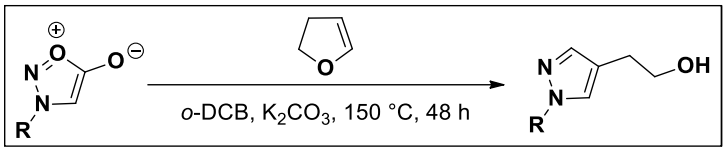

To a sealed tube charged with sydnone (1.0 eq) and K_2CO_3 (2.0 eq) was added *o*-DCB (0.17 M) and the resulting mixture stirred at ambient temperature for 1 hour. 2,3-Dihydrofuran (4 eq) was then added and the mixture heated to 150 °C for 48 hours. After cooling to room temperature the mixture was passed through a silica plug (eluting with 40-60 petroleum ether (100 mL per mmol) and then 10% MeOH/DCM (100 mL per mmol)). Purification by FCC then afforded the target pyrazoles.

General Procedure 19 (GP19)

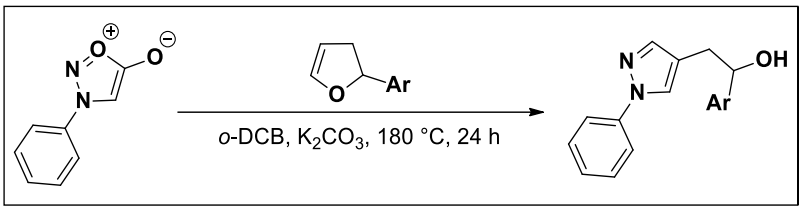

To a sealed tube charged with *N*-phenylsydnone (1.0 eq) and K_2CO_3 (1.0 eq) in *o*-DCB (0.25 M) was added 2-substituted-2,3-dihydrofuran (2.0 eq) and the mixture heated to 180 °C for 24 hours. After cooling to room temperature the mixture was passed through a silica plug (eluting with 40-60 petroleum ether (100 mL per mmol) and then 10% MeOH/DCM (100 mL per mmol)). Purification by FCC then afforded the target pyrazoles.

General Procedure 20 (GP20)

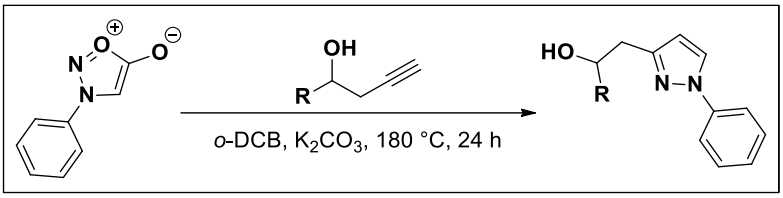

To a sealed tube charged with sydnone (1.0 eq) in *o*-DCB (0.50 M) was added alkyne (3.0 eq) and the resulting mixture heated at 150 °C for 24 hours. After cooling to room temperature the mixture was passed through a silica plug (eluting with 40-60 petroleum ether (100 mL per mmol) and then 10% MeOH/DCM (100 mL per mmol)). Purification by FCC then afforded the target pyrazoles.

5.3 Substrates

5.3.1 Sydnones

N-(*o*-Tolyl)glycine ethyl ester (375).[235]

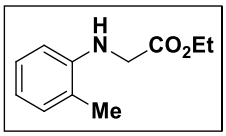

Following GP1 using 2-methylaniline (5.0 g, 47 mmol), ethyl bromoacetate (7.8 g, 47 mmol) and NaOAc (3.8 g, 47 mmol) with FCC (5% EtOAc in 40-60 petroleum ether), *N*-(*o*-tolyl)glycine ethyl ester (**375**) was isolated as an orange oil (7.29 g, 81%).

^{1}H NMR (400 MHz, $CDCl_3$) δ 7.19 – 7.08 (m, 2H), 6.73 (td, *J* = 7.5, 0.5 Hz, 1H), 6.51 (d, *J* = 7.5 Hz, 1H), 4.28 (q, *J* = 7.0 Hz, 2H), 4.23 (br, 1H), 3.96 (s, 2H), 2.24 (s, 3H), 1.33 (t, *J* = 7.0 Hz, 3H); **^{13}C NMR (101 MHz, $CDCl_3$)** δ 171.4, 145.2, 130.3, 127.2, 122.6, 117.9, 110.0, 61.4, 46.0, 17.5, 14.3.

N-(*m*-Tolyl)glycine ethyl ester (376).[235]

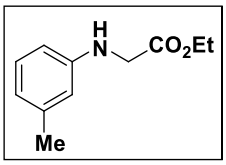

Following GP1 using 3-methylaniline (5.0 g, 47 mmol), ethyl bromoacetate (7.8 g, 47 mmol) and NaOAc (3.8 g, 47 mmol) with FCC (0-20% EtOAc In 40-60 petroleum ether), *N*-(*m*-tolyl)glycine ethyl ester (**376**) was isolated as an orange solid (4.4 g, 43%).

^{1}H NMR (400 MHz, $CDCl_3$) δ 7.13 – 7.06 (m, 1H), 6.62 – 6.56 (m, 1H), 6.47 – 6.40 (m, 2H), 4.25 (q, *J* = 7.0 Hz, 3H), 3.90 (s, 2H), 2.29 (s, 3H), 1.31 (t, *J* = 7.0 Hz, 3H); **^{13}C NMR (101 MHz, $CDCl_3$)** δ 171.5, 147.4, 139.4, 129.5, 119.5, 114.2, 110.5, 61.6, 46.2, 21.9, 14.5.

Synthesis of *N*-(4-Methoxyphenyl)glycine ethyl ester (377).[236]

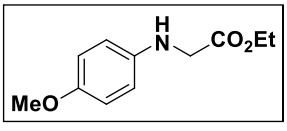

To a solution of *p*-anisidine (10 g, 81 mmol) in Et_3N (200 mL) under N_2 at 0 °C was added ethyl bromoacetate (14 g, 81 mmol) and the resulting solution stirred at room temperature for 20 hours. The solution was then concentrated under vacuum and the residue purified by FCC (10% EtOAc in 40-

60 petroleum ether) to afford *N*-(4-methoxyphenyl)glycine ethyl ester (**377**) as an orange solid (11 g, 62%).

M.P. 56-58 °C (lit.[236] 43 °C); **^{1}H NMR (400 MHz, $CDCl_3$)** δ 6.82 – 6.76 (m, 2H), 6.62 – 6.56 (m, 2H), 4.23 (q, *J* = 7.0 Hz, 2 H), 4.03 (br, 1H), 3.86 (s, 2H), 3.75 (s, 3H), 1.29 (t, *J* = 7.0 Hz, 3H); **^{13}C NMR (101 MHz, $CDCl_3$)** δ 171.5, 152.7, 141.4, 115.0, 114.5, 61.4, 55.9, 47.0, 14.3.

N-(3,4,5-Trimethoxyphenyl)glycine ethyl ester (378).[59]

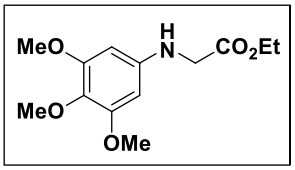

Following GP1 using 3,4,5-trimethoxyaniline (10 g, 55 mmol), ethyl bromoacetate (9.1 g, 55 mmol) and NaOAc (8.9 g, 110 mmol), *N*-(3,4,5-trimethoxyphenyl)glycine ethyl ester (**378**) was isolated as a colourless solid (6.65 g, 45%).

M.P. 70-72 °C (lit.[59] 73-75 °C); **^{1}H NMR (400 MHz, $CDCl_3$)** δ 5.88 (s, 2H), 4.28 (q, *J* = 7.0 Hz, 2H), 3.91 (s, 2H), 3.85 (s, 6H), 3.78 (s, 3H), 1.33 (t, *J* = 7.0 Hz, 3H); **^{13}C NMR (101 MHz, $CDCl_3$)** δ 171.1, 154.0, 143.9, 130.6, 90.6, 61.3, 61.0, 55.9, 46.3, 14.2.

N-(4-Chlorophenyl)glycine ethyl ester (379).[26]

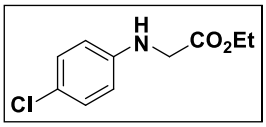

Following GP1 using 4-chloroaniline (10 g, 78 mmol), ethyl bromoacetate (13 g, 78 mmol) and NaOAc (13 g, 160 mmol), *N*-(4-chlorophenyl)glycine ethyl ester (**379**) was isolated as a pale yellow solid (11 g, 64%).

M.P. 90-92 °C (lit.[26] 88 °C); **^{1}H NMR (400 MHz, $CDCl_3$)** δ 7.19 – 7.14 (m, 2H), 6.58 – 6.52 (m, 2H), 4.32 (br, 1H), 4.27 (q, *J* = 7.0 Hz, 2H), 3.89 (d, *J* = 5.5 Hz, 2H), 1.32 (t, *J* = 7.0 Hz, 3H); **^{13}C NMR (101 MHz, $CDCl_3$)** δ 170.8, 145.6, 129.2, 122.9, 114.1, 61.5, 45.9, 14.2.

N-(4-Bromophenyl)glycine ethyl ester (380).[237]

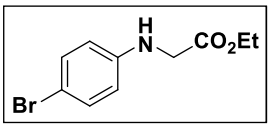

Following GP1 using 4-bromoaniline (10 g, 58 mmol), ethyl bromoacetate (9.7 g, 58 mmol) and NaOAc (9.5 g, 120 mmol), *N*-(4-bromophenyl)glycine ethyl ester (**380**) was isolated as a white solid (6.3 g, 42 %).

M.P. 88-89 °C (lit.[237] 95-96 °C); **^{1}H NMR (400 MHz, $CDCl_3$)** δ 7.32 – 7.26 (m, 2H), 6.53 – 6.47 (m, 2H), 4.35 (br, 1H), 4.27 (q, *J* = 7.0 Hz, 2H), 3.88 (s, 2H), 1.32 (t, *J* = 7.0 Hz, 3H); **^{13}C NMR (101 MHz, $CDCl_3$)** δ 170.8, 146.0, 132.0, 114.6, 109.9, 61.5, 45.7, 14.2.

N-(*o*-Tolyl)glycine (381).[238]

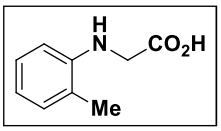

Following GP2 using *N*-(*o*-tolyl)glycine ethyl ester (**375**) (5.0 g, 26 mmol) and NaOH (1.6 g, 39 mmol), *N*-(*o*-tolyl)glycine (**381**) was isolated as a white solid (4.0 g, 94%).

^{1}H NMR (400 MHz, DMSO) δ 7.02 – 6.96 (m, 2H), 6.56 – 6.49 (m, 1H), 6.36 (d, *J* = 8.0 Hz, 1H), 3.83 (s, 2H), 2.10 (s, 3H); **^{13}C NMR (101 MHz, DMSO)** δ 172.7, 145.8, 129.7, 126.7, 121.6, 116.2, 109.1, 44.9, 17.5.

N-(*m*-Tolyl)glycine (382).[238]

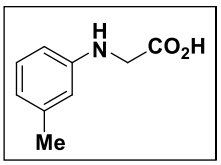

Following GP2 using *N*-(*m*-tolyl)glycine ethyl ester (**376**) (3.3 g, 17 mmol) and NaOH (1.0 g, 26 mmol), *N*-(*m*-tolyl)glycine (**382**) was isolated as a brown powder (2.2 g, 76%).

^{1}H NMR (400 MHz, DMSO) δ 7.05 – 6.94 (m, 1H), 6.47 – 6.35 (m, 3H), 3.80 (s, 2H), 2.22 (s, 3H); **^{13}C NMR (101 MHz, DMSO)** δ 173.7, 149.1, 138.8, 129.6, 118.1, 113.7, 110.4, 45.7, 22.3.

N-(4-Methoxyphenyl)glycine (383).[239]

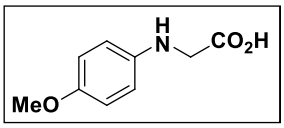

Following GP2 using *N*-(4-methoxyphenyl)glycine ethyl ester (**377**) (5.0 g, 24 mmol) and NaOH (1.4 g, 36 mmol), *N*-(4-methoxyphenyl)glycine (**383**) was isolated as a white powder (3.9 g, 90%).

M.P. 140-141 °C (lit.[239] 140-142 °C); **^{1}H NMR (400 MHz, DMSO)** δ 6.74 – 6.69 (m, 2H), 6.54 – 6.48 (m, 2H), 3.73 (s, 2H), 3.64 (s, 3H), 3.36 (br, 1H); **^{13}C NMR (101 MHz, DMSO)** δ 173.0, 151.0, 142.4, 114.5, 113.2, 55.3, 45.5.

N-(3,4,5-Trimethoxyphenyl)glycine (384).[59]

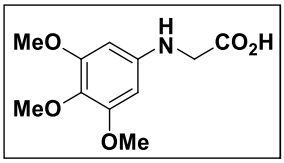

Following GP2 using *N*-(3,4,5-trimethoxyphenyl)glycine ethyl ester (**378**) (5.0 g, 18.6 mmol) and NaOH (1.1 g, 28.0 mmol), *N*-(3,4,5-trimethoxyphenyl)glycine (**384**) was isolated as an orange solid (3.72 g, 83%).

M.P. 110-112 °C (lit.[59] 111-114 °C); **^{1}H NMR (400 MHz, $CDCl_3$)** 5.86 (s, 2H), 3.96 (s, 2H), 3.82 (s, 6H), δ 3.76 (s, 3H); **^{13}C NMR (101 MHz, $CDCl_3$)** δ 175.3, 154.2, 143.5, 131.2, 91.1, 61.2, 56.2, 46.3.

N-(4-Chlorophenyl)glycine (385).[26]

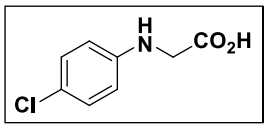

Following GP2 using *N*-(4-chlorophenyl)glycine ethyl ester (**379**) (5.0 g, 23 mmol) and NaOH (1.4 g, 35 mmol), *N*-(4-chlorophenyl)glycine (**385**) was isolated as a white powder (3.7 g, 85%).

M.P. 139-141 °C (lit.[26] 141 °C); **^{1}H NMR (400 MHz, DMSO)** δ 7.12 – 7.07 (m, 2H), 6.60 – 6.53 (m, 2H), 3.79 (s, 2H); **^{13}C NMR (101 MHz, DMSO)** δ 172.9, 147.7, 129.0, 119.8, 114.0, 45.1.

N-(4-Bromophenyl)glycine (386).[31]

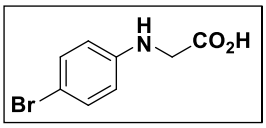

Following GP2 using *N*-(4-bromophenyl)glycine ethyl ester (**380**) (5.2 g, 20 mmol) and NaOH (1.2 g, 30 mmol), *N*-(4-bromophenyl)glycine (**386**) was isolated as a brown powder (3.4 g, 74%).

M.P. 136-139 °C (lit.[31] 105 °C); **^{1}H NMR (400 MHz, DMSO)** δ 7.25 – 7.18 (m, 2H), 6.56 – 6.46 (m, 2H), 3.79 (s, 2H); **^{13}C NMR (101 MHz, DMSO)** δ 172.8, 148.0, 131.8, 114.6, 107.3, 45.0.

N-(4-Trifluoromethylphenyl)glycine (387).[240]

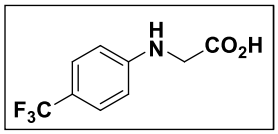

To a solution of glyoxylic acid monohydrate (1.1 g, 12 mmol), $NaB(CN)H_3$ (0.50 g, 8.0 mmol), NaOAc (1.3 g, 16 mmol) and glacial acetic acid (1.9 g, 32 mmol) in MeOH (32 mL) under N_2 at 0 °C was added 4-(trifluoromethyl)aniline (1.3 g, 8.0 mmol) and the resulting mixture stirred at room temperature for 2 hours. The mixture was then filtered through Celite and the solid cake was washed with 1% acetic acid in EtOAc (32 mL) before the addition of brine (32 mL). The mixture was then extracted with EtOAc (3 x 30 mL), dried over anhydrous $MgSO_4$, filtered and concentrated under vacuum. Purification by recrystallisation from EtOH/H_2O (4/1) afforded *N*-(4-trifluoromethylphenyl)glycine (**387**) as a yellow solid (0.76 g, 43%).

M.P. 130-132 °C (lit.[240] 130-132 °C); **^{1}H NMR (400 MHz, DMSO)** δ 7.38 (m, 2H), 6.65 (m, 3H), 3.87 (s, 2H); **^{13}C NMR (101 MHz, DMSO)** δ 172.6, 151.8, 126.6 (q, *J* = 4.0 Hz), 125.8 (q, *J* = 270 Hz), 116.2 (q, *J* = 32 Hz), 112.0, 44.6; **^{19}F NMR (377 MHz, DMSO)** δ -59.0.

N-(4-Nitrophenyl)glycine (388).[241]

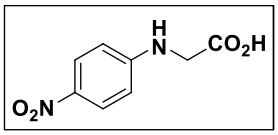

Following GP3 using glycine (5.0 g, 67 mmol), NaOH (2.7 g, 67 mmol), K_2CO_3 (10 g, 73 mmol), tetra-*n*-butylammonium hydroxide (1.0 g, 4.0 mmol) and 1-fluoro-4-nitrobenzene (8.4 g, 59 mmol) with recrystallisation from hot EtOH, *N*-(4-nitrophenyl)glycine (**388**) was isolated as a yellow solid (5.84 g, 50%).

M.P. 208-210 °C dec. (lit.[241] 229 °C); **^{1}H NMR (400 MHz, DMSO)** δ 8.00 (m, 2H), 7.46 (t, *J* = 6.0 Hz, 1H), 6.66 (m, 2H), 3.97 (d, *J* = 6.0 Hz, 2H); **^{13}C NMR (101 MHz, DMSO)** δ 171.8, 154.8, 136.7, 126.5, 111.7, 44.6.

N-(4-Cyanophenyl)glycine (389).[32]

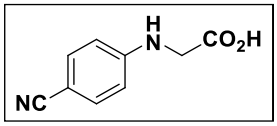

Following GP3 using glycine (5.0 g, 67 mmol), NaOH (2.7 g, 67 mmol), K_2CO_3 (10 g, 73 mmol), tetra-*n*-butylammonium hydroxide (1.0 g, 4.0 mmol) and 4-fluorobenzonitrile (7.2 g, 59 mmol) with recrystallisation from hot EtOH, *N*-(4-cyanophenyl)glycine (**389**) was isolated as a white solid (4.3 g, 41%).

M.P. 212-214 °C dec. (lit.[32] 240-243 °C); **^{1}H NMR (400 MHz, DMSO):** δ 7.46 (m, 2H), 6.92 (t, *J* = 6.0 Hz, 1H), 6.64 (m, 2H), 3.88 (d, *J* = 6.0 Hz, 2H). **^{13}C NMR (101 MHz, DMSO)** δ 172.2, 152.4, 133.8, 121.0, 112.6, 96.8, 44.4.

2-(Phenylamino)propanoic acid (390).[79]

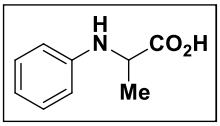

To a suspension of (±)-alanine (2.5 g, 28 mmol), CuI (0.36 g, 1.9 mmol), K_3PO_4 (12 g, 56 mmol) and 2-(dimethylamino)ethanol (5.0 g, 56 mmol) in H_2O (19 mL) under N_2 was added bromobenzene (2.9 g, 19 mmol) and the resulting mixture heated at 90 °C overnight. After cooling to room temperature the mixture was poured onto ice, acidified to pH 6 with 6.0 M HCl and extracted with EtOAc (4 x 30 mL). The combined organic layers were then dried over anhydrous $MgSO_4$, filtered and concentrated under vacuum. Purification by FCC (20% 40-60 petroleum ether in EtOAc) afforded 2-(phenylamino)propanoic acid (**390**) as a tan solid (1.6 g, 52%).

^{1}H NMR (400 MHz, DMSO) δ 7.10 – 7.03 (m, 2H), 6.58 – 6.52 (m, 3H), 3.93 (q, *J* = 7.0 Hz, 1H), 1.36 (d, *J* = 7.0 Hz, 3H); **^{13}C NMR (101 MHz, DMSO)** δ 176.0, 147.8, 128.9, 116.2, 112.4, 51.0, 18.2.

N-Methylsydnone (103).[242]

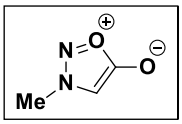

Following GP4 using sarcosine (5.0 g, 56 mmol), IAN (7.2 g, 62 mmol) and TFAA (18 g, 84 mmol), *N*-methylsydnone (**103**) was isolated as an orange oil (1.84 g, 33%).

^{1}H NMR (400 MHz, $CDCl_3$) δ 6.39 (s, 1H), 4.05 (s, 3H); **^{13}C NMR (101 MHz, $CDCl_3$)** δ 169.4, 95.9, 39.4.

N-Isopropylsydnone (104).[243]

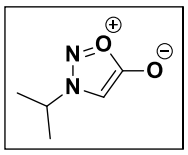

Following GP5 using isopropylamine (10 g, 170 mmol), NaOAc (28 g, 340 mmol), ethyl bromoacetate (28 g, 170 mmol), NaOH (9.1 g, 230 mmol), IAN (20 g, 170 mmol) and TFAA (39 g, 190 mmol), *N*-isopropylsydnone (**104**) was isolated as a yellow solid (4.8 g, 22%).

M.P. 46-48 °C (lit.[243] 54-55 °C); **^{1}H NMR (400 MHz, $CDCl_3$)** δ 6.33 (s, 1H), 4.68 (hept, *J* = 7.0 Hz, 1H), 1.65 (d, *J* = 7.0 Hz, 6H); **^{13}C NMR (101 MHz, $CDCl_3$):** δ 169.5, 92.5, 57.6, 21.7.

N-Benzylsydnone (105).[244]

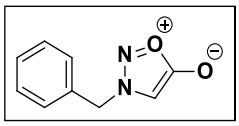

Following GP4 using *N*-benzylglycine hydrochloride (5.0 g, 30 mmol), IAN (3.9 g, 33 mmol) and TFAA (9.5 g, 46 mmol), *N*-benzylsydnone (**105**) was isolated as a white solid (2.81 g, 53%).

M.P. 66-67 °C (lit.[244] 66-67 °C); **^{1}H NMR (400 MHz, $CDCl_3$)** δ 7.51 – 7.31 (m, 5H), 6.22 (s, 1H), 5.37 (s, 2H); **^{13}C NMR (101 MHz, $CDCl_3$)** δ 169.3, 130.6, 130.1, 129.5, 128.8, 94.8, 57.2.

N-(Carboxymethyl)sydnone (106).[79]

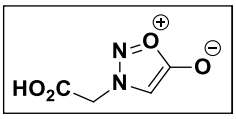

Following GP4 using iminodiacetic acid (10 g, 75 mmol), IAN (9.7 g, 83 mmol) and TFAA (24 g, 110 mmol), *N*-(carboxymethyl)sydnone (**106**) was isolated as a beige solid (10.6 g, 98%).

M.P. 123-126 °C; **^{1}H NMR (400 MHz, D_2O)** δ 6.86 (s, 1H), 5.26 (s, 2H); **^{13}C NMR (101 MHz, DMSO)** δ 169.1, 166.5, 97.6, 53.9.

N-Phenylsydnone (35).[240]

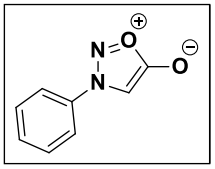

Following GP4 using *N*-Phenylglycine (15 g, 99 mmol), IAN (13 g, 110 mmol) and TFAA (31 g, 150 mmol), *N*-phenylsydnone (**35**) was isolated as a beige solid (14 g, 87%).

M.P. 134-135 °C (lit.[240] 132-134 °C); **^{1}H NMR (400 MHz, $CDCl_3$)** δ 7.78 – 7.60 (m, 5H), 6.76 (s, 1H); **^{13}C NMR (101 MHz, $CDCl_3$)** δ 169.0, 134.8, 132.5, 130.3, 121.3, 93.8.

N-(*o*-Tolyl)sydnone (307).[31]

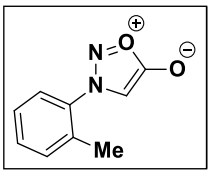

Following GP4 using *N*-(*o*-tolyl)glycine (**381**) (3.0 g, 18 mmol), IAN (2.3 g, 20 mmol) and TFAA (5.7 g, 27 mmol), *N*-(*o*-tolyl)sydnone (**307**) was isolated as a tan solid (2.7 g, 83%).

^{1}H NMR (400 MHz, $CDCl_3$) δ 7.60 – 7.52 (m, 1H), 7.47 – 7.40 (m, 3H), 6.48 (s, 1H), 2.33 (s, 3H); **^{13}C NMR (101 MHz, $CDCl_3$)** δ 169.1, 134.3, 133.4, 132.3, 132.2, 127.6, 125.3, 97.2, 17.3.

N-(*m*-Tolyl)sydnone (391).[245]

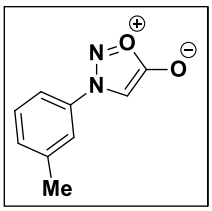

Following GP4 using *N*-(*m*-tolyl)glycine (**382**) (2.2 g, 13 mmol), IAN (1.7 g, 14 mmol) and TFAA (4.1 g, 20 mmol), *N*-(*m*-tolyl)sydnone (**391**) was isolated as a red solid (1.3 g, 56%).

M.P. 80-82 °C (lit.[245] 79 °C); **^{1}H NMR (400 MHz, $CDCl_3$)** δ 7.55 – 7.43 (m, 4H), 6.70 (s, 1H), 2.48 (s, 3H); **^{13}C NMR (101 MHz, $CDCl_3$)** δ 169.3, 141.2, 135.1, 133.5, 130.4, 122.1, 118.7, 94.0, 21.7.

N-(4-Methoxyphenyl)sydnone (46).[240]

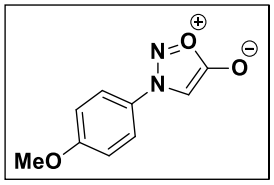

Following GP4 using *N*-(4-methoxyphenyl)glycine (**383**) (3.5 g, 19 mmol), IAN (2.5 g, 21 mmol) and TFAA (6.1 g, 29 mmol), *N*-(4-methoxyphenyl)sydnone (**46**) was isolated as a brown solid (2.8 g, 76%).

M.P. 126 °C (lit.[240] 120-122 °C); **^{1}H NMR (400 MHz, $CDCl_3$)** δ 7.69 – 7.64 (m, 2H), 7.14 – 7.06 (m, 2H), 6.67 (s, 1H), 3.92 (s, 3H); **^{13}C NMR (101 MHz, $CDCl_3$)** δ 169.1, 162.5, 127.7, 122.7, 115.3, 93.4, 55.9.

N-(3,4,5-Trimethoxyphenyl)sydnone (47).[59]

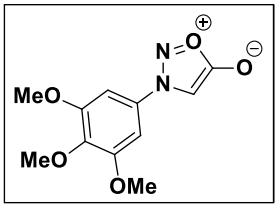

Following GP4 using *N*-(3,4,5-trimethoxyphenyl)glycine (**384**) (3.7 g, 15 mmol), IAN (2.0 g, 17 mmol) and TFAA (4.8 g, 23 mmol), *N*-(3,4,5-trimethoxyphenyl)sydnone (**47**) was isolated as a brown solid (1.75 g, 45%).

M.P. 179-181 °C (lit.[59] 179-182 °C); **^{1}H NMR (400 MHz, $CDCl_3$)** δ 6.96 (s, 2H), 6.81 (s, 1H), 3.95 (s, 6H), 3.92 (s, 3H); **^{13}C NMR (101 MHz, $CDCl_3$)** δ 169.0, 154.1, 141.1, 130.3, 99.1, 94.1, 61.1, 56.7.

N-(4-Fluorophenyl)sydnone (392).[240]

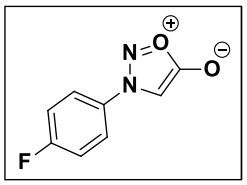

Following GP5 using 4-fluoroaniline (7.5 g, 68 mmol), NaOAc (11 g, 140 mmol), ethyl bromoacetate (11 g, 68 mmol), NaOH (4.1 g, 100 mmol), IAN (7.9 g, 68 mmol) and TFAA (21.2 g, 101 mmol), *N*-(4-fluorophenyl)sydnone (**392**) was isolated as an orange solid (2.8 g, 23%).

M.P. 152 °C (lit.[240] 150-152 °C); **^{1}H NMR (400 MHz, $CDCl_3$)** δ 7.81 – 7.73 (m, 2H), 7.39 – 7.31 (m, 2H), 6.72 (s, 1H); **^{13}C NMR (101 MHz, $CDCl_3$)** δ 168.8, 164.6 (d, *J* = 255.0 Hz), 131.0, 123.6 (d, *J* = 9.2 Hz), 117.6 (d, *J* = 23.7 Hz), 93.9; **^{19}F NMR (377 MHz, $CDCl_3$):** δ -105.34 – -105.43 (m).

N-(4-Chlorophenyl)sydnone (393).[26]

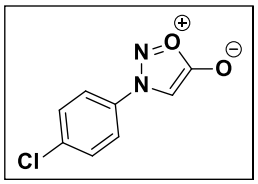

Following GP4 using *N*-(4-chlorophenyl)glycine (**385**) (7.0 g, 37 mmol), IAN (4.8 g, 41 mmol) and TFAA (12 g, 56 mmol), *N*-(4-chlorophenyl)sydnone (**393**) was isolated as a yellow solid (5.56 g, 75%).

M.P. 113-114 °C (lit.[26] 113 °C); **^{1}H NMR (400 MHz, $CDCl_3$)** δ 7.75 – 7.68 (m, 2H), 7.67 – 7.60 (m, 2H), 6.75 (s, 1H); **^{13}C NMR (101 MHz, $CDCl_3$)** δ 168.7, 138.8, 133.2, 130.6, 122.6, 93.6.

N-(4-Bromophenyl)sydnone (394).[34]

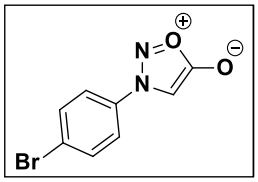

Following GP4 using *N*-(4-bromophenyl)glycine (**386**) (3.2 g, 14 mmol), IAN (1.8 g, 15 mmol) and TFAA (4.4 g, 21 mmol), *N*-(4-bromophenyl)sydnone (**394**) was isolated as a brown solid (2.5 g, 75%).

M.P. 138-140 °C (lit.[34] 137.5-138.5 °C (dec.)); **^{1}H NMR (400 MHz, $CDCl_3$)** δ 7.83 – 7.77 (m, 2H), 7.67 – 7.62 (m, 2H), 6.74 (s, 1H); **^{13}C NMR (101 MHz, $CDCl_3$)** δ 168.8, 133.6, 130.6, 126.9, 122.7, 93.6.

N-(4-Trifluoromethylphenyl)sydnone (395).[240]

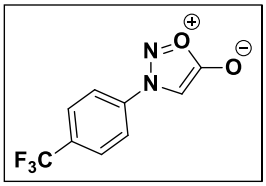

Following GP4 using *N*-(4-trifluoromethylphenyl)glycine (**387**) (500 mg, 2.3 mmol), IAN (290 mg, 2.5 mmol) and TFAA (720 mg, 3.4 mmol), *N*-(4-trifluoromethylphenyl)sydnone (**395**) was isolated as an orange solid (281 mg, 54%).

M.P. 131-133 °C (lit.[240] 132-134 °C); **^{1}H NMR (400 MHz, $CDCl_3$)** δ 8.03 – 7.87 (m, 4H), 6.83 (s, 1H); **^{13}C NMR (101 MHz, $CDCl_3$)** δ 168.7, 137.2, 134.5 (q, *J* = 33.5 Hz), 127.7 (q, *J* = 3.5 Hz), 122.9 (q, *J* = 273.0 Hz) 122.0, 93.9; **^{19}F NMR (377 MHz, $CDCl_3$):** δ -63.1.

N-(4-Nitrophenyl)sydnone (396).[26]

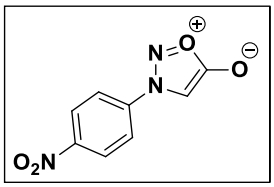

Following GP4 using *N*-(4-nitrophenyl)glycine (**388**) (3.2 g, 16 mmol), IAN (2.1 g, 18 mmol) and TFAA (5.1 g, 25 mmol), *N*-(4-nitrophenyl)sydnone (**396**) was isolated as an orange solid (1.16 g, 34%).

M.P. 147-148 °C (lit.[26] 149 dec.); **^{1}H NMR (400 MHz, $CDCl_3$)** δ 8.58 – 8.52 (m, 2H), 8.04 – 7.98 (m, 2H), 6.86 (s, 1H); **^{13}C NMR (101 MHz, DMSO)** δ 168.8, 149.8, 139.0, 126.0, 123.6, 96.2.

N-(4-Cyanophenyl)sydnone (397).[246]

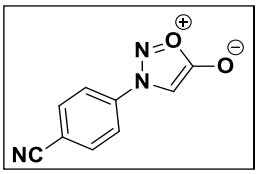

Following GP4 using *N*-(4-cyanophenyl)glycine (**389**) (3.2 g, 18 mmol), IAN (2.3 g, 20 mmol), and TFAA (5.7 g, 27 mmol), *N*-(4-cyanophenyl)sydnone (**397**) was isolated as a white solid (2.3 g, 68%).

M.P. 165-168 °C; **^{1}H NMR (400 MHz, $CDCl_3$)** δ 8.02 – 7.91 (m, 4H), 6.85 (s, 1H); **^{13}C NMR (101 MHz, DMSO)** δ 168.8, 137.9, 134.9, 123.0, 117.9, 115.4, 95.9.

3-Phenyl-4-methylsydnone (308).[79]

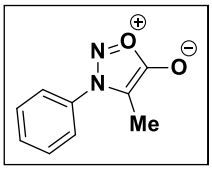

Following GP4 using 2-(phenylamino)propanoic acid (**390**) (1.5 g, 9.1 mmol), IAN (1.2 g, 10 mmol), and TFAA (2.9 g, 14 mmol), 3-phenyl-4-methylsydnone (**308**) was isolated as a brown solid (1.0 g, 65%).

^{1}H NMR (400 MHz, $CDCl_3$) δ 7.72 – 7.62 (m, 3H), 7.56 – 7.51 (m, 2H), 2.15 (s, 3H); **^{13}C NMR (101 MHz, $CDCl_3$)** δ 169.0, 134.1, 132.3, 130.3, 124.6, 105.2, 8.2.

3-Phenyl-4-acetylsydnone (38a).[240]

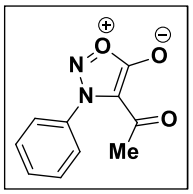

To a solution of *N*-phenylsydnone (**35**) (1.0 g, 6.2 mmol) in Ac_2O (15 mL) under N_2 was added montmorillonite K10 (6.0 g, 6 weight equivalents) and the resulting mixture heated at 110 °C overnight. The reaction mixture was then filtered and the filter cake washed with DCM (2 x 15 mL) and acetone (15 mL) and the combined filtrate was then concentrated under vacuum. Recrystallisation of the crude solid from hot EtOH afforded 3-phenyl-4-acetylsydnone (**38a**) as a yellow solid (0.37 g, 29%).

M.P. 139-141 °C (lit.[240] 138-139); **^{1}H NMR (400 MHz, $CDCl_3$)** δ 7.73 – 7.38 (m, 5H), 2.48 (s, 1H); **^{13}C NMR (101 MHz, $CDCl_3$)** δ 184.1, 166.2, 134.9, 132.3, 129.4, 124.9, 106.1, 28.1.

3-Phenyl-4-carboxysydnone (37).[240]

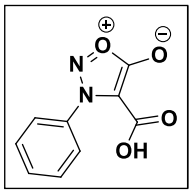

To a solution of *N*-phenylsydnone (**35**) (2.0 g, 12 mmol) in THF (41 mL) under N_2 at -78 °C was added *n*-BuLi (2.5 M in hexanes, 5.4 mL, 14 mmol) dropwise and the resulting mixture stirred at -78 °C for 1 hour. The mixture was then transferred via cannula to a RBF containing dry ice (excess) (**CAUTION:** large evolution of gaseous CO_2) and warmed to room temperature and stirred for 2 hours. The mixture was then diluted with H_2O (20 mL), washed with EtOAc (25 mL) and acidified to pH 1 with conc. HCl. The mixture was then extracted with EtOAc (4 x 25 mL) and the combined organic layers were dried over anhydrous $MgSO_4$, filtered and concentrated under vacuum. Recrystallisation of the crude solid from hot EtOH afforded 3-phenyl-4-carboxysydnone (**37**) as a beige solid (1.3 g, 52%).

M.P. 178-180 °C (lit.[240] 180-182); **^{1}H NMR (400 MHz, DMSO)** δ 13.35 (br, 1H), 7.82 – 7.58 (m, 5H); **^{13}C NMR (101 MHz, DMSO)** δ 164.5, 157.7, 135.3, 132.0, 129.2, 125.7, 100.7.

3-Phenyl-4-(phenylthio)sydnone (309).[210]

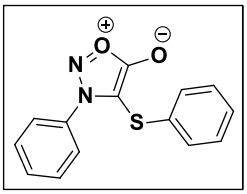

To a solution of *N*-phenylsydnone (**35**) (1.0 g, 6.2 mmol) in THF (10 mL) under N_2 at -78 °C was added *n*-BuLi (2.4 M in hexanes, 2.6 mL, 6.2 mmol) dropwise and the resulting mixture stirred at -78 °C for 1 hour. A solution of *S*-phenyl benzenesulfonothioate (1.6 g, 6.2 mmol) in THF (6.2 mL) was then added dropwise and the resulting mixture warmed to room temperature and stirred overnight. The reaction mixture was then diluted with 1 M HCl (20 mL) and extracted with DCM (4 x 25 mL). The combined organic layers were then dried over anhydrous $MgSO_4$, filtered and concentrated under vacuum. Purification by FCC (30% EtOAc in 40-60 petroleum ether) afforded 3-phenyl-4-(phenylthio)sydnone (**309**) as a tan solid (1.3 g, 78%).

^{1}H NMR (400 MHz, $CDCl_3$) δ 7.70 – 7.64 (m, 1H), 7.61 – 7.55 (m, 2H), 7.51 – 7.45 (m, 2H), 7.30 – 7.18 (m, 5H); **^{13}C NMR (101 MHz, $CDCl_3$)** δ 168.5, 134.1, 133.9, 132.6, 129.8, 129.7, 129.1, 128.0, 125.0, 100.5.

3-Phenyl-4-chlorosydnone (398).[79]

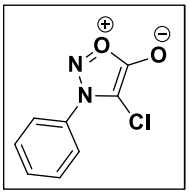

To a solution of *N*-phenylsydnone (**35**) (1.6 g, 10 mmol) in DMF (10 mL) was added *N*-chlorosuccinamide (1.5 g, 11 mmol) and the resulting solution stirred at room temperature for 3 hours. The reaction mixture was then poured onto ice and filtered to afford 3-phenyl-4-chlorosydnone (**398**) as a yellow solid (1.7 g, 86%).

M.P. 111-113 °C (lit.[79] 115-117 °C); **^{1}H NMR (400 MHz, $CDCl_3$)** δ 7.80 – 7.57 (m, 5H); **^{13}C NMR (101 MHz, $CDCl_3$)** δ 164.1, 133.1, 132.9, 130.3, 124.5.

The ^{13}C signal of the *C*4 carbon is not visible.

3-Phenyl-4-((3-hydroxypropyl)carbamoyl)sydnone (107).[77]

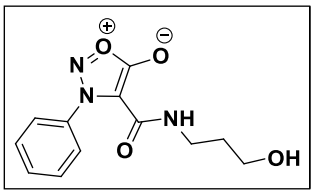

3-Phenyl-4-((3-hydroxypropyl)carbamoyl)sydnone (**107**) was a gift from Dr Andrew Brown and was synthesised according to a literature procedure.[77]

3-Phenyl-4-(4-(benzoyloxy)-3-(benzyloxy)phenyl)sydnone (108).[247]

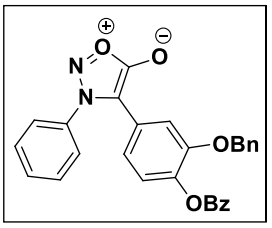

3-Phenyl-4-(4-(benzoyloxy)-3-(benzyloxy)phenyl)sydnone (**108**) was a gift from Dr Andrew Brown and was synthesised according to a literature procedure.[59]

3-Phenyl-4-(*p*-tolyl)sydnone (109).[59]

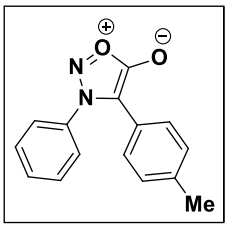

3-Phenyl-4-(*p*-tolyl)sydnone (**109**) was a gift from Dr Andrew Brown and was synthesised according to a literature procedure.[59]

3-Phenyl-4-(pyrazin-2-yl)sydnone (110).[77]

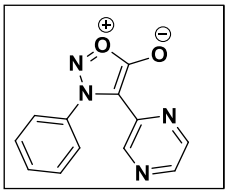

3-Phenyl-4-(pyrazin-2-yl)sydnone (**110**) was a gift from Dr Andrew Brown and was synthesised according to a literature procedure.[59]

3-Phenyl-4-(5-hydroxypentanoyl)sydnone (318).

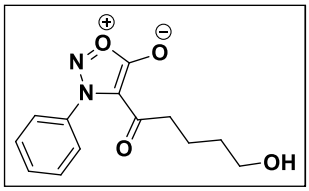

To a solution of *N*-phenylsydnone (**35**) (1.0 g, 6.2 mmol) in THF (25 mL) under N_2 at -78 °C was added *n*-BuLi (2.4 M in hexanes, 2.6 mL, 6.2 mmol) and resulting mixture stirred at -78 °C for 1 hour. δ-Valerolactone (0.31 g, 3.1 mmol) was then added dropwise and the reaction mixture stirred at -78 °C for 3 hours. After warming to room temperature the mixture was diluted with 1 M HCl (20 mL) and extracted with DCM (4 x 25 mL). The combined organic layers were then dried over anhydrous $MgSO_4$, filtered and concentrated under vacuum. Purification by FCC (gradient from 40-70% EtOAc in 40-60 petroleum ether) afforded 3-phenyl-4-(5-hydroxypentanoyl)sydnone (**318**) as a tan solid (1.2 g, 77%).

^{1}H NMR (400 MHz, $CDCl_3$) δ 7.71 – 7.65 (m, 1H), 7.63 – 7.57 (m, 2H), 7.49 – 7.44 (m, 2H), 3.62 (t, *J* = 6.0 Hz, 2H), 2.94 (t, *J* = 7.0 Hz, 2H), 1.78 – 1.66 (m, 3H), 1.64 – 1.55 (m, 2H); **^{13}C NMR (101 MHz, $CDCl_3$)** δ 187.3, 166.2, 135.0, 132.5, 129.6, 124.9, 105.4, 62.1, 39.8, 31.9, 19.5; **FTIR:** ν_{max} 3418, 2939, 2869, 1774, 1671, 1422, 1012 cm^{-1}.

3-Phenyl-4-(5-oxopentanoyl)sydnone (320).

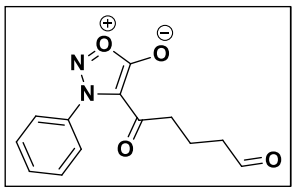

Following GP11 using $(COCl)_2$ (0.13 g, 1.1 mmol), DMSO (0.16 g, 2.1 mmol), 3-phenyl-4-(5-hydroxypentanoyl)sydnone (**318**) (0.25 g, 1.0 mmol) and Et_3N (0.48 g, 4.8 mmol) with purification by FCC (gradient from 40-60% EtOAc in 40-60 petroleum ether), 3-phenyl-4-(5-oxopentanoyl)sydnone (**320**) was isolated as a tan oil (0.16 g, 66%).

^{1}H NMR (400 MHz, $CDCl_3$) δ 9.73 (s, 1H), 7.73 – 7.66 (m, 1H), 7.64 – 7.57 (m, 2H), 7.50 – 7.44 (m, 2H), 2.96 (t, *J* = 7.0 Hz, 2H), 2.51 (td, *J* = 7.0, 1.0 Hz, 2H), 1.93 (p, *J* = 7.0 Hz, 2H); **^{13}C NMR (101 MHz, $CDCl_3$)** δ 202.5, 186.9, 166.0, 134.9, 132.5, 129.6, 125.1, 105.5, 44.0, 40.1, 21.2.

3-Phenyl-4-(6-hydroxyhexanoyl)sydnone (319).

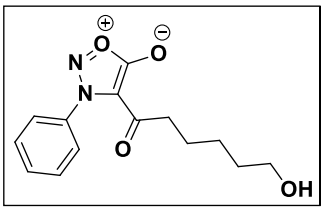

To a solution of *N*-phenylsydnone (**35**) (1.0 g, 6.2 mmol) in THF (25 mL) under N_2 at -78 °C was added *n*-BuLi (2.4 M in hexanes, 2.6 mL, 6.2 mmol) and resulting mixture stirred at -78 °C for 1 hour. ε-Caprolactone (0.35 g, 3.1 mmol) was then added dropwise and the reaction mixture stirred at -78 °C for 3 hours. After warming to room temperature the mixture was diluted with 1 M HCl (20 mL) and extracted with DCM (4 x 25 mL). The combined organic layers were then dried over anhydrous $MgSO_4$, filtered and concentrated under vacuum. Purification by FCC (gradient from 20-60% EtOAc in DCM) afforded 3-phenyl-4-(6-hydroxyhexanoyl)sydnone (**319**) as a tan solid (1.3 g, 75%).

^{1}H NMR (400 MHz, $CDCl_3$) δ 7.71 – 7.65 (m, 1H), 7.64 – 7.57 (m, 2H), 7.50 – 7.44 (m, 2H), 3.61 (t, *J* = 6.5 Hz, 2H), 2.93 (t, *J* = 7.3 Hz, 2H), 1.69 – 1.52 (m, 5H), 1.45 – 1.35 (m, 2H); **^{13}C NMR (101 MHz, $CDCl_3$)** δ 187.4, 166.2, 135.1, 132.5, 129.6, 125.0, 106.1, 62.7, 40.2, 32.5, 25.3, 23.1; **FTIR:** ν_{max} 3373, 2936, 2860, 1774, 1664, 1423, 1303, 1014 cm^{-1}.

3-Phenyl-4-(6-oxohexanoyl)sydnone (321).

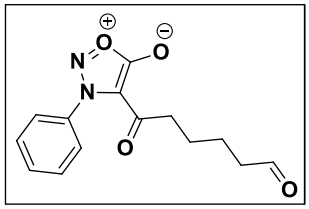

Following GP11 using $(COCl)_2$ (0.15 g, 1.2 mmol), DMSO (0.19 g, 2.4 mmol), 3-phenyl-4-(6-hydroxyhexanoyl)sydnone (**319**) (0.30 g, 1.1 mmol) and Et_3N (0.55 g, 5.5 mmol) with purification by FCC (gradient from 40-60% EtOAc in 40-60 petroleum ether), 3-phenyl-4-(6-oxohexanoyl)sydnone (**321**) was isolated as a yellow oil (0.24 g, 79%).

^{1}H NMR (400 MHz, $CDCl_3$) δ 9.74 (t, *J* = 1.5 Hz, 1H), 7.72 – 7.65 (m, 1H), 7.63 – 7.57 (m, 2H), 7.50 – 7.45 (m, 2H), 2.97 – 2.90 (m, 2H), 2.48 – 2.41 (m, 2H), 1.71 – 1.60 (m, 4H); **^{13}C NMR (101 MHz, $CDCl_3$)** δ 202.3, 186.8, 166.1, 135.0, 132.5, 129.6, 125.0, 106.0, 43.7, 39.9, 22.8, 21.4; **FTIR:** ν_{max} 2940, 1767, 1669, 1419, 1266, 1024 cm^{-1}.

3-Phenyl-4-(6-((*tert*-butyldimethylsilyl)oxy)-1-hydroxyhexyl)sydnone (313).

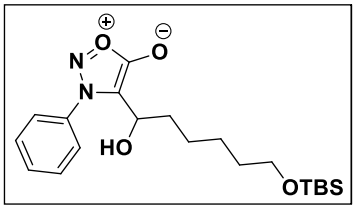

To a solution of *N*-phenylsydnone (**35**) (2.1 g, 13 mmol) in THF (64 mL) under N_2 at -78 °C was added *n*-BuLi (2.4 M in hexanes, 5.9 mL, 14 mmol) and the resulting solution stirred at -78 °C for 1 hour. 6-((*tert*-Butyldimethylsilyl)oxy)hexanal (**312**) (3.3 g, 14 mmol) was then added dropwise and the resulting mixture warmed slowly to room temperature and stirred overnight. The reaction was then diluted with H_2O (100 mL) and extracted with DCM (4 x 75 mL). The combined organic layers were then dried over anhydrous $MgSO_4$, filtered and concentrated under vacuum. Purification by FCC (gradient from 0-20% EtOAc in DCM) afforded 3-phenyl-4-(6-((*tert*-butyldimethylsilyl)oxy)-1-hydroxyhexyl)sydnone (**313**) as an orange oil (4.7 g, 94%).

^{1}H NMR (400 MHz, $CDCl_3$) δ 7.73 – 7.60 (m, 5H), 4.43 (t, *J* = 7.5 Hz, 1H), 3.54 (t, *J* = 6.5 Hz, 2H), 2.81 (br s, 1H), 2.05 – 1.88 (m, 2H), 1.49 – 1.40 (m, 2H), 1.38 – 1.18 (m, 4H), 0.91 – 0.79 (m, 9H), 0.09 – -0.04 (m, 6H); **^{13}C NMR (101 MHz, $CDCl_3$)** δ 167.8, 134.1, 132.7, 130.4, 125.3, 110.0, 64.7, 63.3, 34.2, 32.9, 31.3, 26.3, 26.0, 25.7, 18.7, -5.0; **FTIR ν_{max}** 3384, 2928, 2856, 1720, 1471, 1251, 1058 cm^{-1}; **HRMS** calculated for $C_{20}H_{32}N_2NaO_4Si$ (ES^+)(+Na^+): 415.2024. Found: 415.2034.

3-Phenyl-4-(1-acetoxy-6-((*tert*-butyldimethylsilyl)oxy)hexyl)sydnone (399).

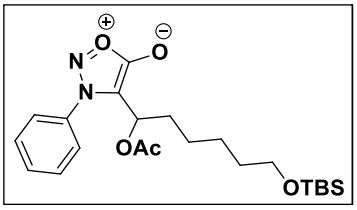

To a solution of 3-phenyl-4-(6-((*tert*-butyldimethylsilyl)oxy)-1-hydroxyhexyl)sydnone (**313**) (0.33 g, 0.84 mmol), pyridine (0.13 g, 1.7 mmol) and DMAP (10 mg, 84 µmol) in DCM (8.5 mL) under N_2 at 0 °C was added Ac_2O (0.17 g, 1.7 mmol) and the resulting mixture stirred at room temperature for 30 minutes before warming to room temperature for 45 minutes. The reaction was then diluted with $NaHCO_3$ (15 mL) and extracted with DCM (3 x 20 mL). The combined organic layers were then washed with 0.50 M HCl (15 mL), dried over anhydrous $MgSO_4$, filtered and concentrated under vacuum. Purification by FCC (gradient from 0-10% EtOAc in DCM) afforded 3-phenyl-4-(1-acetoxy-6-((*tert*-butyldimethylsilyl)oxy)hexyl)sydnone (**399**) as a yellow oil (0.36 g, 97%).

^{1}H NMR (400 MHz, $CDCl_3$) δ 7.73 – 7.68 (m, 1H), 7.67 – 7.61 (m, 2H), 7.58 – 7.52 (m, 2H), 5.42 (t, *J* = 7.5 Hz, 1H), 3.55 (t, *J* = 6.5 Hz, 2H), 2.09 – 1.99 (m, 5H), 1.51 – 1.41 (m, 2H), 1.36 – 1.18 (m, 4H), 0.87 (s, 9H), 0.02 (s, 6H); **^{13}C NMR (101 MHz, $CDCl_3$)** δ 170.7, 167.0, 134.0, 132.8, 130.3, 125.4, 106.8, 66.4, 63.2, 32.9, 31.3, 31.3, 26.3, 25.7, 21.1, 18.7, -5.0; **FTIR ν_{max}** 3485, 2930, 2857, 1738, 1472, 1371, 1228, 1095 cm^{-1}; **HRMS** calculated for $C_{22}H_{34}N_2NaO_5Si$ (ES^+)(+Na^+): 457.2129. Found: 457.2141.

3-Phenyl-4-(1-acetoxy-6-hydroxyhexyl)sydnone (400).

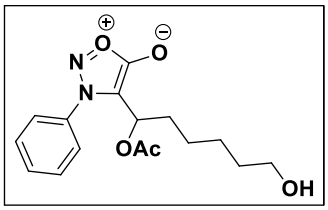

To a solution of 3-phenyl-4-(1-acetoxy-6-((*tert*-butyldimethylsilyl)oxy)hexyl)sydnone (**399**) (0.30 g, 0.69 mmol) in THF (14 mL) under N_2 at 0 °C was added TBAF (1.0 M in THF, 0.69 mL, 0.69 mmol) and the resulting mixture stirred at room temperature for 1 hour. TBAF (1.0 M in THF, 0.69 mL, 0.69 mmol) was then added and the reaction stirred for 1 hour before the addition of sat. $NaHCO_3$ (15 mL). The reaction was then extracted with EtOAc (3 x 30 mL) and the combined organic layers dried over anhydrous $MgSO_4$, filtered and concentrated under vacuum. Purification by FCC (50% EtOAc in DCM) afforded 3-phenyl-4-(1-acetoxy-6-hydroxyhexyl)sydnone (**400**) as a yellow oil (0.15 g, 66%).

^{1}H NMR (400 MHz, $CDCl_3$) δ 7.73 – 7.68 (m, 1H), 7.67 – 7.61 (m, 2H), 7.57 – 7.52 (m, 2H), 5.44 (t, *J* = 7.5 Hz, 1H), 3.59 (t, *J* = 6.5 Hz, 2H), 2.10 – 2.02 (m, 2H), 2.00 (s, 3H), 1.57 – 1.47 (m, 3H), 1.40 – 1.22 (m, 4H); **^{13}C NMR (101 MHz, $CDCl_3$)** δ 170.6, 167.0, 134.0, 132.8, 130.4, 125.4, 106.7, 66.3, 62.9, 32.6, 31.2, 25.5, 25.5, 21.1; **FTIR ν_{max}** 3451, 2938, 2862, 1722, 1242, 909 cm^{-1}; **HRMS** calculated for $C_{16}H_{20}N_2NaO_5$ (ES^+)(+Na^+): 343.1000. Found: 343.1001.

3-Phenyl-4-(1-acetoxy-6-oxohexyl)sydnone (314).

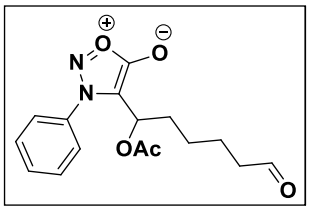

Following GP11 using $(COCl)_2$ (0.17 g, 1.4 mmol), DMSO (0.21 g, 2.7 mmol), 3-phenyl-4-(1-acetoxy-6-hydroxyhexyl)sydnone (**400**) (0.40 g, 1.3 mmol) and Et_3N (0.63 g, 6.3 mmol) with purification by FCC (20% EtOAc in DCM), 3-phenyl-4-(1-acetoxy-6-oxohexyl)sydnone (**314**) was isolated as a yellow oil (0.33 g, 82%).

^{1}H NMR (400 MHz, $CDCl_3$) δ 9.72 (t, *J* = 1.5 Hz, 1H), 7.74 – 7.68 (m, 1H), 7.68 – 7.61 (m, 2H), 7.57 – 7.50 (m, 2H), 5.44 (t, *J* = 7.5 Hz, 1H), 2.42 (t, *J* = 7.0 Hz, 2H), 2.11 – 2.02 (m, 2H), 2.00 (s, 3H), 1.60 (p, *J* = 7.5 Hz, 2H), 1.39 – 1.19 (m, 2H); **^{13}C NMR (101 MHz, $CDCl_3$)** δ 202.3, 170.5, 167.0, 133.9, 132.9, 130.4, 125.4, 106.4, 66.0, 43.7, 30.9, 25.2, 21.6, 21.1; **FTIR ν_{max}** 2938, 2865, 1732, 1475, 1370, 1224, 1017 cm^{-1}; **HRMS** calculated for $C_{16}H_{18}N_2NaO_5$ (ES^+)(+Na^+): 342.1139. Found: 342.1144.

3-Phenyl-4-(6-hydroxyhexyl)sydnone (401).

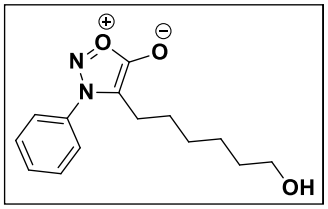

To a solution of 3-phenyl-4-(6-((*tert*-butyldimethylsilyl)oxy)-1-hydroxyhexyl)sydnone (**313**) (1.0 g, 2.6 mmol) and Et_3SiH (0.59 g, 5.1 mmol) in DCM (5.1 mL) under N_2 at 0 °C was added freshly distilled $BF_3.Et_2O$ (0.72 g, 5.1 mmol) and the resulting mixture stirred at room temperature for 45 minutes. The reaction was then diluted with sat. $NaHCO_3$ (25 mL) and extracted with EtOAc (4 x 25 mL). The combined organic layers were then dried over anhydrous $MgSO_4$, filtered and concentrated under vacuum. Purification by FCC (gradient from 40-60% EtOAc in DCM) afforded 3-phenyl-4-(6-hydroxyhexyl)sydnone (**401**) as an orange oil (0.33 g, 50%).

^{1}H NMR (400 MHz, $CDCl_3$) δ 7.73 – 7.62 (m, 3H), 7.53 – 7.48 (m, 2H), 3.58 (t, *J* = 6.5 Hz, 2H), 2.54 – 2.46 (m, 2H), 1.58 – 1.44 (m, 4H), 1.34 – 1.22 (m, 4H); **^{13}C NMR (101 MHz, $CDCl_3$)** δ 168.8, 134.0, 132.3, 130.3, 124.9, 109.5, 62.7, 32.4, 28.7, 27.3, 25.2, 22.3; **FTIR ν_{max}** 3419, 2928, 2857, 1720, 1478, 1236, 1057 cm^{-1}; **HRMS** calculated for $C_{14}H_{19}N_2O_3$ (ES^+)(+H^+): 263.1390. Found: 263.1394.

3-Phenyl-4-(6-oxohexyl)sydnone (315).

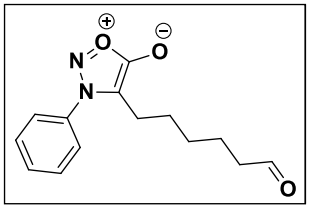

Following GP11 using $(COCl)_2$ (0.18 g, 1.4 mmol), DMSO (0.22 g, 2.8 mmol), 3-phenyl-4-(6-hydroxyhexyl)sydnone (**401**) (0.33 g, 1.3 mmol) and Et_3N (0.64 g, 6.3 mmol) with purification by FCC (gradient from 0-20% EtOAc in DCM), 3-phenyl-4-(6-oxohexyl)sydnone (**315**) was isolated as a brown oil (0.25 g, 75%).

^{1}H NMR (400 MHz, $CDCl_3$) δ 9.71 (t, *J* = 1.5 Hz, 1H), 7.73 – 7.61 (m, 3H), 7.52 – 7.47 (m, 2H), 2.53 – 2.46 (m, 2H), 2.37 (td, *J* = 7.0, 1.5 Hz, 2H), 1.59 – 1.50 (m, 4H), 1.32 – 1.22 (m, 2H); **^{13}C NMR (101 MHz, $CDCl_3$)** δ 202.4, 168.7, 134.0, 132.4, 130.3, 124.9, 109.1, 43.7, 28.5, 27.0, 22.3, 21.5; **FTIR ν_{max}** 2932, 2860, 1720, 1716, 1478, 1235, 1059 cm^{-1}; **HRMS** calculated for $C_{14}H_{16}N_2NaO_3$ (ES^+)(+Na^+): 261.1234. Found: 261.1236.

5.3.2 Dihydrofurans

1-Phenylbut-3-yn-1-ol (163).[248]

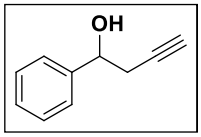

Following GP6 using benzaldehyde (0.50 g, 4.7 mmol), propargyl bromide (80% w/w in toluene, 1.4 g, 9.4 mmol), activated Zn (0.62 g, 9.4 mmol) with purification by FCC (gradient from 5-10% EtOAc in 40-60 petroleum ether), 1-phenylbut-3-yn-1-ol (**163**) was isolated as a colourless oil (0.41 g, 59%).

^{1}H NMR (400 MHz, $CDCl_3$) δ 7.42 – 7.34 (m, 4H), 7.33 – 7.28 (m, 1H), 4.90 – 4.84 (m, 1H), 2.67 – 2.62 (m, 2H), 2.53 (s, 1H), 2.08 (t, *J* = 2.5 Hz, 1H); **^{13}C NMR (101 MHz, $CDCl_3$)** δ 142.6, 128.6, 128.1, 125.9, 80.8, 72.4, 71.1, 29.5.

1-(4-Methoxyphenyl)but-3-yn-1-ol (166).[249]

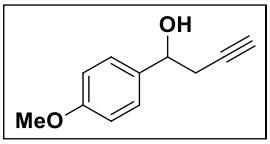

Following GP6 using *p*-anisaldehyde (1.3 g, 9.8 mmol), propargyl bromide (80% w/w in toluene, 2.9 g, 20 mmol), activated Zn (1.3 g, 20 mmol) with purification by FCC (gradient from 0-5% EtOAc in DCM), 1-(4-methoxyphenyl)but-3-yn-1-ol (**166**) was isolated as a yellow oil (0.69 g, 40%).

^{1}H NMR (400 MHz, $CDCl_3$) δ 7.34 – 7.28 (m, 2H), 6.92 – 6.86 (m, 2H), 4.85 – 4.76 (m, 1H), 3.80 (s, 3H), 2.64 – 2.60 (m, 2H), 2.06 (t, *J* = 2.5 Hz, 1H); **^{13}C NMR (101 MHz, $CDCl_3$)** δ 159.4, 134.8, 127.2, 114.0, 81.0, 72.1, 71.0, 55.4, 29.5.

1-(Thiophen-2-yl)but-3-yn-1-ol (167).[249]

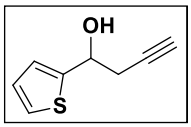

Following GP6 using thiophene-2-carboxaldehyde (1.1 g, 9.8 mmol), propargyl bromide (80% w/w in toluene, 2.9 g, 20 mmol), activated Zn (1.3 g, 20 mmol) with purification by FCC (gradient from 75-100% DCM in 40-60 petroleum ether), 1-(thiophen-2-yl)but-3-yn-1-ol (**167**) was isolated as a green oil (0.60 g, 40%).

^{1}H NMR (400 MHz, $CDCl_3$) δ 7.27 (dd, *J* = 5.0, 1.0 Hz, 1H), 7.04 (d, *J* = 3.5 Hz, 1H), 6.98 (dd, *J* = 5.0, 3.5 Hz, 1H), 5.13 – 5.08 (m, 1H), 2.77 – 2.73 (m, 2H), 2.71 (d, *J* = 4.5 Hz, 1H), 2.10 (t, *J* = 2.5 Hz, 1H); **^{13}C NMR (101 MHz, $CDCl_3$)** δ 146.2, 126.8, 125.0, 124.2, 80.2, 71.6, 68.6, 29.6.

Ethyl 2-hydroxypent-4-ynoate (168).[250]

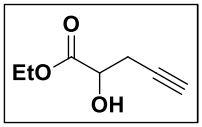

Following GP6 using ethyl glyoxalate (50% w/w in toluene, 2.0 g, 9.8 mmol), propargyl bromide (80% w/w in toluene, 2.9 g, 20 mmol), activated Zn (1.3 g, 20 mmol) with purification by FCC (20% EtOAc in 40-60 petroleum ether), ethyl 2-hydroxypent-4-ynoate (**168**) was isolated as a 70% w/w solution in EtOAc (0.67 g, 33%).

^{1}H NMR (400 MHz, $CDCl_3$) δ 4.31 – 4.18 (m, 3H), 3.22 (d, *J* = 6.5 Hz, 1H), 2.69 (ddd, *J* = 17.0, 5.0, 2.5 Hz, 1H), 2.62 (ddd, *J* = 17.0, 5.0, 2.5 Hz, 1H), 2.02 (t, *J* = 2.5 Hz, 1H), 1.27 (t, *J* = 7.0 Hz, 3H); **^{13}C NMR (101 MHz, $CDCl_3$)** δ 173.1, 78.7, 71.3, 68.8, 62.1, 24.9, 14.2.

2-Phenyl-2,3-dihydrofuran (169).[107]

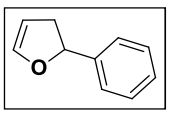

Following GP7 using 1-phenylbut-3-yn-1-ol (**163**) (50 mg, 0.34 mmol), $Mo(CO)_6$ (45 mg, 0.17 mmol) and TMNO (13 mg, 0.17 mmol) with FCC (gradient from 0-5% EtOAc in 40-60 petroleum ether), 2-phenyl-2,3-dihydrofuran (**169**) was isolated as a yellow oil (35 mg, 70%).

Following GP8 using iodobenzene (1.0 g, 4.9 mmol), 2,3-dihydrofuran (**92**) (3.4 g, 49 mmol), TBABr (4.0 g, 12 mmol), KOAc (1.2 g, 12 mmol) and $Pd(OAc)_2$ (55 mg, 0.25 mmol) with purification by FCC (10%

Et_2O in 40-60 petroleum ether), 2-phenyl-2,3-dihydrofuran (**169**) was isolated as a yellow oil (411 mg, 58%).

^{1}H NMR (400 MHz, $CDCl_3$) δ 7.42 – 7.29 (m, 5H), 6.48 (q, *J* = 2.5 Hz, 1H), 5.55 (dd, *J* = 10.5, 8.5 Hz, 1H), 4.99 (q, *J* = 2.5 Hz, 1H), 3.11 (ddt, *J* = 15.0, 10.5, 2.5 Hz, 1H), 2.64 (ddt, *J* = 15.0, 8.5, 2.5 Hz, 1H); **^{13}C NMR (101 MHz, $CDCl_3$)** δ 145.4, 143.1, 128.6, 127.7, 125.6, 99.1, 82.4, 37.9.

2-(4-Methoxyphenyl)-2,3-dihydrofuran (170).[251]

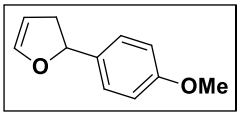

Following GP7 using 1-(4-methoxyphenyl)but-3-yn-1-ol (**166**) (0.41 g, 2.3 mmol), $Mo(CO)_6$ (0.30 g, 1.2 mmol) and TMNO (86 mg, 1.2 mmol) with FCC (gradient from 0-10% EtOAc in 40-60 petroleum ether), 2-(4-methoxyphenyl)-2,3-dihydrofuran (**170**) was isolated as a yellow oil (0.33 g, 88%).

^{1}H NMR (400 MHz, $CDCl_3$) δ 7.34 – 7.29 (m, 1H), 6.94 – 6.87 (m, 1H), 6.44 (q, *J* = 2.5 Hz, 1H), 5.48 (dd, *J* = 10.5, 8.5 Hz, 1H), 4.97 (q, *J* = 2.5 Hz, 1H), 3.81 (s, 2H), 3.04 (ddt, *J* = 15.5, 10.5, 2.5 Hz, 1H), 2.62 (ddt, *J* = 15.5, 8.5, 2.5 Hz, 1H); **^{13}C NMR (101 MHz, $CDCl_3$)** δ 159.3, 145.4, 135.2, 127.2, 114.0, 99.2, 82.3 55.4, 37.8.

2-(Thiophen-2-yl)-2,3-dihydrofuran (171).[251]

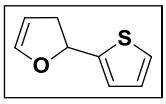

Following GP7 using 1-(thiophen-2-yl)but-3-yn-1-ol (**167**) (0.35 g, 2.3 mmol), $Mo(CO)_6$ (0.30 g, 1.2 mmol) and TMNO (86 mg, 1.2 mmol) with FCC (gradient from 0-10% EtOAc in 40-60 petroleum ether), 2-(thiophen-2-yl)-2,3-dihydrofuran (**171**) was isolated as a yellow oil (0.31 g, 90%).

^{1}H NMR (400 MHz, $CDCl_3$) δ 7.27 (dd, *J* = 5.0, 1.0 Hz, 1H), 7.05 (d, *J* = 3.5 Hz, 1H), 6.98 (dd, *J* = 5.0, 3.5 Hz, 1H), 6.39 (q, *J* = 2.5 Hz, 1H), 5.74 (dd, *J* = 10.5, 8.0 Hz, 1H), 5.00 (q, *J* = 2.5 Hz, 1H), 3.09 (ddt, *J* = 15.0, 10.5, 2.5 Hz, 1H), 2.78 (ddt, *J* = 15.0, 8.0, 2.5 Hz, 1H); **^{13}C NMR (101 MHz, $CDCl_3$)** δ 146.0, 145.0, 126.8, 125.2, 124.6, 99.4, 78.4, 37.9.

Ethyl 2,3-dihydrofuran-2-carboxylate (172).

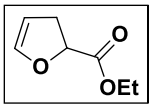

Following GP7 using ethyl 2-hydroxypent-4-ynoate (**168**) (0.33 g, 2.3 mmol), $Mo(CO)_6$ (0.30 g, 1.2 mmol) and TMNO (86 mg, 1.2 mmol) with FCC (gradient from 0-10% EtOAc in 40-60 petroleum ether), ethyl 2,3-dihydrofuran-2-carboxylate (**172**) was isolated as a yellow oil (0.17 g, 52%).

^{1}H NMR (400 MHz, $CDCl_3$) δ 6.35 (q, *J* = 2.5 Hz, 1H), 4.96 – 4.90 (m, 2H), 4.22 (q, *J* = 7.0 Hz, 2H), 2.96 (ddt, *J* = 16.0, 11.5, 2.5 Hz, 1H), 2.76 (ddt, *J* = 16.0, 7.0, 2.5 Hz, 1H), 1.28 (t, *J* = 7.0 Hz, 3H); **^{13}C NMR (101 MHz, $CDCl_3$)** δ 172.0, 145.4, 99.1, 77.8, 61.5, 33.7, 14.3; **FTIR:** ν_{max} 2982, 1752, 1731, 1623, 1274, 1199, 1054 cm^{-1}; **HRMS** calculated for $C_7H_{10}O_3$ (ES^+): 142.0624. Found: 142.0622.

2-(*p*-Tolyl)-2,3-dihydrofuran (174).[251]

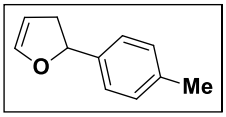

Following GP8 using 4-iodotoluene (1.0 g, 4.6 mmol), 2,3-dihydrofuran (**92**) (3.2 g, 46 mmol), TBABr (3.7 g, 12 mmol), KOAc (1.1 g, 12 mmol) and $Pd(OAc)_2$ (50 mg, 0.23 mmol) with purification by FCC (5% Et_2O in 40-60 petroleum ether), 2-(*p*-tolyl)-2,3-dihydrofuran (**174**) was isolated as a yellow oil (310 mg, 42%).

^{1}H NMR (400 MHz, $CDCl_3$) δ 7.30 (d, *J* = 8.0 Hz, 2H), 7.21 (d, *J* = 8.0 Hz, 2H), 6.48 (q, *J* = 2.5 Hz, 1H), 5.53 (dd, *J* = 10.5, 8.5 Hz, 1H), 5.00 (q, *J* = 2.5 Hz, 1H), 3.09 (ddt, *J* = 15.0, 10.5, 2.5 Hz, 1H), 2.65 (ddt, *J* = 15.0, 8.5, 2.5 Hz, 1H), 2.39 (s, 3H); **^{13}C NMR (101 MHz, $CDCl_3$)** δ 145.3, 140.1, 137.4, 129.2, 125.7, 99.1, 82.4, 37.8, 21.2.

2-(4-Fluorophenyl)-2,3-dihydrofuran (175).[251]

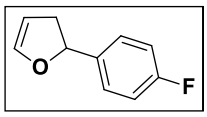

Following GP8 using 4-fluoroiodobenzene (1.0 g, 4.5 mmol), 2,3-dihydrofuran (**92**) (3.2 g, 45 mmol), TBABr (3.7 g, 11 mmol), KOAc (1.1 g, 11 mmol) and $Pd(OAc)_2$ (50 mg, 0.23 mmol) with purification by FCC (10% Et_2O in 40-60 petroleum ether), 2-(4-fluorophenyl)-2,3-dihydrofuran (**175**) was isolated as a colourless oil (366 mg, 50%).

^{1}H NMR (400 MHz, $CDCl_3$) δ 7.40 – 7.33 (m, 2H), 7.12 – 7.03 (m, 2H), 6.47 (q, *J* = 2.5 Hz, 1H), 5.52 (dd, *J* = 10.5, 8.5 Hz, 1H), 4.99 (q, *J* = 2.5 Hz, 1H), 3.10 (ddt, *J* = 15.5, 10.5, 2.5 Hz, 1H), 2.60 (ddt, *J* = 15.5, 8.5, 2.5 Hz, 1H); **^{13}C NMR (101 MHz, $CDCl_3$)** δ 162.3 (d, *J* = 245.5 Hz), 145.3, 138.9, 127.4 (d, *J* = 8.0 Hz), 115.4 (d, *J* = 21.5 Hz), 99.1, 81.7, 37.9; **^{19}F{^{1}H} NMR (377 MHz, $CDCl_3$)** δ -114.98; **FTIR:** ν_{max} 2932, 2860, 1621, 1509, 1224, 1136, 1051 cm^{-1}; **HRMS** calculated for $C_{10}H_{10}FO$ (ES^+)($+H^+$): 164.0632. Found: 164.0630.

2-(4-Nitrophenyl)-2,3-dihydrofuran (176).

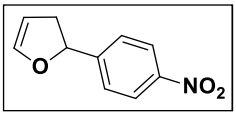

Following GP8 using 4-iodonitrobenzene (1.0 g, 4.0 mmol), 2,3-dihydrofuran (**92**) (2.8 g, 40 mmol), TBABr (3.3 g, 10 mmol), KOAc (0.99 g, 10 mmol) and $Pd(OAc)_2$ (45 mg, 0.2 mmol) with purification by FCC (10% Et_2O in 40-60 petroleum ether), 2-(4-nitrophenyl)-2,3-dihydrofuran (**176**) was isolated as a yellow oil (433 mg, 56%).

^{1}H NMR (400 MHz, $CDCl_3$) δ 8.24 – 8.19 (m, 2H), 7.52 (d, *J* = 8.5 Hz, 2H), 6.48 (q, *J* = 2.5 Hz, 1H), 5.62 (dd, *J* = 11.0, 8.0 Hz, 1H), 4.99 (q, *J* = 2.5 Hz, 1H), 3.19 (ddt, *J* = 15.5, 11.0, 2.5 Hz, 1H), 2.55 (ddt, *J* = 15.5, 8.0, 2.5 Hz, 1H); **^{13}C NMR (101 MHz, $CDCl_3$)** δ 150.6, 147.3, 145.3, 126.2, 123.8, 99.1, 81.0, 38.0; **FTIR:** ν_{max} 2934, 2860, 1599, 1518, 1345, 1047 cm^{-1}; **HRMS** calculated for $C_{10}H_{10}NO_3$ (ES^+)($+H^+$): 191.0577. Found: 191.0575.

5.3.3 Enol Ethers

(2-Methoxyvinyl)benzene (118).[252]

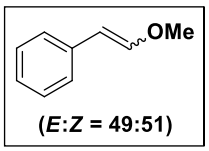

Following GP9 using hexamethyldisilazane (1.1 g, 6.5 mmol), *n*-BuLi (2.5 M in hexanes, 2.6 mL, 6.5 mmol), (methoxymethyl)triphenylphosphonium chloride (2.2 g, 6.5 mmol) and benzaldehyde (0.53 g, 5.0 mmol), (2-methoxyvinyl)benzene (**118**) was isolated as an inseparable mixture of isomers (***E***:*Z* = **49**:51) (0.62 g, 93%).

^{1}H NMR (400 MHz, $CDCl_3$) δ 7.64 – 7.60 (m, 2H), 7.38 – 7.26 (m, 6H), 7.21 – 7.15 (m, 2H), **7.09** (d, *J* = 13.0 Hz, 1H, *E* isomer), 6.17 (d, *J* = 7.0 Hz, 1H, *Z* isomer), **5.86** (d, *J* = 13.0 Hz, 1H, *E* isomer), 5.27 (d, *J* =

7.0 Hz, 1H, *Z* isomer), 3.80 (s, 3H), 3.71 (s, 3H); **^{13}C NMR (101 MHz, $CDCl_3$)** δ 148.9, 148.0, 136.4, 136.0, 128.7 (2C), 128.3 (4C), 125.8, 125.7, 125.2 (2C), 105.7, 105.1, 60.7, 56.5.

1-Methoxy-4-(2-methoxyvinyl)benzene (119).[253]

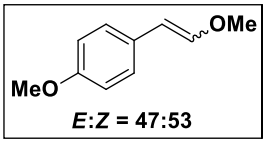

Following GP9 using hexamethyldisilazane (1.1 g, 6.5 mmol), *n*-BuLi (2.2 M in hexanes, 3.0 mL, 6.5 mmol), (methoxymethyl)triphenylphosphonium chloride (2.2 g, 6.5 mmol) and *p*-anisaldehyde (0.68 g, 5.0 mmol), 1-methoxy-4-(2-methoxyvinyl)benzene (**119**) was isolated as an inseparable mixture of isomers (***E***:*Z* = **47**:53) (0.76 g, 93%).

^{1}H NMR (400 MHz, $CDCl_3$) δ 7.57 – 7.52 (m, 2H), 7.21 – 7.15 (m, 2H), **6.96** (d, *J* = 13.0 Hz, 1H, *E* isomer), 6.89 – 6.82 (m, 4H), 6.07 (d, *J* = 7.0 Hz, 1H, *Z* isomer), **5.81** (d, *J* = 13.0 Hz, 1H, E isomer), 5.20 (d, *J* = 7.0 Hz, 1H, *Z* isomer), 3.82 – 3.79 (m, 6H), 3.77 (s, 3H), 3.68 (s, 3H); **^{13}C NMR (101 MHz, $CDCl_3$)** δ 157.9, 157.7, 147.6, 146.4, 129.5 (2C), 129.0, 128.9, 126.3 (2C), 114.2 (2C), 113.7 (2C), 105.3, 104.7, 60.6, 56.5, 55.4, 55.3.

(3-Methoxyallyl)benzene (120).[254]

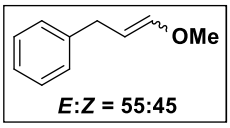

Following GP9 using hexamethyldisilazane (1.1 g, 6.5 mmol), *n*-BuLi (2.2 M in hexanes, 3.0 mL, 6.5 mmol), (methoxymethyl)triphenylphosphonium chloride (2.2 g, 6.5 mmol) and phenylacetaldehyde (0.60 g, 5.0 mmol), (3-methoxyallyl)benzene (**120**) was isolated as an inseparable mixture of isomers (***E***:*Z* = **55**:45) (0.35 g, 47%).

^{1}H NMR (400 MHz, $CDCl_3$) δ 7.36 – 7.19 (m, 10H), **6.48 – 6.42** (m, 1H, *E* isomer), 6.05 (dt, *J* = 6.0, 1.5 Hz, 1H, *Z* isomer), **4.94** (dt, *J* = 12.5, 7.5 Hz, 1H, *E* isomer), 4.62 (td, *J* = 7.5, 6.0 Hz, 1H, *Z* isomer), 3.67 (s, 3H), 3.57 (s, 3H), 3.47 (d, *J* = 7.5 Hz, 2H, *Z* isomer), **3.31** (d, *J* = 7.5 Hz, 2H, *E* isomer); **^{13}C NMR (101 MHz, $CDCl_3$)** δ 148.2, 146.8, 141.8, 141.8, 128.5 (2C), 128.4 (2C), 128.4 (4C), 126.1, 125.8, 105.6, 102.0, 59.7, 56.0, 34.1, 30.2.

1-Methoxyhept-1-ene (121).[255]

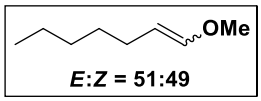

Following GP9 using hexamethyldisilazane (6.0 g, 37 mmol), *n*-BuLi (2.2 M in hexanes, 17 mL, 37 mmol), (methoxymethyl)triphenylphosphonium chloride (13 g, 37 mmol) and hexanal (2.8 g, 28 mmol), 1-methoxyhept-1-ene (**121**) was isolated as an inseparable mixture of isomers (***E***:*Z* = **51**:49) (3.0 g, 84%).

^{1}H NMR (400 MHz, $CDCl_3$) δ **6.27** (dt, *J* = 12.5, 1.5 Hz, 1H, *E* isomer), 5.85 (dt, *J* = 6.0, 1.5 Hz, 1H, *Z* isomer), **4.72** (dt, *J* = 12.5, 7.5 Hz, 1H, *E* isomer), 4.33 (td, *J* = 7.5, 6.0 Hz, 1H, *Z* isomer), 3.57 (s, 3H, *Z* isomer), **3.49** (s, 3H, *E* isomer), 2.05 (qd, *J* = 7.5, 1.5 Hz, 2H), 1.94 – 1.87 (m, 2H), 1.39 – 1.24 (m, 12H), 0.93 – 0.84 (m, 6H); **^{13}C NMR (101 MHz, $CDCl_3$)** 147.1, 145.8, 106.6, 101.8, 58.5, 54.5, 31.1 (2C), 30.5, 29.5, 27.9, 23.5, 22.3 (2C), 13.9 (2C).

Trimethyl((1-phenylvinyl)oxy)silane (122).[256]

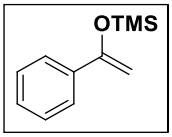

Following GP10 using acetophenone (0.50 g, 4.2 mmol), TMSCl (0.91 g, 8.4 mmol), Et_3N (0.64 g, 6.3 mmol) and NaI (0.94 g, 6.3 mmol) with purification by FCC (40-60 petroleum ether), trimethyl((1-phenylvinyl)oxy)silane (**122**) was isolated as a colourless oil (0.50 g, 62%).

^{1}H NMR (400 MHz, $CDCl_3$) δ 7.69 – 7.62 (m, 2H), 7.41 – 7.30 (m, 3H), 4.98 (d, *J* = 1.5 Hz, 1H), 4.49 (d, *J* = 1.5 Hz, 1H), 0.36 – 0.30 (m, 9H); **^{13}C NMR (101 MHz, $CDCl_3$)** δ 155.7, 137.5, 128.2, 128.1, 125.2, 91.1, 0.1.

(*Z*)-Trimethyl(styryloxy)silane (123).[252]

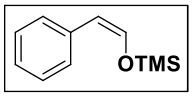

Following GP10 using phenylacetaldehyde (0.50 g, 4.2 mmol), TMSCl (0.91 g, 8.4 mmol), Et_3N (0.64 g, 6.3 mmol) and NaI (0.94 g, 6.3 mmol), (*Z*)-trimethyl(styryloxy)silane (**123**) was isolated as a colourless oil (0.24 g, 30%).

^{1}H NMR (400 MHz, $CDCl_3$) δ 7.69 (dd, *J* = 8.0, 1.0 Hz, 2H), 7.35 (td, *J* = 7.5, 3.5 Hz, 2H), 7.24 – 7.17 (m, 1H), 6.47 (d, *J* = 6.5 Hz, 1H), 5.40 (d, *J* = 6.5 Hz, 1H), 0.36 – 0.32 (m, 9H); **^{13}C NMR (101 MHz, $CDCl_3$)** δ 139.9, 136.3, 128.3, 128.2, 125.8, 109.5, -0.4.

5.3.4 Aldehydes

6-((*tert*-Butyldimethylsilyl)oxy)hexan-1-ol (402).[257]

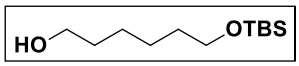

To a solution of 1,6-hexanediol (8.9 g, 75 mmol) and imidazole (6.8 g, 100 mmol) in DCM (50 mL) under N_2 at room temperature was added a solution of *tert*-butyldimethylsilyl chloride (7.5 g, 50 mmol) in DCM (25 mL) dropwise. The reaction was stirred at room temperature overnight and then filtered through silica (eluting with 40% EtOAc in 40-60 petroleum ether). Purification by FCC (gradient from 5-50% EtOAc in 40-60 petroleum ether) afforded 6-((*tert*-butyldimethylsilyl)oxy)hexan-1-ol (**402**) as a colourless oil (6.7 g, 58%).

^{1}H NMR (400 MHz, $CDCl_3$) δ 3.57 (t, *J* = 6.5 Hz, 4H), 2.21 (s, 1H), 1.58 – 1.45 (m, 4H), 1.38 – 1.25 (m, 4H), 0.92 – 0.79 (m, 9H), 0.05 – -0.05 (m, 6H); **^{13}C NMR (101 MHz, $CDCl_3$)** δ 63.3, 62.9, 32.9, 32.8, 26.1, 25.7, 25.6, 18.5, -5.2.

6-((*tert*-Butyldimethylsilyl)oxy)hexanal (312).[258]

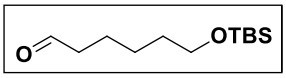

Following GP11 using $(COCl)_2$ (1.5 g, 12 mmol), DMSO (1.8 g, 24 mmol), 6-((*tert*-butyldimethylsilyl)oxy)hexan-1-ol (**402**) (2.5 g, 11 mmol) and Et_3N (5.5 g, 54 mmol) with purification by FCC (gradient from 0-50% EtOAc in 40-60 petroleum ether), 6-((*tert*-butyldimethylsilyl)oxy)hexanal (**312**) was isolated as a yellow oil (2.1 g, 82%).

^{1}H NMR (400 MHz, $CDCl_3$) δ 9.69 (t, *J* = 1.5 Hz, 1H), 3.54 (t, *J* = 6.5 Hz, 2H), 2.37 (td, *J* = 7.5, 1.5 Hz, 2H), 1.63 – 1.53 (m, 2H), 1.51 – 1.42 (m, 2H), 1.36 – 1.27 (m, 2H), 0.82 (s, 9H), -0.03 (s, 6H); **^{13}C NMR (101 MHz, $CDCl_3$)** δ 203.0, 63.0, 44.0, 32.6, 26.1, 25.6, 22.0, 18.5, -5.2.

tert-Butyl(hept-6-en-1-yloxy)dimethylsilane (403).[259]

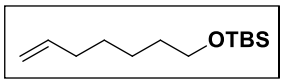

To a solution of methyltriphenylphosphonium bromide (4.7 g, 13 mmol) in THF (20 mL) under N_2 at room temperature was added *t*-BuOK (1.5 g, 13 mmol) and the resulting suspension stirred for 45 minutes. A solution of 6-((*tert*-butyldimethylsilyl)oxy)hexanal (**312**) (1.5 g, 6.5 mmol) in THF (8 mL) was then added and the reaction stirred overnight at room temperature. The reaction was then diluted with hexane (150 mL) and filtered through silica to afford *tert*-butyl(hept-6-en-1-yloxy)dimethylsilane (**403**) as a colourless oil (1.4 g, 94%).

^{1}H NMR (400 MHz, $CDCl_3$) δ 5.81 (ddt, *J* = 17.0, 10.0, 6.5 Hz, 1H), 4.99 (ddd, *J* = 17.0, 3.5, 1.5 Hz, 1H), 4.96 – 4.90 (m, 1H), 3.60 (t, *J* = 6.5 Hz, 2H), 2.09 – 2.02 (m, 2H), 1.57 – 1.48 (m, 2H), 1.44 – 1.29 (m, 4H), 0.92 – 0.87 (m, 9H), 0.07 – 0.02 (m, 6H); **^{13}C NMR (101 MHz, $CDCl_3$)** δ 139.2, 114.4, 63.4, 33.9, 32.9, 28.9, 26.1, 25.5, 18.5, -5.1.

Hept-6-en-1-ol (404).[260]

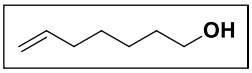

To a solution of *tert*-butyl(hept-6-en-1-yloxy)dimethylsilane (**403**) (2.3 g, 9.9 mmol) in MeOH (40 mL) was added CSA (1.2 g, 5.0 mmol) and the reaction stirred at room temperature overnight. The reaction was then diluted with Et_3N (3.0 g, 30 mmol) and concentrated under vacuum. Purification by FCC (gradient from 0-50% EtOAc in 40-60 petroleum ether) afforded hept-6-en-1-ol (**404**) as a yellow oil (0.70 g, 61%).

^{1}H NMR (400 MHz, $CDCl_3$) δ 5.74 (ddt, *J* = 17.0, 10.0, 6.5 Hz, 1H), 4.94 (ddd, *J* = 17.0, 3.5, 1.5 Hz, 1H), 4.87 (ddt, *J* = 10.0, 2.0, 1.0 Hz, 1H), 3.53 (t, *J* = 6.5 Hz, 2H), 3.08 (br, 1H), 2.05 – 1.95 (m, 2H), 1.55 – 1.45 (m, 2H), 1.40 – 1.25 (m, 4H); **^{13}C NMR (101 MHz, $CDCl_3$)** δ 138.9, 114.3, 62.5, 33.7, 32.5, 28.7, 25.3.

Hept-6-enal (327).[261]

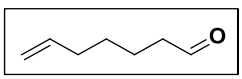

Following GP11 using $(COCl)_2$ (1.8 g, 14 mmol), DMSO (2.3 g, 29 mmol), hept-6-en-1-ol (**404**) (1.5 g, 13 mmol) and Et_3N (6.6 g, 66 mmol) with purification by FCC (gradient from 20-30% EtOAc in 40-60 petroleum ether), hept-6-enal (**327**) was isolated as a 50% w/w solution in EtOAc (1.0 g, 64%).

^{1}H NMR (400 MHz, $CDCl_3$) δ 9.67 (dd, *J* = 3.0, 1.5 Hz, 1H), 5.69 (ddt, *J* = 17.0, 10.0, 6.5 Hz, 1H), 4.95 – 4.84 (m, 2H), 2.39 – 2.32 (m, 2H), 2.03 – 1.95 (m, 2H), 1.60 – 1.51 (m, 2H), 1.39 – 1.30 (m, 2H); **^{13}C NMR (101 MHz, $CDCl_3$)** δ 202.5, 138.2, 114.7, 43.6, 33.4, 28.2, 20.9.

2-Cyclohexylacetaldehyde (405).[262]

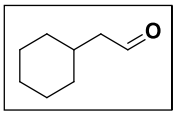

Following GP11 using $(COCl)_2$ (5.0 g, 39 mmol), DMSO (6.1 g, 78 mmol), 2-cyclohexylethanol (5.0 g, 39 mmol) and Et_3N (20 g, 200 mmol) with purification by FCC (15% EtOAc in 40-60 petroleum ether), 2-cyclohexylacetaldehyde (**405**) was isolated as a yellow oil (3.7 g, 75%).

^{1}H NMR (400 MHz, $CDCl_3$) δ 9.69 (t, *J* = 2.5 Hz, 1H), 2.23 (dd, *J* = 7.0, 2.5 Hz, 2H), 1.89 – 1.77 (m, 1H), 1.71 – 1.56 (m, 5H), 1.30 – 1.17 (m, 2H), 1.16 – 1.06 (m, 1H), 1.00 – 0.88 (m, 2H); **^{13}C NMR (101 MHz, $CDCl_3$)** δ 202.8, 51.4, 33.2, 32.7, 26.1, 26.1.

tert-Butyl 4-(2-oxoethyl)piperidine-1-carboxylate (406).[263]

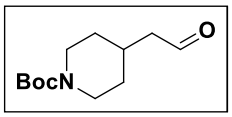

To a solution of hexamethyldisilazane (2.5 g, 15 mmol) in THF (47 mL) under N_2 at 0 °C was added *n*-butyllithium (2.4 M in hexanes, 6.3 mL, 15 mmol) and the resulting mixture stirred at 0 °C for 45 minutes. (methoxymethyl)triphenylphosphonium chloride (5.2 g, 15 mmol) was then added portionwise and the reaction stirred for 45 minutes before cooling to -78 °C. A solution of *tert*-butyl 4-formylpiperidine-1-carboxylate (2.5 g, 12 mmol) in THF (47 mL) was then added slowly and the reaction stirred at -78 °C for 4 hours. After warming to room temperature the reaction was diluted with pentane (150 mL), filtered through silica and the filtrate concentrated under vacuum. The crude oil was then dissolved in THF (29 mL) and 2.0 M HCl (29 mL, 58 mmol) added dropwise. After stirring for 2 hours at room temperature the reaction was extracted with DCM (4 x 40 mL) and the combined organic layers dried over anhydrous $MgSO_4$, filtered and concentrated under vacuum. Purification by FCC (gradient from 25-40% EtOAc in 40-60 petroleum ether) afforded *tert*-butyl 4-(2-oxoethyl)piperidine-1-carboxylate (**406**) as a colourless oil (1.6 g, 61%).

^{1}H NMR (400 MHz, $CDCl_3$) δ 9.75 (t, *J* = 1.5 Hz, 1H), 4.05 (br, 2H), 2.71 (t, *J* = 11.5 Hz, 2H), 2.36 (dd, *J* = 7.0, 1.5 Hz, 2H), 2.08 – 1.96 (m, 1H), 1.66 (d, *J* = 13.5 Hz, 2H), 1.42 (s, 9H), 1.21 – 1.07 (m, 2H); **^{13}C NMR (101 MHz, $CDCl_3$)** δ 201.7, 154.9, 79.5, 50.5, 43.5, 32.0, 30.7, 28.5.

Methyl 5-oxopentanoate (407).[264]

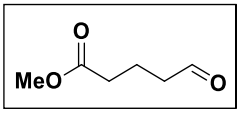

Step 1: To a solution of δ-valerolactone (1.0 g, 10 mmol) in MeOH (20 mL) was added conc. H_2SO_4 (0.097 g, 0.99 mmol) and the reaction heated to reflux overnight. Solid $NaHCO_3$ (0.17 g, 2.0 mmol) was added and the reaction stirred for 10 minutes before dilution with H_2O (25 mL) and extraction with EtOAc (3 x 50 mL). The combined organic layers were then dried over anhydrous $MgSO_4$, filtered and concentrated under vacuum.

Step 2: Following GP11 using $(COCl)_2$ (1.4 g, 11 mmol), DMSO (1.7 g, 22 mmol), the crude oil from **step 1** (1.2 g) and Et_3N (5.1 g, 50 mmol) with purification by FCC (gradient from 0-40% EtOAc in 40-60 petroleum ether), methyl 5-oxopentanoate (**407**) was isolated as a yellow oil (0.75 g, 57%).

^{1}H NMR (400 MHz, $CDCl_3$) δ 9.74 (t, *J* = 1.0 Hz, 1H), 3.64 (s, 3H), 2.50 (td, *J* = 7.0, 1.0 Hz, 2H), 2.35 (t, *J* = 7.5 Hz, 2H), 1.92 (p, *J* = 7.0 Hz, 2H); **^{13}C NMR (101 MHz, $CDCl_3$)** δ 201.6, 173.4, 51.7, 43.0, 33.0, 17.4.

N-Methoxy-*N*-methyl-5-oxopentanamide (408).[265]

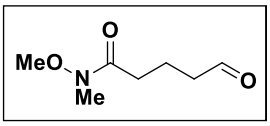

Step 1: To a solution of *N*,*O*-dimethylhydroxylamine hydrochloride (2.9 g, 30 mmol) in DCM (17 mL) under nitrogen at -78 °C was added trimethylaluminium (2.0 M in hexanes, 15 mL, 30 mmol) dropwise over 15 minutes and the resulting mixture warmed to room temperature and stirred for 4 hours. The reaction was then cooled to 0 °C and δ-valerolactone (1.0 g, 10 mmol) added dropwise. After stirring at room temperature overnight the reaction was cooled to 0 °C and diluted with H_2O (10 mL) and 10% H_2SO_4 (25 mL) and then extracted with DCM (4 x 30 mL). The combined organic layers were then washed with brine (30 mL), dried over anhydrous $MgSO_4$, filtered and concentrated under vacuum.

Step 2: Following GP11 using $(COCl)_2$ (1.4 g, 11 mmol), DMSO (1.7 g, 22 mmol), the crude oil from **step 1** (1.0 g) and Et_3N (5.1 g, 50 mmol) with purification by FCC (gradient from 40-70% EtOAc in 40-60 petroleum ether), *N*-methoxy-*N*-methyl-5-oxopentanamide (**408**) was isolated as a yellow oil (0.42 g, 26%).

^{1}H NMR (400 MHz, $CDCl_3$) δ 9.74 (s, 1H), 3.64 (s, 3H), 3.14 (s, 3H), 2.50 (td, *J* = 7.0, 1.0 Hz, 2H), 2.45 (t, *J* = 7.0 Hz, 2H), 1.93 (p, *J* = 7.0 Hz, 2H); **^{13}C NMR (101 MHz, $CDCl_3$)** δ 202.3, 176.7, 61.3, 43.2, 32.2, 30.8, 17.1.

2-Cyclopropylacetaldehyde (330).[266]

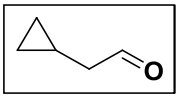

2-Cyclopropylacetaldehyde (**330**) was synthesised according to a literature procedure.[266]

^{1}H NMR (400 MHz, $CDCl_3$) δ 9.79 (t, *J* = 2.0 Hz, 1H), 2.29 (dd, *J* = 7.0, 2.0 Hz, 2H), 1.03 – 0.92 (m, 1H), 0.66 – 0.53 (m, 2H), 0.23 – 0.10 (m, 2H); **^{13}C NMR (101 MHz, $CDCl_3$)** δ 202.5, 52.9, 6.0 (2C), 0.

5.3.5 Enamines

(*E*)-1-(Hex-1-en-1-yl)piperidine (138).[267]

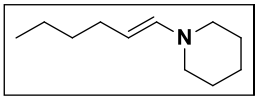

Following GP12 using hexanal (2.0 g, 20 mmol), piperidine (3.7 g, 44 mmol) and K_2CO_3 (5.5 g, 40 mmol), (*E*)-1-(hex-1-en-1-yl)piperidine (**138**) was isolated as a colourless oil (3.0 g, 91%).

^{1}H NMR (400 MHz, $CDCl_3$) δ 5.83 – 5.76 (m, 1H), 4.37 (dt, *J* = 14.0, 7.0 Hz, 1H), 2.74 – 2.67 (m, 4H), 1.98 – 1.89 (m, 2H), 1.59 – 1.44 (m, 6H), 1.33 – 1.24 (m, 4H), 0.91 – 0.83 (m, 3H); **^{13}C NMR (101 MHz, $CDCl_3$)** δ 140.3, 101.7, 50.3, 33.7, 30.4, 27.2, 25.6, 25.2, 24.5, 22.2, 14.1.

(*E*)-1-(Hex-1-en-1-yl)pyrrolidine (288).[267]

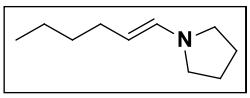

Following GP12 using hexanal (1.0 g, 10 mmol), pyrrolidine (1.6 g, 22 mmol) and K_2CO_3 (2.8 g, 20 mmol), (*E*)-1-(hex-1-en-1-yl)pyrrolidine (**288**) was isolated as a colourless oil (1.3 g, 84%).

^{1}H NMR (400 MHz, $CDCl_3$) δ 6.16 (d, *J* = 14.0 Hz, 1H), 4.12 (dt, *J* = 14.0, 7.0 Hz, 1H), 2.98 – 2.92 (m, 4H), 2.00 – 1.92 (m, 2H), 1.85 – 1.78 (m, 4H), 1.34 – 1.26 (m, 4H), 0.92 – 0.85 (m, 3H); **^{13}C NMR (101 MHz, $CDCl_3$)** δ 135.9, 99.3, 49.3, 34.2, 30.4, 24.9, 22.2, 14.1.

(*E*)-*N*,*N*-Diethylhex-1-en-1-amine (289).[268]

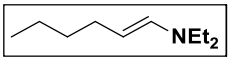

Following GP12 using hexanal (0.5 g, 5.0 mmol), diethylamine (0.80 g, 11 mmol) and K_2CO_3 (1.4 g, 10 mmol), (*E*)-*N*,*N*-diethylhex-1-en-1-amine (**289**) was isolated as a colourless oil (0.55 g, 71%).

^{1}H NMR (400 MHz, $CDCl_3$) δ 5.84 (dt, *J* = 14.0, 1.0 Hz, 1H), 4.17 (dt, *J* = 14.0, 7.0 Hz, 1H), 2.92 (q, *J* = 7.0 Hz, 4H), 1.99 – 1.92 (m, 2H), 1.34 – 1.26 (m, 4H), 1.03 (t, *J* = 7.0 Hz, 6H), 0.91 – 0.85 (m, 3H); **^{13}C NMR (101 MHz, $CDCl_3$)** δ 137.1, 98.4, 44.6, 34.1, 30.6, 22.2, 14.2, 12.4.

Benzyl 3,4-dihydropyridine-1(2*H*)-carboxylate (84).[92]

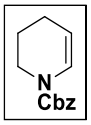

To a solution of δ-valerolactam (3.0 g, 30 mmol) in THF (120) under N_2 at -78 °C was added *n*-BuLi (2.4 M in hexanes, 12.5 mL, 30 mmol) dropwise and the resulting solution stirred at -78 °C for 30 minutes. A solution of benzyl chloroformate (5.2 g, 30 mmol) in THF (30 mL) was added dropwise and the mixture stirred at -78 °C for 4 hours. The reaction was then diluted with sat. NH_4Cl (50 mL) and extracted with Et_2O (3 x 50 mL). The combined organic layers were then washed with brine (50 mL), dried over anhydrous $MgSO_4$, filtered and concentrated under vacuum.

The crude oil was dissolved in MeOH (100 mL) and the solution cooled to 0 °C before the addition of $NaBH_4$ (1.5 g, 40 mmol) portionwise. After stirring for 45 minutes at 0 °C the reaction mixture was poured onto ice and extracted with EtOAc (3 x 100 mL). The combined organic layers were then washed with brine (50 mL), dried over anhydrous $MgSO_4$, filtered and concentrated under vacuum.

The crude oil was dissolved in THF (50 mL) before the addition of conc. H_2SO_4 (0.25 mL) and the resulting mixture stirred at room temperature for 1.5 hours. The reaction was then diluted with sat. $NaHCO_3$ (100 mL) and extracted with EtOAc (3 x 100 mL). The combined organic layers were then dried over anhydrous $MgSO_4$, filtered and concentrated under vacuum. Purification by FCC (20% EtOAc in 40-60 petroleum ether) afforded benzyl 3,4-dihydropyridine-1(2*H*)-carboxylate (**84**) as a colourless oil (two rotamers = **59**:41) (2.3 g, 41%).

^{1}H NMR (400 MHz, $CDCl_3$) δ 7.43 – 7.31 (m, 10H), 6.91 (d, *J* = 8.5 Hz, 1H, minor), **6.81** (d, *J* = 8.5 Hz, 1H, major), 5.19 (s, 4H), 5.02 – 4.95 (m, 1H, minor), **4.91 – 4.84** (m, 1H, major), 3.69 – 3.59 (m, 4H), 2.10 – 2.00 (m, 4H), 1.89 – 1.76 (m, 4H); **^{13}C NMR (101 MHz, $CDCl_3$)** δ 153.5, 153.1, 136.4 (2C), 128.6 (2C), 128.5 (2C), 128.4, 128.3, 128.1 (2C), 128.0 (2C), 125.4, 124.9, 106.7, 106.4, 67.4, 67.3, 42.4, 42.2, 21.6 (2C), 21.5, 21.3.

Benzyl (4,4-diethoxybutyl)carbamate (145).[104]

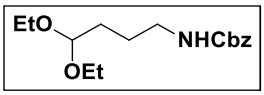

To a solution of 4,4-diethoxybutan-1-amine (**144**) (1.0 g, 6.2 mmol) in DCM (19 mL) was added a solution of Na_2CO_3 (2.2 g, 21 mmol) in H_2O (19 mL) and the resulting mixture cooled to 0 °C. Benzylchloroformate (1.2 g, 6.8 mmol) was added dropwise and the resulting mixture was then warmed to room temperature and stirred for 3 hours. The layers were then separated and the aqueous layer was extracted with EtOAc (2 x 20 mL). The combined organic layers were then dried over anhydrous $MgSO_4$, filtered and concentrated under vacuum to afford benzyl (4,4-diethoxybutyl)carbamate (**145**) as a colourless oil (1.83 g, quant.)

^{1}H NMR (400 MHz, $CDCl_3$) δ 7.37 – 7.27 (m, 5H), 5.08 (s, 2H), 4.99 (s, 1H), 4.46 (t, *J* = 5.0 Hz, 1H), 3.67 – 3.57 (m, 2H), 3.51 – 3.42 (m, 2H), 3.20 (dd, *J* = 12.5, 6.5 Hz, 2H), 1.67 – 1.52 (m, 4H), 1.18 (t, *J* = 7.0 Hz, 6H); **^{13}C NMR (101 MHz, $CDCl_3$)** δ 156.5, 136.8, 128.6, 128.1, 128.1, 102.7, 66.6, 61.4, 40.9, 31.0, 25.1, 15.4.

Benzyl 2,3-dihydro-1*H*-pyrrole-1-carboxylate (146).[104]

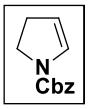

To a solution of PPTS (1.6 g, 6.2 mmol) in acetone (17 mL) and H_2O (4 mL) was added benzyl (4,4-diethoxybutyl)carbamate (**145**) (1.8 g, 6.2 mmol) and the resulting mixture heated at 45 °C overnight. After cooling to room temperature the volatiles were removed under vacuum and the residual oil partitioned between EtOAc (25 mL) and H_2O (25 mL). The aqueous layer was then extracted with EtOAc (3 x 25 mL) and the combined organic layers were washed with brine (25 mL), dried over anhydrous $MgSO_4$, filtered and concentrated under vacuum. The crude oil was then dissolved in toluene (50 mL) and the resulting mixture heated at reflux for 4 hours. After cooling to room temperature the volatiles were removed under vacuum and the residual oil purified by FCC (gradient from 10-20% EtOAc in 40-60 petroleum ether) to afford benzyl 2,3-dihydro-1*H*-pyrrole-1-carboxylate (**146**) as a colourless oil (two rotamers = **55**:45) (0.40 g, 32%).

^{1}H NMR (400 MHz, $CDCl_3$) δ 7.41 – 7.29 (m, 10H), 6.66 – 6.62 (m, 1H, minor), **6.57 – 6.52** (m, 1H, major), 5.17 (s, 4H), 5.11 – 5.07 (m, 1H, minor), **5.05 – 5.01** (m, 1H, major), 3.85 – 3.73 (m, 4H), 2.71 – 2.59 (m, 4H); **^{13}C NMR (101 MHz, $CDCl_3$)** δ 152.9, 152.2, 136.7 (2C), 129.8, 129.1, 128.6 (2C), 128.1, 128.1, 128.0, 127.9, 108.9, 108.7, 67.1, 66.9, 45.3, 45.1, 29.8, 28.7.

1-(1-(4-Methoxyphenyl)vinyl)piperidine (140).[269]

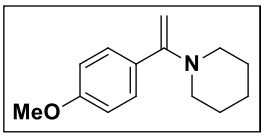

1-(1-(4-Methoxyphenyl)vinyl)piperidine (**140**) was a gift from Dr Taban Kakaawla and was synthesised according to a literature procedure.[270]

1-(1-(4-Chlorophenyl)vinyl)piperidine (141).[271]

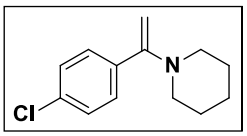

1-(1-(4-Chlorophenyl)vinyl)piperidine (**141**) was a gift from Dr Taban Kakaawla and was synthesised according to a literature procedure.[270]

(*E*)-4-(Piperidin-1-yl)but-3-en-2-one (142).[272]

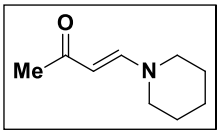

(*E*)-4-(Piperidin-1-yl)but-3-en-2-one (**142**) was a gift from Dr Taban Kakaawla and was synthesised according to a literature procedure.[271]

5.3.6 Others

N-Benzylidene-1-benzylamine *N*-oxide (409).[273]

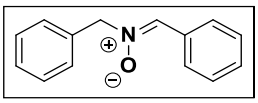

To a solution of benzaldehyde (0.60 g, 5.7 mmol) in DCM (6 mL) under N_2 was added Na_2SO_4 (1.6 g, 11.4 mmol), Et_3N (0.82 g, 8.1 mmol) and *N*-benzylhydroxylamine (1.0 g, 8.1 mmol) and the resulting mixture stirred at room temperature overnight. The mixture was then diluted with 5% v/v HCl (20 mL) and extracted with DCM (4 x 25 mL). The combined organic layers were then washed with sat. $NaHCO_3$ (20 mL), dried over anhydrous $MgSO_4$, filtered and concentrated under vacuum. Purification by FCC (10% 40-60 petroleum ether in EtOAc) afforded *N*-benzylidene-1-benzylamine *N*-oxide (**409**) as a white solid (1.0 g, 86%).

M.P. 67-69 °C (lit[273] 82-83 °C); **^{1}H NMR (400 MHz, $CDCl_3$)** δ 8.24 – 8.19 (m, 2H), 7.51 – 7.46 (m, 2H), 7.44 – 7.37 (m, 7H), 5.07 (s, 2H); **^{13}C NMR (101 MHz, $CDCl_3$)** δ 192.5, 134.5, 133.3, 130.6, 130.5, 129.4, 129.1, 128.8, 128.6, 71.4.

2-Benzyl-3-phenyl-2,3-dihydroisoxazole (134).[274]

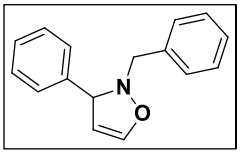

N-Benzylidene-1-benzylamine *N*-oxide (**409**) (0.16 g, 0.78 mmol) was dissolved in vinyl acetate (0.40 g, 4.7 mmol) under argon and the resulting mixture was heated at reflux in the dark for 72 hours. After cooling to room temperature the volatiles were removed under vacuum and the residue purified by FCC (40% Et_2O in 40-60 petroleum ether). The resulting oil (0.2 g, 0.67 mmol) was then dissolved in NMP (3.4 mL) under argon. BSTFA (0.21 g, 0.80 mmol) was added dropwise and the resulting mixture cooled to 0 °C before the dropwise addition of TMSOTf (14 mg, 67 µmol). The reaction mixture was then stirred at room temperature overnight in the dark before cooling to 0 °C. The mixture was then diluted with sat. $NaHCO_3$ (5 mL) and Et_2O (5 mL) and the mixture stirred at room temperature for 5 minutes. The layers were separated and the organic layer was washed with H_2O (4 x 5 mL), dried over anhydrous $MgSO_4$, filtered and concentrated under vacuum. Purification by FCC (gradient from 5-15% EtOAc in 40-60 petroleum ether) afforded 2-benzyl-3-phenyl-2,3-dihydroisoxazole (**134**) as a yellow oil (96 mg, 52%).

^{1}H NMR (400 MHz, $CDCl_3$) δ 7.50 – 7.44 (m, 2H), 7.42 – 7.26 (m, 8H), 6.64 (t, *J* = 2.0 Hz, 1H), 5.08 (t, *J* = 2.5 Hz, 1H), 4.98 (t, *J* = 2.0 Hz, 1H), 4.38 (d, *J* = 13.0 Hz, 1H), 4.09 (d, *J* = 13.0 Hz, 1H); **^{13}C NMR (101 MHz, $CDCl_3$)** δ 142.1, 136.6 (2C), 129.4, 128.6, 128.5, 127.7, 127.6, 127.1, 100.2, 72.2, 63.4.

(*E*)-1-Iodooct-1-ene (136-*E*).[103]

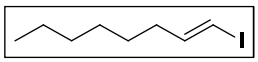

To a solution of 1-octyne (1.1 g, 10 mmol) in hexane (10 mL) under N_2 was added DIBAL-H (1.0 M in toluene, 15 mL, 15 mmol) and the resulting mixture heated at 55 °C for 6 hours. The reaction mixture was then cooled to -50 °C before the dropwise addition of a solution of I_2 (2.8 g, 11 mmol) in THF (15 mL). The mixture was then warmed to room temperature over 1 hour and stirred at room temperature for 12 hours before cooling to 0 °C. The reaction mixture was then diluted with 10% v/v H_2SO_4 (25 mL) and extracted with hexane (3 x 20 mL). The combined organic layers were then washed with brine, dried over anhydrous $MgSO_4$, filtered and concentrated under vacuum. Purification by FCC (gradient

from 0-5% EtOAc in 40-60 petroleum ether) afforded (*E*)-1-iodooct-1-ene (**136-*E***) as a colourless oil (1.3 g, 56%).

^{1}H NMR (400 MHz, $CDCl_3$) δ 6.51 (dt, *J* = 14.5, 7.5 Hz, 1H), 5.97 (dt, *J* = 14.5, 1.5 Hz, 1H), 2.04 (qd, *J* = 7.5, 1.5 Hz, 2H), 1.43 – 1.34 (m, 2H), 1.33 – 1.22 (m, 6H), 0.92 – 0.85 (m, 3H); **^{13}C NMR (101 MHz, $CDCl_3$)** δ 146.9, 74.4, 36.2, 31.7, 28.7, 28.5, 22.7, 14.2.

1-Iodooct-1-yne (410).[275]

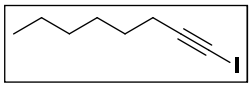

To a solution of 1-octyne (1.1 g, 10 mmol) in hexane (5 mL) under N_2 at -78 °C was added *n*-BuLi (2.4 M in hexanes, 4.3 mL, 10 mmol) dropwise and the resulting mixture stirred at -78 °C for 1.5 hours. A solution of iodine (2.8 g, 11 mmol) in Et_2O (15 mL) was then added dropwise over 15 minutes and the resulting mixture warmed to room temperature and stirred for 1 hour. The reaction mixture was then diluted with H_2O (10 mL), stirred for 10 minutes and extracted with hexane (3 x 20 mL). The combined organic layers were then washed with H_2O (2 x 20 mL), 20% $Na_2S_2O_3$ (10 mL) and dried over anhydrous $MgSO_4$, filtered and concentrated under vacuum. Filtration through silica (eluting with 5% EtOAc in 40-60 petroleum ether) afforded 1-iodooct-1-yne (**410**) as a colourless oil (1.8 g, 78%).

^{1}H NMR (400 MHz, $CDCl_3$) δ 2.35 (t, *J* = 7.0 Hz, 2H), 1.55 – 1.46 (m, 2H), 1.41 – 1.24 (m, 6H), 0.89 (t, *J* = 7.0 Hz, 3H); **^{13}C NMR (101 MHz, $CDCl_3$)** δ 95.0, 31.4, 28.6 (2C), 22.7, 21.0, 14.2. (The C≡**C**-I signal lies outside the spectral window at ~ -7ppm)

(*Z*)-1-Iodooct-1-ene (136-*Z*).[276]

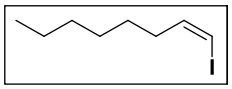

To a solution of BH_3.DMS (0.53 g, 7.0 mmol) in Et_2O (10 mL) under N_2 at 0 °C was added cyclohexene (1.2 g, 14 mmol) and the resulting mixture stirred at 0 °C for 15 minutes before warming to room temperature and stirring for 1 hour. The mixture was then cooled to 0 °C and 1-iodooct-1-yne (**410**) (1.5 g, 6.4 mmol) was added and the reaction mixture stirred at 0 °C for 30 minutes. The mixture was then warmed to room temperature and stirred for 1 hour before cooling to 0 °C. AcOH (3.1 mL) was added dropwise and the resulting mixture was stirred at room temperature for 2 hours before dilution with Et_2O (10 mL). The layers were then separated and the combined organic layers were washed with H_2O (4 x 10 mL), dried over anhydrous $MgSO_4$, filtered and concentrated under vacuum. Purification by FCC (40-60 petroleum ether) afforded (*Z*)-1-iodooct-1-ene (**136-*Z***) as a colourless oil (1.1 g, 74%).

^{1}H NMR (400 MHz, $CDCl_3$) δ 6.20 – 6.13 (m, 2H), 2.18 – 2.08 (m, 2H), 1.47 – 1.39 (m, 2H), 1.37 – 1.26 (m, 6H), 0.93 – 0.85 (m, 3H); **^{13}C NMR (101 MHz, $CDCl_3$)** δ 141.6, 82.3, 34.9, 31.8, 28.9, 28.1, 22.7, 14.2.

5.4 Cycloaddition Reactions

5.4.1 Pyrazoles

1-Phenyl-1*H*-pyrazole (112).[231]

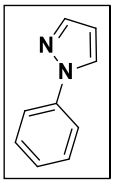

Following GP14 using *N*-phenylsydnone (**35**) (81 mg, 0.50 mmol) and ethyl vinyl ether (**111a**) (140 mg, 2.0 mmol) with filtration through a silica plug (eluting with 10% MeOH in DCM), 1-phenyl-1*H*-pyrazole (**112**) was isolated as a brown oil (68 mg, 94%).

Following GP14 using *N*-phenylsydnone (**35**) (50 mg, 0.31 mmol) and cyclohexyl vinyl ether (**111b**) (160 mg, 1.2 mmol) with FCC (gradient from 0-10% EtOAc in 40-60 petroleum ether), 1-phenyl-1*H*-pyrazole (**112**) was isolated as a yellow oil (24 mg, 54%).

Following GP14 using *N*-phenylsydnone (**35**) (50 mg, 0.31 mmol) and *tert*-butyl vinyl ether (**111c**) (120 mg, 1.2 mmol) with FCC (gradient from 0-10% EtOAc in 40-60 petroleum ether), 1-phenyl-1*H*-pyrazole (**112**) was isolated as a yellow oil (33 mg, 73%).

^{1}H NMR (400 MHz, $CDCl_3$) δ 7.92 (d, *J* = 2.4 Hz, 1H), 7.76 – 7.66 (m, 3H), 7.49 – 7.41 (m, 2H), 7.32 – 7.25 (m, 1H), 6.48 – 6.44 (m, 1H); **^{13}C NMR (101 MHz, $CDCl_3$)** δ 141.1, 140.2, 129.5, 126.8, 126.5, 119.2, 107.7.

4-Methyl-1-phenyl-1*H*-pyrazole (114a).[277]

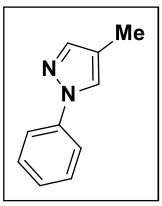

Following GP13 using *N*-phenylsydnone (**35**) (81 mg, 0.5 mmol) and propionaldehyde (87 mg, 1.5 mmol) with FCC (gradient from 5-10% Et_2O in 40-60 petroleum ether), 4-methyl-1-phenyl-1*H*-pyrazole (**114a**) was isolated as a yellow oil (50 mg, 64%).

Following GP14 using *N*-phenylsydnone (**35**) (81 mg, 0.5 mmol) and ethyl propenyl ether (**113**) (170 mg, 2.0 mmol) with FCC (gradient from 0-20% EtOAc in 40-60 petroleum ether), 4-methyl-1-phenyl-1*H*-pyrazole (**114a**) was obtained as a brown oil (55 mg, 70%).

^{1}H NMR (400 MHz, $CDCl_3$) δ 7.70 (s, 1H), 7.67 – 7.63 (m, 2H), 7.54 (s, 1H), 7.46 – 7.40 (m, 2H), 7.28 – 7.22 (m, 1H), 2.16 (s, 3H); **^{13}C NMR (101 MHz, $CDCl_3$)** δ 142.1, 140.6, 129.7, 126.3, 125.6, 119.0, 118.5, 9.3.

3-Methyl-1-phenyl-1*H*-pyrazole (114b).[278]

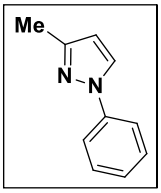

Following GP14 using *N*-phenylsydnone (**35**) (50 mg, 0.31 mmol) and 2-methoxypropene (**143**) (90 mg, 1.2 mmol) with FCC (gradient from 0-5% EtOAc in 40-60 petroleum ether), 3-methyl-1-phenyl-1*H*-pyrazole (**114b**) was isolated as a yellow oil (26 mg, 54%).

^{1}H NMR (400 MHz, $CDCl_3$) δ 7.81 (d, *J* = 2.5 Hz, 1H), 7.65 (dd, *J* = 8.5, 1.0 Hz, 2H), 7.46 – 7.39 (m, 2H), 7.27 – 7.21 (m, 1H), 6.24 (d, *J* = 2.5 Hz, 1H), 2.38 (s, 3H); **^{13}C NMR (101 MHz, $CDCl_3$)** δ 150.7, 140.3, 129.5, 127.5, 126.1, 119.0, 107.6, 13.9.

4-Butyl-1-phenyl-1*H*-pyrazole (287a).[279]

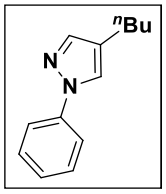

Following GP13 using *N*-phenylsydnone (**35**) (81 mg, 0.5 mmol) and hexanal (150 mg, 1.5 mmol) with FCC (gradient from 0-5% Et_2O in 40-60 petroleum ether), 4-butyl-1-phenyl-1*H*-pyrazole (**287a**) was isolated as a yellow oil (86 mg, 86%).

^{1}H NMR (400 MHz, $CDCl_3$) δ 7.70 (d, *J* = 0.5 Hz, 1H), 7.69 – 7.64 (m, 2H), 7.55 (s, 1H), 7.46 – 7.39 (m, 2H), 7.28 – 7.21 (m, 1H), 2.53 (t, *J* = 7.5 Hz, 2H), 1.65 – 1.56 (m, 2H), 1.45 – 1.35 (m, 2H), 0.95 (t, *J* = 7.5 Hz, 3H); **^{13}C NMR (101 MHz, $CDCl_3$)** δ 141.3, 140.6, 129.6, 126.2, 125.0, 124.3, 119.0, 33.2, 24.2, 22.6, 14.2.

4-Pentyl-1-phenyl-1*H*-pyrazole (132a).[32]

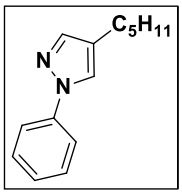

Following GP14 using *N*-phenylsydnone (**35**) (81 mg, 0.50 mmol) and 1-methoxyhept-1-ene (**121**) (0.26 g, 2.0 mmol) with purification by FCC (gradient from 0-10% EtOAc in 40-60 petroleum ether), 4-pentyl-1-phenyl-1*H*-pyrazole (**132a**) was isolated as a yellow oil (32 mg, 30%).

^{1}H NMR (400 MHz, $CDCl_3$) δ 7.71 (s, 1H), 7.68 – 7.64 (m, 2H), 7.55 (s, 1H), 7.46 – 7.40 (m, 2H), 7.27 – 7.22 (m, 2H), 2.53 (t, *J* = 7.5 Hz, 2H), 1.66 – 1.57 (m, 2H), 1.40 – 1.32 (m, 4H), 0.94 – 0.89 (m, 3H); **^{13}C NMR (101 MHz, $CDCl_3$)** δ 140.8, 140.2, 129.4, 125.8, 124.6, 124.0, 118.7, 31.5, 30.5, 24.2, 22.5, 14.1.

4-Isopropyl-1-phenyl-1*H*-pyrazole (291a).[280]

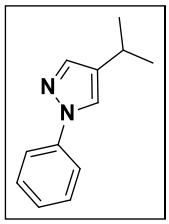

Following GP13 using *N*-phenylsydnone (**35**) (81 mg, 0.5 mmol) and isovaleraldehyde (130 mg, 1.5 mmol) with FCC (gradient from 5-15% Et_2O in 40-60 petroleum ether), 4-isopropyl-1-phenyl-1*H*-pyrazole (**291a**) was isolated as a yellow oil (75 mg, 81%).

^{1}H NMR (400 MHz, $CDCl_3$) δ 7.70 (s, 1H), 7.69 – 7.63 (m, 2H), 7.59 (s, 1H), 7.47 – 7.39 (m, 2H), 7.28 – 7.21 (m, 1H), 2.92 (hept, *J* = 7.0 Hz, 1H), 1.28 (d, *J* = 7.0 Hz, 6H); **^{13}C NMR (101 MHz, $CDCl_3$)** δ 140.5, 139.8, 131.4, 129.6, 126.2, 123.6, 119.0, 24.6, 24.0.

4-Cyclohexyl-1-phenyl-1*H*-pyrazole (298a).[280]

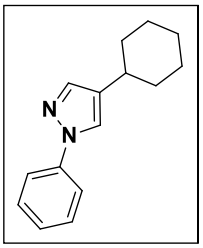

Following GP13 using *N*-phenylsydnone (**35**) (81 mg, 0.5 mmol) and 2-cyclohexylacetaldehyde (**405**) (190 mg, 1.5 mmol) with FCC (gradient from 5-15% Et_2O in 40-60 petroleum ether), 4-cyclohexyl-1-phenyl-1*H*-pyrazole (**298a**) was isolated as a yellow oil (96 mg, 85%).

^{1}H NMR (400 MHz, $CDCl_3$) δ 7.69 (s, 1H), 7.68 – 7.64 (m, 2H), 7.58 (s, 1H), 7.45 – 7.39 (m, 2H), 7.27 – 7.21 (m, 1H), 2.60 – 2.50 (m, 1H), 2.06 – 1.94 (m, 2H), 1.87 – 1.68 (m, 3H), 1.44 – 1.20 (m, 5H); **^{13}C NMR (101 MHz, $CDCl_3$)** δ 140.6, 139.8, 130.6, 129.6, 126.2, 123.6, 119.0, 34.7, 34.3, 26.7, 26.4.

4-Benzyl-1-phenyl-1*H*-pyrazole (131a).

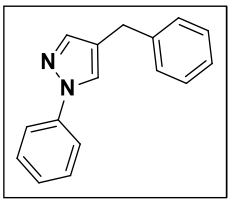

Following GP13 using *N*-phenylsydnone (**35**) (81 mg, 0.5 mmol) and hydrocinnamaldehyde (200 mg, 1.5 mmol) with FCC (DCM), 4-benzyl-1-phenyl-1*H*-pyrazole (**131a**) was isolated as a white solid (91 mg, 77%).

Following GP14 using *N*-phenylsydnone (**35**) (41 mg, 0.25 mmol) and (3-methoxyallyl)benzene (**120**) (150 mg, 1.0 mmol) with FCC (gradient from 0-5% EtOAc in 40-60 petroleum ether), 4-benzyl-1-phenyl-1*H*-pyrazole (**131a**) was isolated as an orange solid (24 mg, 41%).

M.P. 82-84 °C; **^{1}H NMR (400 MHz, $CDCl_3$)** δ 7.71 – 7.64 (m, 3H), 7.59 (s, 1H), 7.47 – 7.39 (m, 2H), 7.38 – 7.31 (m, 2H), 7.31 – 7.23 (m, 4H), 3.92 (s, 2H); **^{13}C NMR (101 MHz, $CDCl_3$)** δ 141.5, 140.9, 140.5, 129.6, 128.9, 128.8, 126.6, 126.4, 125.7, 123.1, 119.1, 30.9; **FTIR ν_{max}** 3024, 2906, 1593, 1492, 1396, 1217, 952 cm^{-1}; **HRMS** calculated for $C_{16}H_{15}N_2$ (ES^+)($+H^+$): 235.1230. Found: 235.1237.

1,4-Diphenyl-1*H*-pyrazole (302a).[279]

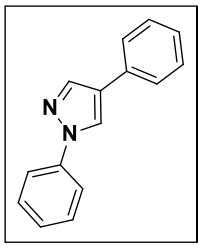

Following GP13 using *N*-phenylsydnone (**35**) (81 mg, 0.5 mmol) and phenylacetaldehyde (180 mg, 1.5 mmol) with FCC (gradient from 0-5% EtOAc in 40-60 petroleum ether), 1,4-diphenyl-1*H*-pyrazole (**302a**) was isolated as a yellow solid (51 mg, 46%).

M.P. 91-95 °C (lit.[279] 95-96 °C); **^{1}H NMR (400 MHz, $CDCl_3$)** δ 8.17 (s, 1H), 8.01 (s, 1H), 7.74 (d, *J* = 8.0 Hz, 2H), 7.57 (d, *J* = 7.5 Hz, 2H), 7.48 (t, *J* = 8.0 Hz, 2H), 7.41 (t, *J* = 7.5 Hz, 2H), 7.35 – 7.24 (m, 2H); **^{13}C NMR (101 MHz, $CDCl_3$)** δ 140.4, 139.2, 132.4, 129.8, 129.3, 127.2, 126.9, 126.1, 125.3, 123.7, 119.4.

Methyl 3-(1-phenyl-1*H*-pyrazol-4-yl)propanoate (304a).

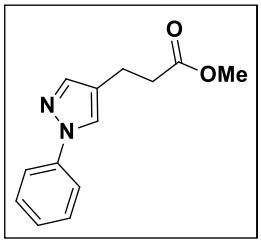

Following GP13 using *N*-phenylsydnone (**78**) (81 mg, 0.5 mmol) and methyl 5-oxopentanoate (**407**) (200 mg, 1.5 mmol) with FCC (20% EtOAc in 40-60 petroleum ether), methyl 3-(1-phenyl-1*H*-pyrazol-4-yl)propanoate (**304a**) was isolated as a yellow oil (79 mg, 69%).

^{1}H NMR (400 MHz, $CDCl_3$) δ 7.74 (s, 1H), 7.67 – 7.61 (m, 2H), 7.55 (s, 1H), 7.44 – 7.38 (m, 2H), 7.27 – 7.21 (m, 1H), 3.67 (s, 3H), 2.86 (t, *J* = 7.5 Hz, 2H), 2.61 (t, *J* = 7.5 Hz, 2H); **^{13}C NMR (101 MHz, $CDCl_3$)** δ 173.5, 141.0 , 140.4, 129.6, 126.5, 125.4, 122.3, 119.1, 51.9, 35.5, 19.9; **FTIR ν_{max}** 2951, 1731, 1501, 1397, 1172, 953 cm^{-1}; **HRMS** calculated for $C_{13}H_{15}N_2O_2$ (ES^+)($+H^+$): 231.1128. Found: 231.1132.

N-Methoxy-*N*-methyl-3-(1-phenyl-1*H*-pyrazol-4-yl)propanamide (305a).

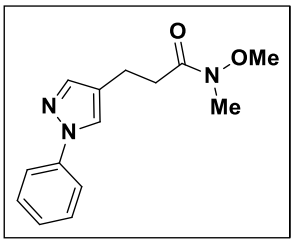

Following GP13 using *N*-phenylsydnone (**35**) (81 mg, 0.5 mmol) and *N*-methoxy-*N*-methyl-5-oxopentanamide (**408**) (240 mg, 1.5 mmol) with FCC (60% EtOAc in 40-60 petroleum ether), *N*-methoxy-*N*-methyl-3-(1-phenyl-1*H*-pyrazol-4-yl)propanamide (**305a**) was isolated as an orange oil (87 mg, 67%).

^{1}H NMR (400 MHz, $CDCl_3$) δ 7.77 (s, 1H), 7.66 – 7.61 (m, 2H), 7.57 (s, 1H), 7.44 – 7.37 (m, 2H), 7.26 – 7.20 (m, 1H), 3.63 (s, 3H), 3.17 (s, 3H), 2.87 (t, *J* = 7.5 Hz, 2H), 2.72 (t, *J* = 7.5 Hz, 2H); **^{13}C NMR (101 MHz, $CDCl_3$)** δ 141.2, 140.5, 129.6, 126.4, 125.6, 122.9, 121.6, 119.1, 61.5, 33.4, 32.5, 19.4; **FTIR ν_{max}** 3489, 2965, 2937, 2245, 1752, 1659, 1504, 1397, 1178, 954 cm^{-1}; **HRMS** calculated for $C_{14}H_{18}N_3O_2$ (ES^+)($+H^+$): 260.1394. Found: 260.1401.

4-(4-((*tert*-Butyldimethylsilyl)oxy)butyl)-1-phenyl-1*H*-pyrazole (303a).

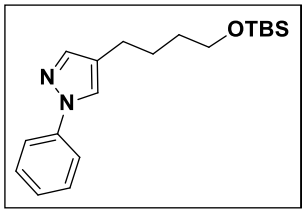

Following GP13 using *N*-phenylsydnone (**35**) (81 mg, 0.5 mmol) and 6-((*tert*-butyldimethylsilyl)oxy)hexanal (**312**) (350 mg, 1.5 mmol) with FCC (gradient from 0-10% Et_2O in 40-60 petroleum ether), 4-(4-((*tert*-butyldimethylsilyl)oxy)butyl)-1-phenyl-1*H*-pyrazole (**303a**) was isolated as a yellow oil (100 mg, 62%).

^{1}H NMR (400 MHz, $CDCl_3$) δ 7.71 (d, *J* = 0.5 Hz, 1H), 7.68 – 7.63 (m, 2H), 7.55 (s, 1H), 7.45 – 7.39 (m, 2H), 7.27 – 7.21 (m, 1H), 3.65 (t, *J* = 6.0 Hz, 2H), 2.55 (t, *J* = 7.5 Hz, 2H), 1.71 – 1.56 (m, 4H), 0.90 (s, 9H), 0.06 (s, 6H); **^{13}C NMR (101 MHz, $CDCl_3$)** δ 141.3, 140.6, 129.7, 126.3, 125.1, 124.2, 119.1, 63.3, 32.7, 27.4, 26.3, 24.3, 18.7, -4.9; **FTIR ν_{max}** 2928, 2856, 1601, 1505, 1395, 1252, 1099, 952 cm^{-1}; **HRMS** calculated for $C_{19}H_{31}N_2OSi$ (ES^+)($+H^+$): 331.2200. Found: 331.2209.

tert-Butyl 4-(1-phenyl-1*H*-pyrazol-4-yl)piperidine-1-carboxylate (306a).

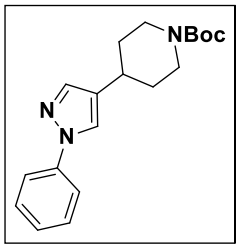

Following GP13 using *N*-phenylsydnone (**35**) (81 mg, 0.5 mmol) and *tert*-butyl 4-(2-oxoethyl)piperidine-1-carboxylate (**406**) (340 mg, 1.5 mmol) with FCC (gradient from 20-30% Et_2O in 40-60 petroleum ether), *tert*-butyl 4-(1-phenyl-1*H*-pyrazol-4-yl)piperidine-1-carboxylate (**306a**) was isolated as a white solid (120 mg, 73%).

M.P. 109-111 °C; **^{1}H NMR (400 MHz, $CDCl_3$)** δ 7.70 (s, 1H), 7.67 – 7.62 (m, 2H), 7.57 (s, 1H), 7.46 – 7.40 (m, 2H), 7.28 – 7.22 (m, 1H), 4.17 (s, 2H), 2.89 – 2.77 (m, 2H), 2.71 (tt, *J* = 11.5, 3.5 Hz, 1H), 1.98 – 1.90 (m, 2H), 1.64 – 1.49 (m, 2H), 1.47 (s, 9H); **^{13}C NMR (101 MHz, $CDCl_3$)** δ 155.2, 140.5, 139.7, 129.7, 128.6, 126.5, 123.9, 119.2, 79.8, 44.2, 33.5, 32.7, 28.8; **FTIR ν_{max}** 2969, 2917, 2864, 1663, 1598, 1421, 1237, 1169, 952 cm^{-1}; **HRMS** calculated for $C_{19}H_{26}N_3O_2$ (ES^+)($+H^+$): 328.2020. Found: 328.2032.

4-Methyl-1-(4-nitrophenyl)-1*H*-pyrazole (115a).

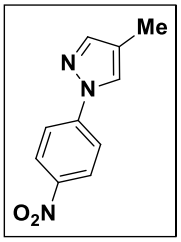

Following GP14 using *N*-(4-nitrophenyl)sydnone (**396**) (100 mg, 0.50 mmol) and ethyl propenyl ether (**113**) (170 mg, 2.0 mmol) and *o*-DCB (0.5 mL) with FCC (gradient from 0-10% EtOAc in DCM), 4-methyl-1-(4-nitrophenyl)-1*H*-pyrazole (**115a**) was isolated as a yellow solid (87 mg, 85%).

M.P. 122-124 °C; **^{1}H NMR (400 MHz, $CDCl_3$)** δ 8.32 – 8.26 (m, 2H), 7.83 – 7.77 (m, 3H), 7.59 (s, 1H), 2.17 (s, 3H); **^{13}C NMR (101 MHz, $CDCl_3$)** δ 145.1, 144.6, 143.9, 125.5, 125.5, 120.3, 118.1, 9.1; **FTIR:** ν_{max} 3125, 2922, 1597, 1508, 1330, 1109, 946 cm^{-1}; **HRMS** calculated for $C_{10}H_{10}N_3O_2$ (ES^+)($+H^+$): 204.0768. Found: 204.0769.

1-(4-Methoxyphenyl)-4-methyl-1*H*-pyrazole (116a).[281]

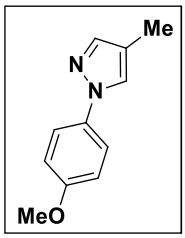

Following GP14 using *N*-(4-methoxyphenyl)sydnone (**46**) (96 mg, 0.50 mmol) and ethyl propenyl ether (**113**) (170 mg, 2.0 mmol) and *o*-DCB (0.5 mL) with FCC (gradient from 0-10% EtOAc in DCM), 1-(4-methoxyphenyl)-4-methyl-1*H*-pyrazole (**116a**) was isolated as an orange solid (62 mg, 66%).

M.P. 48-50 °C; **^{1}H NMR (400 MHz, $CDCl_3$)** δ 7.58 (s, 1H), 7.56 – 7.50 (m, 2H), 7.48 (s, 1H), 6.96 – 6.89 (m, 2H), 3.80 (s, 3H), 2.13 (s, 3H); **^{13}C NMR (101 MHz, $CDCl_3$)** δ 157.9, 141.3, 134.2, 125.5, 120.4, 117.8, 114.5, 55.6, 9.0; **HRMS** calculated for $C_{11}H_{13}N_2O$ (ES^+)($+H^+$): 189.1022. Found: 189.1024.

5-Chloro-4-methyl-1-phenyl-1*H*-pyrazole (117a).[282]

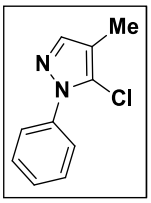

Following GP14 using 3-phenyl-4-chlorosydnone (**398**) (99 mg, 0.50 mmol) and ethyl propenyl ether (**113**) (170 mg, 2.0 mmol) and *o*-DCB (0.5 mL) with FCC (gradient from 0-10% EtOAc in 40-60 petroleum ether), 5-chloro-4-methyl-1-phenyl-1*H*-pyrazole (**117a**) was isolated as a yellow oil (39 mg, 41%).

^{1}H NMR (400 MHz, $CDCl_3$) δ 7.59 – 7.53 (m, 3H), 7.50 – 7.44 (m, 2H), 7.41 – 7.36 (m, 1H), 2.10 (s, 3H); **^{13}C NMR (101 MHz, $CDCl_3$)** δ 141.0, 138.8, 129.0, 128.0, 125.4, 124.8, 115.1, 8.6.

4-Isopropyl-1-(4-methoxyphenyl)-1*H*-pyrazole (292a).

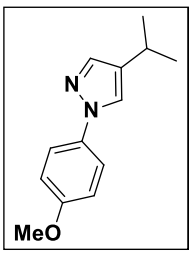

Following GP13 using *N*-(4-methoxyphenyl)sydnone (**46**) (81 mg, 0.50 mmol) and isovaleraldehyde (130 mg, 1.5 mmol) with FCC (gradient from 5-10% EtOAc in 40-60 petroleum ether), 4-isopropyl-1-(4-methoxyphenyl)-1*H*-pyrazole (**292a**) was isolated as an orange oil (86 mg, 80%).

^{1}H NMR (400 MHz, $CDCl_3$) δ 7.60 (s, 1H), 7.58 – 7.53 (m, 3H), 6.97 – 6.92 (m, 2H), 3.82 (s, 3H), 2.90 (hept, *J* = 7.0 Hz, 1H), 1.26 (d, *J* = 7.0 Hz, 6H); **^{13}C NMR (101 MHz, $CDCl_3$)** δ 158.2, 139.3, 134.5, 131.1, 123.8, 120.7, 114.7, 55.8, 24.7, 24.2; **FTIR ν_{max}** 2959, 1515, 1463, 1397, 1242, 1042, 954 cm^{-1}; **HRMS** calculated for $C_{13}H_{17}N_2O$ (ES^+)($+H^+$): 217.1335. Found: 217.1344.

4-(4-Isopropyl-1*H*-pyrazol-1-yl)benzonitrile (293a).

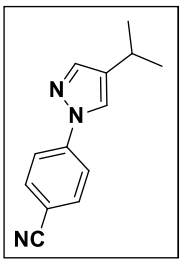

Following GP13 using *N*-(4-cyanophenyl)sydnone (**397**) (94 mg, 0.5 mmol) and isovaleraldehyde (130 mg, 1.5 mmol) with FCC (gradient from 0-30% EtOAc in 40-60 petroleum ether), 4-(4-isopropyl-1*H*-pyrazol-1-yl)benzonitrile (**293a**) was isolated as a colourless oil (53 mg, 50%).

^{1}H NMR (400 MHz, $CDCl_3$) δ 7.81 – 7.77 (m, 2H), 7.76 – 7.70 (m, 3H), 7.63 (s, 1H), 2.92 (hept, *J* = 7.0 Hz, 1H), 1.28 (d, *J* = 7.0 Hz, 6H); **^{13}C NMR (101 MHz, $CDCl_3$)** δ 143.4, 141.6, 133.9, 133.0, 123.6, 118.9, 118.7, 109.2, 24.7, 23.9; **FTIR ν_{max}** 2961, 2872, 2219, 1605, 1514, 1392, 1175, 945 cm^{-1}; **HRMS** calculated for $C_{13}H_{14}N_3$ (ES^+)($+H^+$): 212.1182. Found: 212.1190.

1-(4-Fluorophenyl)-4-isopropyl-1*H*-pyrazole (294a).

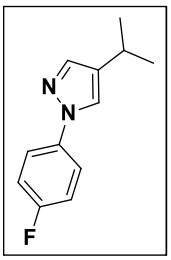

Following GP13 using *N*-(4-fluorophenyl)sydnone (**392**) (90 mg, 0.5 mmol) and isovaleraldehyde (130 mg, 1.5 mmol) with FCC (gradient from 5-10% Et_2O in 40-60 petroleum ether), 1-(4-fluorophenyl)-4-isopropyl-1*H*-pyrazole (**294a**) was isolated as a yellow oil (84 mg, 82%).

^{1}H NMR (400 MHz, $CDCl_3$) δ 7.64 – 7.59 (m, 3H), 7.57 (s, 1H), 7.14 – 7.08 (m, 2H), 2.91 (hept, *J* = 7.0 Hz, 1H), 1.27 (d, *J* = 7.0 Hz, 6H); **^{13}C NMR (101 MHz, $CDCl_3$)** δ 161.1 (d, *J* = 245.0 Hz), 139.9, 137.0, 131.7, 123.8, 120.8 (d, *J* = 8.0 Hz), 116.4 (d, *J* = 23.0 Hz), 24.7, 24.1; **^{19}F NMR (377 MHz, $CDCl_3$)** δ -116.7 – -116.8 (m); **FTIR ν_{max}** 2961, 2872, 1512, 1395, 1226, 952 cm^{-1}; **HRMS** calculated for $C_{12}H_{14}FN_2$ (ES^+)($+H^+$): 205.1136. Found: 205.1140.

1-(4-Chlorophenyl)-4-isopropyl-1*H*-pyrazole (295a).

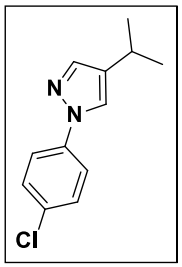

Following GP13 using *N*-(4-chlorophenyl)sydnone (**393**) (98 mg, 0.5 mmol) and isovaleraldehyde (130 mg, 1.5 mmol) with FCC (toluene), 1-(4-chlorophenyl)-4-isopropyl-1*H*-pyrazole (**295a**) was isolated as a yellow solid (86 mg, 78%).

M.P. 47-48 °C; **^{1}H NMR (400 MHz, $CDCl_3$)** δ 7.65 (s, 1H), 7.62 – 7.56 (m, 3H), 7.41 – 7.35 (m, 2H), 2.91 (hept, *J* = 7.0 Hz, 1H), 1.27 (d, *J* = 7.0 Hz, 6H); **^{13}C NMR (101 MHz, $CDCl_3$)** δ 140.2, 139.2, 131.9, 131.6, 129.7, 123.6, 120.1, 24.7, 24.1; **FTIR ν_{max}** 2960, 2931, 2869, 1497, 1393, 1093, 949 cm^{-1}; **HRMS** calculated for $C_{12}H_{14}ClN_2$ (^{35}Cl)(ES^+)($+H^+$): 221.0840. Found: 221.0850.

1-(4-Bromophenyl)-4-isopropyl-1*H*-pyrazole (296a).

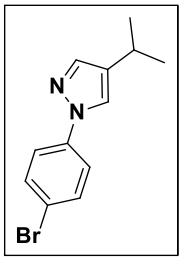

Following GP13 using *N*-(4-bromophenyl)sydnone (**394**) (120 mg, 0.5 mmol) and isovaleraldehyde (130 mg, 1.5 mmol) with FCC (gradient from 5-10% Et_2O in 40-60 petroleum ether), 1-(4-bromophenyl)-4-isopropyl-1*H*-pyrazole (**296a**) was isolated as a yellow solid (110 mg, 83%).

M.P. 42-43 °C; **^{1}H NMR (400 MHz, $CDCl_3$)** δ 7.66 (s, 1H), 7.58 (s, 1H), 7.57 – 7.51 (m, 4H), 2.91 (hept, *J* = 7.0 Hz, 1H), 1.27 (d, *J* = 7.0 Hz, 6H); **^{13}C NMR (101 MHz, $CDCl_3$)** δ 140.3, 139.7, 132.7, 132.0, 123.5, 120.5, 119.4, 24.7, 24.1; **FTIR ν_{max}** 2958, 2867, 1590, 1493, 1392, 1304, 1208, 948 cm^{-1}; **HRMS** calculated for $C_{12}H_{14}BrN_2$ (^{79}Br)(ES^+)($+H^+$): 267.0315. Found: 267.0318.

4-Isopropyl-1-(4-(trifluoromethyl)phenyl)-1*H*-pyrazole (297a).[280]

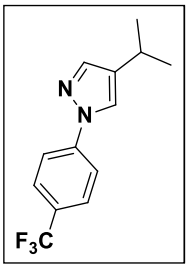

Following GP13 using *N*-(4-(trifluoromethyl)phenyl)sydnone (**395**) (120 mg, 0.5 mmol) and isovaleraldehyde (130 mg, 1.5 mmol) with FCC (gradient from 5-10% EtOAc in 40-60 petroleum ether), 4-isopropyl-1-(4-(trifluoromethyl)phenyl)-1*H*-pyrazole (**297a**) was isolated as an orange oil (73 mg, 57%).

^{1}H NMR (400 MHz, $CDCl_3$) δ 7.79 (d, *J* = 8.5 Hz, 2H), 7.75 (s, 1H), 7.68 (d, *J* = 8.5 Hz, 2H), 7.62 (s, 1H), 2.93 (hept, *J* = 7.0 Hz, 1H), 1.28 (d, *J* = 7.0 Hz, 6H); **^{13}C NMR (101 MHz, $CDCl_3$)** δ 143.0, 141.0, 132.5, 128.0 (q, *J* = 33.0 Hz), 127.0 (q, *J* = 4.0 Hz), 124.4 (q, *J* = 272.0 Hz), 123.6, 118.6, 24.8, 24.0; **^{19}F NMR (377 MHz, $CDCl_3$)** δ -62.2.

4-Isopropyl-1-(*m*-tolyl)-1*H*-pyrazole (301a).

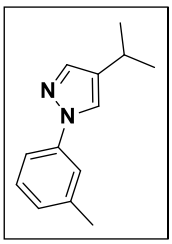

Following GP13 using *N*-(*m*-tolyl)sydnone (**391**) (88 mg, 0.5 mmol) and isovaleraldehyde (130 mg, 1.5 mmol) with FCC (5% Et_2O in 40-60 petroleum ether), 4-isopropyl-1-(*m*-tolyl)-1*H*-pyrazole (**301a**) was isolated as a yellow oil (81 mg, 81%).

^{1}H NMR (400 MHz, $CDCl_3$) δ 7.69 (s, 1H), 7.58 (s, 1H), 7.52 (s, 1H), 7.46 – 7.41 (m, 1H), 7.30 (t, *J* = 7.5 Hz, 1H), 7.06 (d, *J* = 7.5 Hz, 1H), 2.92 (hept, *J* = 7.0 Hz, 1H), 2.41 (s, 3H), 1.28 (d, *J* = 7.0 Hz, 6H); **^{13}C NMR (101 MHz, $CDCl_3$)** δ 140.6, 139.7, 131.4, 129.4, 127.1, 123.7, 119.9, 116.1, 24.7, 24.1, 21.8; **FTIR ν_{max}** 2961, 2871, 1611, 1499, 1391, 1178, 966 cm^{-1}; **HRMS** calculated for $C_{13}H_{17}N_2$ (ES^+)($+H^+$): 201.1386. Found: 201.1392.

4-Cyclohexyl-1-(4-methoxyphenyl)-1*H*-pyrazole (299a).[75]

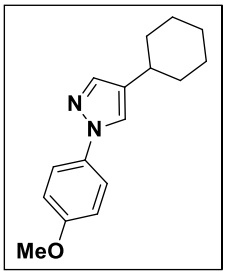

Following GP13 using *N*-(4-methoxyphenyl)sydnone (**46**) (81 mg, 0.50 mmol) and 2-cyclohexylacetaldehyde (**405**) (190 mg, 1.5 mmol) with FCC (gradient from 5-10% EtOAc in 40-60 petroleum ether), 4-cyclohexyl-1-(4-methoxyphenyl)-1*H*-pyrazole (**299a**) was isolated as an orange oil (110 mg, 85%).

^{1}H NMR (400 MHz, $CDCl_3$) δ 7.59 (s, 1H), 7.58 – 7.52 (m, 3H), 6.97 – 6.91 (m, 2H), 3.82 (s, 3H), 2.59 – 2.47 (m, 1H), 2.03 – 1.94 (m, 2H), 1.84 – 1.69 (m, 3H), 1.42 – 1.19 (m, 5H); **^{13}C NMR (101 MHz, $CDCl_3$)** δ 158.1, 139.3, 134.5, 130.2, 123.8, 120.7, 114.7, 55.8, 34.7, 34.3, 26.7, 26.4.

1-(4-Chlorophenyl)-4-cyclohexyl-1*H*-pyrazole (300a).

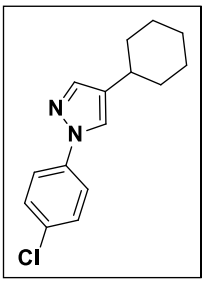

Following GP13 using *N*-(4-chlorophenyl)sydnone (**393**) (98 mg, 0.5 mmol) and 2-cyclohexylacetaldehyde (**405**) (190 mg, 1.5 mmol) with FCC (toluene), 1-(4-chlorophenyl)-4-cyclohexyl-1*H*-pyrazole (**300a**) was isolated as a yellow solid (110 mg, 83%).

M.P. 63-65 °C; **^{1}H NMR (400 MHz, $CDCl_3$)** δ 7.64 (s, 1H), 7.62 – 7.56 (m, 3H), 7.41 – 7.35 (m, 2H), 2.59 – 2.49 (m, 1H), 2.03 – 1.94 (m, 2H), 1.85 – 1.68 (m, 3H), 1.45 – 1.18 (m, 5H); **^{13}C NMR (101 MHz, $CDCl_3$)** δ 140.2, 139.2, 131.6, 131.0, 129.7, 123.6, 120.1, 34.7, 34.3, 26.7, 26.4; **FTIR ν_{max}** 2919, 2849, 1598, 1498, 1445, 1096, 950 cm^{-1}; **HRMS** calculated for $C_{15}H_{18}ClN_2$ (^{35}Cl)(ES^+)($+H^+$): 261.1155. Found: 261.1153.

1-Phenyl-5,6-dihydro-1*H*-indazol-7(4*H*)-one (323).

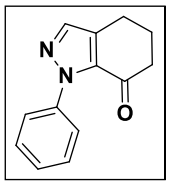

Following GP13 using 3-phenyl-4-(6-oxohexanoyl)sydnone (**321**) (140 mg, 0.50 mmol) with FCC (gradient from 20-30% EtOAc in 40-60 petroleum ether), 1-phenyl-5,6-dihydro-1*H*-indazol-7(4*H*)-one (**323**) was isolated as a yellow oil (13 mg, 12%).

^{1}H NMR (400 MHz, $CDCl_3$) δ 7.59 (s, 1H), 7.52 – 7.48 (m, 2H), 7.47 – 7.37 (m, 3H), 2.85 (t, *J* = 6.0 Hz, 2H), 2.60 (dd, *J* = 7.0, 6.0 Hz, 2H), 2.22 – 2.13 (m, 2H); **^{13}C NMR (101 MHz, $CDCl_3$)** δ 188.1, 140.2, 138.1, 134.6, 132.1, 128.6, 128.4, 125.3, 40.2, 24.9, 21.5; **FTIR:** ν_{max} 2950, 2920, 1680, 1496, 1404, 1285, 895 cm^{-1};

1-Phenyl-4,5,6,7-tetrahydro-1*H*-indazole (324).[230]

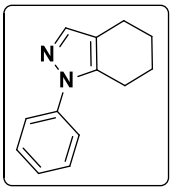

Following GP13 using 3-phenyl-4-(6-oxohexyl)sydnone (**315**) (130 mg, 0.5 mmol) with FCC (gradient from 10-20% EtOAc in 40-60 petroleum ether), 1-phenyl-4,5,6,7-tetrahydro-1*H*-indazole (**324**) was isolated as a yellow oil (77 mg, 78%).

^{1}H NMR (400 MHz, $CDCl_3$) δ 7.53 – 7.41 (m, 5H), 7.33 – 7.28 (m, 1H), 2.73 (t, *J* = 5.0 Hz, 2H), 2.59 (t, *J* = 5.0 Hz, 2H), 1.87 – 1.75 (m, 4H); **^{13}C NMR (101 MHz, $CDCl_3$)** δ 140.3, 139.0, 138.3, 129.2, 126.7, 123.2, 117.9, 23.8, 23.3, 22.9, 20.9.

1-Phenyl-4,5,6,7-tetrahydro-1*H*-indazol-7-yl acetate (325).

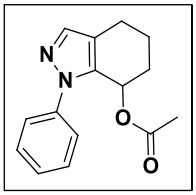

Following GP13 using 3-phenyl-4-(1-acetoxy-6-oxohexyl)sydnone (**314**) (40 mg, 0.13 mmol) with FCC (20% EtOAc in 40-60 petroleum ether), 1-phenyl-4,5,6,7-tetrahydro-1*H*-indazol-7-yl acetate (**325**) was isolated as a yellow oil (17 mg, 52%).

^{1}H NMR (400 MHz, $CDCl_3$) δ 7.51 (s, 1H), 7.46 – 7.40 (m, 4H), 7.38 – 7.32 (m, 1H), 6.03 (t, *J* = 4.5 Hz, 1H), 2.72 (dt, *J* = 15.5, 4.5 Hz, 1H), 2.60 – 2.49 (m, 1H), 2.06 – 1.76 (m, 7H); **^{13}C NMR (101 MHz, $CDCl_3$)** δ 170.1, 140.1, 138.6, 135.8, 129.2, 127.8, 124.1, 121.0, 63.9, 29.8, 20.9, 20.7, 19.2; ; **FTIR ν_{max}** 2922, 2851, 1725, 1597, 1502, 1371, 1231, 1053, 960 cm^{-1}; **HRMS** calculated for $C_{15}H_{17}N_2O_2$ (ES^+)($+H^+$): 257.1285. Found: 257.1288.

1,5-diphenyl-3-(*p*-tolyl)-1*H*-pyrazole (411).[283]

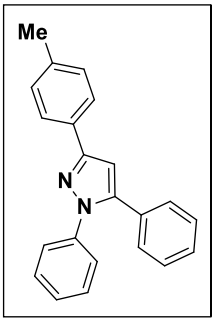

A flame-dried screw cap vial was charged with 3-phenyl-4-(*p*-tolyl)sydnone (**109**) (130mg, 0.50 mmol), $Ru(bpy)_3(PF_6)_2$ (21 mg, 25 µmol) and EVI_2 (230 mg, 0.50 mmol) under N_2. Anhydrous, degassed NMP (5.0 mL) was then added via syringe followed by phenylacetylene (150 mg, 1.5 mmol). The vial was then subjected to three vacuum/nitrogen cycles, sealed and irradiated at room temperature using a kessil A160WE tuna blue aquarium light for 48 hours. The reaction was then diluted with H_2O (40 mL) and extracted with Et_2O or EtOAc (4 x 25 mL). The combined organic layers were then washed with brine (25 mL), dried over anhydrous $MgSO_4$, filtered and concentrated under vacuum. Purification by FCC (gradient from 10-20% Et_2O in 40-60 petroleum ether) afforded 1,5-diphenyl-3-(*p*-tolyl)-1*H*-pyrazole (**411**) as a yellow solid (16 mg, 10%).

^{1}H NMR (400 MHz, $CDCl_3$) δ 7.84 – 7.79 (m, 2H), 7.40 – 7.27 (m, 10H), 7.26 – 7.22 (m, 2H), 6.80 (s, 1H), 2.39 (s, 3H); **^{13}C NMR (101 MHz, $CDCl_3$)** δ 152.2, 144.4, 140.3, 137.9, 130.8, 130.4, 129.5, 129.0, 128.9, 128.6, 128.4, 127.5, 125.9, 125.5, 105.2, 21.5.

4-isopropyl-1-phenyl-3-(*p*-tolyl)-1*H*-pyrazole (412).[284]

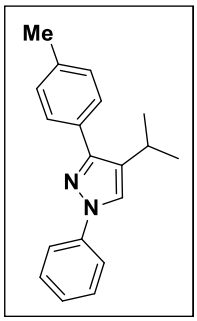

Following GP13 using 3-phenyl-4-(*p*-tolyl)sydnone (**109**) (130mg, 0.50 mmol) and isovaleraldehyde (130 mg, 1.5 mmol) with FCC (10% Et_2O in 40-60 petroleum ether), 4-isopropyl-1-phenyl-3-(*p*-tolyl)-1*H*-pyrazole (**412**) was isolated as a red oil (14 mg, 10%).

^{1}H NMR (400 MHz, $CDCl_3$) δ 7.79 (s, 1H), 7.76 – 7.72 (m, 2H), 7.63 – 7.58 (m, 2H), 7.46 – 7.41 (m, 2H), 7.27 – 7.22 (m, 4H), 3.17 (hept, *J* = 7.0 Hz, 1H), 2.40 (s, 3H), 1.26 (d, *J* = 7.0 Hz, 6H); **^{13}C NMR (101 MHz, $CDCl_3$)** δ 151.2, 140.4, 137.6, 131.4, 129.4, 129.3, 128.2, 126.0, 124.4, 118.8, 30.5, 24.4, 21.4; **FTIR:** ν_{max} 2959, 1599, 1502, 1403, 1327, 1060 cm^{-1}.

***tert*-Butyl (2-(1-phenyl-1*H*-pyrazol-4-yl)ethyl)carbamate (79a).**

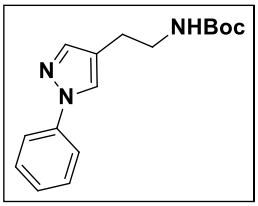

Following GP15 using *N*-phenylsydnone (**35**) (81 mg, 0.5 mmol), *N*-Boc-2,3-dihydropyrrole (**77**) (170 mg, 1.0 mmol) and *o*-DCB (0.50 mL) with FCC (5% EtOAc in 40-60 petroleum ether), *tert*-butyl (2-(1-phenyl-1*H*-pyrazol-4-yl)ethyl)carbamate (**79a**) was isolated as a brown oil (7.2 mg, 5%). This compound was analysed by ^{1}H NMR only due to a lack of available material.

^{1}H NMR (400 MHz, $CDCl_3$) δ 7.77 (s, 1H), 7.66 (d, *J* = 8.0 Hz, 2H), 7.57 (s, 1H), 7.44 (t, *J* = 8.0 Hz, 2H), 7.30 – 7.26 (m, 1H), 4.63 (br, 1H), 3.43 – 3.32 (m, 2H), 2.74 (t, *J* = 7.0 Hz, 2H), 1.44 (s, 9H).

tert-Butyl (3-(1-phenyl-1*H*-pyrazol-4-yl)propyl)carbamate (78a).

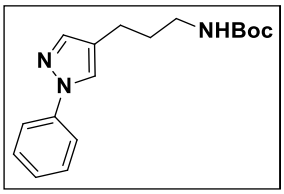

Following GP15 using *N*-phenylsydnone (**35**) (81 mg, 0.5 mmol), *N*-Boc-3,4-dihydro-2H-pyridine (**76**) (180 mg, 1.0 mmol) and xylenes (0.50 mL) with FCC (5% EtOAc in 40-60 petroleum ether), *tert*-butyl (3-(1-phenyl-1*H*-pyrazol-4-yl)propyl)carbamate (**78a**) was isolated as brown oil (12 mg, 8%). This compound was analysed by ^{1}H NMR only due to a lack of available material.

^{1}H NMR (400 MHz, $CDCl_3$) δ 7.74 (s, 1H), 7.65 (d, *J* = 8.0 Hz, 2H), 7.55 (s, 1H), 7.43 (t, *J* = 8.0 Hz, 2H), 7.25 (t, *J* = 7.5 Hz, 1H), 4.57 (br, 1H), 3.25 – 3.12 (m, 2H), 2.57 (t, *J* = 7.5 Hz, 2H), 1.80 (p, *J* = 7.5 Hz, 2H), 1.45 (s, 9H).

2-(Phenylamino)-1-(piperidin-1-yl)ethanone (139).[285]

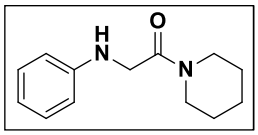

Following GP15 using *N*-phenylsydnone (**35**) (81 mg, 0.50 mmol) and (*E*)-1-(hex-1-en-1-yl)piperidine (**138**) (370 mg, 2.0 mmol) with purification by FCC (gradient from 0-40% EtOAc in 40-60 petroleum ether) afforded 2-(phenylamino)-1-(piperidin-1-yl)ethanone (**139**) as a yellow oil (110 mg, quant.). This compound was analysed by ^{1}H NMR only because it was not a target of the study and ^{1}H NMR provided sufficient information to inform further experiments.

^{1}H NMR (400 MHz, $CDCl_3$) δ 7.22 – 7.16 (m, 2H), 6.75 – 6.69 (m, 1H), 6.65 – 6.61 (m, 2H), 3.85 (s, 2H), 3.64 – 3.59 (m, 2H), 3.40 – 3.33 (m, 2H), 1.72 – 1.65 (m, 2H), 1.64 – 1.55 (m, 4H).

Benzyl (2-(1-phenyl-1*H*-pyrazol-4-yl)ethyl)carbamate (147a) + benzyl benzyl(2-(1-phenyl-1*H*-pyrazol-4-yl)ethyl)carbamate (148a).

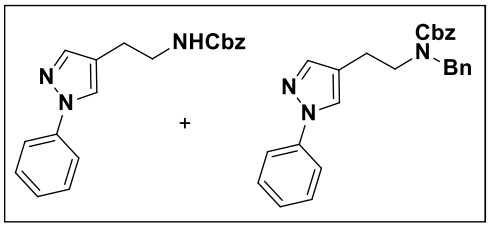

To a solution of *N*-phenylsydnone (**35**) (40 mg, 0.25 mmol) in *o*-DCB (1.0 mL) was added benzyl 2,3-dihydro-1*H*-pyrrole-1-carboxylate (**146**) (100 mg, 0.50 mmol) and the resulting mixture heated at 150 °C for 24 hours. After cooling to room temperature the reaction was purified by FCC (gradient from 10-50% EtOAc in 40-60 petroleum ether) to afford an inseparable mixture of benzyl (2-(1-phenyl-1*H*-pyrazol-4-yl)ethyl)carbamate (**147a**) and benzyl benzyl(2-(1-phenyl-1*H*-pyrazol-4-yl)ethyl)carbamate (**148a**) (21 mg, 24%, 60:40). These compounds were analysed by ^{1}H NMR and LC-MS only.

^{1}H NMR (400 MHz, $CDCl_3$) δ 7.75 (s, 2H), 7.66 – 7.60 (m, 4H), 7.56 (s, 2H), 7.47 – 7.41 (m, 4H), 7.39 – 7.31 (m, 15H), 7.29 – 7.24 (m, 2H), 5.11 (s, 4H), 4.88 (s, 2H, minor), 3.45 (dd, *J* = 13.0, 6.5 Hz, 4H), 2.76 (t, *J* = 6.5 Hz, 4H).

1-Phenyl-4-(3-((tetrahydro-2*H*-pyran-2-yl)oxy)propyl)-1*H*-pyrazole (88a).

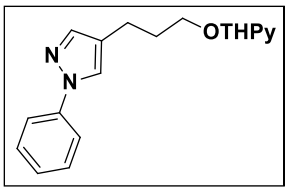

Following GP16 using *N*-phenylsydnone (**35**) (81 mg, 0.50 mmol) and 3,4-dihydro-2*H*-pyran (**86**) (170 mg, 2.0 mmol) with FCC (gradient from 0-10% EtOAc in DCM), 1-phenyl-4-(3-((tetrahydro-2*H*-pyran-2-yl)oxy)propyl)-1*H*-pyrazole (**88a**) was isolated as a brown oil (56 mg, 39%).

^{1}H NMR (400 MHz, $CDCl_3$) δ 7.75 (s, 1H), 7.70 – 7.64 (m, 2H), 7.58 (s, 1H), 7.48 – 7.38 (m, 2H), 7.30 – 7.21 (m, 1H), 4.63 – 4.58 (m, 1H), 3.95 – 3.78 (m, 2H), 3.58 – 3.41 (m, 2H), 2.74 – 2.58 (m, 2H), 2.01 – 1.80 (m, 3H), 1.80 – 1.69 (m, 1H), 1.67 – 1.47 (m, 4H); **^{13}C NMR (101 MHz, $CDCl_3$)** δ 141.0, 140.3, 129.4, 126.0, 124.9, 123.3, 118.7, 112.7, 99.0, 66.7, 62.5, 30.8, 25.5, 20.9, 19.8; **FTIR:** ν_{max} 2939, 2864, 1599, 1502, 1396, 1135, 1118, 1030, 953 cm^{-1}; **HRMS** calculated for $C_{17}H_{23}N_2O_2$ (ES^+)($+H^+$): 287.1754. Found: 287.1751.

1-(4-Methoxyphenyl)-4-(3-((tetrahydro-2*H*-pyran-2-yl)oxy)propyl)-1*H*-pyrazole (89a).

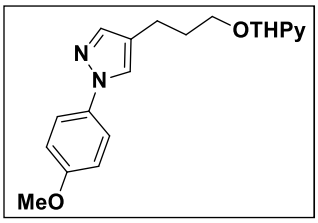

Following GP16 using *N*-(4-methoxyphenyl)sydnone (**46**) (96 mg, 0.50 mmol) and 3,4-dihydro-2*H*-pyran (**86**) (170 mg, 2.0 mmol) with FCC (20% EtOAc in 40-60 petroleum ether), 1-(4-methoxyphenyl)-4-(3-((tetrahydro-2*H*-pyran-2-yl)oxy)propyl)-1*H*-pyrazole (**89a**) was isolated as a yellow oil (38 mg, 24%).

^{1}H NMR (400 MHz, $CDCl_3$) δ 7.66 (s, 1H), 7.60 – 7.54 (m, 3H), 6.99 – 6.95 (m, 2H), 4.61 (dd, *J* = 4.0, 3.0 Hz, 1H), 3.86 (s, 3H), 3.84 – 3.76 (m, 2H), 3.57 – 3.43 (m, 2H), 2.72 – 2.59 (m, 2H), 1.98 – 1.84 (m, 3H), 1.80 – 1.71 (m, 1H), 1.66 – 1.52 (m, 4H).**^{13}C NMR (101 MHz, $CDCl_3$)** δ 157.9, 140.4, 134.2, 125.0, 122.9, 120.4, 114.5, 99.0, 66.8, 62.5, 55.6, 30.9, 30.8, 25.5, 20.9, 19.8; **FTIR:** ν_{max} 2937, 2864, 1513, 1242, 1028, 955, 828 cm^{-1}; **HRMS** calculated for $C_{18}H_{25}N_2O_3$ (ES^+)($+H^+$): 317.1860. Found: 317.1857.

1-(4-Fluorophenyl)-4-(3-((tetrahydro-2*H*-pyran-2-yl)oxy)propyl)-1*H*-pyrazole (91a).

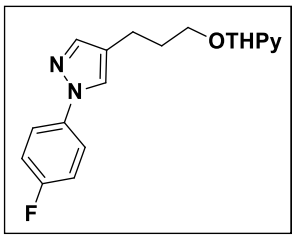

Following GP16 using *N*-(4-fluorophenyl)sydnone (**392**) (90 mg, 0.50 mmol) and 3,4-dihydro-2*H*-pyran (**86**) (170 mg, 2.0 mmol) with FCC (gradient from 0-40% EtOAc in 40-60 petroleum ether), 1-(4-fluorophenyl)-4-(3-((tetrahydro-2*H*-pyran-2-yl)oxy)propyl)-1*H*-pyrazole (**91a**)was isolated as a yellow oil (53 mg, 35%).

^{1}H NMR (400 MHz, $CDCl_3$) δ 7.68 (s, 1H), 7.66 – 7.59 (m, 2H), 7.56 (s, 1H), 7.18 – 7.09 (m, 2H), 4.60 (dd, *J* = 4.5, 3.0 Hz, 1H), 3.94 – 3.78 (m, 2H), 3.57 – 3.42 (m, 2H), 2.72 – 2.58 (m, 2H), 2.02 – 1.81 (m, 3H), 1.80 – 1.69 (m, 1H), 1.67 – 1.49 (m, 4H); **^{13}C NMR (101 MHz, $CDCl_3$)** δ 160.9 (d, *J* = 245.0 Hz), 141.0, 136.7, 125.0, 123.0, 120.5 (d, *J* = 8.0 Hz), 116.1 (d, *J* = 23.0 Hz), 99.1, 66.7, 62.5, 30.8, 30.7, 25.5, 20.9, 19.8; **^{19}F NMR (377 MHz, $CDCl_3$)** δ -116.6 – -116.7 (m); **FTIR:** ν_{max} 2940, 2865, 1512, 1397, 1224, 1134, 1030, 953, 833 cm^{-1}; **HRMS** calculated for $C_{17}H_{22}FN_2O_2$ (ES^+)($+H^+$): 305.1660. Found: 305.1653.

4-(4-(3-((Tetrahydro-2*H*-pyran-2-yl)oxy)propyl)-1*H*-pyrazol-1-yl)benzonitrile (90a).

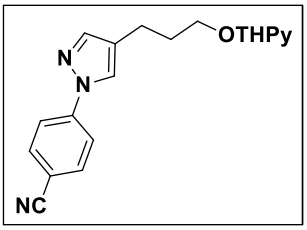

Following GP16 using *N*-(4-cyanophenyl)sydnone (**397**) (94 mg, 0.50 mmol) and 3,4-dihydro-2*H*-pyran (**86**) (170 mg, 2.0 mmol) with FCC (gradient from 0-10% EtOAc in DCM), 4-(4-(3-((tetrahydro-2*H*-pyran-2-yl)oxy)propyl)-1*H*-pyrazol-1-yl)benzonitrile (**90a**) was isolated as an orange oil (75 mg, 48%).

^{1}H NMR (400 MHz, $CDCl_3$) δ 7.82 – 7.75 (m, 3H), 7.74 – 7.68 (m, 2H), 7.61 (s, 1H), 4.58 (dd, *J* = 4.5, 3.0 Hz, 1H), 3.92 – 3.76 (m, 2H), 3.54 – 3.41 (m, 2H), 2.71 – 2.57 (m, 2H), 1.98 – 1.78 (m, 3H), 1.77 – 1.68 (m, 1H), 1.64 – 1.47 (m, 4H); **^{13}C NMR (101 MHz, $CDCl_3$)** δ 143.0, 142.6, 133.6, 124.8, 118.5, 118.4, 113.7, 108.9, 99.1, 66.6, 62.6, 30.8, 30.5, 25.5, 20.8, 19.8; **FTIR:** ν_{max} 2940, 2865, 2226, 1606, 1516, 1394, 1030, 947, 839 cm^{-1}; **HRMS** calculated for $C_{18}H_{22}N_3O_2$ (ES^+)($+H^+$): 312.1707. Found: 312.1706.

1-Phenyl-4-(2-((tetrahydrofuran-2-yl)oxy)ethyl)-1*H*-pyrazole (94a).

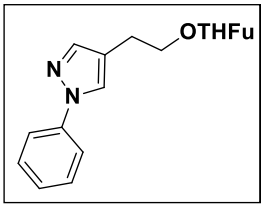

Following GP17 using *N*-phenylsydnone (**35**) (81 mg, 0.50 mmol) and 2,3-dihydrofuran (**92**) (140 mg, 2.0 mmol) with FCC (gradient from 0-50% EtOAc in 40-60 petroleum ether), 1-phenyl-4-(2-((tetrahydrofuran-2-yl)oxy)ethyl)-1*H*-pyrazole (**94a**) was isolated as a yellow oil (86mg, 67%).

^{1}H NMR (400 MHz, $CDCl_3$) δ 7.79 (s, 1H), 7.72 – 7.64 (m, 2H), 7.61 (s, 1H), 7.48 – 7.40 (m, 2H), 7.31 – 7.24 (m, 1H), 5.18 (dd, *J* = 4.0, 2.0 Hz, 1H), 3.95 – 3.84 (m, 3H), 3.61 (dt, *J* = 9.5, 7.0 Hz, 1H), 2.82 (t, *J* = 7.0 Hz, 2H), 2.11 – 1.80 (m, 4H); **^{13}C NMR (101 MHz, $CDCl_3$)** δ 141.3, 140.3, 129.4, 126.1, 125.3, 120.6, 118.8, 103.9, 67.3, 67.0, 32.4, 25.0, 23.5; **FTIR:** ν_{max} 2875, 1724, 1599, 1502, 1395, 1034, 952 cm^{-1}; **HRMS** calculated for $C_{15}H_{19}N_2O_2$ (ES^+)($+H^+$): 259.1441. Found: 259.1447.

1-(4-Methoxyphenyl)-4-(2-((tetrahydrofuran-2-yl)oxy)ethyl)-1*H*-pyrazole (95a).

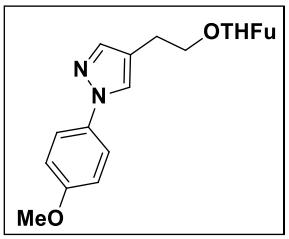

Following GP17 using *N*-(4-methoxyphenyl)sydnone (**46**) (96 mg, 0.50 mmol) and 2,3-dihydrofuran (**92**) (140 mg, 2.0 mmol) with FCC (30% EtOAc in 40-60 petroleum ether), 1-(4-methoxyphenyl)-4-(2-((tetrahydrofuran-2-yl)oxy)ethyl)-1*H*-pyrazole (**95a**) was isolated as a yellow oil (72 mg, 50%).

^{1}H NMR (400 MHz, $CDCl_3$) δ 7.69 (s, 1H), 7.59 – 7.55 (m, 3H), 6.99 – 6.95 (m, 2H), 5.16-5.19 (m, 1H), 3.92 – 3.86 (m, 3H), 3.85 (s, 3H), 3.60 (dt, *J* = 9.5, 7.0 Hz, 1H), 2.81 (t, *J* = 7.0 Hz, 2H), 2.09 – 1.76 (m, 4H); **^{13}C NMR (101 MHz, $CDCl_3$)** δ 158.0, 140.7, 134.1, 125.4, 120.5, 120.1, 114.5, 103.9, 67.4, 67.0, 55.6, 32.4, 25.0, 23.5; **FTIR:** ν_{max} 2935, 1775, 1514, 1243, 1091, 1032, 955, 829 cm^{-1}; **HRMS** calculated for $C_{16}H_{21}N_2O_3$ (ES^+)($+H^+$): 289.1547. Found: 289.1551.

4-(2-((Tetrahydrofuran-2-yl)oxy)ethyl)-1-(3,4,5-trimethoxyphenyl)-1*H*-pyrazole (96a).

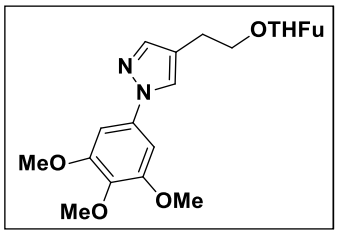

Following GP17 using *N*-(3,4,5-trimethoxyphenyl)sydnone (**47**) (63 mg, 0.25 mmol) and 2,3-dihydrofuran (**92**) (70 mg, 1.0 mmol) with FCC (20% EtOAc and 5% MeOH in 40-60 petroleum ether), 4-(2-((tetrahydrofuran-2-yl)oxy)ethyl)-1-(3,4,5-trimethoxyphenyl)-1*H*-pyrazole (**96a**) was isolated as a brown oil (44 mg, 51%).

^{1}H NMR (400 MHz, $CDCl_3$) δ 7.74 (s, 1H), 7.59 (s, 1H), 6.89 (s, 2H), 5.18 (dd, *J* = 4.0, 2.0 Hz, 1H), 3.96 – 3.93 (m, 6H), 3.91 – 3.86 (m, 6H), 3.61 (dt, *J* = 9.5, 7.0 Hz, 1H), 2.8 (t, *J* = 7.0 Hz, 2H), 2.09 – 1.80 (m, 4H); **^{13}C NMR (101 MHz, $CDCl_3$)** δ 153.7, 141.1, 136.5, 125.6, 120.5, 103.9, 97.0, 96.8, 67.3, 67.0, 61.0, 56.3, 32.4, 25.0, 23.5.; **FTIR:** ν_{max} 2939, 1721, 1600, 1508, 1468, 1227, 1124, 1033, 977 cm^{-1}; **HRMS** calculated for $C_{18}H_{25}N_2O_5$ (ES^+)($+H^+$): 349.1758. Found: 349.1760.

1-(4-Nitrophenyl)-4-(2-((tetrahydrofuran-2-yl)oxy)ethyl)-1*H*-pyrazole (97a).

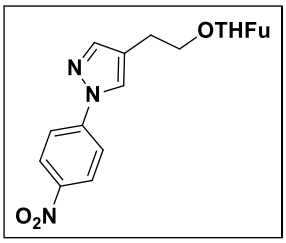

Following GP17 using *N*-(4-nitrophenyl)sydnone (**396**) (100 mg, 0.50 mmol) and 2,3-dihydrofuran (**92**) (140 mg, 2.0 mmol) with FCC (gradient from 20-40% EtOAc in 40-60 petroleum ether), 1-(4-nitrophenyl)-4-(2-((tetrahydrofuran-2-yl)oxy)ethyl)-1*H*-pyrazole (**97a**) was isolated as an orange oil (90 mg, 60%).

^{1}H NMR (400 MHz, $CDCl_3$) δ 8.34 – 8.29 (m, 2H), 7.89 (s, 1H), 7.86 – 7.81 (m, 2H), 7.68 (s, 1H), 5.16 (dd, *J* = 4.0, 2.0 Hz, 1H), 3.93 – 3.84 (m, 3H), 3.61 (dt, *J* = 9.5, 6.5 Hz, 1H), 2.82 (t, *J* = 6.5 Hz, 2H), 2.08 – 1.78 (m, 4H); **^{13}C NMR (101 MHz, $CDCl_3$)** δ 145.1, 144.5, 143.3, 125.5, 125.4, 122.6, 118.1, 104.0, 67.0, 66.9, 32.4, 24.9, 23.6; **FTIR:** ν_{max} 3123, 2878, 1724, 1596, 1517, 1505, 1334, 1031, 945, 851 cm^{-1}; **HRMS** calculated for $C_{15}H_{18}N_3O_4$ (ES^+)($+H^+$): 304.1292. Found: 304.1295.

4-(4-(2-((Tetrahydrofuran-2-yl)oxy)ethyl)-1*H*-pyrazol-1-yl)benzonitrile (99a).

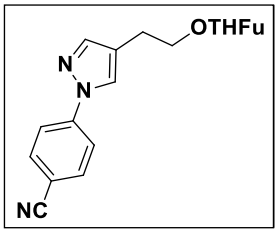

Following GP17 using *N*-(4-cyanophenyl)sydnone (**397**) (94 mg, 0.50 mmol) and 2,3-dihydrofuran (**92**) (140 mg, 2.0 mmol) with FCC (gradient from 10-20% EtOAc in DCM), 4-(4-(2-((tetrahydrofuran-2-yl)oxy)ethyl)-1*H*-pyrazol-1-yl)benzonitrile (**99a**) was isolated as a yellow oil (80 mg, 57%).

^{1}H NMR (400 MHz, $CDCl_3$) δ 7.84 (s, 1H), 7.80 – 7.75 (m, 2H), 7.74 – 7.68 (m, 2H), 7.64 (s, 1H), 5.15 (dd, *J* = 4.0, 2.0 Hz, 1H), 3.92 – 3.81 (m, 3H), 3.59 (dt, *J* = 9.5, 6.5 Hz, 1H), 2.79 (t, *J* = 6.5 Hz, 2H), 2.05 – 1.76 (m, 4H); **^{13}C NMR (101 MHz, $CDCl_3$)** δ 143.0, 142.9, 133.6, 125.2, 122.2, 118.5, 118.4, 109.0, 103.9, 67.0, 66.9, 32.4, 24.9, 23.5; **FTIR:** ν_{max} 2878, 2226, 1722, 1606, 1515, 1393, 1032, 946, 838 cm^{-1}; **HRMS** calculated for $C_{16}H_{18}N_3O_2$ (ES^+)($+H^+$): 284.1394. Found: 284.1399.

1-(4-Fluorophenyl)-4-(2-((tetrahydrofuran-2-yl)oxy)ethyl)-1*H*-pyrazole (100a).

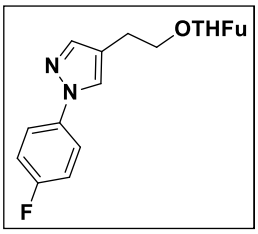

Following GP17 using *N*-(4-fluorophenyl)sydnone (**392**) (90 mg, 0.50 mmol) and 2,3-dihydrofuran (**92**) (140 mg, 2.0 mmol) with FCC (30% EtOAc in 40-60 petroleum ether), 1-(4-fluorophenyl)-4-(2-((tetrahydrofuran-2-yl)oxy)ethyl)-1*H*-pyrazole (**100a**) was isolated as a yellow oil (81 mg, 59%).

^{1}H NMR (400 MHz, $CDCl_3$) δ 7.72 (s, 1H), 7.66 – 7.60 (m, 2H), 7.60 (s, 1H), 7.18 – 7.10 (m, 2H), 5.20 – 5.15 (m, 1H), 3.94 – 3.84 (m, 3H), 3.60 (dt, *J* = 9.5, 6.5 Hz, 1H), 2.81 (t, *J* = 6.5 Hz, 2H), 2.11 – 1.79 (m, 4H); **^{13}C NMR (101 MHz, $CDCl_3$)** δ 160.9 (d, *J* = 245.0 Hz), 141.3, 136.7 (d, *J* = 2.5 Hz), 125.5, 120.7, 120.5 (d, *J* = 8.0 Hz), 116.2 (d, *J* = 23.0 Hz), 103.9, 67.3, 67.0, 32.4, 25.0, 23.5; **^{19}F NMR (377 MHz, $CDCl_3$)** δ -116.5 – -116.6 (m); **FTIR:** ν_{max} 2877, 1724, 1571, 1513, 1396, 1220, 1033, 953, 834 cm^{-1}; **HRMS** calculated for $C_{15}H_{18}FN_2O_2$ (ES^+)($+H^+$): 277.1347. Found: 277.1352.

1-(4-Chlorophenyl)-4-(2-((tetrahydrofuran-2-yl)oxy)ethyl)-1*H*-pyrazole (101a).

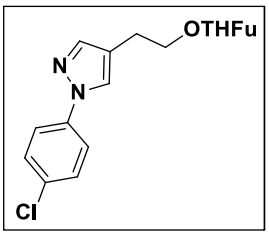

Following GP17 using *N*-(4-chlorophenyl)sydnone (**393**) (99 mg, 0.50 mmol) and 2,3-dihydrofuran (**92**) (140 mg, 2.0 mmol) with FCC (gradient from 0-20% EtOAc in DCM), 1-(4-chlorophenyl)-4-(2-((tetrahydrofuran-2-yl)oxy)ethyl)-1*H*-pyrazole (**101a**) was isolated as a yellow oil (100 mg, 70%).

^{1}H NMR (400 MHz, $CDCl_3$) δ 7.74 (s, 1H), 7.61 (s, 1H), 7.60 – 7.56 (m, 2H), 7.42 – 7.36 (m, 2H), 5.16 (dd, *J* = 4.0, 2.0 Hz, 1H), 3.92 – 3.83 (m, 3H), 3.59 (dt, *J* = 9.5, 7.0 Hz, 1H), 2.80 (t, *J* = 7.0 Hz, 2H), 2.07 – 1.77 (m, 4H); **^{13}C NMR (101 MHz, $CDCl_3$)** δ 141.6, 138.8, 131.4, 129.4, 125.2, 121.0, 119.8, 103.9, 67.2, 67.0, 32.4, 25.0, 23.5; **FTIR:** ν_{max} 2876, 1723, 1498, 1396, 1092, 1033, 951, 828 cm^{-1}; **HRMS** calculated for $C_{15}H_{18}ClN_2O_2$ (^{35}Cl)(ES^+)($+H^+$): 293.1051. Found: 293.1057.

1-(4-Bromophenyl)-4-(2-((tetrahydrofuran-2-yl)oxy)ethyl)-1*H*-pyrazole (102a).

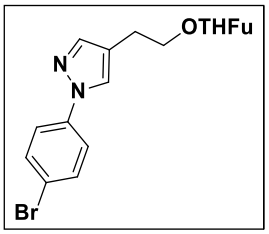

Following GP17 using *N*-(4-bromophenyl)sydnone (**394**) (120 mg, 0.50 mmol) and 2,3-dihydrofuran (**92**) (140 mg, 2.0 mmol) with FCC (gradient from 0-20% EtOAc in DCM), 1-(4-bromophenyl)-4-(2-((tetrahydrofuran-2-yl)oxy)ethyl)-1*H*-pyrazole (**102a**) was isolated as a colourless oil (110 mg, 67%).

^{1}H NMR (400 MHz, $CDCl_3$) δ 7.73 (s, 1H), 7.58 (s, 1H), 7.52 (s, 4H), 5.14 (dd, *J* = 4.0, 2.0 Hz, 1H), 3.92 – 3.80 (m, 3H), 3.57 (dt, *J* = 9.5, 6.5 Hz, 1H), 2.78 (t, *J* = 6.5 Hz, 2H), 2.06 – 1.75 (m, 4H); **^{13}C NMR (101 MHz, $CDCl_3$)** δ 141.6, 138.8, 131.4, 129.4, 125.2, 121.0, 119.8, 103.9, 67.2, 67.0, 32.4, 25.0, 23.5; **FTIR:** ν_{max} 2876, 1722, 1592, 1494, 1395, 1032, 950, 825 cm^{-1}; **HRMS** calculated for $C_{15}H_{18}BrN_2O_2$ (^{79}Br)(ES^+)($+H^+$): 337.0546. Found: 337.0551.

4-(2-((Tetrahydrofuran-2-yl)oxy)ethyl)-1-(4-(trifluoromethyl)phenyl)-1*H*-pyrazole (98a).

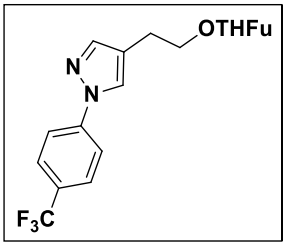

Following GP17 using *N*-(4-(trifluoromethyl)phenyl)sydnone (**395**) (120 mg, 0.50 mmol) and 2,3-dihydrofuran (**92**) (140 mg, 2.0 mmol) with FCC (gradient from 10-30% EtOAc in 40-60 petroleum ether), 4-(2-((tetrahydrofuran-2-yl)oxy)ethyl)-1-(4-(trifluoromethyl)phenyl)-1*H*-pyrazole (**98a**) was isolated as an orange oil (110 mg, 67%).

^{1}H NMR (400 MHz, $CDCl_3$) δ 7.85 (s, 1H), 7.82 – 7.78 (m, 2H), 7.73 – 7.69 (m, 2H), 7.65 (s, 1H), 5.18 (dd, *J* = 4.0, 2.0 Hz, 1H), 3.95 – 3.85 (m, 3H), 3.62 (dt, *J* = 9.5, 6.5 Hz, 1H), 2.83 (t, *J* = 6.5 Hz, 2H), 2.09 – 1.80 (m, 4H); **^{13}C NMR (101 MHz, $CDCl_3$)** δ 142.6, 142.3, 127.8 (q, *J* = 33.0 Hz), 126.7 (q, *J* = 3.5 Hz), 125.3, 122.6, 121.6, 118.3, 103.9, 67.1, 67.0, 32.4, 24.9, 23.5; **^{19}F NMR (377 MHz, $CDCl_3$)** δ -62.2; **FTIR:** ν_{max} 2923, 1617, 1526, 1397, 1324, 1121, 1069, 1035, 950, 843 cm^{-1}; **HRMS** calculated for $C_{16}H_{18}F_3N_2O_2$ (ES^+)($+H^+$): 327.1315. Found: 327.1320.

2-(1-Phenyl-1*H*-pyrazol-4-yl)ethanol (93a).

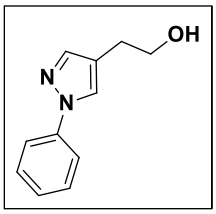

Following GP18 using *N*-Phenylsydnone (**35**) (81 mg, 0.5 mmol), 2,3-dihydrofuran (**92**) (140 mg, 2.0 mmol) and K_2CO_3 (138 mg, 1.0 mmol) with FCC (30% EtOAc in 40-60 petroleum ether), 2-(1-phenyl-1*H*-pyrazol-4-yl)ethanol (**93a**) was isolated as a brown oil (66 mg, 70%).

^{1}H NMR (400 MHz, $CDCl_3$) δ 7.82 (s, 1H), 7.71 – 7.63 (m, 2H), 7.60 (s, 1H), 7.49 – 7.38 (m, 2H), 7.32 – 7.24 (m, 1H), 3.84 (t, *J* = 6.5 Hz, 2H), 2.80 (t, *J* = 6.5 Hz, 2H), 2.02 (br, 1H); **^{13}C NMR (101 MHz, $CDCl_3$)** δ 141.2, 140.1, 129.4, 126.3, 125.7, 119.9, 118.9, 63.0, 27.8; **FTIR:** ν_{max} 3343, 2927, 2871, 1598, 1500, 1397, 1042, 953 cm^{-1}; **HRMS** calculated for $C_{11}H_{13}N_2O$ (ES^+)($+H^+$): 189.1022. Found: 189.1024.

2-(1-(4-Methoxyphenyl)-1*H*-pyrazol-4-yl)ethanol (153a).

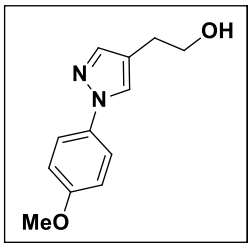

Following GP18 using *N*-(4-methoxyphenyl)sydnone (**46**) (96 mg, 0.5 mmol), 2,3-dihydrofuran (**92**) (140 mg, 2.0 mmol) and K_2CO_3 (138 mg, 1.0 mmol) with FCC (gradient from 20-40% EtOAc in DCM), 2-(1-(4-methoxyphenyl)-1*H*-pyrazol-4-yl)ethanol (**153a**) was isolated as a brown amorphous solid (71 mg, 65%).

^{1}H NMR (400 MHz, $CDCl_3$) δ 7.70 (s, 1H), 7.59 – 7.50 (m, 3H), 7.00 – 6.91 (m, 2H), 3.86 – 3.77 (m, 5H), 2.77 (t, *J* = 6.5 Hz, 2H), 2.26 (br, 1H); **^{13}C NMR (101 MHz, $CDCl_3$)** δ 158.1, 140.6, 134.0, 125.9, 120.6, 119.5, 114.5, 63.0, 55.6, 27.8; **FTIR:** ν_{max} 3349, 2934, 2836, 1514, 1399, 1243, 1043, 956 cm^{-1}; **HRMS** calculated for $C_{12}H_{15}N_2O_2$ (ES^+)($+H^+$): 219.1128. Found: 219.1130.

2-(1-(4-Nitrophenyl)-1*H*-pyrazol-4-yl)ethanol (154a).

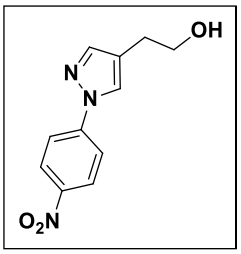

Following GP18 using *N*-(4-nitrophenyl)sydnone (**396**) (103 mg, 0.5 mmol), 2,3-dihydrofuran (**92**) (140 mg, 2.0 mmol) and K_2CO_3 (138 mg, 1.0 mmol) with FCC (gradient from 20-40% EtOAc in DCM), 2-(1-(4-nitrophenyl)-1*H*-pyrazol-4-yl)ethanol (**154a**) was isolated as an orange oil (35 mg, 30%).

^{1}H NMR (400 MHz, $CDCl_3$) δ 8.36 – 8.28 (m, 2H), 7.95 (s, 1H), 7.88 – 7.81 (m, 2H), 7.70 (s, 1H), 3.89 (t, *J* = 6.5 Hz, 2H), 2.83 (t, *J* = 6.5 Hz, 2H), 1.77 (br, 1H); **^{13}C NMR (101 MHz, $CDCl_3$)** δ 145.2, 144.4, 143.2, 125.8, 125.4, 122.0, 118.2, 62.7, 27.6; **FTIR:** ν_{max} 3369, 3122, 2931, 1596, 1506, 1334, 1110, 946 cm^{-1}; **HRMS** calculated for $C_{11}H_{12}N_3O_3$ (ES^+)($+H^+$): 234.0873. Found: 234.0873.

4-(4-(2-Hydroxyethyl)-1*H*-pyrazol-1-yl)benzonitrile (155a).

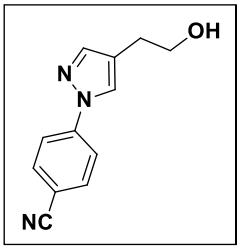

Following GP18 using *N*-(4-cyanophenyl)sydnone (**397**) (93.5 mg, 0.5 mmol), 2,3-dihydrofuran (**92**) (140 mg, 2.0 mmol) and K_2CO_3 (138 mg, 1.0 mmol) with FCC (gradient from 20-40% EtOAc in DCM), 4-(4-(2-hydroxyethyl)-1*H*-pyrazol-1-yl)benzonitrile (**155a**) was isolated as a brown oil (69 mg, 65%).

^{1}H NMR (400 MHz, $CDCl_3$) δ 7.89 (s, 1H), 7.82 – 7.76 (m, 2H), 7.74 – 7.69 (m, 2H), 7.66 (s, 1H), 3.86 (t, *J* = 6.5 Hz, 2H), 2.80 (t, *J* = 6.5 Hz, 2H), 2.02 (br, 1H); **^{13}C NMR (101 MHz, $CDCl_3$)** δ 142.9, 142.8, 133.7, 125.7, 121.7, 118.6, 118.5, 109.2, 62.7, 27.6; **FTIR:** ν_{max} 3401, 2927, 2226, 1606, 1515, 1394, 947 cm^{-1}; **HRMS** calculated for $C_{12}H_{12}N_3O$ (ES^+)($+H^+$): 214.0975. Found: 214.0971.

2-(1-(4-Fluorophenyl)-1*H*-pyrazol-4-yl)ethanol (156a).

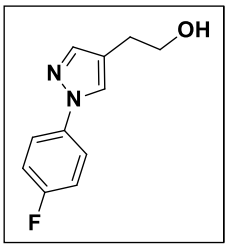

Following GP18 using *N*-(4-fluorophenyl)sydnone (**392**) (90 mg, 0.5 mmol), 2,3-dihydrofuran (**92**) (140 mg, 2.0 mmol) and K_2CO_3 (138 mg, 1.0 mmol) with FCC (gradient from 20-40% EtOAc in DCM), 2-(1-(4-fluorophenyl)-1*H*-pyrazol-4-yl)ethanol (**156a**) was isolated as an orange oil (60 mg, 58%).

^{1}H NMR (400 MHz, $CDCl_3$) δ 7.77 (s, 1H), 7.63 (m, 3H), 7.19 – 7.10 (m, 2H), 3.86 (t, *J* = 6.5 Hz, 2H), 2.82 (t, *J* = 6.5 Hz, 2H), 1.67 (br, 1H); **^{13}C NMR (101 MHz, $CDCl_3$)** δ 161.0 (d, *J* = 245.5 Hz), 141.2, 136.5, 125.9, 120.6 (d, *J* = 8.5 Hz), 120.1, 116.2 (d, *J* = 23.0 Hz), 62.9, 27.7; **^{19}F NMR (377 MHz, $CDCl_3$)** δ -116.2 – 116.3 (m); **FTIR:** ν_{max} 3323, 2929, 2869, 1512, 1398, 1226, 1035, 954 cm^{-1}; **HRMS** calculated for $C_{11}H_{12}FN_2O$ (ES^+)($+H^+$): 207.0928. Found: 207.0931.

2-(1-(4-Chlorophenyl)-1*H*-pyrazol-4-yl)ethanol (157a).

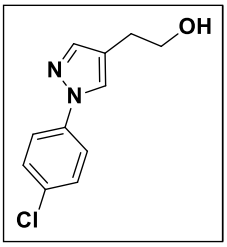

Following GP18 using *N*-(4-chlorophenyl)sydnone (**393**) (99 mg, 0.5 mmol), 2,3-dihydrofuran (**92**) (140 mg, 2.0 mmol) and K_2CO_3 (138 mg, 1.0 mmol) with FCC (gradient from 20-40% EtOAc in DCM), 2-(1-(4-chlorophenyl)-1*H*-pyrazol-4-yl)ethanol (**157a**) was isolated as a brown oil (39 mg, 35%).

^{1}H NMR (400 MHz, $CDCl_3$) δ 7.80 (s, 1H), 7.66 – 7.57 (m, 3H), 7.45 – 7.36 (m, 2H), 3.85 (t, *J* = 6.5 Hz, 2H), 2.81 (t, *J* = 6.5 Hz, 2H), 1.80 (br, 1H); **^{13}C NMR (101 MHz, $CDCl_3$)** δ 141.5, 138.7, 131.7, 129.5, 125.6, 120.3, 120.0, 62.9, 27.7; **FTIR:** ν_{max} 3350, 2927, 2875, 1499, 1397, 1093, 952 cm^{-1}; **HRMS** calculated for $C_{11}H_{12}ClN_2O$ (^{35}Cl)(ES^+)($+H^+$): 223.0633. Found: 223.0635.

1-Phenyl-2-(1-phenyl-1*H*-pyrazol-4-yl)ethanol (177a).

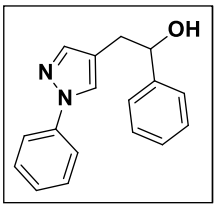

Following GP19 using *N*-phenylsydnone (**35**) (50 mg, 0.31 mmol), 2-phenyl-2,3-dihydrofuran (**169**) (90 mg, 0.62 mmol) and K_2CO_3 (43 mg, 0.31 mmol) with FCC (50% EtOAc in 40-60 petroleum ether), 1-phenyl-2-(1-phenyl-1*H*-pyrazol-4-yl)ethanol (**177a**) was isolated as a brown solid (39 mg, 48%).

^{1}H NMR (400 MHz, $CDCl_3$) δ 7.68 (s, 1H), 7.65 – 7.59 (m, 2H), 7.49 (s, 1H), 7.45 – 7.39 (m, 2H), 7.38 – 7.23 (m, 6H), 4.89 – 4.81 (m, 1H), 3.00 – 2.92 (m, 2H), 2.36 (br, 1H); **^{13}C NMR (101 MHz, $CDCl_3$)** δ 143.8, 141.6, 140.1, 129.4, 128.5, 127.8, 126.2, 126.2, 126.0, 119.2, 118.9, 74.6, 34.4; **FTIR:** ν_{max} 3352, 2918, 1598, 1502, 1398, 1042, 953 cm^{-1}; **HRMS** calculated for $C_{17}H_{17}N_2O$ (ES^+)($+H^+$): 265.1335. Found: 265.1345.

1-(4-Methoxyphenyl)-2-(1-phenyl-1*H*-pyrazol-4-yl)ethanol (178a).

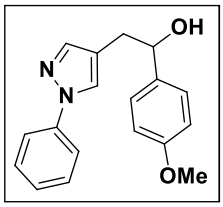

Following GP19 using *N*-phenylsydnone (**35**) (50 mg, 0.31 mmol), 2-(4-methoxyphenyl)-2,3-dihydrofuran (**170**) (109 mg, 0.62 mmol) and K_2CO_3 (43 mg, 0.31 mmol) with FCC (gradient from 0-20% EtOAc in DCM), 1-(4-methoxyphenyl)-2-(1-phenyl-1*H*-pyrazol-4-yl)ethanol (**178a**) was isolated as a brown oil (42 mg, 46%).

^{1}H NMR (400 MHz, $CDCl_3$) δ 7.67 (s, 1H), 7.63 – 7.59 (m, 2H), 7.46 (s, 1H), 7.41 (t, *J* = 8.0 Hz, 2H), 7.30 – 7.22 (m, 3H), 6.91 – 6.86 (m, 2H), 4.82 – 4.76 (m, 1H), 3.80 (s, 3H), 2.96 (dd, *J* = 14.5, 7.5 Hz, 1H), 2.91 (dd, *J* = 14.5, 5.5 Hz, 1H), 2.35 (br, 1H); **^{13}C NMR (101 MHz, $CDCl_3$)** δ 159.3, 141.7, 140.2, 136.1, 129.5, 127.3, 126.3, 126.2, 119.4, 118.9, 113.9, 74.3, 55.4, 34.4; **FTIR:** ν_{max} 3364, 2932, 1599, 1503, 1397, 1244, 1033, 953 cm^{-1}; **HRMS** calculated for $C_{18}H_{19}N_2O_2$ (ES^+)($+H^+$): 295.1441. Found: 295.1452.

2-(1-Phenyl-1*H*-pyrazol-4-yl)-1-(thiophen-2-yl)ethanol (179a).

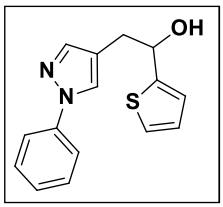

Following GP19 using *N*-phenylsydnone (**35**) (50 mg, 0.31 mmol), 2-(thiophen-2-yl)-2,3-dihydrofuran (**171**) (94 mg, 0.62 mmol) and K_2CO_3 (43 mg, 0.31 mmol) with FCC (gradient from 0-20% EtOAc in DCM), 2-(1-phenyl-1*H*-pyrazol-4-yl)-1-(thiophen-2-yl)ethanol (**179a**) was isolated as a brown oil (37 mg, 44%).

^{1}H NMR (400 MHz, $CDCl_3$) δ 7.73 (s, 1H), 7.65 – 7.60 (m, 2H), 7.52 (s, 1H), 7.42 (t, *J* = 8.0 Hz, 2H), 7.29 – 7.24 (m, 2H), 7.00 – 6.95 (m, 2H), 5.14 – 5.08 (m, 1H), 3.10 – 3.05 (m, 2H), 2.44 (br, 1H); **^{13}C NMR (101 MHz, $CDCl_3$)** δ 147.8, 141.7, 140.2, 129.9, 129.5, 126.8, 126.4, 124.9, 124.2, 119.0, 118.8, 70.7, 34.7; **FTIR:** ν_{max} 3322, 2919, 1598, 1501, 1398, 1041, 953 cm^{-1}; **HRMS** calculated for $C_{15}H_{15}N_2OS$ (ES^+)($+H^+$): 271.0900. Found: 271.0907.

Ethyl 2-hydroxy-3-(1-phenyl-1*H*-pyrazol-4-yl)propanoate (180a).

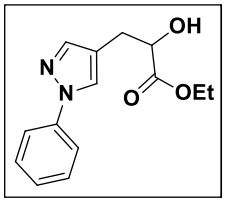

Following GP19 using *N*-phenylsydnone (**35**) (50 mg, 0.31 mmol), ethyl 2,3-dihydrofuran-2-carboxylate (**172**) (88 mg, 0.62 mmol) and K_2CO_3 (43 mg, 0.31 mmol) with FCC (gradient from 0-20% EtOAc in DCM), ethyl 2-hydroxy-3-(1-phenyl-1*H*-pyrazol-4-yl)propanoate (**180a**) was isolated as a brown oil (39 mg, 49%).

^{1}H NMR (400 MHz, $CDCl_3$) δ 7.84 (s, 1H), 7.68 – 7.62 (m, 2H), 7.56 (s, 1H), 7.46 – 7.40 (m, 3H), 7.29 – 7.24 (m, 2H), 4.40 (dd, *J* = 5.5, 4.5 Hz, 1H), 4.29 – 4.20 (m, 2H), 3.06 (dd, *J* = 15.0, 4.5 Hz, 1H), 2.96 (dd, *J* = 15.0, 5.5 Hz, 2H), 1.30 (t, *J* = 7.0 Hz, 3H); **^{13}C NMR (101 MHz, $CDCl_3$)** δ 174.2, 141.6, 140.2, 129.5, 126.4, 126.4, 119.0, 117.5, 70.6, 62.1, 29.4, 14.4; **FTIR:** ν_{max} 3320, 2927, 1732, 1599, 1501, 1398, 1208, 1095 cm^{-1}; **HRMS** calculated for $C_{14}H_{17}N_2O_3$ (ES^+)($+H^+$): 261.1234. Found: 261.1234.

1-(4-Fluorophenyl)-2-(1-phenyl-1*H*-pyrazol-4-yl)ethanol (181a).

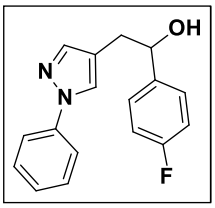

Following GP19 using *N*-phenylsydnone (**35**) (50 mg, 0.31 mmol), 2-(4-fluorophenyl)-2,3-dihydrofuran (**175**) (100 mg, 0.62 mmol) and K_2CO_3 (43 mg, 0.31 mmol) with FCC (30% EtOAc in 40-60 petroleum ether), 1-(4-fluorophenyl)-2-(1-phenyl-1*H*-pyrazol-4-yl)ethanol (**181a**) was isolated as orange crystals (46 mg, 53%).

M.P. 139-142 °C; **^{1}H NMR (400 MHz, $CDCl_3$)** δ 7.72 (s, 1H), 7.67-7.62 (m, 2H), 7.51 (s, 1H), 7.48-7.42 (m, 2H), 7.39 – 7.26 (m, 3H), 7.11 – 7.02 (m, 2H), 4.88 – 4.82 (m, 1H), 2.96 – 2.92 (m, 2H), 2.26 (br, 1H); **^{13}C NMR (101 MHz, $CDCl_3$)** δ 162.3 (d, *J* = 245.5 Hz), 141.6, 140.1, 139.5, 139.4, 129.4, 127.6 (d, *J* = 8.0 Hz), 126.3, 126.1, 118.9, 115.3 (d, *J* = 21.5 Hz), 74.0, 34.5; **^{19}F{^{1}H} NMR (377 MHz, $CDCl_3$)** δ -114.7; **FTIR:** ν_{max} 3276, 2912, 1599, 1500, 1399, 1220, 833 cm^{-1}; **HRMS** calculated for $C_{17}H_{16}FN_2O$ (ES^+)($+H^+$): 283.1241. Found: 283.1243.

2-(1-Phenyl-1*H*-pyrazol-4-yl)-1-(*p*-tolyl)ethanol (182a).

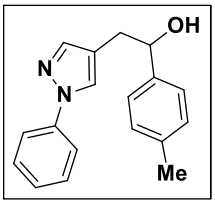

Following GP19 using *N*-phenylsydnone (**35**) (50 mg, 0.31 mmol), 2-(*p*-tolyl)-2,3-dihydrofuran (**174**) (99 mg, 0.62 mmol) and K_2CO_3 (43 mg, 0.31 mmol) with FCC (30% EtOAc in 40-60 petroleum ether), 2-(1-phenyl-1*H*-pyrazol-4-yl)-1-(*p*-tolyl)ethanol (**182a**) was isolated as an orange solid (52 mg, 61%).

^{1}H NMR (400 MHz, $CDCl_3$) δ 7.73 (s, 1H), 7.68 – 7.63 (m, 2H), 7.52 (s, 1H), 7.49 – 7.41 (m, 2H), 7.32 – 7.25 (m, 3H), 7.20 (d, *J* = 8.0 Hz, 2H), 4.89 – 4.83 (m, 1H), 3.01 (dd, *J* = 15.0, 7.5 Hz, 1H), 2.97 (dd, *J* = 15.0, 5.5 Hz, 1H), 2.38 (s, 3H), 2.10 (br, 1H); **^{13}C NMR (101 MHz, $CDCl_3$)** δ 141.6, 140.8, 140.2, 137.5, 129.4, 129.2, 126.2, 126.1, 125.9, 119.3, 118.9, 74.5, 34.4, 21.2; **FTIR:** ν_{max} 3308, 2917, 1599, 1502, 1398, 1043 cm^{-1}; **HRMS** calculated for $C_{18}H_{19}N_2O$ (ES^+)($+H^+$): 279.1492. Found: 279.1499.

1-(4-Nitrophenyl)-2-(1-phenyl-1*H*-pyrazol-4-yl)ethanol (183a).

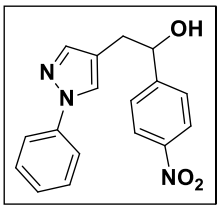

Following GP19 using *N*-phenylsydnone (**35**) (50 mg, 0.31 mmol), 2-(4-nitrophenyl)-2,3-dihydrofuran (**176**) (118 mg, 0.62 mmol) and K_2CO_3 (43 mg, 0.31 mmol) with FCC (40% EtOAc in 40-60 petroleum ether), 1-(4-nitrophenyl)-2-(1-phenyl-1*H*-pyrazol-4-yl)ethanol (**183a**) was isolated containing minor impurities (34 mg).

^{1}H NMR (400 MHz, $CDCl_3$) δ 8.25 – 8.20 (m, 2H), 7.76 (s, 1H), 7.67 – 7.61 (m, 2H), 7.58 – 7.51 (m, 3H), 7.49 – 7.42 (m, 2H), 7.34 – 7.26 (m, 1H), 5.00 (dd, *J* = 8.0, 5.0 Hz, 1H), 3.02 (dd, *J* = 14.5, 5.0 Hz, 1H), 2.95 (dd, *J* = 14.5, 8.0 Hz, 1H), 2.58 (br, 1H); **^{13}C NMR (101 MHz, $CDCl_3$)** δ 151.0, 147.4, 141.4, 139.9, 129.5, 126.7, 126.5, 126.3, 123.7, 118.9, 118.1, 73.5, 34.5; **HRMS** calculated for $C_{17}H_{16}N_3O_3$ (ES^+)($+H^+$): 310.1186. Found: 310.1193.

1-Phenyl-2-(1-phenyl-1*H*-pyrazol-3-yl)ethanol (177b).

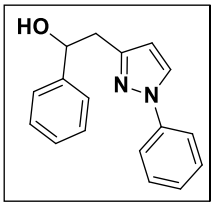

Following GP20 using *N*-phenylsydnone (**35**) (50 mg, 0.31 mmol) and 1-phenylbut-3-yn-1-ol (**163**) (150 mg, 0.92 mmol) with FCC (gradient from 0-10% EtOAc in DCM), 1-phenyl-2-(1-phenyl-1*H*-pyrazol-3-yl)ethanol (**177b**) was isolated as an orange oil (38 mg, 42%).

^{1}H NMR (400 MHz, $CDCl_3$) δ 7.86 (d, *J* = 2.5 Hz, 1H), 7.73 – 7.62 (m, 2H), 7.49 – 7.42 (m, 4H), 7.37 (t, *J* = 7.5 Hz, 2H), 7.29 (t, *J* = 7.5 Hz, 2H), 6.26 (d, *J* = 2.5 Hz, 1H), 5.15 – 5.04 (m, 1H), 3.86 (d, *J* = 2.5 Hz, 1H), 3.14 (dd, *J* = 15.0, 4.0 Hz, 1H), 3.09 (dd, *J* = 15.0, 8.0 Hz, 1H); **^{13}C NMR (101 MHz, $CDCl_3$)** δ 152.1, 143.9, 140.0, 129.5, 128.5, 127.6, 127.5, 126.4, 126.0, 119.0, 107.7, 73.3, 38.4; **FTIR:** ν_{max} 3172, 3055, 2904, 1757, 1597, 1495, 1390, 1213, 1045 cm^{-1}; **HRMS** calculated for $C_{17}H_{17}N_2O$ (ES^+)($+H^+$): 265.1335. Found: 265.1329.

1-(4-Methoxyphenyl)-2-(1-phenyl-1*H*-pyrazol-3-yl)ethanol (178b).

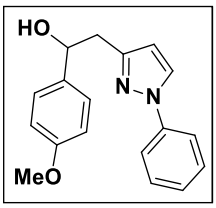

Following GP20 using *N*-phenylsydnone (**35**) (50 mg, 0.31 mmol) and 1-(4-methoxyphenyl)but-3-yn-1-ol (**166**) (160 mg, 0.92 mmol) with FCC (gradient from 0-10% EtOAc in DCM), 1-(4-methoxyphenyl)-2-(1-phenyl-1*H*-pyrazol-3-yl)ethanol (**178b**) was isolated as an orange oil (19 mg, 20%).

^{1}H NMR (400 MHz, $CDCl_3$) δ 7.85 (d, *J* = 2.5 Hz, 1H), 7.70 – 7.65 (m, 2H), 7.48 – 7.42 (m, 2H), 7.40 – 7.36 (m, 2H), 7.31 – 7.27 (m, 1H), 6.93 – 6.88 (m, 2H), 6.25 (d, *J* = 2.5 Hz, 1H), 5.07 – 5.02 (m, 1H), 3.81 (s, 3H), 3.12 – 3.06 (m, 2H), 1.65 (br, 1H); **^{13}C NMR (101 MHz, $CDCl_3$)** δ 159.1, 152.2, 140.1, 136.1, 129.6, 127.6, 127.2, 126.5, 119.1, 113.9, 107.8, 73.0, 55.4, 38.4; **FTIR:** ν_{max} 3386, 2928, 1683, 1598, 1510, 1389, 1244, 1173, 1031 cm^{-1}; **HRMS** calculated for $C_{18}H_{18}N_2O_2Na$ (ES^+)($+Na^+$): 317.1260. Found: 317.1265.

2-(1-Phenyl-1*H*-pyrazol-3-yl)-1-(thiophen-2-yl)ethanol (179b).

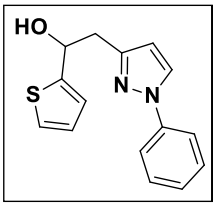

Following GP20 using *N*-phenylsydnone (**35**) (50 mg, 0.31 mmol) and 1-(thiophen-2-yl)but-3-yn-1-ol (**167**) (140 mg, 0.92 mmol) with FCC (gradient from 0-10% EtOAc in DCM), 2-(1-phenyl-1*H*-pyrazol-3-yl)-1-(thiophen-2-yl)ethanol (**179b**) was isolated as a brown oil (30 mg, 36%).

^{1}H NMR (400 MHz, $CDCl_3$) δ 7.85 (d, *J* = 2.5 Hz, 1H), 7.66 (d, *J* = 8.0 Hz, 1H), 7.45 (t, *J* = 8.0 Hz, 1H), 7.31 – 7.22 (m, 1H), 7.02 (d, *J* = 3.5 Hz, 1H), 6.98 (dd, *J* = 5.0, 3.5 Hz, 1H), 6.29 (d, *J* = 2.5 Hz, 1H), 5.37 (dd, *J* = 8.0, 4.5 Hz, 1H), 4.13 (br, 1H), 3.26 (dd, *J* = 15.0, 4.5 Hz, 1H), 3.21 (dd, *J* = 15.0, 8.0 Hz, 1H); **^{13}C NMR (101 MHz, $CDCl_3$)** δ 151.6, 147.8, 140.0, 129.6, 127.6, 126.7, 126.5, 124.5, 123.6, 119.0, 107.8, 69.6, 38.3; **FTIR:** ν_{max} 3139, 2923, 1666, 1597, 1498, 1387, 1151, 1045 cm^{-1}; **HRMS** calculated for $C_{15}H_{15}N_2OS$ (ES^+)($+H^+$): 271.0900. Found: 271.0901.

Ethyl 2-hydroxy-3-(1-phenyl-1*H*-pyrazol-3-yl)propanoate (180b).

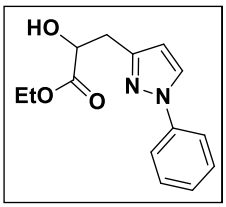

Following GP20 using *N*-phenylsydnone (**35**) (50 mg, 0.31 mmol) and ethyl 2-hydroxypent-4-ynoate (**168**) (190 mg, 0.92 mmol) with FCC (gradient from 0-10% EtOAc in DCM), ethyl 2-hydroxy-3-(1-phenyl-1*H*-pyrazol-3-yl)propanoate (**180b**) was isolated as an orange oil (29 mg, 36%).

^{1}H NMR (400 MHz, $CDCl_3$) δ 7.84 (d, *J* = 2.5 Hz, 1H), 7.63 (d, *J* = 8.0 Hz, 2H), 7.42 (t, *J* = 8.0 Hz, 2H), 7.26 (t, *J* = 7.5 Hz, 1H), 6.33 (d, *J* = 2.5 Hz, 1H), 4.58 – 4.51 (m, 1H), 4.23 (q, *J* = 7.0 Hz, 2H), 3.58 (d, *J* = 6.5 Hz, 1H), 3.26 (dd, *J* = 15.0, 4.0 Hz, 1H), 3.14 (dd, *J* = 15.0, 6.5 Hz, 1H), 1.27 (t, *J* = 7.0 Hz, 4H); **^{13}C NMR (101 MHz, $CDCl_3$)** δ 174.0, 150.1, 140.1, 129.5, 127.6, 126.4, 119.0, 107.8, 70.3, 61.7, 33.2, 14.3; **FTIR:** ν_{max} 3452, 2981, 1731, 1599, 1500, 1389, 1193, 1096 cm^{-1}; **HRMS** calculated for $C_{14}H_{17}N_2O_3$ (ES^+)($+H^+$): 261.1234. Found: 261.1244.

5.4.2 Control Reactions

Competition reactions between 2,3-dihydrofuran (92) and 3,4-dihydro-2*H*-pyran (86).

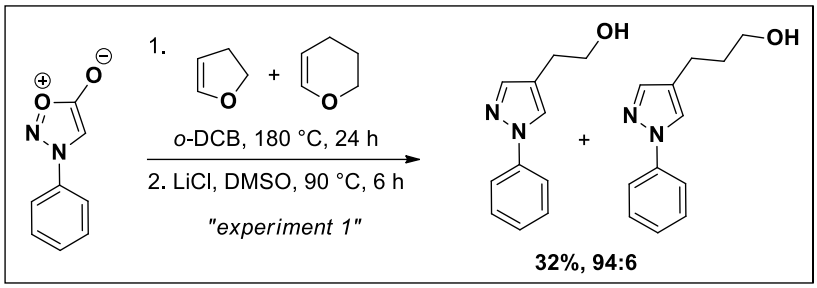

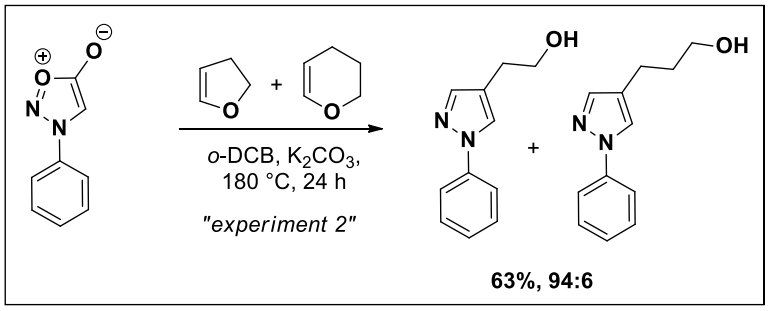

Competition experiment 1: To a solution of *N*-phenylsydnone (**35**) (100 mg, 0.62 mmol) in *o*-DCB (0.62 mL) was added 2,3-dihydrofuran (**92**) (170 mg, 2.5 mmol) and 3,4-dihydro-2*H*-pyran (**86**) (210 mg, 2.5 mmol) and the resulting mixture heated at 180 °C for 24 hours. After cooling to room temperature the reaction was filtered through a silica plug (eluting with 10% MeOH in DCM) and the solvent removed

under vacuum. The crude oil was then dissolved in a mixture of DMSO (10 mL) and H_2O (0.11 mL, 6.2 mmol) containing LiCl (130 mg, 3.1 mmol) and the resulting mixture heated at 90 °C for 6 hours. After cooling to room temperature the reaction mixture was diluted with H_2O (10 mL) and extracted with Et_2O (3 x 25 mL). The combined organic layers were then dried over anhydrous $MgSO_4$, filtered and concentrated under vacuum. Purification by FCC (20-40% EtOAc in DCM) afforded an inseparable mixture of 2-(1-phenyl-1*H*-pyrazol-4-yl)ethanol (**93a**) + 3-(1-phenyl-1*H*-pyrazol-4-yl)propan-1-ol (**87a**) as a yellow oil (38 mg, 32%, 94:6).

Competition experiment 2: To a solution of *N*-phenylsydnone (**35**) (100 mg, 0.62 mmol) and K_2CO_3 (170 mg, 1.24 mmol) in *o*-DCB (3.64 mL) was added 2,3-dihydrofuran (**92**) (170 mg, 2.5 mmol) and 3,4-dihydro-2*H*-pyran (**86**) (210 mg, 2.5 mmol) and the resulting mixture heated at 180 °C for 48 hours. After cooling to room temperature the reaction mixture was purified by FCC (30-50% EtOAc in 40-60 petroleum ether) to afford a mixture of 2-(1-phenyl-1*H*-pyrazol-4-yl)ethanol (**93a**) + 3-(1-phenyl-1*H*-pyrazol-4-yl)propan-1-ol (**87a**) as a yellow oil (73 mg, 63%, 94:6).

^{1}H NMR (400 MHz, $CDCl_3$) δ 7.79 (d, *J* = 0.5 Hz, 1H, major), 7.72 (d, *J* = 0.5 Hz, 1H, minor), 7.67 – 7.62 (m, 4H), 7.58 (s, 1H, major), 7.54 (s, 1H, minor), 7.46 – 7.40 (m, 4H), 7.29 – 7.23 (m, 2H), 3.82 (t, *J* = 6.5 Hz, 2H, major), 3.69 (t, *J* = 6.5 Hz, 2H, minor), 2.78 (t, *J* = 6.5 Hz, 2H, major), 2.62 (t, *J* = 7.5 Hz, 2H, minor), 2.01 (br, 2H), 1.91 – 1.83 (m, 2H, minor).

This reaction was analysed by ^{1}H NMR only.

Competition reaction between 2,3-dihydrofuran (92) and ethyl vinyl ether (111a).

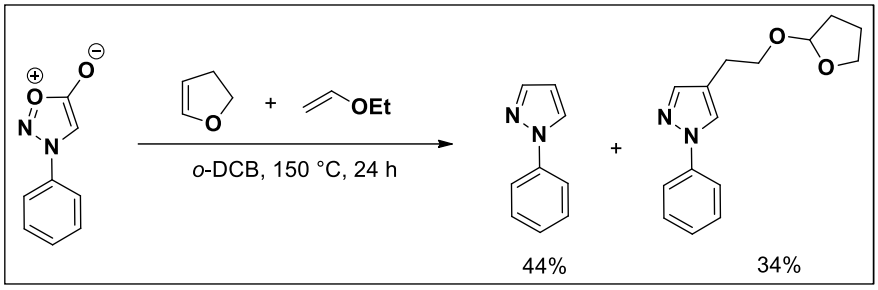

To a solution of *N*-phenylsydnone (**35**) (81 mg, 0.50 mmol) in *o*-DCB (0.50 mL) was added 2,3-dihydrofuran (**92**) (140 mg, 2.0 mmol) and ethyl vinyl ether (**111a**) (140 mg, 2.0 mmol) and the resulting mixture heated at 150 °C for 24 hours. After cooling to room temperature the reaction mixture was purified by FCC (gradient from 0-30% EtOAc in DCM) to afford 1-phenyl-1*H*-pyrazole (**112**) as a yellow oil (31 mg, 44%) and 1-phenyl-4-(2-((tetrahydrofuran-2-yl)oxy)ethyl)-1*H*-pyrazole (**94a**) as a yellow oil (44 mg, 34%).

1-phenyl-1*H*-pyrazole (112).

^{1}H NMR (400 MHz, $CDCl_3$) δ 7.92 (d, *J* = 2.4 Hz, 1H), 7.76 – 7.66 (m, 3H), 7.49 – 7.41 (m, 2H), 7.32 – 7.25 (m, 1H), 6.48 – 6.44 (m, 1H); **^{13}C NMR (101 MHz, $CDCl_3$)** δ 141.1, 140.2, 129.5, 126.8, 126.5, 119.2, 107.7.

1-phenyl-4-(2-((tetrahydrofuran-2-yl)oxy)ethyl)-1*H*-pyrazole (94a).

^{1}H NMR (400 MHz, $CDCl_3$) δ 7.79 (s, 1H), 7.72 – 7.64 (m, 2H), 7.61 (s, 1H), 7.48 – 7.40 (m, 2H), 7.31 – 7.24 (m, 1H), 5.18 (dd, *J* = 4.0, 2.0 Hz, 1H), 3.95 – 3.84 (m, 3H), 3.61 (dt, *J* = 9.5, 7.0 Hz, 1H), 2.82 (t, *J* = 7.0 Hz, 2H), 2.11 – 1.80 (m, 4H); **^{13}C NMR (101 MHz, $CDCl_3$)** δ 141.3, 140.3, 129.4, 126.1, 125.3, 120.6, 118.8, 103.9, 67.3, 67.0, 32.4, 25.0, 23.5.

For full characterisation see the individual compounds entries.

Reaction of *N*-phenylsydnone (35) with but-3-yn-1-ol (158).

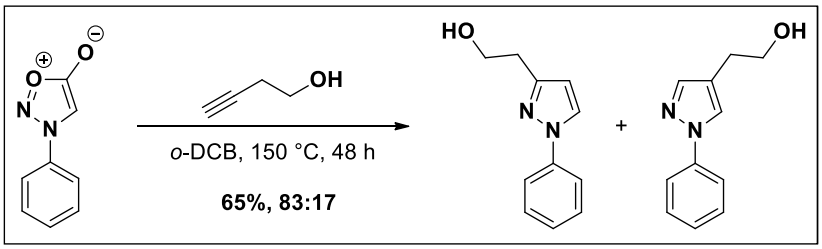

To a solution of *N*-phenylsydnone (**35**) (81 mg, 0.50 mmol) in *o*-DCB (2.0 mL) was added but-3-yn-1-ol (**158**) (140 mg, 2.0 mmol) and the resulting mixture heated at 150 °C for 48 h. After cooling to room temperature the reaction was purified by FCC (gradient from 0-50% EtOAc in 40-60 petroleum ether) to afford an inseparable mixture of 2-(1-phenyl-1*H*-pyrazol-4-yl)ethanol (**93a**) and 2-(1-phenyl-1*H*-pyrazol-3-yl)ethanol (**93b**) as a yellow oil (61 mg, 65%, 17:83).

^{1}H NMR (400 MHz, $CDCl_3$) δ 7.82 (d, *J* = 2.5 Hz, 1H, major), 7.78 (s, 1H, minor), 7.67 – 7.59 (m, 4H), 7.57 (s, 1H, minor), 7.41 (t, *J* = 8.0 Hz, 4H), 7.24 (t, *J* = 7.5 Hz, 2H), 6.29 (d, *J* = 2.5 Hz, 1H, major), 3.95 (t, *J* = 6.0 Hz, 2H, major), 3.79 (t, *J* = 6.5 Hz, 2H, minor), 2.95 (t, *J* = 6.0 Hz, 2H, major), 2.75 (t, *J* = 6.5 Hz, 2H, minor); **^{13}C NMR (101 MHz, $CDCl_3$)** δ 152.6 (minor), 141.2 (major), 140.0, 132.5 (minor), 130.3 (minor), 129.4 (major), 127.5 (major), 126.3 (major), 125.7 (minor), 121.3 (minor), 118.9 (major), 107.2 (major), 62.9 (minor), 61.8 (major), 31.3 (major), 27.8 (minor).

For full characterisation see the individual compounds entries.

Reaction of *N*-phenylsydnone (35) with 1-hexyne

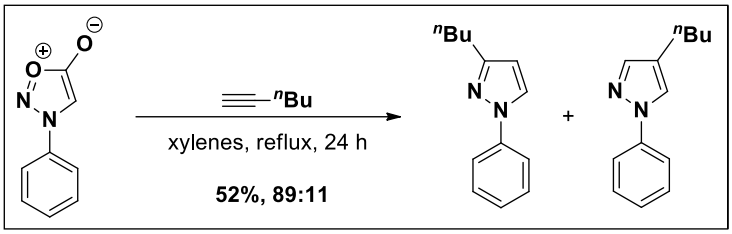

To a solution of *N*-phenylsydnone (**35**) (81 mg, 0.50 mmol) in xylenes (1.0 mL) was added 1-hexyne (120 mg, 1.5 mmol) and the resulting mixture heated at reflux for 20 h. After cooling to room temperature the reaction was purified by FCC (gradient from 0-5% Et2O in 40-60 petroleum ether) to afford an inseparable mixture of 4-butyl-1-phenyl-1*H*-pyrazole (**287a**) and 3-butyl-1-phenyl-1*H*-pyrazole (**287b**) as a yellow oil (52 mg, 52%, 11:89).

^{1}H NMR (400 MHz, $CDCl_3$) δ 7.81 (d, *J* = 2.5 Hz, 1H, major), 7.71 (s, 1H, minor), 7.68 – 7.64 (m, 4H), 7.55 (s, 1H, minor), 7.46 – 7.39 (m, 4H), 7.28 – 7.21 (m, 2H), 6.26 (d, *J* = 2.5 Hz, 1H, major), 2.73 (t, *J* = 8.0 Hz, 2H, major), 2.54 (t, *J* = 7.5 Hz, 2H, minor), 1.75 – 1.65 (m, 2H, major), 1.65 – 1.56 (m, 2H, minor), 1.49 – 1.36 (m, 4H), 0.99 – 0.92 (m, 6H); **^{13}C NMR (101 MHz, $CDCl_3$)** δ 155.5 (minor), 141.1 (major), 140.4, 129.5 (major), 129.1 (minor), 128.1 (minor), 127.3 (major), 126.1 (minor), 126.0 (major), 124.8 (minor), 119.0 (major), 118.8 (minor), 106.6 (major), 33.1 (minor), 32.0 (major), 28.3 (major), 24.0 (minor), 22.7 (major), 22.5 (minor), 14.07.

For full characterisation see the individual compounds entries.

5.5 PSEC Mechanistic Experiments

5.5.1 Radical Trapping Experiments

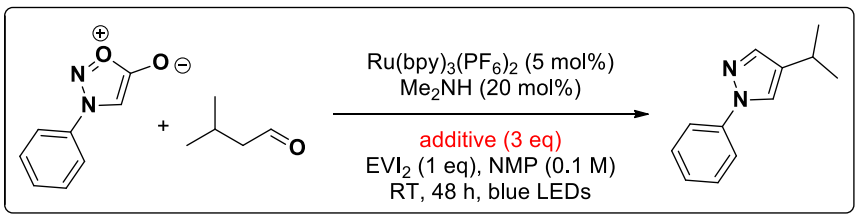

A flame-dried screw cap vial was charged with *N*-phenylsydnone (**35**) (81 mg, 0.5 mmol), $Ru(bpy)_3(PF_6)_2$ (21 mg, 25 µM) and EVI_2 (230 mg, 0.5 mmol) under N_2. Anhydrous, degassed NMP (5 mL) was then added via syringe followed by isovaleraldehyde (130 mg, 1.5 mmol), dimethylamine (0.05 mL, 2.0 M in THF) and radical trapping agent (1.5 mmol). The vial was then subjected to three vacuum/nitrogen cycles, sealed and irradiated using a kessil A160WE tuna blue aquarium light for 48 hours. The reaction was then diluted with H_2O (40 mL) and extracted with Et_2O or EtOAc (4 x 25 mL).

The combined organic layers were then washed with brine (25 mL), dried over anhydrous $MgSO_4$, filtered and concentrated under vacuum. Purification by FCC (gradient from 5-15% Et_2O in 40-60 petroleum ether) afforded 4-isopropyl-1-phenyl-1*H*-pyrazole (**291a**) as a yellow oil.

Additive	**Yield [%]**
None	81
TEMPO	78
1,1-diphenylethylene	76

5.5.2 Radical Clock Experiments

4-Cyclopropyl-1-phenyl-1*H*-pyrazole (331a).[75]

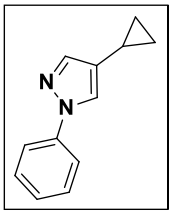

Following GP13 using *N*-phenylsydnone (**35**) (29 mg, 0.18 mmol) and 2-cyclopropylacetaldehyde (**330**) (46 mg, 0.55 mmol) with FCC (5% Et_2O in 40-60 petroleum ether), 4-cyclopropyl-1-phenyl-1*H*-pyrazole (**331a**) was isolated as a yellow oil (18 mg, 55%).

^{1}H NMR (400 MHz, $CDCl_3$) δ 7.67 (s, 1H), 7.66 – 7.61 (m, 2H), 7.50 (s, 1H), 7.46 – 7.39 (m, 2H), 7.27 – 7.22 (m, 1H), 1.76 (tt, *J* = 8.5, 5.0 Hz, 1H), 0.90 (ddd, *J* = 8.5, 6.0, 4.5 Hz, 2H), 0.61 – 0.56 (m, 2H); **^{13}C NMR (101 MHz, $CDCl_3$)** δ 140.6, 140.1, 129.7, 127.0, 126.4, 124.3, 119.1, 8.2, 5.8.

4-(Pent-4-en-1-yl)-1-phenyl-1*H*-pyrazole (328a).

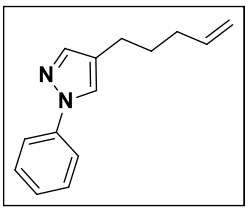

Following GP13 using *N*-phenylsydnone (**35**) (81 mg, 0.50 mmol) and hept-6-enal (**327**) (50% w/w in EtOAc, 300 mg, 1.5 mmol) with FCC (gradient from 0-10% Et_2O in 40-60 petroleum ether), 4-(pent-4-en-1-yl)-1-phenyl-1*H*-pyrazole (**328a**) was isolated as a yellow oil (82 mg, 78%).

^{1}H NMR (400 MHz, $CDCl_3$) δ 7.71 (s, 1H), 7.69 – 7.64 (m, 2H), 7.55 (s, 1H), 7.46 – 7.40 (m, 2H), 7.28 – 7.22 (m, 1H), 5.84 (ddt, *J* = 17.0, 10.0, 6.5 Hz, 1H), 5.08 – 4.97 (m, 2H), 2.58 – 2.52 (m, 2H), 2.18 – 2.10

(m, 2H), 1.76 – 1.68 (m, 2H); **^{13}C NMR (101 MHz, $CDCl_3$)** δ 141.2, 140.5, 138.7, 129.6, 126.3, 125.0, 123.9, 119.0, 115.2, 33.5, 30.2, 23.8; **FTIR ν_{max}** 3074, 2928, 2858, 1599, 1503, 1395, 953, 908 cm^{-1}; **HRMS** calculated for $C_{14}H_{17}N_2$ (ES^+)($+H^+$): 213.1386. Found: 213.1386.

5.5.3 Stern-Volmer Analysis

Stern-volmer experiments were conducted on a Fluoromax 3 spectrofluorometer. Stock solutions of $Ru(bpy)_3(PF_6)_2$ (100 µM) and quenchers (50 mM) were prepared in HPLC grade DMF. The solutions were mixed and purged with argon for 5 minutes, then sealed and placed inside the spectrofluorometer in the dark for 2 minutes prior to data acquisition. The samples were then excited at 465 nm and emission data recorded at 610 nm. I_0/I values were calculated from the average of three scans per data point.

Solution	volume of $Ru(bpy)_3(PF_6)_2$ stock/ µL	Volume of quencher stock/ µL	volume of DMF/ µL	total volume/ µL	[quencher]/ mM
1	40	0	360	400	0
2	40	40	320	400	5
3	40	80	280	400	10
4	40	120	240	400	15
5	40	160	200	400	20

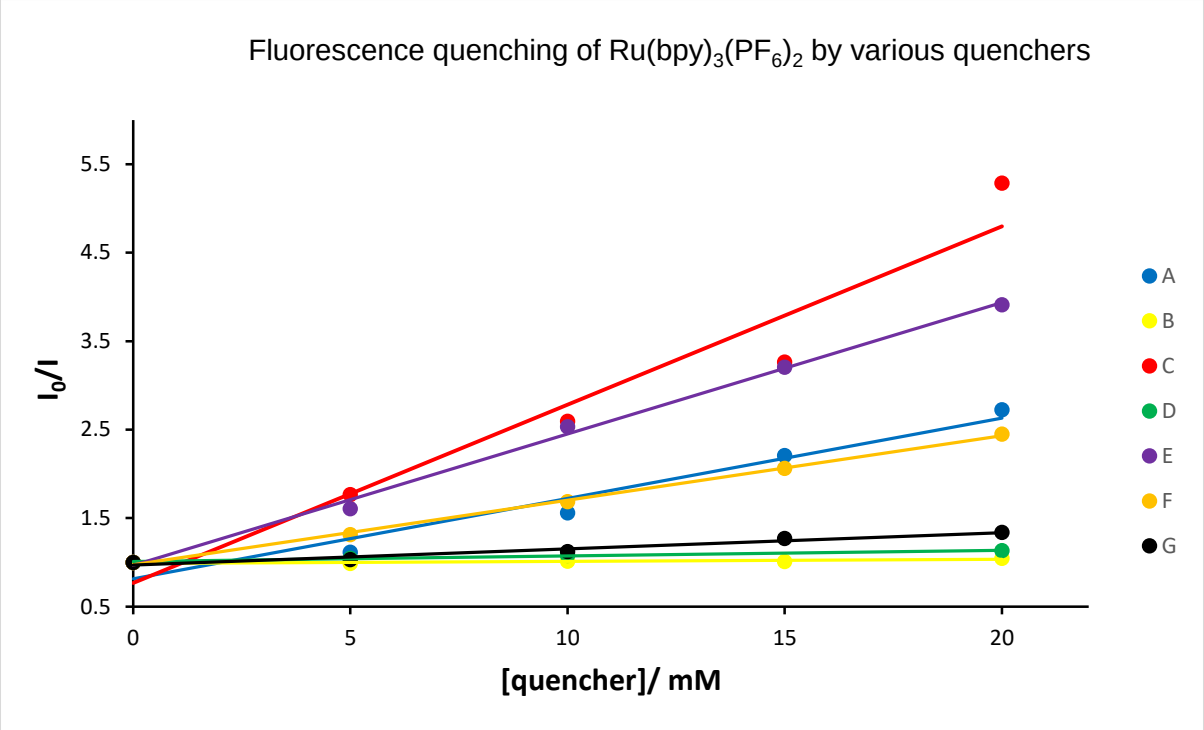

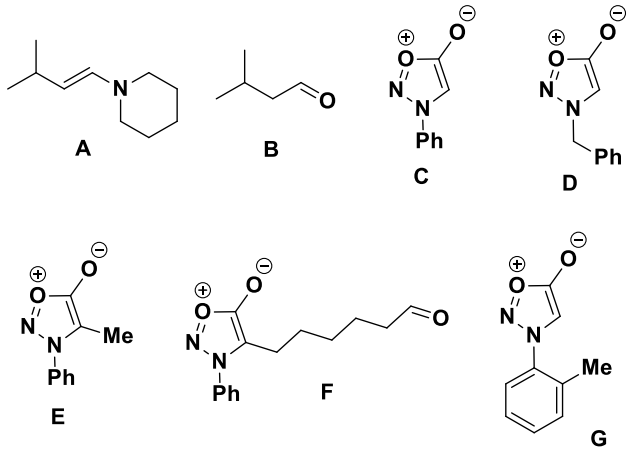

Quencher	K_{SV} [M^{-1}]
(*E*)-1-(3-methylbut-1-en-1-yl)piperidine (**A**)	90.8
Isovaleraldehyde (**B**)	2.3
N-phenylsydnone (**C**)	201.4
N-benzylsydnone (**D**)	6.4
3-phenyl-4-methylsydnone (**E**)	148.4
4-(6-oxohexyl)-3-phenylsydnone (**F**)	72.9
N-(*o*-tolyl)sydnone (**G**)	18.3

5.5.4 Cyclic Voltammetry

Cyclic Voltammetry was carried out on a VersaSTAT 3 workstation using a Pt wire working electrode, Ag wire reference electrode and Pt wire counter electrode. The measurements were taken at room temperature in anhydrous, degassed MeCN containing 0.1 M Bu_4NPF_6 as the electrolyte. 2 mg of *N*-phenylsydnone was dissolved in 5 mL of this solution and 1 crystal of ferrocene was added as a reference. Reported spectra were recorded at 200 mV/s.

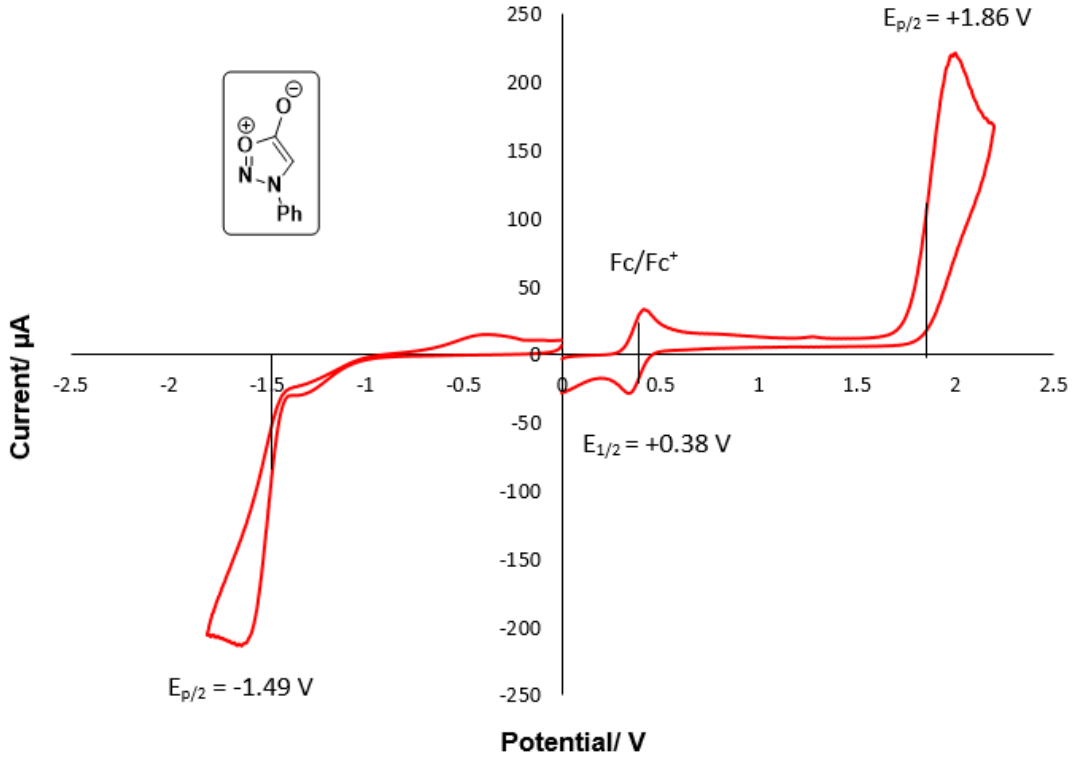

Measured $E_{1/2}$ (Fc/Fc^+) = + 0.38 V

- $E_{p/2}$ refers to the voltage at which the current value has reached half of the peak current.[233]

The *N*-phenylsydnone oxidation peak ($E_{p/2}$ = +1.48 V vs. Fc/Fc^+) exceeds the oxidation potential of $Ru(bpy)_3(PF_6)_2$ ($E_{1/2}$ = +0.89 V vs. Fc/Fc^+) thus rendering a reductive quench of the photocatalyst highly endergonic. Additionally the *N*-phenylsydnone reduction peak ($E_{p/2}$ = -1.87 V vs. Fc/Fc^+) exceeds the reduction potential of $Ru(bpy)_3(PF_6)_2$ ($E_{1/2}$ = -1.73 V vs. Fc/Fc^+) rendering an oxidative quench of the photocatalyst endergonic. Therefore an energy transfer (photosensitisation) mechanism is more likely operative under the PSEC cycloaddition reaction conditions.

5.5.5 Reaction with non-quenching Dipolarophile

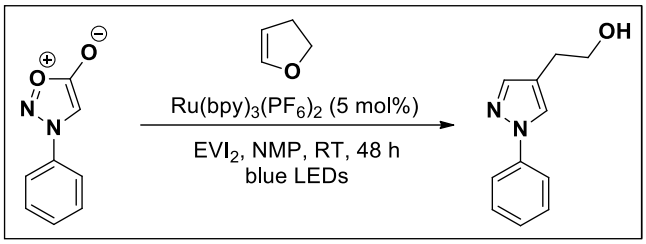

A flame-dried screw cap vial was charged with *N*-phenylsydnone (**35**) (81 mg, 0.5 mmol), $Ru(bpy)_3(PF_6)_2$ (21 mg, 25 µM) and EVI_2 (230 mg, 0.5 mmol) under N_2. Anhydrous, degassed NMP (5 mL) was then added via syringe followed by 2,3-dihydrofuran (**92**) (110 mg, 1.5 mmol). The vial was then subjected to three vacuum/nitrogen cycles, sealed and irradiated using a kessil A160WE tuna blue aquarium light for 72 hours. The reaction was then diluted with H_2O (40 mL) and extracted with Et_2O (4 x 25 mL). The combined organic layers were then washed with brine (25 mL), dried over anhydrous $MgSO_4$ and concentrated under vacuum. Purification by FCC (gradient from 10-40% EtOAc in DCM) afforded 2-(1-phenyl-1*H*-pyrazol-4-yl)ethanol (**93a**) as an orange oil (36 mg, 38%).

^{1}H NMR (400 MHz, $CDCl_3$) δ 7.79 (d, *J* = 0.5 Hz, 1H), 7.67 – 7.62 (m, 2H), 7.58 (s, 1H), 7.46 – 7.39 (m, 2H), 7.29 – 7.23 (m, 1H), 3.82 (t, *J* = 6.5 Hz, 2H), 2.78 (t, *J* = 6.5 Hz, 2H), 1.99 (s, 1H); **^{13}C NMR (101 MHz, $CDCl_3$)** δ 141.5, 140.4, 129.7, 126.6, 126.0, 120.2, 119.2, 63.3, 28.1; **FTIR ν_{max}** 3343, 2927, 2871, 1598, 1500, 1397, 1042, 953 cm^{-1}; **HRMS** calculated for $C_{11}H_{13}N_2O$ (ES^+)($+H^+$): 189.1022. Found: 189.1024.

5.5.6 Isotopic Labelling Experiment

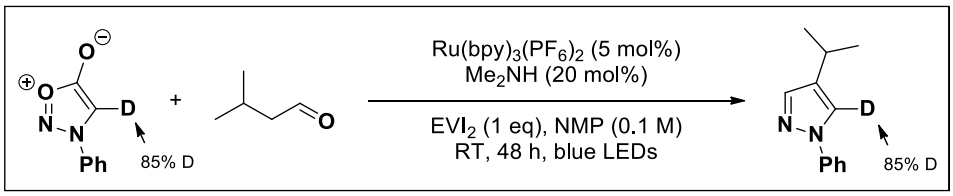

4-isopropyl-1-phenyl-1*H*-pyrazole-*5-d* (*D*-291a).

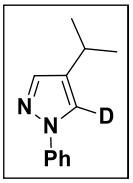

Following GP13 using 3-phenylsydnone-*4-d* (***D*-35**) (81 mg, 0.5 mmol) and isovaleraldehyde (130 mg, 1.5 mmol) with FCC (5% Et_2O in 40-60 petroleum ether), 4-isopropyl-1-phenyl-1*H*-pyrazole-*5-d* (***D*-291a**) was isolated as a yellow oil (82 mg, 87%).

^{1}H NMR (400 MHz, $CDCl_3$) δ 7.70 (s, 0.15H), 7.69 – 7.65 (m, 2H), 7.60 (s, 1H), 7.46 – 7.39 (m, 2H), 7.27 – 7.22 (m, 1H), 2.92 (hept, *J* = 7.0 Hz, 1H), 1.28 (d, *J* = 7.0 Hz, 6H); **^{13}C NMR (101 MHz, $CDCl_3$)** δ 140.4, 139.6, 131.2, 129.4, 126.0, δ 123.2 (t, *J* = 28.5 Hz), 118.8, 24.5, 23.9; **FTIR:** ν_{max} 2960, 1600, 1502, 1390, 993, 944, 854 cm^{-1};

See Appendix 3 and Appendix 4 for ^{1}H and ^{13}C NMR spectra.

5.5.7 UV-Vis Spectrum

UV visible spectra were determined on an Agilent Cary 300 UV-Vis spectrophotometer in a 1 cm^2 quartz cuvette. *N*-phenylsydnone was dissolved in HPLC grade acetonitrile to a concentration of 50 µM.

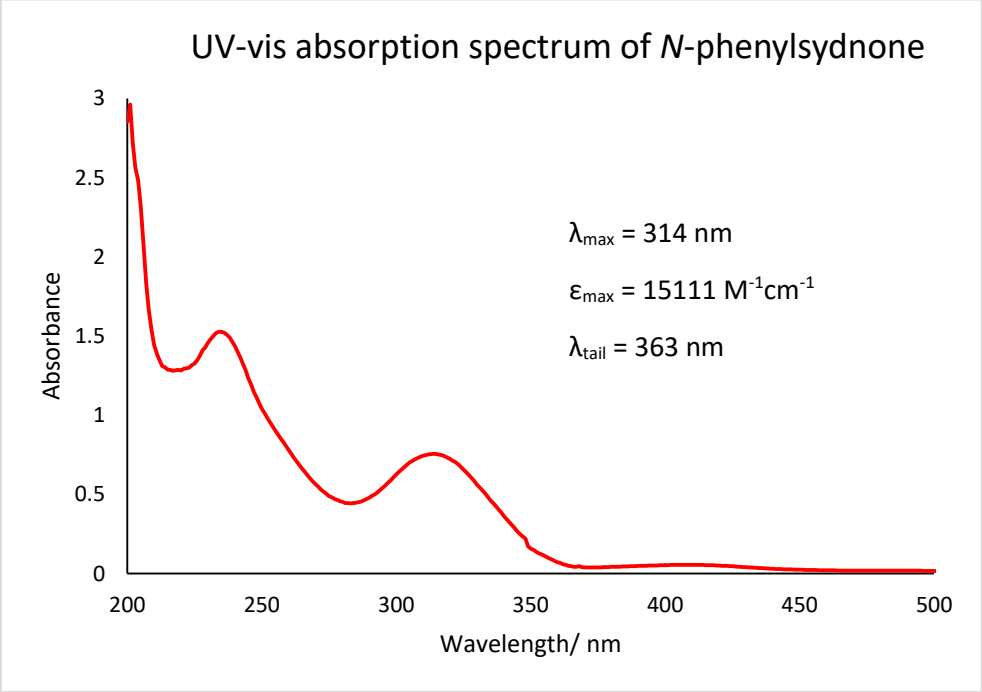

Estimating the singlet energy

An estimate of the singlet excited state energy for a given compound can be obtained from the UV-vis spectrum of the compound according to the following equation:

$$E_{00}(X^*/X) \sim hc \,/\, \lambda_{tail}$$

Where:

$E_{00}(X^*/X)$ = the energy of the singlet excited state (eV)

h = Planck's constant (4.135667696 x 10^{-15} eV.s)

c = speed of light (299762458 $m.s^{-1}$)

λ_{tail} = wavelength at the tail of the absorption peak (nm)

$$N - \text{phenylsydnone singlet energy} = \frac{(4.135667696\ x10^{-15}).(299792458)}{363\ x10^{-9}} = 3.42\ eV$$

Comparison of the estimated singlet energy of *N*-phenylsydnone with the literature value for the triplet energy of $[Ru(bpy)_3]^{2+}$ (E_T = 2.12 eV) indicates that the formation of a singlet excited sydnone species is not possible under the PSEC reaction conditions.

6 References

(1) Knorr, L. *Berichte der Dtsch. Chem. Gesellschaft* **1883**, *16*, 2597–2599.
(2) Penning, T. D.; Talley, J. J.; Bertenshaw, S. R.; Carter, J. S.; Collins, P. W.; Docter, S.; Graneto, M. J.; Lee, L. F.; Malecha, J. W.; Miyashiro, J. M. *J. Med. Chem.* **1997**, *40*, 1347–1365.
(3) Van Gaal, L. F.; Rissanen, A. M.; Scheen, A. J.; Ziegler, O.; Rössner, S. *Lancet* **2005**, *365*, 1389–1397.
(4) Vidau, C.; Brunet, J.-L.; Badiou, A.; Belzunces, L. P. *Toxicol. Vitr.* **2009**, *23*, 589–597.
(5) Cole, L. M.; Nicholson, R. A.; Casida, J. E. *Pestic. Biochem. Physiol.* **1993**, *46*, 47–54.
(6) Fustero, S.; Sánchez-Roselló, M.; Barrio, P.; Simón-Fuentes, A. *Chem. Rev.* **2011**, *111*, 6984–7034.
(7) Singh, S. P.; Kumar, D.; Batra, H.; Naithani, R.; Rozas, I.; Elguero, J. *Can. J. Chem.* **2000**, *78*, 1109–1120.
(8) Maddila, S.; Jonnalagadda, S. B.; Maddila, K. K. G. and S. N. *Current Organic Synthesis*. 2017, pp 634–653.
(9) Katritzky, A. R.; Wang, M.; Zhang, S.; Voronkov, M. V; Steel, P. J. *J. Org. Chem.* **2001**, *66*, 6787–6791.
(10) Aggarwal, V. K.; de Vicente, J.; Bonnert, R. V. *J. Org. Chem.* **2003**, *68*, 5381–5383.
(11) Muruganantham, R.; Mobin, S. M.; Namboothiri, I. N. N. *Org. Lett.* **2007**, *9*, 1125–1128.
(12) Ohira, S. *Synth. Commun.* **1989**, *19*, 561–564.
(13) Müller, S.; Liepold, B.; Roth, G. J.; Bestmann, H. J. *Synlett* **1996**, *6*, 521–522.
(14) Oh, L. M. *Tetrahedron Lett.* **2006**, *47*, 7943–7946.
(15) Donohue, S. R.; Halldin, C.; Pike, V. W. *Tetrahedron Lett.* **2008**, *49*, 2789–2791.
(16) Donohue, A. C.; Pallich, S.; McCarthy, T. D. *J. Chem. Soc. Perkin Trans. 1* **2001**, No. 21, 2817–2822.
(17) Abunada, M. N.; Hassaneen, M. H.; Kandile, G. N.; Miqdad, A. O. *Molecules*. 2008, pp 1501–1517.
(18) Kirar, E. P.; Uroš, G.; Amalija, G.; Franc, P.; Sebastijan, R.; Bogdan, Š.; Jurij, S. *Zeitschrift für Naturforschung B*. 2018, p 467.
(19) Earl, J. C.; Mackney, A. W. *J. Chem. Soc.* **1935**, No. 0, 899–900.
(20) Baker, W.; Ollis, W. D. *Q. Rev. Chem. Soc.* **1957**, *11*, 15–29.
(21) Stewart, F. H. C. *Chem. Rev.* **1964**, *64*, 129–147.
(22) Moustafa, M. A.; Gineinah, M. M.; Nasr, M. N.; Bayoumi, W. A. H. *Arch. Pharm. (Weinheim).* **2004**, *337*, 427–433.
(23) Wagner, H.; Hill, J. B. *J. Med. Chem.* **1974**, *17*, 1337–1338.
(24) Dunkley, C. S.; Thoman, C. J. *Bioorg. Med. Chem. Lett.* **2003**, *13*, 2899–2901.
(25) Browne, D. L.; Harrity, J. P. A. *Tetrahedron* **2010**, *66*, 553–568.
(26) Baker, W.; Ollis, W. D.; Poole, V. D. *J. Chem. Soc.* **1949**, No. 0, 307–314.
(27) KENNER, J.; MACKAY, K. *Nature* **1946**, *158*, 909–910.
(28) Tin-Lok, C.; Miller, J.; Stansfield, F. *J. Chem. Soc.* **1964**, No. 0, 1213–1216.
(29) Greco, C. V; O'Reilly, B. P. *J. Heterocycl. Chem.* **1970**, *7*, 1433–1434.
(30) Thoman, C. J.; Voaden, D. J. *Org. Synth.* **1965**, *45*, 96.
(31) Azarifar, D.; Ghasemnejad-Bosra, H. *Synthesis (Stuttg).* **2006**, 1123–1126.
(32) Specklin, S.; Decuypere, E.; Plougastel, L.; Aliani, S.; Taran, F. *J. Org. Chem.* **2014**, *79*, 7772–7777.
(33) Greco, C. V; Pesce, M.; Franco, J. M. *J. Heterocycl. Chem.* **1966**, *3*, 391–392.
(34) Eade, R. A.; Earl, J. C. *J. Chem. Soc.* **1948**, No. 0, 2307–2310.
(35) Tien, H.-J.; Yeh, M.-Y.; Huang, C.-Y. *J. Chinese Chem. Soc.* **1985**, *32*, 461–465.
(36) Tien, H.-J.; Nonaka, T.; Sekine, T. *Chem. Lett.* **1979**, *8*, 283–286.
(37) Turnbull, K. *J. Heterocycl. Chem.* **1985**, *22*, 965–968.
(38) Dumitraşcu, F.; Drâghici, C.; Dumitrescu, D.; Tarko, L.; Râileanu, D. *Liebigs Ann.* **1997**, *1997*,

2613–2616.
(39) Dumitrascu, F.; Mitan, C. I.; Dumitrescu, D.; Draghici, C.; Caproiu, M. T. *Arkivoc* **2002**, *2002*, 80.
(40) Liu, H.; Audisio, D.; Plougastel, L.; Decuypere, E.; Buisson, D.-A.; Koniev, O.; Kolodych, S.; Wagner, A.; Elhabiri, M.; Krzyczmonik, A. *Angew. Chemie Int. Ed.* **2016**, *55*, 12073–12077.
(41) Hung, W.-J.; Tien, H.-J. *J. Chinese Chem. Soc.* **1993**, *40*, 637–639.
(42) Turnbull, K. *Synth.* **1986**, 334–336.
(43) Turnbull, K.; Saljoughian, M. *Synth. Commun.* **1986**, *16*, 461–466.
(44) McChord, K. L.; Tullis, S. A.; Turnbull, K. *Synth. Commun.* **1989**, *19*, 2249–2253.
(45) Yashunskii, V. G.; Vasil'eva, V. F. *Dokl. Akad. Nauk USSR* **1960**, *130*, 350–352.
(46) Mahoney, J.; Turnbull, K.; Cubberley, M. *Synth. Commun.* **2012**, *42*, 3220–3229.
(47) Balaguer, A.; Selhorst, R.; Turnbull, K. *Synth. Commun.* **2013**, *43*, 1626–1632.
(48) Balaguer, A. M.; Rumple, A. C.; Turnbull, K. *Org. Prep. Proced. Int.* **2014**, *46*, 363–369.
(49) Nicolaou, K. C.; Bulger, P. G.; Sarlah, D. *Angew. Chemie Int. Ed.* **2005**, *44*, 4442–4489.
(50) Magano, J.; Dunetz, J. R. *Chem. Rev.* **2011**, *111*, 2177–2250.
(51) Kalinin, V. N.; Min, S. F. *J. Organomet. Chem.* **1988**, *352*, C34–C36.
(52) A. Cherepanov, I.; D. Bronova, D.; Y. Balantseva, E.; N. Kalinin, V. *Mendeleev Commun.* **1997**, *7*, 93–94.
(53) Turnbull, K.; Krein, D. M.; Tullis, S. A. *Synth. Commun.* **2003**, *33*, 2209–2214.
(54) Browne, D. L.; Taylor, J. B.; Plant, A.; Harrity, J. P. A. *J. Org. Chem.* **2009**, *74*, 396–400.
(55) Chen, Z.; Wang, B.; Zhang, J.; Yu, W.; Liu, Z.; Zhang, Y. *Org. Chem. Front.* **2015**, *2*, 1107–1295.
(56) Yeung, C. S.; Dong, V. M. *Chem. Rev.* **2011**, *111*, 1215–1292.
(57) Rodriguez, A.; Moran, W. J. *Synth.* **2009**, 650–654.
(58) Rodriguez, A.; Fennessy, R. V; Moran, W. J. *Tetrahedron Lett.* **2009**, *50*, 3942–3944.
(59) Brown, A. W.; Harrity, J. P. A. *J. Org. Chem.* **2015**, *80*, 2467–2472.
(60) Martin, R.; Buchwald, S. L. *Acc. Chem. Res.* **2008**, *41*, 1461–1473.
(61) Huisgen, R.; Grashey, R.; Gotthardt, H.; Schmidt, R. *Angew. Chemie Int. Ed. English* **1962**, *1*, 48–49.
(62) Maffrand, J.-P. *Heterocycles* **1981**, *16*, 35–37.
(63) Padwa, A.; Burgess, E. M.; Gingrich, H. L.; Roush, D. M. *J. Org. Chem.* **1982**, *47*, 786–791.
(64) Chang, E.-M.; Wong, F. F.; Chen, T.-H.; Chiang, K.-C.; Yeh, M.-Y. *Heterocycles* **2006**, *68*, 1007–1015.
(65) Browne, D. L.; Helm, M. D.; Plant, A.; Harrity, J. P. A. *Angew. Chemie Int. Ed.* **2007**, *46*, 8656–8658.
(66) Decuypere, E.; Specklin, S.; Gabillet, S.; Audisio, D.; Liu, H.; Plougastel, L.; Kolodych, S.; Taran, F. *Org. Lett.* **2015**, *17*, 362–365.
(67) Delaunay, T.; Genix, P.; Es-Sayed, M.; Vors, J.-P.; Monteiro, N.; Balme, G. *Org. Lett.* **2010**, *12*, 3328–3331.
(68) Delaunay, T.; Es-Sayed, M.; Vors, J.-P.; Monteiro, N.; Balme, G. *European J. Org. Chem.* **2011**, *2011*, 3837–3848.
(69) Browne, D. L.; Taylor, J. B.; Plant, A.; Harrity, J. P. A. *J. Org. Chem.* **2010**, *75*, 984–987.
(70) Browne, D. L.; Vivat, J. F.; Plant, A.; Gomez-Bengoa, E.; Harrity, J. P. A. *J. Am. Chem. Soc.* **2009**, *131*, 7762–7769.
(71) Kolb, H. C.; Finn, M. G.; Sharpless, K. B. *Angew. Chemie Int. Ed.* **2001**, *40*, 2004–2021.
(72) Moses, J. E.; Moorhouse, A. D. *Chem. Soc. Rev.* **2007**, *36*, 1249–1262.
(73) Meldal, M.; Tornøe, C. W. *Chem. Rev.* **2008**, *108*, 2952–3015.
(74) Kolodych, S.; Rasolofonjatovo, E.; Chaumontet, M.; Nevers, M.-C.; Créminon, C.; Taran, F. *Angew. Chemie Int. Ed.* **2013**, *52*, 12056–12060.
(75) Comas-Barceló, J.; Foster, R. S.; Fiser, B.; Gomez-Bengoa, E.; Harrity, J. P. A. *Chem. – A Eur. J.* **2015**, *21*, 3257–3263.
(76) Comas-Barceló, J.; Blanco-Ania, D.; van den Broek, S. A. M. W.; Nieuwland, P. J.; Harrity, J. P.

A.; Rutjes, F. P. J. T. *Catal. Sci. Technol.* **2016**, *6*, 4718–4723.
(77) Brown, A. W.; Comas-Barceló, J.; Harrity, J. P. A. *Chem. – A Eur. J.* **2017**, *23*, 5228–5231.
(78) Wallace, S.; Chin, J. W. *Chem. Sci.* **2014**, *5*, 1742–1744.
(79) Plougastel, L.; Koniev, O.; Specklin, S.; Decuypere, E.; Créminon, C.; Buisson, D.-A.; Wagner, A.; Kolodych, S.; Taran, F. *Chem. Commun.* **2014**, *50*, 9376–9378.
(80) Tao, H.; Liu, F.; Zeng, R.; Shao, Z.; Zou, L.; Cao, Y.; Murphy, J. M.; Houk, K. N.; Liang, Y. *Chem. Commun.* **2018**, *54*, 5082–5085.
(81) Narayanam, M. K.; Liang, Y.; Houk, K. N.; Murphy, J. M. *Chem. Sci.* **2016**, *7*, 1257–1261.
(82) Huisgen, R.; Gotthardt, H.; Grashey, R. *Angew. Chemie Int. Ed. English* **1962**, *1*, 49.
(83) Sun, K. K. *Tetrahedron Lett.* **1986**, *27*, 317–320.
(84) Huisgen, R.; Grashey, R.; Gotthardt, H. *Chem. Ber.* **1968**, *101*, 829–838.
(85) Sun, K. K. *Macromolecules* **1987**, *20*, 726–729.
(86) Intemann, J. J.; Huang, W.; Jin, Z.; Shi, Z.; Yang, X.; Yang, J.; Luo, J.; Jen, A. K.-Y. *ACS Macro Lett.* **2013**, *2*, 256–259.
(87) Sasaki, T.; Manabe, T.; Nishida, S. *J. Org. Chem.* **1980**, *45*, 479–482.
(88) Ranganathan, D.; Bamezai, S. *Tetrahedron Lett.* **1983**, *24*, 1067–1070.
(89) Larsen, S. D.; Martinborough, E. *Tetrahedron Lett.* **1989**, *30*, 4625–4628.
(90) Lopchuk, J. M.; Hughes, R. P.; Gribble, G. W. *Org. Lett.* **2013**, *15*, 5218–5221.
(91) Applegate, J.; Turnbull, K. *Synthesis (Stuttg).* **1988**, 1011–1012.
(92) De Simone, F.; Gertsch, J.; Waser, J. *Angew. Chemie Int. Ed.* **2010**, *49*, 5767–5770.
(93) Hladikova, V.; Váňa, J.; Hanusek, J. *Beilstein J. Org. Chem.* **2018**, *14*, 1317–1348.
(94) Huisgen, R.; Gotthardt, H. *Chem. Ber.* **1968**, *101*, 1059–1071.
(95) Houk, K. N.; Sims, J.; Duke, R. E.; Strozier, R. W.; George, J. K. *J. Am. Chem. Soc.* **1973**, *95*, 7287–7301.
(96) Gimadiev, T. R.; Klimchuk, O.; Nugmanov, R. I.; Madzhidov, T. I.; Varnek, A. *J. Mol. Struct.* **2019**, *1198*, 126897.
(97) Oshima, M.; Murao, T.; Sakurai, Y.; Sasaki, Y.; Nanbu, N. *Acad. Reports Fac. Eng. Tokyo. Polytech. Univ.* **2007**, *30*, 59–65.
(98) Anslyn, E. V.; Dougherty, D. A. *Modern Physical Organic Chemistry*; University Science Books: Sausalito, CA, 2006.
(99) Newcomb, M.; Shen, R.; Choi, S.-Y.; Toy, P. H.; Hollenberg, P. F.; Vaz, A. D. N.; Coon, M. J. *J. Am. Chem. Soc.* **2000**, *122*, 2677–2686.
(100) Connors, D. M.; Goroff, N. S. *Org. Lett.* **2016**, *18*, 4262–4265.
(101) Fischer, R.; Lackovičová, D.; Fišera, L. *Synthesis (Stuttg).* **2012**, *44*, 3783–3788.
(102) Denmark, S. E.; Wang, Z. *Org. Synth.* **2005**, *81*, 42.
(103) Shakhmaev, R. N.; Ishbaeva, A. U.; Zorin, V. V. *Russ. J. Org. Chem.* **2012**, *48*, 908–913.
(104) Macdonald, S. J. F.; Spooner, J. E.; Dowle, M. D. *Synlett* **1998**, No. December, 1375–1377.
(105) Edwards, J. T.; Merchant, R. R.; McClymont, K. S.; Knouse, K. W.; Qin, T.; Malins, L. R.; Vokits, B.; Shaw, S. A.; Bao, D.-H.; Wei, F.-L. *Nature* **2017**, *545*, 213–218.
(106) Gao, P.; Shen, Y.-W.; Fang, R.; Hao, X.-H.; Qiu, Z.-H.; Yang, F.; Yan, X.-B.; Wang, Q.; Gong, X.-J.; Liu, X.-Y. *Angew. Chemie Int. Ed.* **2014**, *53*, 7629–7633.
(107) McDonald, F. E.; Connolly, C. B.; Gleason, M. M.; Towne, T. B.; Treiber, K. D. *J. Org. Chem.* **1993**, *58*, 6952–6953.
(108) Fearnley, S. P.; Lory, P. *Tetrahedron Lett.* **2014**, *55*, 5207–5209.
(109) Carrow, B. P.; Hartwig, J. F. *J. Am. Chem. Soc.* **2010**, *132*, 79–81.
(110) Prier, C. K.; Rankic, D. A.; MacMillan, D. W. C. *Chem. Rev.* **2013**, *113*, 5322–5363.
(111) Shaw, M. H.; Twilton, J.; MacMillan, D. W. C. *J. Org. Chem.* **2016**, *81*, 6898–6926.
(112) Marzo, L.; Pagire, S. K.; Reiser, O.; König, B. *Angew. Chemie - Int. Ed.* **2018**, *57*, 10034–10072.
(113) Noel, T.; Wang, X.; Hessel, V. *Chim. Oggi* **2013**, *31*, 10–14.
(114) Garlets, Z. J.; Nguyen, J. D.; Stephenson, C. R. J. *Isr. J. Chem.* **2014**, *54*, 351–360.
(115) Nicewicz, D. A.; MacMillan, D. W. C. *Science (80-.).* **2008**, *322*, 77–80.

(116) Ischay, M. A.; Anzovino, M. E.; Du, J.; Yoon, T. P. *J. Am. Chem. Soc.* **2008**, *130*, 12886–12887.
(117) Narayanam, J. M. R.; Tucker, J. W.; Stephenson, C. R. J. *J. Am. Chem. Soc.* **2009**, *131*, 8756–8757.
(118) Zhou, Q. Q.; Zou, Y. Q.; Lu, L. Q.; Xiao, W. J. *Angew. Chemie - Int. Ed.* **2019**, *58*, 1586–1604.
(119) Protti, S.; Fagnoni, M.; Ravelli, D. *ChemCatChem* **2015**, *7*, 1516–1523.
(120) Xuan, J.; Lu, L. Q.; Chen, J. R.; Xiao, W. J. *European J. Org. Chem.* **2013**, No. 30, 6755–6770.
(121) Chen, J. R.; Hu, X. Q.; Lu, L. Q.; Xiao, W. J. *Acc. Chem. Res.* **2016**, *49*, 1911–1923.
(122) Michelin, C.; Hoffmann, N. *ACS Catal.* **2018**, *8*, 12046–12055.
(123) Scholz, S. O.; Farney, E. P.; Kim, S.; Bates, D. M.; Yoon, T. P. *Angew. Chemie Int. Ed.* **2016**, *55*, 2239–2242.
(124) Sarabia, F. J.; Ferreira, E. M. *Org. Lett.* **2017**, *19*, 2865–2868.
(125) Larsen, C. B.; Wenger, O. S. *Chem. - A Eur. J.* **2018**, *24*, 2039–2058.
(126) Hockin, B. M.; Li, C.; Robertson, N.; Zysman-Colman, E. *Catal. Sci. Technol.* **2019**, *9*, 889–915.
(127) Cismesia, M. A.; Yoon, T. P. *Chem. Sci.* **2015**, *6*, 5426–5434.
(128) Tyson, E. L.; Farney, E. P.; Yoon, T. P. *Org. Lett.* **2012**, *14*, 1110–1113.
(129) Du, J.; Skubi, K. L.; Schultz, D. M.; Yoon, T. P. *Science (80-.).* **2014**, *344*, 392–396.
(130) Ischay, M. A.; Lu, Z.; Yoon, T. P. *J. Am. Chem. Soc.* **2010**, *132*, 8572–8574.
(131) Ischay, M. A.; Ament, M. S.; Yoon, T. P. *Chem. Sci.* **2012**, *3*, 2807–2811.
(132) Parrish, J. D.; Ischay, M. A.; Lu, Z.; Guo, S.; Peters, N. R.; Yoon, T. P. *Org. Lett.* **2012**, *14*, 1640–1643.
(133) Li, R.; Ma, B. C.; Huang, W.; Wang, L.; Wang, D.; Lu, H.; Landfester, K.; Zhang, K. A. I. *ACS Catal.* **2017**, *7*, 3097–3101.
(134) Romero, N. A.; Nicewicz, D. A. *Chem. Rev.* **2016**, *116*, 10075–10166.
(135) Ikezawa, H.; Kutal, C.; Yasufuku, K.; Yamazaki, H. *J. Am. Chem. Soc.* **1986**, *108*, 1589–1594.
(136) Lu, Z.; Yoon, T. P. *Angew. Chemie Int. Ed.* **2012**, *51*, 10329–10332.
(137) Hurtley, A. E.; Lu, Z.; Yoon, T. P. *Angew. Chemie Int. Ed.* **2014**, *53*, 8991–8994.
(138) Zhao, J.; Brosmer, J. L.; Tang, Q.; Yang, Z.; Houk, K. N.; Diaconescu, P. L.; Kwon, O. *J. Am. Chem. Soc.* **2017**, *139*, 9807–9810.
(139) Pagire, S. K.; Hossain, A.; Traub, L.; Kerres, S.; Reiser, O. *Chem. Commun.* **2017**, *53*, 12072–12075.
(140) Wang, C.; Lu, Z. *Org. Lett.* **2017**, *19*, 5888–5891.
(141) Zhu, M.; Zheng, C.; Zhang, X.; You, S.-L. *J. Am. Chem. Soc.* **2019**, *141*, 2636–2644.
(142) Zhao, L.-M.; Lei, T.; Liao, R.-Z.; Xiao, H.; Chen, B.; Ramamurthy, V.; Tung, C.-H.; Wu, L.-Z. *J. Org. Chem.* **2019**, *84*, 9257–9269.
(143) Mojr, V.; Svobodová, E.; Straková, K.; Neveselý, T.; Chudoba, J.; Dvořáková, H.; Cibulka, R. *Chem. Commun.* **2015**, *51*, 12036–12039.
(144) Mojr, V.; Pitrová, G.; Straková, K.; Prukała, D.; Brazevic, S.; Svobodová, E.; Hoskovcová, I.; Burdziński, G.; Slanina, T.; Sikorski, M. *ChemCatChem* **2018**, *10*, 849–858.
(145) Blum, T. R.; Miller, Z. D.; Bates, D. M.; Guzei, I. A.; Yoon, T. P. *Science (80-.).* **2016**, *354*, 1391–1395.
(146) Miller, Z. D.; Lee, B. J.; Yoon, T. P. *Angew. Chemie Int. Ed.* **2017**, *56*, 11891–11895.
(147) Yu, H.; Dong, S.; Yao, Q.; Chen, L.; Zhang, D.; Liu, X.; Feng, X. *Chem. – A Eur. J.* **2018**, *24*, 19361–19367.
(148) Skubi, K. L.; Kidd, J. B.; Jung, H.; Guzei, I. A.; Baik, M.-H.; Yoon, T. P. *J. Am. Chem. Soc.* **2017**, *139*, 17186–17192.
(149) Müller, C.; Bauer, A.; Bach, T. *Angew. Chemie Int. Ed.* **2009**, *48*, 6640–6642.
(150) Guo, H.; Herdtweck, E.; Bach, T. *Angew. Chemie Int. Ed.* **2010**, *49*, 7782–7785.
(151) Müller, C.; Bauer, A.; Maturi, M. M.; Cuquerella, M. C.; Miranda, M. A.; Bach, T. *J. Am. Chem. Soc.* **2011**, *133*, 16689–16697.
(152) Brimioulle, R.; Guo, H.; Bach, T. *Chem. – A Eur. J.* **2012**, *18*, 7552–7560.
(153) Maturi, M. M.; Wenninger, M.; Alonso, R.; Bauer, A.; Pöthig, A.; Riedle, E.; Bach, T. *Chem. – A*

Eur. J. **2013**, *19*, 7461–7472.
(154) Brimioulle, R.; Bach, T. *Science (80-.).* **2013**, *342*, 840–843.
(155) Alonso, R.; Bach, T. *Angew. Chemie Int. Ed.* **2014**, *53*, 4368–4371.
(156) Vallavoju, N.; Selvakumar, S.; Jockusch, S.; Sibi, M. P.; Sivaguru, J. *Angew. Chemie Int. Ed.* **2014**, *53*, 5604–5608.
(157) Maturi, M. M.; Bach, T. *Angew. Chemie Int. Ed.* **2014**, *53*, 7661–7664.
(158) Brimioulle, R.; Bach, T. *Angew. Chemie Int. Ed.* **2014**, *53*, 12921–12924.
(159) Coote, S. C.; Pöthig, A.; Bach, T. *Chem. – A Eur. J.* **2015**, *21*, 6906–6912.
(160) Brimioulle, R.; Bauer, A.; Bach, T. *J. Am. Chem. Soc.* **2015**, *137*, 5170–5176.
(161) Poplata, S.; Bauer, A.; Storch, G.; Bach, T. *Chem. – A Eur. J.* **2019**, *25*, 8135–8148.
(162) Lu, Z.; Shen, M.; Yoon, T. P. *J. Am. Chem. Soc.* **2011**, *133*, 1162–1164.
(163) Amador, A. G.; Sherbrook, E. M.; Yoon, T. P. *J. Am. Chem. Soc.* **2016**, *138*, 4722–4725.
(164) Huang, X.; Lin, J.; Shen, T.; Harms, K.; Marchini, M.; Ceroni, P.; Meggers, E. *Angew. Chemie Int. Ed.* **2018**, *57*, 5454–5458.
(165) Zhao, G.; Yang, C.; Guo, L.; Sun, H.; Lin, R.; Xia, W. *J. Org. Chem.* **2012**, *77*, 6302–6306.
(166) Maity, S.; Zhu, M.; Shinabery, R. S.; Zheng, N. *Angew. Chemie Int. Ed.* **2012**, *51*, 222–226.
(167) Lu, Z.; Parrish, J. D.; Yoon, T. P. *Tetrahedron* **2014**, *70*, 4270–4278.
(168) Nguyen, T. H.; Morris, S. A.; Zheng, N. *Adv. Synth. Catal.* **2014**, *356*, 2831–2837.
(169) Wang, C.; Ren, X.; Xie, H.; Lu, Z. *Chem. – A Eur. J.* **2015**, *21*, 9676–9680.
(170) Sarabia, F. J.; Li, Q.; Ferreira, E. M. *Angew. Chemie Int. Ed.* **2018**, *57*, 11015–11019.
(171) Xuan, J.; Xia, X. D.; Zeng, T. T.; Feng, Z. J.; Chen, J. R.; Lu, L. Q.; Xiao, W. J. *Angew. Chemie - Int. Ed.* **2014**, *53*, 5653–5656.
(172) Albrecht, E.; Averdung, J.; Bischof, E. W.; Heidbreder, A.; Kirschberg, T.; Müller, F.; Mattay, J. *J. Photochem. Photobiol. A Chem.* **1994**, *82*, 219–232.
(173) Zeng, T.-T.; Xuan, J.; Ding, W.; Wang, K.; Lu, L.-Q.; Xiao, W.-J. *Org. Lett.* **2015**, *17*, 4070–4073.
(174) Deng, Q.-H.; Zou, Y.-Q.; Lu, L.-Q.; Tang, Z.-L.; Chen, J.-R.; Xiao, W.-J. *Chem. – An Asian J.* **2014**, *9*, 2432–2435.
(175) Ding, Y.; Zhang, T.; Chen, Q.-Y.; Zhu, C. *Org. Lett.* **2016**, *18*, 4206–4209.
(176) Zou, Y.-Q.; Lu, L.-Q.; Fu, L.; Chang, N.-J.; Rong, J.; Chen, J.-R.; Xiao, W.-J. *Angew. Chemie Int. Ed.* **2011**, *50*, 7171–7175.
(177) Rueping, M.; Leonori, D.; Poisson, T. *Chem. Commun.* **2011**, *47*, 9615–9617.
(178) Chandrasekhar, D.; Borra, S.; Kapure, J. S.; Shivaji, G. S.; Srinivasulu, G.; Maurya, R. A. *Org. Chem. Front.* **2015**, *2*, 1308–1312.
(179) Chandrasekhar, D.; Borra, S.; Nanubolu, J. B.; Maurya, R. A. *Org. Lett.* **2016**, *18*, 2974–2977.
(180) Fujiya, A.; Tanaka, M.; Yamaguchi, E.; Tada, N.; Itoh, A. *J. Org. Chem.* **2016**, *81*, 7262–7270.
(181) Thierry, T.; Lebargy, C.; Pfund, E.; Lequeux, T. *J. Org. Chem.* **2019**, *84*, 5877–5885.
(182) Hou, H.; Zhu, S.; Pan, F.; Rueping, M. *Org. Lett.* **2014**, *16*, 2872–2875.
(183) Haun, G.; Paneque, A. N.; Almond, D. W.; Austin, B. E.; Moura-Letts, G. *Org. Lett.* **2019**, *21*, 1388–1392.
(184) Jang, G. S.; Lee, J.; Seo, J.; Woo, S. K. *Org. Lett.* **2017**, *19*, 6448–6451.
(185) Svejstrup, T. D.; Zawodny, W.; Douglas, J. J.; Bidgeli, D.; Sheikh, N. S.; Leonori, D. *Chem. Commun.* **2016**, *52*, 12302–12305.
(186) Horibe, T.; Ishihara, K. *Chem. Lett.* **2020**, *49*, 107–113.
(187) Lin, S.; Ischay, M. A.; Fry, C. G.; Yoon, T. P. *J. Am. Chem. Soc.* **2011**, *133*, 19350–19353.
(188) Stevenson, S. M.; Shores, M. P.; Ferreira, E. M. *Angew. Chemie Int. Ed.* **2015**, *54*, 6506–6510.
(189) Hurtley, A. E.; Cismesia, M. A.; Ischay, M. A.; Yoon, T. P. *Tetrahedron* **2011**, *67*, 4442–4448.
(190) Wang, J.; Zheng, N. *Angew. Chemie Int. Ed.* **2015**, *54*, 11424–11427.
(191) Yang, B.; Lu, Z. *J. Org. Chem.* **2016**, *81*, 7288–7300.
(192) Lin, S.; Lies, S. D.; Gravatt, C. S.; Yoon, T. P. *Org. Lett.* **2017**, *19*, 368–371.
(193) Wang, L.; Wu, F.; Chen, J.; Nicewicz, D. A.; Huang, Y. *Angew. Chemie Int. Ed.* **2017**, *56*, 6896–6900.

(194) Higgins, R. F.; Fatur, S. M.; Shepard, S. G.; Stevenson, S. M.; Boston, D. J.; Ferreira, E. M.; Damrauer, N. H.; Rappé, A. K.; Shores, M. P. *J. Am. Chem. Soc.* **2016**, *138*, 5451–5464.
(195) Yang, Y.; Liu, Q.; Zhang, L.; Yu, H.; Dang, Z. *Organometallics* **2017**, *36*, 687–698.
(196) Stevenson, S. M.; Higgins, R. F.; Shores, M. P.; Ferreira, E. M. *Chem. Sci.* **2017**, *8*, 654–660.
(197) Higgins, R. F.; Fatur, S. M.; Damrauer, N. H.; Ferreira, E. M.; Rappé, A. K.; Shores, M. P. *ACS Catal.* **2018**, *8*, 9216–9225.
(198) Arai, N.; Ohkuma, T. *J. Org. Chem.* **2017**, *82*, 7628–7636.
(199) Yadav, A. K.; Yadav, L. D. S. *Tetrahedron Lett.* **2017**, *58*, 552–555.
(200) Tanaka, K.; Omata, D.; Asada, Y.; Hoshino, Y.; Honda, K. *J. Org. Chem.* **2019**, *84*, 10669–10678.
(201) Krauch, C. H.; Kuhls, J.; Piek, H.-J. *Tetrahedron Lett.* **1966**, *7*, 4043–4048.
(202) George, M. V; Angadiyavar, C. S. *J. Org. Chem.* **1971**, *36*, 1589–1594.
(203) Huseya, Y.; Chinone, A.; Ohta, M. *Bull. Chem. Soc. Jpn.* **1971**, *44*, 1667–1668.
(204) Gotthardt, H.; Reiter, F. *Chem. Ber.* **1979**, *112*, 1635–1649.
(205) Bhattacharyya, K.; Ramaiah, D.; Das, P. K.; George, M. V. *J. Photochem.* **1987**, *36*, 63–84.
(206) Stößer, R.; Lieberenz, M.; Csongár, C.; Tomaschewski, G. *zeitschrift für chemie* **1983**, *23*, 184.
(207) Stößer, R.; Csongár, C.; Lieberenz, M.; Tomaschewski, G. *J. Photochem. Photobiol. A Chem.* **1991**, *61*, 245–252.
(208) Veedu, R. N.; Kvaskoff, D.; Wentrup, C. *Aust. J. Chem.* **2014**, *67*, 457–468.
(209) Gotthardt, H.; Reiter, F. *Tetrahedron Lett.* **1971**, *12*, 2749–2752.
(210) Gotthardt, H.; Reiter, F. *Chem. Ber.* **1979**, *112*, 1206–1225.
(211) Pfoertner, K.-H.; Foricher, J. *Helv. Chim. Acta* **1980**, *63*, 653–657.
(212) Gotthardt, H.; Reiter, F. *Chem. Ber.* **1981**, *114*, 1737–1745.
(213) Meier, H.; Heimgartner, H. *Helv. Chim. Acta* **1986**, *69*, 927–940.
(214) Butković, K.; Basarić, N.; Lovreković, K.; Marinić, Ž.; Višnjevac, A.; Kojić-Prodić, B.; Šindler-Kulyk, M. *Tetrahedron Lett.* **2004**, *45*, 9057–9060.
(215) Butković, K.; Vuk, D.; Marinić, Ž.; Penić, J.; Šindler-Kulyk, M. *Tetrahedron* **2010**, *66*, 9356–9362.
(216) Butković, K.; Marinić, Ž.; Molčanov, K.; Kojić-Prodić, B.; Šindler-Kulyk, M. *Beilstein J. Org. Chem.* **2011**, *7*, 1663–1670.
(217) Lim, R. K. V; Lin, Q. *Acc. Chem. Res.* **2011**, *44*, 828–839.
(218) Zhang, L.; Zhang, X.; Yao, Z.; Jiang, S.; Deng, J.; Li, B.; Yu, Z. *J. Am. Chem. Soc.* **2018**, *140*, 7390–7394.
(219) Yao, Z.; Wu, X.; Zhang, X.; Xiong, Q.; Jiang, S.; Yu, Z. *Org. Biomol. Chem.* **2019**, *17*, 6777–6781.
(220) Zhang, X.; Wu, X.; Jiang, S.; Gao, J.; Yao, Z.; Deng, J.; Zhang, L.; Yu, Z. *Chem. Commun.* **2019**, *55*, 7187–7190.
(221) Lin, S.; Padilla, C. E.; Ischay, M. A.; Yoon, T. P. *Tetrahedron Lett.* **2012**, *53*, 3073–3076.
(222) Koike, T.; Akita, M. *Chem. Lett.* **2009**, *38*, 166–167.
(223) Farney, E. P.; Chapman, S. J.; Swords, W. B.; Torelli, M. D.; Hamers, R. J.; Yoon, T. P. *J. Am. Chem. Soc.* **2019**, *141*, 6385–6391.
(224) Fu, Y.; Li, R.-Q.; Liu, L.; Guo, Q.-X. *Res. Chem. Intermed.* **2004**, *30*, 279–286.
(225) Bowry, V. W.; Lusztyk, J.; Ingold, K. U. *J. Am. Chem. Soc.* **1991**, *113*, 5687–5698.
(226) Zhang, Y.; Du, Y.; Huang, Z.; Xu, J.; Wu, X.; Wang, Y.; Wang, M.; Yang, S.; Webster, R. D.; Chi, Y. R. *J. Am. Chem. Soc.* **2015**, *137*, 2416–2419.
(227) Buzzetti, L.; Crisenza, G. E. M.; Melchiorre, P. *Angew. Chemie Int. Ed.* **2019**, *58*, 3730–3747.
(228) Kalyanasundaram, K. *Coord. Chem. Rev.* **1982**, *46*, 159–244.
(229) Eber, G.; Schneider, S.; Dörr, F. *Berichte der Bunsengesellschaft für Phys. Chemie* **1980**, *84*, 281–285.
(230) Mendoza, J. de; Prados, P.; Elguero, J. *Heterocycles* **1985**, *23*, 2629–2634.
(231) Echevarría, A.; Elguero, J.; Meutermans, W. *J. Heterocycl. Chem.* **1993**, *30*, 957–960.
(232) Lorenz, K. T.; Bauld, N. L. *J. Am. Chem. Soc.* **1987**, *109*, 1157–1160.
(233) Roth, H. G.; Romero, N. A.; Nicewicz, D. A. *Synlett* **2016**, *27*, 714–723.

(234) Teders, M.; Bernard, S.; Gottschalk, K.; Schwarz, J. L.; Standley, E. A.; Decuypere, E.; Daniliuc, C. G.; Audisio, D.; Taran, F.; Glorius, F. *Org. Lett.* **2019**, *21*, 9747–9752.
(235) Sreenilayam, G.; Fasan, R. *Chem. Commun.* **2015**, *51*, 1532–1534.
(236) Saalfrank, R. W.; Weiß, B. *Chem. Ber.* **1985**, *118*, 2626–2634.
(237) Schoeller, W.; Schrauth, W.; Goldacker, P. *Berichte der Dtsch. Chem. Gesellschaft* **1911**, *44*, 1300–1312.
(238) Ikeda, S.; Murata, S. *J. Photochem. Photobiol. A Chem.* **2002**, *149*, 121–130.
(239) Zhang, G.; Li, S.; Lei, J.; Zhang, G.; Xie, X.; Ding, C.; Liu, R. *Synlett* **2016**, *27*, 956–960.
(240) Wezeman, T.; Comas-Barceló, J.; Nieger, M.; Harrity, J. P. A.; Bräse, S. *Org. Biomol. Chem.* **2017**, *15*, 1575–1579.
(241) Lantz, R. L.; Obellianne, P. *Bull. Soc. Chim. Fr.* **1956**, 311–317.
(242) Fang, Y.; Wu, C.; Larock, R. C.; Shi, F. *J. Org. Chem.* **2011**, *76*, 8840–8851.
(243) Kier, L. B.; Dhawan, D. *J. Pharm. Sci.* **1962**, *51*, 1058–1061.
(244) Nakajima, M.; Anselme, J. P. *J. Org. Chem.* **1983**, *48*, 1444–1448.
(245) Hammick, D. L.; Voaden, D. J. *J. Chem. Soc.* **1961**, No. 0, 3303–3308.
(246) Li, L.; Wang, H.; Yang, X.; Kong, L.; Wang, F.; Li, X. *J. Org. Chem.* **2016**, *81*, 12038–12045.
(247) Brown, A. W.; Fisher, M.; Tozer, G. M.; Kanthou, C.; Harrity, J. P. A. *J. Med. Chem.* **2016**, *59*, 9473–9488.
(248) Liu, P. N.; Su, F. H.; Wen, T. B.; Sung, H. H.-Y.; Williams, I. D.; Jia, G. *Chem. – A Eur. J.* **2010**, *16*, 7889–7897.
(249) Ma, X.; Wang, J.-X.; Li, S.; Wang, K.-H.; Huang, D. *Tetrahedron* **2009**, *65*, 8683–8689.
(250) Jiang, X.; Vogel, E. B.; Smith, M. R.; Baker, G. L. *Macromolecules* **2008**, *41*, 1937–1944.
(251) El-Sepelgy, O.; Brzozowska, A.; Sklyaruk, J.; Jang, Y. K.; Zubar, V.; Rueping, M. *Org. Lett.* **2018**, *20*, 696–699.
(252) Ladjama, D.; Rieel, J. J. *Synth.* **1979**, 504–507.
(253) Brown, C. E.; McNulty, J.; Bordón, C.; Yolken, R.; Jones-Brando, L. *Org. Biomol. Chem.* **2016**, *14*, 5951–5955.
(254) Vatele, J.-M. *Tetrahedron Lett.* **1984**, *25*, 5997–6000.
(255) Levinger, S.; Shatzmiller, S. *Tetrahedron* **1978**, *34*, 563–567.
(256) Kerr, W. J.; Watson, A. J. B.; Hayes, D. *Org. Biomol. Chem.* **2008**, *6*, 1238–1243.
(257) Suess, A. M.; Uehling, M. R.; Kaminsky, W.; Lalic, G. *J. Am. Chem. Soc.* **2015**, *137*, 7747–7753.
(258) Bull, J. A.; Charette, A. B. *J. Am. Chem. Soc.* **2010**, *132*, 1895–1902.
(259) Saikia, B.; Devi, T. J.; Barua, N. C. *Tetrahedron* **2013**, *69*, 2157–2166.
(260) Zaed, A. M.; Swift, M. D.; Sutherland, A. *Org. Biomol. Chem.* **2009**, *7*, 2678–2680.
(261) Hoye, T. R.; Danielson, M. E.; May, A. E.; Zhao, H. *Angew. Chemie Int. Ed.* **2008**, *47*, 9743–9746.
(262) Stratakis, M.; Nencka, R.; Rabalakos, C.; Adam, W.; Krebs, O. *J. Org. Chem.* **2002**, *67*, 8758–8763.
(263) Beeson, T. D.; MacMillan, D. W. C. *J. Am. Chem. Soc.* **2005**, *127*, 8826–8828.
(264) Gannett, P. M.; Nagel, D. L.; Reilly, P. J.; Lawson, T.; Sharpe, J.; Toth, B. *J. Org. Chem.* **1988**, *53*, 1064–1071.
(265) Molander, G. A.; McWilliams, J. C.; Noll, B. C. *J. Am. Chem. Soc.* **1997**, *119*, 1265–1276.
(266) Horiuchi, T.; Takeda, Y.; Haginoya, N.; Miyazaki, M.; Nagata, M.; Kitagawa, M.; Akahane, K.; Uoto, K. *Chem. Pharm. Bull.* **2011**, *59*, 991–1002.
(267) Ahmed, M.; Seayad, A. M.; Jackstell, R.; Beller, M. *Angew. Chemie Int. Ed.* **2003**, *42*, 5615–5619.
(268) Ikeda, S.; Chatani, N.; Kajikawa, Y.; Ohe, K.; Murai, S. *J. Org. Chem.* **1992**, *57*, 2–4.
(269) Hu, B.; Chen, H.; Liu, Y.; Dong, W.; Ren, K.; Xie, X.; Xu, H.; Zhang, Z. *Chem. Commun.* **2014**, *50*, 13547–13550.
(270) Carlson, R.; Nilsson, Å. *Acta Chem. Scand. B* **1984**, *38*, 49–53.
(271) Kakaawla, T. K. K.; Harrity, J. P. A. *Org. Lett.* **2018**, *20*, 201–203.

(272) Jin, X.; Kataoka, K.; Yatabe, T.; Yamaguchi, K.; Mizuno, N. *Angew. Chemie Int. Ed.* **2016**, *55*, 7212–7217.
(273) Imada, Y.; Iida, H.; Ono, S.; Murahashi, S.-I. *J. Am. Chem. Soc.* **2003**, *125*, 2868–2869.
(274) Fischer, R.; Lackovičová, D.; Fišera, L. *Synth.* **2012**, *44*, 3783–3788.
(275) Yamagishi, M.; Nishigai, K.; Hata, T.; Urabe, H. *Org. Lett.* **2011**, *13*, 4873–4875.
(276) Ilardi, E. A.; Stivala, C. E.; Zakarian, A. *Org. Lett.* **2008**, *10*, 1727–1730.
(277) Patra, T.; Agasti, S.; Modak, A.; Maiti, D. *Chem. Commun.* **2013**, *49*, 8362–8364.
(278) Zhu, L.; Guo, P.; Li, G.; Lan, J.; Xie, R.; You, J. *J. Org. Chem.* **2007**, *72*, 8535–8538.
(279) Majumder, S.; Gipson, K. R.; Staples, R. J.; Odom, A. L. *Adv. Synth. Catal.* **2009**, *351*, 2013–2023.
(280) Schmitt, D. C.; Taylor, A. P.; Flick, A. C.; Kyne, R. E. *Org. Lett.* **2015**, *17*, 1405–1408.
(281) Romero, N. A.; Margrey, K. A.; Tay, N. E.; Nicewicz, D. A. *Science (80-.).* **2015**, *349*, 1326 LP – 1330.
(282) Iwasawa, Yoshihiro Yamamoto, Susumu Suzuki, K.; Murakami, H.; Suzuki, F. EP0366329, 1990.
(283) Landge, S. M.; Schmidt, A.; Outerbridge, V.; Török, B. *Synlett* **2007**, *10*, 1600–1604.
(284) Xu, Z.-L.; Li, H.-X.; Ren, Z.-G.; Du, W.-Y.; Xu, W.-C.; Lang, J.-P. *Tetrahedron* **2011**, *67*, 5282–5288.
(285) Johnson, D.; Suschitzky, H. *J. Chem. Soc. Perkin Trans. 1* **1976**, No. 10, 1062–1064.

Appendix

Appendix 1 – On/Off Experiment

The on off experiment was performed under standard conditions (GP13) using *N*-phenylsydnone (**35**) (81 mg, 0.5 mmol), isovaleraldehyde (**326**) (130 mg, 1.5 mmol), dimethylamine (2.0 M in THF, 0.05 mL, 0.1 mmol), $Ru(bpy)_3(PF_6)_2$ (25 µmol), EVI_2 (0.5 mmol) and NMP (5 mL). Light was switched off/on in 2 hour intervals. Every 30 minutes a 0.1 mL aliquot of the reaction mixture was removed, filtered through silica (eluting with EtOAc/petrol (1:1)) and concentrated under vacuum. The conversion was then estimated by ^{1}H-NMR by comparing the ratio of starting material:product. The obtained data indicates product formation is halted in the absence of irradiation, confirming the light promoted nature of the reaction.

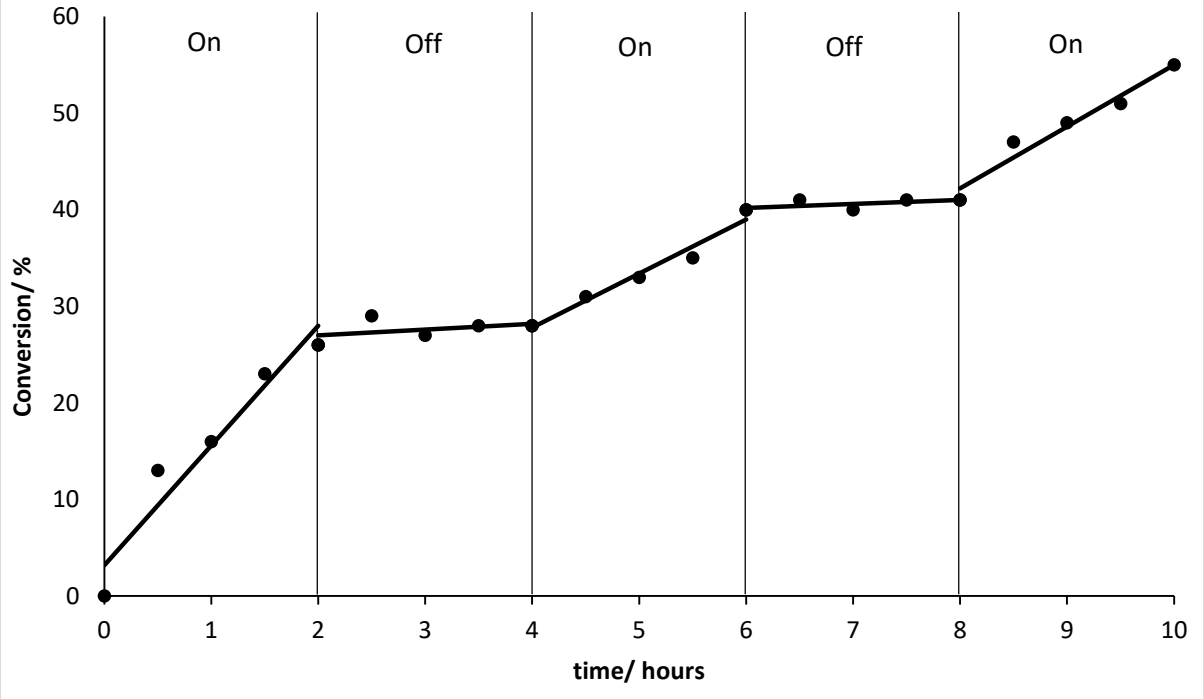

Appendix 2 – Stern-Volmer Analysis of 2,3-Dihydrofuran (92)

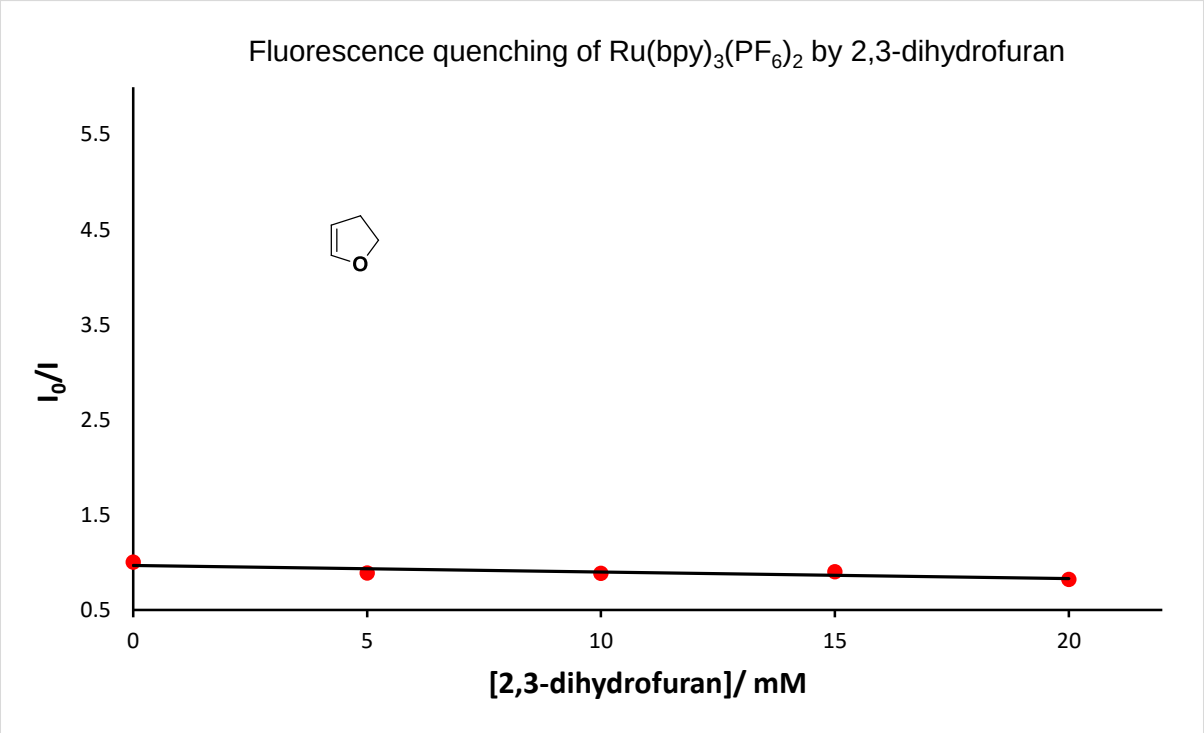

As can be seen, the trendline is parallel to the x-axis, therefore 2,3-dihydrofuran is not a quencher of the excited state catalyst.

Appendix 3 – ^{1}H NMR spectra of 291a and *D*-291a

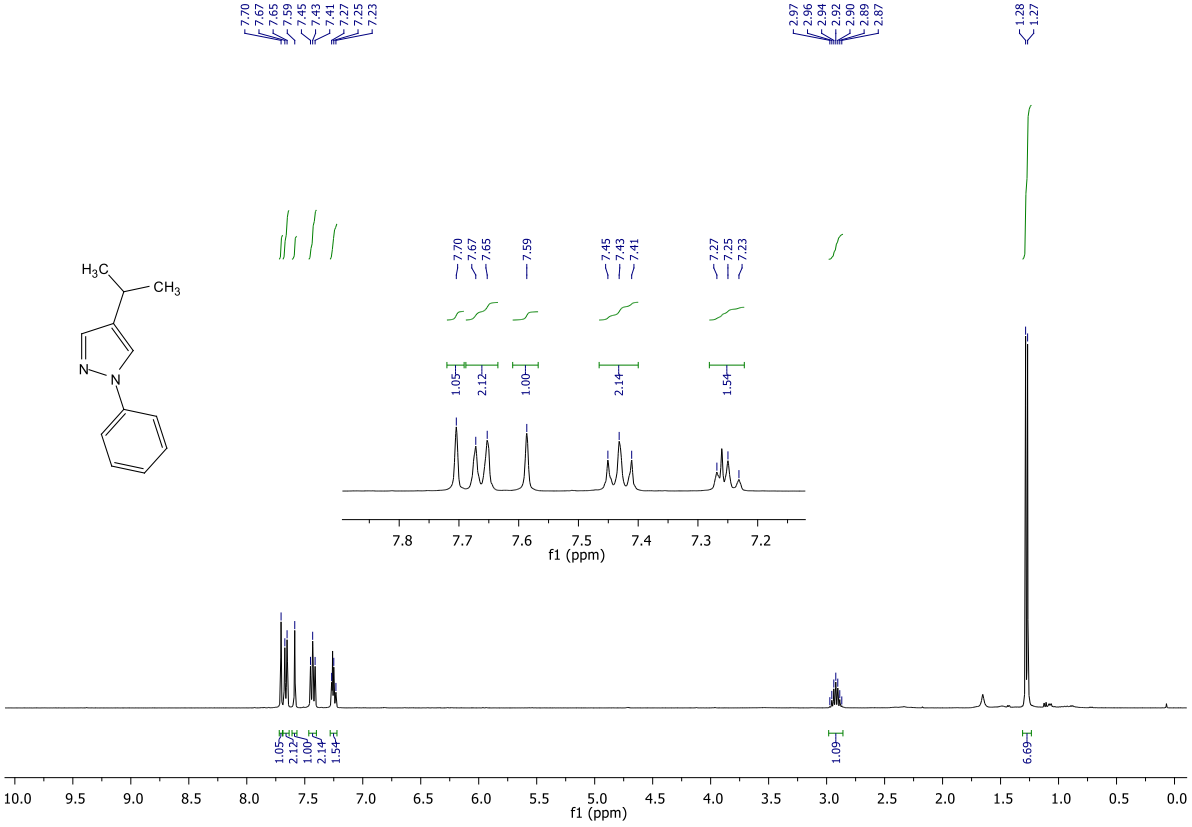

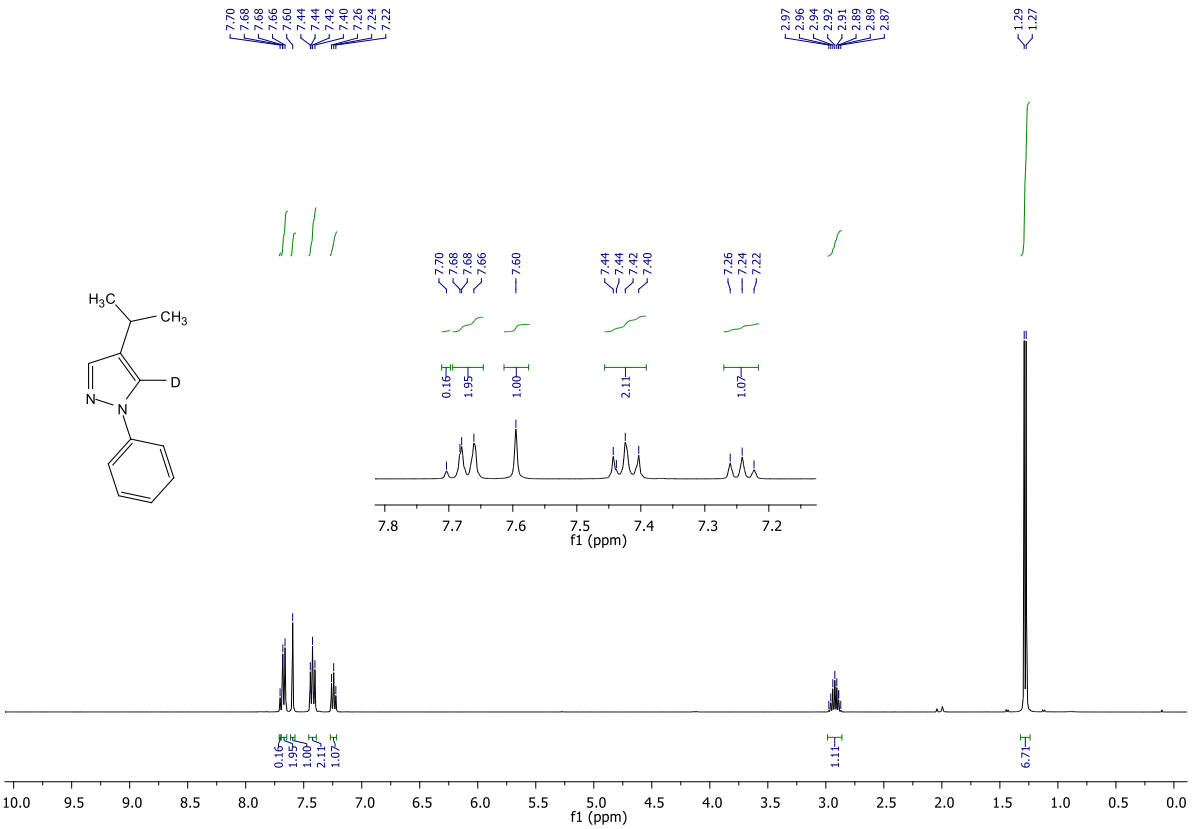

Appendix 4 – ^{13}C NMR spectra of 291a and *D*-291a